Study of MeCP2 function in a mouse model of Rett syndrome

Skirmantas Kriaucionis

Thesis presented for the degree of Doctor of Philosophy

Wellcome Trust Centre for Cell Biology

University of Edinburgh

2004

Acknowledgments

First of all I would like to acknowledge my supervisor Adrian Bird for taking me into his laboratory (even when I had difficulties in drawing structure of 5-methyl-cytosine), further guidance and fruitful discussions. Everybody in the laboratory was very kind, supportive and helped me in many different ways. Specifically, Jim Selfridge for professionalism in teaching me the mouse gene targeting technique, Jacky Guy who introduced me to tissue culture and ES cell manipulations, Catherine Millar for advise on two-hybrid screen, Rob Klose on chromatin IP assay, Hannah Moore on the bisulfide DNA sequencing and Helle Jorgensen for immunohistochemistry expertise. In general, scientific advice of Donald Macleod, Miho Suzuki, Jennifer Berger, Heather McQueen and Brian Hendrich were very helpful. Technical help from Christine Struthers, Aileen Greig, Helen Barr and Karen Wilson was indispensable.

I am grateful to Darwin Trust for the funding of these studies.

Finally I would like to thank my wife Lina for the care and understanding. The delicious home food made by my talented wife was a necessary ingredient of every success.

Abstract

DNA methylation is a common modification in vertebrates that is mainly restricted to CpG dinucleotides. It is an essential component of a genome, which is important for proper development, imprinting, X-chromosome inactivation and for transcriptional silencing in general. MeCP2 was initially identified as a protein that binds methylated CpG. Transient transfection studies and identification of protein partners suggested that MeCP2 is a transcriptional repressor.

Mutations in the *MECP2* gene are frequently found in patients with Rett syndrome. It is now commonly agreed that Rett syndrome is a monogenic neurological disease caused by mutations in *MECP2* gene. Rett syndrome mainly occurs in girls and it is characterised by a period of normal development until around 6 - 18 months, followed by a rapid regression. After the regression, symptoms persist as severe mental retardation, reduced head size, seizures, ataxia, hyperventilation and repetitive hand wringing movements.

The phenotype of mice with a deleted *Mecp2* gene mimics some Rett syndrome symptoms. The *Mecp2*-null mouse develops normally until about 6 weeks of age after which tremors, irregular breathing, lack of mobility and hindlimb clasping develop.

The main goal of this thesis is to understand how the mutation in *MECP2* gene causes Rett syndrome. The search for MeCP2 regulated genes was initiated in *Mecp2*-null mouse brain. Examination of candidate genes revealed that *Bdnf* is down-regulated and *Hes1* is up-regulated in pre, early and late symptomatic *Mecp2*-null mice. Further, global analysis of gene expression was examined by ADDER differential display. Some mis-regulated genes were identified, two of which are involved in mitochondrial respiration. Oxygen electrode measurements revealed defects in brain mitochondrial respiration, which commenced coincident with symptom onset in *Mecp2*-null mice. This finding suggests mitochondrial involvement in the pathogenesis of Rett syndrome symptoms.

In the course of these studies, the structure of the *Mecp2* gene was re-investigated, leading to the identification of a new MeCP2 isoform. Data in this thesis demonstrates that the new isoform is the major form of MeCP2 in both mouse and human brain.

Abbreviations

A_{600}	Absorption at the 600 nm wavelength
ADDER	amplification of double stranded cDNA end restriction fragments
ADP	adenosine diphosphate
ATP	adenosine triphosphate
bp	base-pair
BSA	bovine serum albumine
Da	dalton
DAPI	4',6-diamidino-2-phenylindole
dATP	deoxyadenosine triphosphate
dCTP	deoxycytidine triphosphate
dDTP	dATP + dGTP + dTTP
DEPC	diethylpyrocarbonate
dGTP	deoxyguanosine triphosphate
DIG	digoxigenin
DMR	differential methylated region
DMSO	dimethyl sulfoxide
DNA	deoxyribonucleic acid
DNase	deoxyribonuclease

dNTP	dATP + dGTP + dTTP + dCTP
Dox	doxycycline
dTTP	deoxythymidine triphosphate
EB	embryoid bodies
ECL	enhanced chemical luminescence
EDTA	diaminoethanetetraacetic acid
EEG	electroencephalogram
ELISA	enzyme-linked immunosorbent assay
ES	embryonic stem
EST	expressed sequence tag
FISH	fluorescent *in situ* hybridisation
h	hour
j	joules
kb	kilobase
kDa	kilodalton
l	liter
LB	Luria broth
M	molar
MBD	Methyl CpG binding domain
min	minutes
MOPS	3-(N-morpholino) propanesulphonic acid

NAD	nicotinamide adenine dinucleotide
NADH	nicotinamide adenine dinucleotide (reduced form)
ORF	open reading frame
PBS	phosphate buffer saline
PCR	polymerase chain reaction
PDL	poly-D lysine
RCR	respiratory control ratio
R-M	restriction-modification
RNA	ribonucleic acid
RNase	ribonuclease
rpm	revolutions per minute
rtTA	reverse tetracycline trans-activator
s	second
SAM	S-adenosyl-L-methionine
SDS	sodium dodecyl sulphate
TAM	tamoxifen
TEM	transmission electron microscopy
Tet	tetracycline
tetO	tetracycline operator
TRD	Transcriptional repression domain
Tris	2-amino-2(hydroxymethyl)-1,2,-propanediol

tTA	tetracycline trans-activator
TUNEL	terminal deoxynucleotidyl transferase-mediated dUTP nick end labeling
UV	ultra violet
V	volts

Table of contents

DECLARATION **2**

ACKNOWLEDGMENTS **3**

ABSTRACT **4**

ABBREVIATIONS **6**

TABLE OF CONTENTS **10**

LIST OF FIGURES **14**

LIST OF TABLES **16**

1. CHAPTER ONE. LITERATURE REVIEW **17**

1.1. OVERVIEW 18

1.2. DNA METHYLATION 18

1.2.1. Common theme *18*

1.2.2. Biology of DNA methylation in prokaryotes *19*

1.2.3. 5-methyl cytosine in different eukaryotes *21*

1.2.4. Biological functions in mammals related to DNA methylation *23*

1.2.5. Understanding DNA methylation through investigation of DNA methyltransferases .. *25*

1.2.6. Interplay between DNA methylation and histone modifications *28*

1.3. METHYL CPG BINDING PROTEINS 29

1.4. MECP2 33

1.4.1. MeCP2 specific binding to methylated CpGs *33*

1.4.2. MeCP2 as transcriptional repressor *36*

1.5. RETT SYNDROME 38

1.6. MECP2 MUTATIONS IN MOUSE 44

1.7. MECP2 STUDIES IN BRAIN 46

1.8. DISCUSSION 48

1.9. THESIS OBJECTIVES 50

2. CHAPTER TWO. MATERIALS AND METHODS **52**

2.1. MATERIALS 53

2.1.1. Common solutions and reagents *53*

2.1.2. Protein manipulation solutions *54*

2.1.3. Cell culture solutions *54*

2.1.4. *Microbiological solutions and reagents* 55
2.2. SPECIFIC REAGENTS 55
2.2.1. *Antibodies* 55
2.2.2. *Primers* 56
2.3. PROTOCOLS 61
2.3.1. *RNA and genomic DNA extraction* 61
2.3.2. *Crude genomic DNA extraction for the genotyping of mice* 62
2.3.3. *Preparation of frozen competent E.coli* 62
2.3.4. *Restriction digestion of DNA* 63
2.3.5. *DNA electrophoresis and gel purification* 63
2.3.6. *DNA ligation* 64
2.3.7. *Plasmid DNA transformation of competent E.coli* 64
2.3.8. *Small scale crude plasmid DNA preparation* 64
2.3.9. *Large, medium and small scale plasmid DNA purification* 65
2.3.10. *DNA labelling by direct incorporation of radioactive nucleotides* 65
2.3.11. *DNA end labelling by phosphate group transfer* 66
2.3.12. *Southern blot using alkali transfer* 66
2.3.13. *Northern blot* 67
2.3.14. *Nascent RNA fluorescent in situ hybridization (FISH) on mouse brain tissue sections* 67
2.3.15. *Immuno-staining of monolayer cells* 69
2.3.16. *cDNA synthesis* 70
2.3.17. *Western blotting* 70
2.3.18. *DNA sequencing* 71
2.3.19. *Site-directed mutagenesis* 71
2.3.20. *Real Time PCR* 72
2.3.21. *Mammalian monolayer cell culture* 74
2.3.22. *Monolayer cell transient transfection* 75
2.3.23. *Embryonic stem (ES) cell differentiation into neurons* 75
2.3.24. *ADDER differential display* 78
2.3.25. *Bisulfite DNA modification* 80
2.3.26. *Chromatin Immunoprecipitation* 81
2.3.27. *TUNEL staining* 82
2.3.28. *Screening for mutations in exon 1 of the Mecp2 gene in Rett syndrome patients* 83
2.3.29. *Generation of a mouse with a targeted mutation* 84
2.3.30. *Luciferase activity measurements* 86
2.3.31. *Generation of amino acid sequence alignments* 86
2.3.32. *BLAST searches* 87
2.3.33. *Examination of condition of Mecp2-null mice* 87

3. CHAPTER THREE. GENE EXPRESSION ANALYSIS IN *MECP2*-NULL MOUSE BRAIN 89

3.1. INTRODUCTION 90

3.2. LITERATURE OVERVIEW OF PREVIOUSLY IDENTIFIED MECP2 TARGET GENES BY A CANDIDATE APPROACH 91

3.3. PREVIOUSLY DESCRIBED ATTEMPTS TO IDENTIFY MECP2 TARGET GENES BY GLOBAL ANALYSIS OF GENE EXPRESSION 93

3.4. MECP2 TARGET GENES IDENTIFIED BY CANDIDATE APPROACH 94

3.4.1. Bdnf mRNA is down-regulated in Mecp2-null mouse brain 94

3.4.2. Ss18l1 (Crest) mRNA is not mis-regulated in Mecp2-null mouse brain 98

3.4.3. Mammalian homolog of Hairy2a is up-regulated in the Mecp2-null mouse brain 99

3.4.4. Verification and syptom-course analysis of Sgk and Fkbp5 expression 99

3.5. GLOBAL ANALYSIS OF GENE EXPRESSION 104

3.5.1. Gene expression analysis in Mecp2-null mouse brain by a variant of differential display 104

3.6. BIOLOGICAL CAUSES AND CONSEQUENCES OF GENE MIS-REGULATION IN MECP2-NULL MOUSE BRAIN 110

3.6.1. Meg3/gtl2 up-regulation is not due to bi-allelic expression 110

3.6.2. Mis-regulation of Uqcrc1 correlates with mitochondrial respiration defect in Mecp2-null mouse brain 115

3.6.3. Mitochondrial respiration dysfunction does not lead to increased apoptosis in Mecp2-null mouse brain 121

3.7. SUMMARY AND CONCLUSIONS 124

4. CHAPTER FOUR. MECP2 ISOFORMS 128

4.1. INTRODUCTION 129

4.2. IDENTIFICATION OF MECP2 SPLICE VARIANT IN EST DATABASES 130

4.3. MECP2E1 IS THE MAJOR MRNA SPLICE VARIANT IN VIVO 131

4.4. THE MECP2E1 SPLICE VARIANT IS MORE EFFICIENTLY TRANSLATED IN VIVO 134

4.5. LOCALISATION OF DIFFERENT MECP2 ISOFORMS IN MOUSE CELLS 137

4.6. SCREENING OF ISOFORM SPECIFIC SEQUENCE VARIATIONS IN HUMANS 137

4.7. GENERATION OF MECP2 ISOFORM SPECIFIC ANTIBODIES 138

4.8. DISCUSSION 141

5. CHAPTER FIVE. INDUCIBLE MECP2 EXPRESSION IN A MOUSE 144

5.1. INTRODUCTION 145

5.2. CONSTRUCTION OF THE INDUCIBLE MECP2 ALLELE IN MICE 146

5.3. CRE-ER^T MEDIATED MECP2 KNOCK-OUT IN ADULT MICE 151

5.4. SUMMARY AND DISCUSSION 153

6. CHAPTER SIX. FINAL CONCLUSIONS 155

6.1. FINAL SUMMARY AND DISCUSSION 156

REFERENCE LIST 161

PUBLISHED PAPERS 184

List of Figures

Figure 1-1. Biologically acquired DNA modifications found in living organisms..... 20
Figure 1-2. Methyl-CpG binding proteins..... 30
Figure 1-3. Representative structure of MBD (from MBD1) in complex with DNA..... 35
Figure 1-4. MECP2 alignment and sequence variations found in humans..... 40
Figure 1-5. Distribution of different Rett syndrome causing mutations..... 41
Figure 1-6. Frequencies of different Rett syndrome causing mutations in the MECP2 gene..... 42
Figure 2-1. Evaluation of the Real Time PCR assay..... 73
Figure 2-2. Neurons derived by *in vitro* differentiation of ES cells..... 77
Figure 2-3 Schematic diagram shows steps involved in ADDER differential display..... 79
Figure 3-1. *Bdnf* expression in the *Mecp2*-null mouse brain during progression of symptoms... 95
Figure 3-2. Contribution of different *Bdnf* promoters to the total Bdnf mRNA under-representation in pre-symptomatic *Mecp2*-null mouse brain..... 97
Figure 3-3. *Ntrk2* and *Ss18l1* are not mis-regulated in late symptomatic *Mecp2*-null mouse brain..... 98
Figure 3-4. *Hes1* is significantly up-regulated at all stages of disease examined..... 100
Figure 3-5. *Fkbp5* and *Sgk* are significantly up-regulated in pre, early and late symptomatic mice..... 101
Figure 3-6. MeCP2 presence at the two different regions of *Fkbp5* and one region of *Sgk* is not abolished after the infusion of corticosterone..... 103
Figure 3-7. ADDER differential display analysis from *Mecp2*-null and *wt* mice brains..... 105
Figure 3-8. An example of a standart procedure used for the identification of genes from differential display screen..... 107
Figure 3-9. Nascent RNA FISH experiment scheme..... 111
Figure 3-10. Results from the nascent RNA FISH experiment..... 113
Figure 3-11. Nascent RNA FISH images..... 114
Figure 3-12. The mitochondrial respiration chain..... 115
Figure 3-13. Real Time PCR data showing *Uqcrc1* and *mt-Nd2* mis-regulation in *Mecp2*-null mouse brain..... 116
Figure 3-14. MeCP2 binds the promoter region of *Uqcrc1* gene..... 118
Figure 3-15. Investigation of the respiratory chain in mitochondria isolated from whole brain of *wt* and *Mecp2*-null mice..... 120
Figure 3-16. TUNEL staining on late symptomatic *Mecp2*-null mouse and *wt* litter mate brain section..... 123
Figure 4-1. Alternative splicing of MeCP2 mRNA..... 132

Figure 4-2. Relative abundance of splice variant mRNAs in mouse tissues, human brain and differentiating ES cells. 133
Figure 4-3. Western blot analysis of mouse cells transfected with MeCP2e1 and MeCP2e2. ... 135
Figure 4-4. Reduced abundance of MeCP2e2 due to translational interference by an upstream ORF..... 136
Figure 4-5. Both MeCP2 isoforms co-localise with methyl-CpG-rich DAPI bright spots..... 137
Figure 4-6. Western blot analysis of isoform specific anti-sera..... 140
Figure 5-1. Mechanism of "Tet-on" inducible gene expression for induction of *Mecp2*. 147
Figure 5-2. Strategy for the production of an inducible MeCP2 in mouse..... 148
Figure 5-3. The targeting of ROSA26 locus with the tetracycline trans-acivator. 150
Figure 5-4. *Luciferase* reporter induction in N-nlsrtTA targeted ES cells 150
Figure 5-5. Generation of ligand inducible mutation in the *Mecp2* gene using Cre-ER^T technology..... 152
Figure 5-6. Southern blot analysis of *loxP* recombination at the *Mecp2* locus after administration of 1 mg of TAM per day..... 152
Figure 5-7. Southern blot of *Mecp2* loxP recombination following administration of 3 mg of TAM per day for 5 consecutive days..... 153

List of Tables

Table 2-1. Antibodies used in the different experiments presented in this thesis. 55

Table 2-2. Primers used for ADDER differential display. 56

Table 2-3. Primers used for the Real Time PCR. 57

Table 2-4. PCR primers used for the genotyping of mice. 61

Table 2-5. Classification of *Mecp2*-null mice according to the manifestation of phenotype. 88

Table 3-1. List of genes found to be mis-regulated in *Mecp2*-null mouse brain by ADDER and confirmed by Real Time PCR 109

Table 4-1. Physical characteristics of human and mouse MeCP2 isoforms. 131

1. Chapter one.

Literature review

1.1. Overview

The literature review provides a background about the MeCP2 protein and Rett syndrome, the main subjects investigated in this thesis. MeCP2 is a methyl-CpG binding protein and a lot of the MeCP2 research is related to the understanding of DNA methylation function in different organisms. The initial section describes the known properties of the DNA methylation in prokaryotes and eukaryotes. The studies of DNA methyltransferases in mouse has provided significant input to the understanding of the *in vivo* importance of methylation, therefore substantial attention is paid to this topic. Next, the evidence of histone modifications' connection with DNA methylation is discussed. The general part of the introduction is finished by a description of the protein family which share a similar methylated DNA recognition domain. The subsequent sections describe the most important evidence showing DNA binding and transcriptional repression properties of MeCP2. Next, Rett syndrome and MeCP2 mutation distribution are discussed, followed by, a description of existing mouse models. In the discussion section, the different theories concerning MeCP2 function are put forward. The final section formulates the objectives of this thesis.

1.2. DNA Methylation

1.2.1. Common theme

There is only one common type of biologically acquired DNA modification present in most living organisms – methylation. DNA can be modified by addition of a methyl group to either the endocyclic carbon-5 in cytosine (Hotchkiss, 1948), or the exocyclic nitrogen-4 (Janulaitis et al., 1983) of cytosine or the nitrogen-6 (DUNN and SMITH, 1955) of adenine (Figure 1-1). Cytosine was additionally shown to harbour two methyl groups, on both the C5 and N4 positions, however the *in vivo* presence of such modification is unclear (Klimasauskas et al., 2002). The methyl group is added post-replication by DNA methyltransferase enzymes, which use S-adenosyl-L-methionine (SAM) as a methyl group donor. Determination of primary

protein sequences for different classes of methyltransferases followed by alignments, led to a conclusion, that different DNA methyltransferases share common homologous motifs (Klimasauskas et al., 1989). The close structural similarity between DNA methyltransferases was shown, when more structures became available (Cheng and Roberts, 2001). The most conserved part is the catalytic domain which has 10 conserved motifs (Kumar et al., 1994). The structure of *Hha* I cytosine-5 DNA methyltransferase in complex with DNA revealed that the mechanism by which DNA is methylated involves flipping out of the cytosine from the double helix of DNA, exposing it to a catalytical pocket where the methyl group is transferred from SAM to cytosine (Klimasauskas et al., 1994).

1.2.2. Biology of DNA methylation in prokaryotes

Bacteria can have methylation on cytosine-5, cytosine-4 and adenine-4 residues. Often methyltransferases are linked with restriction endonucleases. These cases are described as restriction-modification (R-M) systems and the biological function of restriction-modification is to defend against invading phage genomes (Wilson and Murray, 1991). When foreign DNA enters a bacterial cell it can be attacked by restriction endonuclease. The host cell, however, in addition to endonuclease, harbours DNA methyltransferase, which maintains the host genome methylated and resistant to endonuclease activity. Some phage genomes acquired a methyltransferase to protect their genome from digestion. The constant competition between bacteria and bacteriophages resulted in the evolution of a whole range of R-M systems with different DNA sequence specificities. Often one bacterial strain has more than one R-M system, for example *Neisseria gonorrheae* has as many as 14 R-M systems (Stein et al., 1995). Usually R-M systems are not essential for normal growth of bacteria, because the mutation in them does not give rise to a phenotype. This suggests that the main advantage of R-M systems is in natural settings, where the organism is subjected to pathogen induced competition.

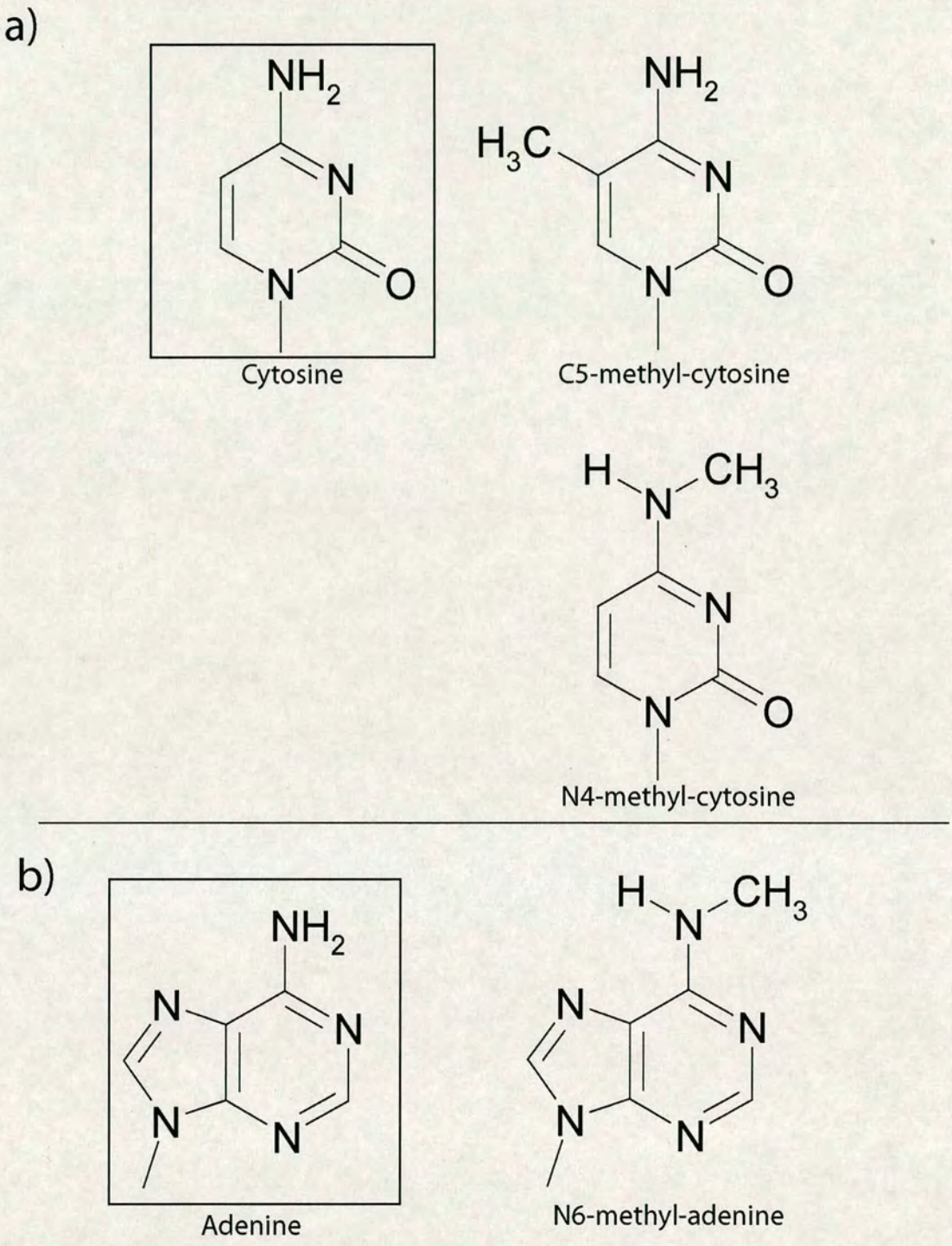

Figure 1-1. Biologically acquired DNA modifications found in living organisms. a) The common base cytosine is shown in the square. Cytosine can be modified by DNA methyltransferases, which add a methyl group to the cyclic carbon on position 5 or exocyclic nitrogen 4. b) The adenine is shown in the box. Methylation of adenine occurs only at exocyclic nitrogen 6.

Another described biological function of DNA methylation in bacteria is in mismatch repair. Because cytosine methylation occurs after replication, there is a period when the parental strand of the DNA double helix is methylated and the newly synthesized strand is un-methylated, resulting in the hemi-methylated DNA. If there were any mismatch errors made during replication, methylation mark help to distinguish the parental strand hence the mutated daughter strand could be repaired. For that purpose *E. coli* has DAM methyltransferase which methylates adenine in the sequence context GATC at most places in the genome (Palmer and Marinus, 1994). The deletion of DAM methyltransferase is, therefore, associated with an increased mutability phenotype (Bale et al., 1979). Additionally, it has been reported that DAM methylation is important for replication initiation and regulation of expression of several genes.

1.2.3. 5-methyl cytosine in different eukaryotes

In eukaryotes, DNA methylation is common but limited to 5-methyl cytosine. There are some species without detectable DNA methylation (such as yeast *Saccaromyces cerevisiae, Schizosaccharomyces pombe*, worm *Caenorhabditis elegans*), however there is no known vertebrate or plant genome that does not contain DNA methylation.

Insects have variable levels of DNA methylation which ranges from 0 – 10% of total cytosines methylated (Field et al., 2004). In the widely used model organism fruit-fly, *Drosophila melanogaster,* it has been challenging to find any methylation. However recent studies suggest that *D. melanogaster* embryos have 0.4% methylation which drops sharply to approximately 0.1% in the larval stage and then gradually decreases to less than 0.1% in adults (Lyko et al., 2000; Lyko, 2001). Bisulfite sequencing determined that in fruit-flies genomic methylation is most common in CpA and CpG dinucleotide sequences. In the cabbage moth, *Mamestra brassicae,* overall DNA methylation has been reported to be very high, reaching approximately 9% in larvae and adults. Restriction digestion with methyl sensitive enzymes determined that part of the moth's genome has CpG methylation, however,

CpG methylation was absent in several transposons and ribosomal repeats, which are often methylated in plants and vertebrates (Mandrioli and Volpi, 2003). Yet more detailed bisulfite sequencing analysis is required to investigate the possibility of non CpG methylation in the repeats.

In plant genomes in addition to frequently methylated cytosine in CpG context, there is a significant presence of symmetric methylation in CNG and asymmetric methylation in CNN sequences (Tariq and Paszkowski, 2004). It is now well described, that methylation in plants is required for silencing of transposons and viruses, regulation of imprinted genes and is essential for normal development (Tariq and Paszkowski, 2004). Mutant *Arabidopsis thaliana* plants lacking approximately 25 - 50% of methylation (met1-1 and met1-2 alleles), display late flowering and loss of gene silencing (Ronemus et al., 1996; Finnegan et al., 1996; Kankel et al., 2003). Other mutants that get rid of almost all CpG methylation are not viable (Saze et al., 2003).

The fungus, *Neurospora crassa,* has evolved different methylation patterns. Most of the cytosines in the *Neurospora* genome are unmethylated. The methylated cytosines are found in sequences which have been subjected to repeat induced point mutations (RIP) (Singer et al., 1995). Surprisingly, mutation of the methyltransferase DIM-2, which causes genome wide demethylation, does not display any obvious phenotype (Kouzminova and Selker, 2001).

In humans, methylated cytosine represents ~ 1% of the genome and is mainly observed in the context of CpG dinucleotides. Initially it was thought that cytosine methylation is present exclusively at CpG residues, however several recent studies show the presence of CpA and CpT methylation but at a much lower frequency (Ramsahoye et al., 2000; Haines et al., 2001; Dodge et al., 2002; White et al., 2002). In mammalian cells, methylated DNA is dispersed through out the genome with the majority of methylated CpGs located in transcribed regions and intergenic DNA. Exceptions to these observations are CpG islands, which are mostly unmethylated. CpG islands are defined as 1-2 kb CG rich regions (60-70%), which are found at the promoter regions of about 60% of RNA polymerase II transcribed genes (Antequera and Bird, 1993; Waterston et al., 2002).

In mammals, DNA methylation has been reported to play an important role in development, imprinting, X-chromosome inactivation, DNA mutability and cancers (Bird and Wolffe, 1999; Laird, 2003; Jaenisch and Bird, 2003; Li, 2002; Jones, 2002; Prokhortchouk and Hendrich, 2002). Numerous studies have shown that promoter methylation often correlates with silencing of a gene (Makar et al., 2003; Issa et al., 1994; Issa et al., 1996), however, not every silenced gene is methylated. There are several examples of tissue specific genes that are silenced and un-methylated (Bird, 2002).

There are several theories addressing the evolution of DNA methylation. One argues that the primary function of DNA methylation is to silence transposons and viral elements, serving as a defence against damage caused by intracellular parasites (Jahner et al., 1982; Bestor, 1990). Another theory says that silencing of repeat sequences evolved as a secondary mechanism in vertebrates, when genomes became large suggesting the primary function of DNA methylation is silencing of transcriptional noise (Bird and Tweedie, 1995).

1.2.4. Biological functions in mammals related to DNA methylation

DNA methylation is involved in a variety of biological functions, many of them involving gene silencing. As mentioned before these include genomic imprinting, X-chromosome inactivation, tumorigenesis and genome stability.

Imprinting is a common mechanism of gene dosage management and it is present from plants to humans. Genomic imprinting occurs when one parental allele is expressed and another is silenced. The role of DNA methylation in imprinting was noted with the finding that as well as parental specific gene expression patterns, there are parental specific heritable methylation patterns (Li et al., 1993). These parental origin specific methylation marks were termed imprinting control regions (ICR). One of the suggested models of how ICR works is through binding of the CTCF insulator protein, which has a reduced affinity to methylated sites. It has been demonstrated that in the *H19/Igf2* locus CTCF blocks the enhancer from activating the *Igf2* promoter. At the paternal locus, CTCF is unable to bind methylated sites and thus

can not block the enhancer, permitting *Igf2* activation (Hark et al., 2000; Bell and Felsenfeld, 2000; Kanduri et al., 2000). Another model proposes that antisense RNA transcription is necessary for the establishment of imprinting and later the methylation is required for propagation of stable silencing (Constancia et al., 1998). A good example for antisense RNA involvement is the *Igf2r* gene, whose imprinting is lost when the promoter of the antisense RNA is deleted (Lerchner and Barlow, 1997).

X chromosome inactivation has many similarities to imprinting (discussed in (Lee, 2003)). It has endured as a way of solving the gene dosage problem in mammals, where almost the whole of one X chromosome is inactivated in females. In humans, the X-chromosome is inactivated randomly both in the embryonic and extra-embryonic tissue, but in mice extra-embryonic tissue has imprinted paternal X chromosome inactivation, whereas the embryo has a random X chromosome inactivation. One of the important events in X chromosome inactivation is DNA methylation of CpG islands on inactive chromosome and of the *Xist* gene on the active X. *Xist* is a non-coding RNA essential for proper X-inactivation (reviewed in (Brockdorff, 2002)).

Numerous studies have shown that cancer cells have altered DNA methylation profiles. Global hypomethylation and some local CpG island hypermethylation are often observed in cancer cells (Baylin and Herman, 2000; Plass, 2002). It is widely argued whether altered methylation profiles are the cause or consequence of tumorigenesis, but it is commonly agreed that DNA methylation plays a significant role in cancer. The genetic link between DNA methylation and development of cancer was demonstrated in mice with DNA methyltransferase 1 (*Dnmt1*) hypomorphic allele, which results the reduced level of DNA methylation (~10%). These mice were shown to develop aggressive T cell lymphomas (Gaudet et al., 2003; Eden et al., 2003).

In mouse development, global DNA methylation has been shown to change dynamically. The paternal genome is actively de-methylated within hours after fertilization, before any DNA replication. The maternal genome is de-methylated later by a passive mechanism. Both genomes are methylated again before

implantation. A second wave of de-methylation occurs in primordial germ cells until E13 - E14, which is later followed by *de novo* methylation during gametogenesis (Reik et al., 2001).

One potentially dangerous "side effect" of DNA methylation is its increased susceptibility to mutation. After spontaneous deamination, un-methylated cytosine becomes uracil, which is not a DNA base, and therefore can be easily distinguished by the DNA repair machinery and removed. However deamination of methylated cytosine leads to thymine, which is a common base in DNA. The resulting G:T mismatch can be repaired to G:C, which would result in correction, or replicated causing G:C and A:T strands one of which (A:T) would have a mutation. Because DNA methylation in mammals is primarily found in the CpG dinucleotide context, mammalian genomes become depleted in CpG sequences, leaving the majority of CpGs in the unmethylated promoter regions, which are called CpG islands (Cooper et al., 1983). As predicted (Cooper and Youssoufian, 1988), the remaining methylated CpG's in the genome are hot spots for disease causing point mutations. For example the majority of *MECP2* point mutations in humans are in CpG to TpG transitions.

1.2.5. Understanding DNA methylation through investigation of DNA methyltransferases

There are four known DNA methyltransferases in mammals falling into three distinct families: DNMT1, DNMT2 and DNMT3. Clear evidence exist that DNMT1 and two members of DNMT3 family (DNMT3A and DNMT3B) are active methyltransferases. DNMT2 has all ten methyltransferase motifs and is conserved in different mammals, insects and even yeast, but so far detection of any methyltransferase activity has been challenging *in vitro* or *in vivo* (Dong et al., 2001; Okano et al., 1998b; Hermann et al., 2003). Only recently, several independent reports showed, that overexpression of DNMT2 in flies increases genomic methylation levels at CpA and CpT sites, suggesting that DNMT2 is capable of methylating the genome (Kunert et al., 2003; Mund et al., 2004; Tang et al., 2003).

The first methyltransferase to be cloned and characterized was DNA methyltransferase 1 (DNMT1) (Bestor, 1988). DNMT1 shows a strong preference (5 to 30 fold) for hemimethylated DNA as a substrate, therefore it has been suggested that its main role is to maintain DNA methylation patterns after replication of DNA (Yoder et al., 1997). Further evidence supporting this role of DNMT1 together with a mechanistic insight, was demonstrated by the interaction of DNMT1 with PCNA, which is major DNA replication protein found at the replication fork (Iida et al., 2002). The enzymatic activity of DNMT1 on hemimethylated substrate was also enhanced by the presence of PCNA, suggesting that PCNA is responsible for keeping and stimulating DNMT1 activity during replication, when daughter strand is being methylated. Other studies have also demonstrated DNMT1 co-purification with replication activity (Vertino et al., 2002). In mouse fibroblasts, Dnmt1 co-localises with replication foci in S-phase (Leonhardt et al., 1992; Bestor, 2000). These and other studies established a model that after semi-conservative DNA replication, when DNA becomes hemimethylated, DNMT1 methylates the daughter strand. Therefore the replication machinery, via protein-protein interactions, keeps DNMT1 in close proximity to perform this.

A great deal of insight into the role of DNA methylation in mammals has come from *Dnmt1* knock-out experiments in mice. *Dnmt1* knock-outs in embryonic stem (ES) cells were viable and resulted in a loss of about one third of the total methylation (Li et al., 1992). These ES cells were used to generate *Dnmt1* deficient mice, which were developmentally delayed and died around mid-gestation (Li et al., 1992). Additionally, DNA methylation loss resulted in the reactivation of imprinted silent paternal allele of *H19* gene and repression of maternally expressed *Igf2r* and paternally expressed *Igf2* (Li et al., 1993). These findings confirmed the importance of DNA methylation in imprinting.

Previously it has been shown that in a female mouse the *Xist* gene on the active X chromosome is silent and methylated, whereas it is active and unmethylated on the inactive X (Brown et al., 1991b; Brown et al., 1991a). In males, the *Xist* gene promoter is always methylated and silent. Evidence that methylation is an important component of *Xist* regulation came again from the *Dnmt1*-null embryos. *Xist*

becomes demethylated and reactivated in the male X chromosome in *Dnmt1*-null embryos, but in ES cells, *Xist* expression is not affected (Beard et al., 1995).

An elevated gene mutation rate was demonstrated when *Hprt* and *HSV-Tk* transgenes were introduced in *Dnmt1* deficient ES cells (Chen et al., 1998). Most of the mutations were found to be recombination derived, rather then point mutations, suggesting a role for methylation in genome stability. In contrast other group have observed reduced HSV-TKNeo transgene loss in ES cells lacking DNMT1 (Chan et al., 2001). The discrepancy between these results was explained by the possibility that different mechanisms may act at different chromosomal loci.

Mouse oocytes and preimplantation embryos have an isoform of Dnmt1 lacking N-terminal 118 amino acids (Dnmt1o) (Mertineit et al., 1998). Specific *Dnmt1o* knock-out mice were apparently normal if the parents were heterozygous for the mutant allele. However, null females were infertile, resulting in embryonic death of offspring at day E14 - 21 of gestation. Global methylation patterns were not affected, but imprinted genes *h19* and *Snrpn* were abnormally expressed from both paternal and maternal alleles (Howell et al., 2001). It has been suggested that Dnmt1o is required for faithful maintenance of certain imprints in early development, when there is no Dnmt1 present in the nucleus.

Dnmt3 family members were identified by sequence homology to bacterial DNA methyltransferases. *Dnmt3a* and *Dnmt3b* mRNA were found to be highly abundant in ES cells, suggesting that they might be responsible for the residual DNA methylation present in *Dnmt1*-null ES cells (Okano et al., 1998a). Just like *Dnmt1*-nulls, *Dnmt3a* and *Dnmt3b* single and double null ES cells were shown to be viable (Okano et al., 1999). *Dnmt3a*-null mice were born alive, but runted and died at 4 weeks of age. *Dnmt3b* mutation in mice were embryonic lethal with abnormalities starting at E9.5 (Okano et al., 1999). *De novo* methylation activity was tested by infecting mutant ES cells with recombinant retrovirus, which in *wt* (or *Dnmt1*-null) cells becomes silenced by DNA methylation. The retrovirus was methylated in single *Dnmt3a* or *Dnmt3b* nulls, but failed to become methylated in double nulls (Okano et al., 1999). *De novo* methylation is a slow event – it takes 8 days for the retrovirus to become methylated. Prolonged (up to 5 months) culturing of *Dnmt3a* or *Dnmt3b*

double null ES cells leads to the loss of methylation from repeats and some single copy genes. Re-introducing either *Dnmt3a* or *Dnmt3b* methyltransferase restores the methylation profile, but overexpression of *Dnmt1* does not (Chen et al., 2003a). These experiments provided a clear distinction between the role of Dnmt1 and Dnmt3 families of methyltransferases. Recently, cre-lox mediated knock-outs in primordial germ cells demonstrated that Dnmt3a plays an important role in establishing paternal and maternal imprints (Kaneda et al., 2004). Interestingly, a similar loss of imprint phenotype is caused by *Dnmt3L* knock-out (Bourc'his et al., 2001). The *Dnmt3L* gene does not encode a functional methyltransferase (although it is similar to other methyltransferases, it lacks important catalytic motifs), therefore its function is likely to be related with the recruitment of a functional methyltransferase.

Mutations in the *de novo* DNA methyltransferase *DNMT3B* result in a rare disorder called ICF (immunodeficiency centromere instability and facial abnormalities) syndrome (Wijmenga et al., 1998). The typical symptoms are immunodeficiency, instability of pericentromeric heterochromatin, facial abnormalities and mental retardation (Hendrich and Bickmore, 2001). Interestingly in ICF patients methylation is lost in satellite DNA and few non-satellite repeats, suggesting that DNMT3B might act at specific loci (Kondo et al., 2000).

1.2.6. Interplay between DNA methylation and histone modifications

In addition to DNA modification, which is limited only to 5-methyl-cytosine, there are many known histone modifications. Arginine can be mono or dimethylated, lysine can be mono-, di- or tri-methylated, acetylated, ubiquitylated and SUMOylated, serine and threonine can be phosphorylated (reviewed in (Fischle et al., 2003)). It has been demonstrated, that not only does type of modification matter for the biological role, but also the position of the modified amino acid. A good illustration for this statement is the methylation of lysine 4 or 9 on the histone H3 tail. Lysine 4 methylation correlates well with actively transcribed chromatin, whereas lysine 9 methylation is a mark for silent heterochromatin (Litt et al., 2001).

Data from fungi and plants suggests that crosstalk occurs between the DNA methylation and histone modifications. In the fungus, the *Neurospora crassa* mutation dim-5 causes loss of DNA methylation. Surprisingly, dim-5 mutation was identified in Set domain protein, which *in vitro* methylates H3 lysine 9 (Tamaru and Selker, 2001). In the plant *Arabidobsis thaliana,* mutation in the H3 lysine 9 methyltransferase KRYPTONITE leads to loss of cytosine methylation in CpNpG sites (Jackson et al., 2002; Malagnac et al., 2002). These findings suggest that in fungi and plants H3 lysine 9 methylation is required for DNA methylation. Subsequently, evidence that DNA methylation is required for H3 lysine 9 methylation was demonstrated. In *Dnmt1* null plants, which lack CpG methylation loss of H3 lysine 9 methylation was demonstrated (Tariq et al., 2003). In mouse ES cells, knock-out of H3 lysine 9 methyltransferase Suv39h leads to a decrease in methylation at pericentric satellite repeats. However H3 lysine 9 methylation in pericentric heterochromatin is not perturbed in *Dnmt1*-null or *Dnmt3a* and *Dnmt3b* double null cells, suggesting that histone methylation guides DNA methylation at satellite DNA (Lehnertz et al., 2003). The suggested mechanism for the crosstalk between DNA and histone methylation may involve direct interaction of Dnmt3b with HP1 alpha (which binds to methylated H3 lysine 9), which in turn interacts with Suv39h histone methyltransferase (Lehnertz et al., 2003).

1.3. Methyl CpG binding proteins

The methylation mark is postulated to act by two mechanisms. The first is by directly preventing binding of DNA binding proteins like Ets1 (Ets-1) or CTCF (Maier et al., 2003; Bell and Felsenfeld, 2000), which demonstrate restricted binding to methylated sequences, but bind to the same sequence when it is unmethylated. The second mechanism involves a group of proteins which bind the methylated CpG sequence. Currently there are four known proteins that bind methylated CpG independent of its sequence context: MeCP2, MBD1, MBD2 and MBD4 (Figure 1-2). Kaiso is the fifth protein binding methylated DNA, however it requires at least two symmetrically methylated CpGs in a context dependent manner (Prokhortchouk et al., 2001).

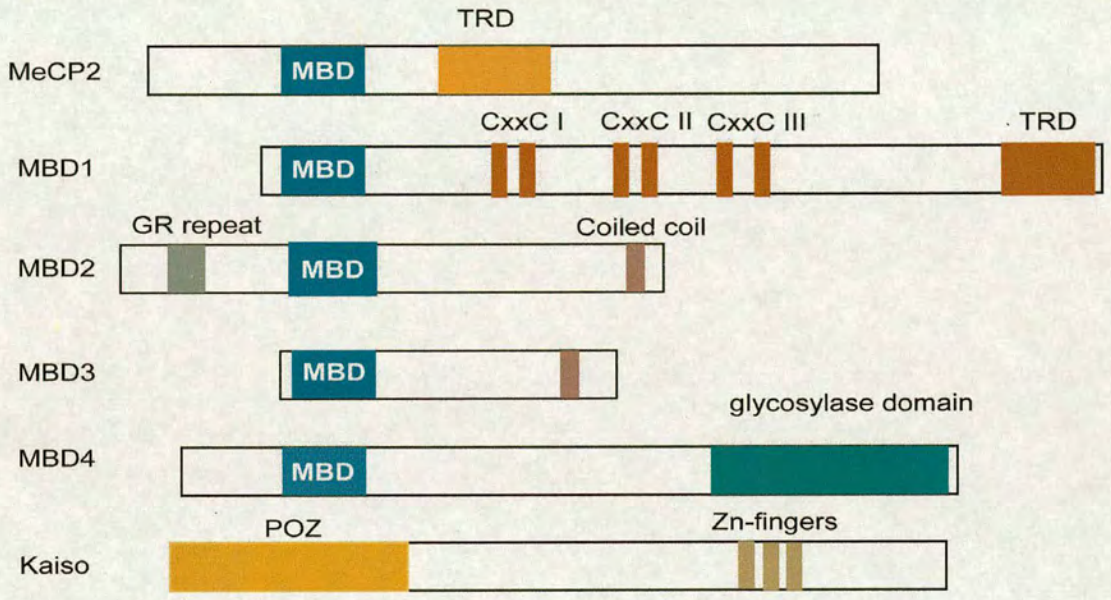

Figure 1-2. Methyl-CpG binding proteins. MeCP2, MBD1, MBD2, MBD3 and MBD4 have homologous domains (MBD) for recognising methyl-CpG dinucleotide. Kaiso uses zinc fingers to recognise at least two methylated CpGs. MeCP2 and MBD1 have transcriptional repression domains (TRD), which have been shown to be required for transcriptional repression. CxxC III domain in MBD1 binds non methylated CpGs. MBD3 is the part of Mi-2/NuRD repressor complex, which interacts with MBD2. MBD4 is a DNA T:G mismatch glycosylase.

The first cloned methyl-CpG binding protein was MeCP2 (Lewis et al., 1992). After narrowing down a region of MeCP2 responsible for binding to methylated CpG (MBD domain), the search for homologous MBD domains revealed another four genes, which were assigned to the MBD family – *Mbd1*, *Mbd2*, *Mbd3* and *Mbd4* (Hendrich and Bird, 1998). Mbd1, Mbd2 and Mbd3 have been described as transcriptional repressors, whereas Mbd4 is a DNA glycosylase. Mbd1 is the largest family member, which has several alternative splicing isoforms (Hendrich and Bird, 1998; Fujita et al., 1999; Jorgensen et al., 2004) and represses transcription when fused to Gal-4 DNA binding domain (Ng et al., 2000). Different approaches have identified MBD1 interacting proteins such as histone methyltransferase Suv39h1 and chromatin assembly factor MCAF (Fujita et al., 2003b; Fujita et al., 2003a), which are suggested to act as a transcriptional co-repressors for MBD1. Mice lacking *Mbd1* are viable and look normal. However, behavioural tests revealed spatial learning difficulties in *Mbd1* nulls, which could be explained by reduced forebrain weight and cell density in dentate gyrus (Zhao et al., 2003). Adult neural stem cells derived from null mice show increased expression of IAP and increased genomic instability (Zhao et al., 2003). Recently, another DNA binding domain was identified in Mbd1. The CxxC III domain was noticed to be similar to one found in CpG binding protein, which binds non-methylated CpG (Fisscher et al., 1996). Electrophoretic mobility shift experiments, together with localisation studies in DNA methylation deficient cells, demonstrated that MBD1 binds non-methylated CpGs via its CxxC III domain (Jorgensen et al., 2004). Interestingly, CxxC III mediated MBD1 binding to non methylated promoters also leads to transcriptional repression (Jorgensen et al., 2004). This finding makes understanding of MBD1 function difficult and further experiments are required to investigate MBD1 binding sites in the genome and potential target genes.

MBD2 and MBD3 are similar proteins (~70% homology), which are suggested to have evolved from a single common MBD2/3 ancestral form (Hendrich and Tweedie, 2003). The mammalian form of MBD2 binds methylated DNA, but MBD3 does not (Hendrich and Bird, 1998). Frogs have two forms of MBD3, one of which

binds methyl-CpG and another which does not (Wade et al., 1999). MBD3 is the integral part of Mi2/NuRD histone deacetylation and nucleosome remodelling complex (Wade et al., 1999; Zhang et al., 1999). In addition MBD2 was found to co-purify with the NuRD complex (Feng and Zhang, 2001). MBD2-NuRD complex was previously seen in the methyl-CpG specific electrophoresis mobility shift and was called MeCP1 (Meehan et al., 1989). Therefore biochemical experiments suggest that MBD2 recruits NuRD for transcriptional repression. The biological role of *Mbd2* and *Mbd3* genes was investigated by knock-out experiments. *Mbd3*-null mice are not viable and display multiple abnormalities at day E8.5 (Hendrich et al., 2001). *Mbd2*-null mice are viable, look normal, but have impaired maternal behaviour (Hendrich et al., 2001). The analysis of helper T cells lacking *Mbd2* revealed defects in differentiation, and demonstrated that *Il-4* is a target gene for MBD2 repression (Hutchins et al., 2002). Another phenotype of *Mbd2* deficiency was noticed when the *Mbd2*-null mouse was crossed to the Min mouse, which has a mutation in one of the *Apc* alleles and is prone to intestinal tumours (Sansom et al., 2003). Min mice develop tumours and die around 8 months old. Interestingly, *Mbd2* deficient Min mice, developed only few tumours and most of them survived longer than a year (Sansom et al., 2003). The observation is similar to that seen in the mice with reduced levels of DNA methylation (*Dnmt1* heterozygous mice fed with 5-aza-deoxycytidine), although, the molecular basis of the tumour suppression mechanism is not clear (Laird et al., 1995). Further determination of MBD2 target genes could help to understand the link between MBD2 and cancer.

MBD4, in addition to methyl-CpG binding domain, has a glycosylase domain (Figure 1-2), which was shown be a functional T:G mismatch glycosylase (Hendrich and Bird, 1998; Petronzelli et al., 2000). Because T:G mismatches frequently arise from deamination of methyl-cytosine (as described in 1.2.4), it has been proposed that MBD4 activity could help to repair them. *In vivo* experimental evidence to support this hypothesis was acquired, when mice lacking *Mbd4* were crossed with "Big Blue" reporter mice, which has λ-phage genome transgene (Millar et al., 2002). The λ-phage transgene can be recovered from the mouse genome and used as a readout for mutations. *Mbd4*-null mice were shown to have approximately 3 times increased C to T transition rate (Millar et al., 2002). At the moment, the role of the

MBD in MBD4 has not been demonstrated. The simple explanation is that MBD targets MBD4 to sites, which are highly methylated, and therefore have the biggest probability of deamination occurring. However, there is a lack of experimental data yet to support this hypothesis.

Kaiso was purified following its ability to shift methylated probe from CSML-0 adenocarcinoma cell line (Prokhortchouk et al., 2001). Unlike MBD family members, Kaiso uses a zinc finger domain to bind DNA and requires at least two methylated CpG's (Prokhortchouk et al., 2001). Interestingly, in addition to methylated CpGs, Kaiso can bind to specific non-methylated sequences (Daniel et al., 2002). In human cells Kaiso was shown to co-purify with N-CoR complex and repress transcription from the *MTA2* gene promoter in a methylation dependent manner (Yoon et al., 2003).

1.4. MeCP2

1.4.1. MeCP2 specific binding to methylated CpGs

The first described methyl-CpG binding activity was MeCP1, which was discovered in crude nuclear extracts by its ability to bind a methylated DNA probe containing 12 or more methylated CpG's (Meehan et al., 1989). Later MeCP2 was purified as an 80 kDa protein that binds a single methylated CpG in South-Western assays (Lewis et al., 1992). In mouse cells MeCP2 localises to pericentromeric heterochromatin, which comprises mainly highly methylated satellite DNA (Nan et al., 1996). The methyl-CpG binding domain (MBD) in MeCP2 was mapped by the construction of deletion mutants, and was found to be located in the N-terminal region of the protein. DNase I *in vitro* footprinting indicated that the MBD from MeCP2 can protect a 12 nucleotide region surrounding a methyl-CpG site, and has an approximate dissociation constant of 10^{-9} M. Bandshift experiments have shown, that symmetrically methylated CpG is required for binding, with no noticeable affinity for hemimethylated DNA (Nan et al., 1993). A recent study suggested that *in vitro* MeCP2 binds oligonucleosome arrays and compacts the chromatin (Georgel et al., 2003). However the results are very ambiguous, because non-methylated DNA was

used in the study, ignoring all previous experimental evidence that shows preferential MeCP2 binding to methylated DNA.

It was suggested that MeCP2 can bind methylated CpG's without major impediment from a nucleosome surface (Chandler et al., 1999). This finding was supported by solving the structure of the MBD (from MBD1) in complex with DNA (Ohki et al., 2001). Methyl groups in the CpG dinucleotide point to the major groove. Therefore the MBD utilises the DNA major groove as an access surface (Figure 1-3). The way MBD faces DNA and has limited contacts with DNA suggested that access to methyl-CpG sites should not interfere with nucleosome – DNA binding (Ohki et al., 2001).

Several regions were examined for the presence of MeCP2 using the chromatin immunoprecipitation (ChIP) technique. Results clearly indicate that MeCP2 is bound to methylated DNA *in vivo*. Some targets include: the maternally methylated U2af1-rs1 differentially methylated region (DMR) in mouse liver, the methylated *H19* DMR in cultured mouse cells, the silent and methylated MT-I promoter, the *NaCh II* promoter in Rat-1 cells, methylated p14(ARF)/p16(INK4A) CpG islands in human cancer cells and others (Fournier et al., 2002; Fuks et al., 2003; Ghoshal et al., 2002; Koizume et al., 2002; Lunyak et al., 2002; El Osta et al., 2002; Nguyen et al., 2001). Recently, MeCP2 was found to bind the brain derived neurotrophic factor *(Bdnf)* promoter in cultured mouse and rat neurons (Chen et al., 2003b; Martinowich et al., 2003). Interestingly, after treating neuronal cultures with KCl (which induces Ca^{2+} influx), MeCP2 was shown to become phosphorylated and subsequently leave the *Bdnf* promoter. South - Western analysis suggested that the phosphorylated version of MeCP2 may have lost its methylated DNA binding affinity. Surprisingly, KCl treatment does not displace MeCP2 from the *H19* gene, even when around half of MeCP2 is phosphorylated (Chen et al., 2003b).

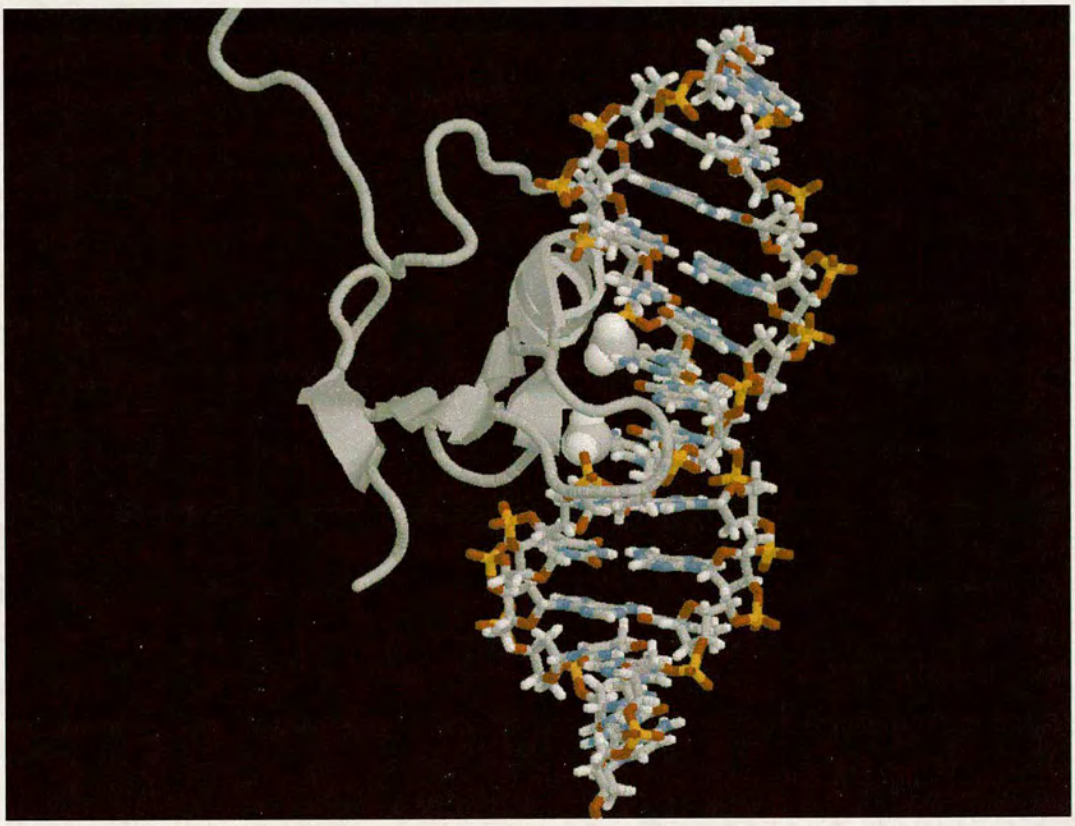

Figure 1-3. Representative structure of MBD (from MBD1) in complex with DNA. Methyl groups are displayed as space-filling balls and are pointing towards the major groove of double DNA helix. MBD accesses and specifically recognises methyl groups from the major groove side. Because the MBD does not interfere with the other DNA side which could be a binding surface for histones, it has been suggested that an MBD could bind DNA on the nucleosome surface (Ohki et al., 2001).

Previously, MeCP2 was seen as a static transcriptional repressor that binds methylated genes and ensures proper silencing. Discovery of MeCP2 involvement in *Bdnf* regulation suggested that there might be dual MeCP2 roles. The dynamic, phosphorylation mediated, MeCP2 role could be on inducible promoters (example *Bdnf* promoter III), when after a signal MeCP2 leaves the promoter. The "static" MeCP2 could be responsible for constant silencing of permanently silent regions of a genome (example *H19* DMR). Another possible explanation of the dynamic MeCP2 association and dissociation could be the appearance or disappearance of the methylation at a given locus. Therefore release of MeCP2 from *Bdnf* promoter III might be explained not only by phosphorylation, but also by a decrease in methylation after induction with KCl (Martinowich et al., 2003).

The above mentioned studies strongly suggest that MeCP2 binds the methylated CpGs and that the MBD is responsible for recruiting it to methylated DNA in various cell lines and some tissues.

1.4.2. MeCP2 as transcriptional repressor

Many genes are shown to be silent when the promoter is, or becomes, methylated. Therefore, MeCP2 was initially hypothesized to be a transcriptional repressor. Transient transfection studies using reporter gene under the control of a methylated promoter show that MeCP2 is able to repress transcription both in cells and *in vitro* (Meehan et al., 1992; Nan et al., 1997). MeCP2 repression properties were investigated by monitoring reporter gene (β-gal) expression, using a GAL4 fusion with various parts of the *Mecp2* gene (Nan et al., 1997). A 100 amino acid region in the middle of the protein was mapped as a minimal region which is able to repress transcription (TRD). GAL4-MeCP2 and MeCP2 on its own were shown to repress transcription up to 2 kb from the transcription initiation site (Nan et al., 1997).

Initial GST-MeCP2 "pull downs" from HeLa nuclear extracts and partial MeCP2 complex purification from *Xenopus laevis* oocytes, suggest that MeCP2 is found in a stable complex with a co-repressor mSin3A/HDAC1,2 (Nan et al., 1998; Jones et al., 1998). However, later MeCP2 purification from rat brain and different other sources

demonstrated that MeCP2 does not exist in a stable complex with any other proteins (Klose and Bird, 2004). Therefore, it is likely that mSin3A co-repressor complex is recruited to the target genes only. Treating cells with the HDAC inhibitor TSA partially relieves MeCP2 mediated repression, supporting HDAC involvement in transcriptional repression (Nan et al., 1998; Jones et al., 1998). Different approaches identified other interacting proteins including the transcription factor TFIIB, proto oncogene c-ski, DNA methyltransferase DNMT1, histone methyltransferase Suv39H1, transcription factor PU.1 and nuclear co-repressor NcoR (Lunyak et al., 2002; Kaludov and Wolffe, 2000; Kimura and Shiota, 2003; Kokura et al., 2001; Fuks et al., 2003; Suzuki et al., 2003; Rietveld et al., 2002). The *in vivo* occurrence and significance of later interactions is not yet clear, however, it may represent different ways by which MeCP2 is involved in regulating different genes. The biological importance of the interaction between MeCP2 and Sin3A/HDAC and SMRT co-repressor complexes was elegantly demonstrated in *Xenopus* (Stancheva et al., 2003). Antisense morpholino - mediated translational MeCP2 knock-out demonstrates developmental arrest, which could subsequently be rescued by injection of *wt* mRNA. Identification of target genes downstream of the *Delta/Notch* signalling cascade suggested potential co-repressors which are involved in silencing *Hairy/Enhancer of Split* genes. Interactions with Sin3A and SMRT co-repressors were demonstrated by reciprocal GST pull-downs. Finally, chromatin IP confirmed that both MeCP2 and SMRT are displaced from the *Hairy2a* promoter after activation with the Notch intracellular domain (Stancheva et al., 2003). This study provided the first molecular example of the function of MeCP2 in the endogenous gene repression *in vivo*. The second example is the *Bdnf* gene, which is up to 2 fold up-regulated in neuronal cultures established from *Mecp2*-null mouse (Chen et al., 2003b). Similarly to *Hairy2a* gene promoter, MeCP2, Sin3a and HDAC1 are found on the promoter III of *Bdnf* and all together leave the promoter after *Bdnf* is induced by KCl (Martinowich et al., 2003). Interestingly, the disappearance of the repressor complex is accompanied by changes in the chromatin structure with a reduction of H3 lysine 9 di-methylation and an increase in H3 lysine 4 di-methylation and H4 acetylation (Martinowich et al., 2003).

1.5. Rett syndrome

Rett syndrome is a frequent form of mental retardation and occurs sporadically once every 10 000 – 22 000 female births. A typical Rett syndrome case is characterised by a period of normal development until around 1 year, followed by a rapid regression including loss of acquired speech and motor skills, microcephaly, seizures, autism, ataxia, intermittent hyperventilation and stereotypic hand movements (Armstrong, 2002; Glaze, 2002; Hagberg, 2002; Jellinger, 2003; Kerr, 2002; Segawa, 2001). Classical Rett syndrome progression after the period of normal development was divided into four stages:

I. **Onset** of the disease is characterised by reduced head grow, reduced communication and hypotonia. It often happens between 6 – 18 months and girls at that time do not display any other abnormalities.

II. **Rapid regression** occurs at 1 to 4 years of age and is characterised by the further loss of communication, loss hand skills and appearance of typical hand wringing, loss of language, irritability, the first signs of mental retardation and possibly seizures.

III. At the **pseudo-stationary** phase girls have developed severe mental retardation, ataxia, persistence of seizures, irregular breathing, typical hand movements, teeth grinding, hyperventilation and early scoliosis. This stage is usually apparent at preschool age and can continue for years.

IV. The **late motor deterioration** stage is characterised by progressive scoliosis, wheelchair dependence, tropic disturbance, but with fewer seizures and improved communication.

After the initial regression symptoms stabilise, patients often survive into adulthood. Apart from "classical" Rett syndrome there are some variations. Girls having "preserved speech" variant are able to speak, "*formes frustes*" has a longer period of normal development and "congenital onset" have no period of normal development.

Several recent studies showed that after the initial symptom onset period there is no further regression, suggesting a non-degenerative nature of the disease (Cass et al., 2003; Armstrong, 2002). Some of the best described neuropathological features of Rett syndrome are the reduced brain size and reduced dendritic branching (Armstrong, 2001). In nine different age Rett syndrome girls brain size was found decreased to 66% - 88% of expected values (Jellinger et al., 1988). The sizes of individual neurons and dendritic trees were found reduced in different areas of the cortex (Bauman et al., 1995; Armstrong, 1995). EEG is clearly abnormal and abnormalities are most prominent at disease stages II and III (Dunn and MacLeod, 2001).

A familial Rett syndrome case allowed mapping of the disease to the region Xq28 (Amir et al., 1999). Screening candidate genes in the region identified *MECP2* gene mutations as a frequent event in Rett patients (Amir et al., 1999). Later, numerous mutation screenings confirmed that approximately 80% of Rett syndrome cases are caused by mutation in the *MECP2* gene.

Rett syndrome causing mutations are a valuable tool for the highlighting the important regions of MeCP2 (Figure 1-4). Numerous laboratories initiated screens and a lot of information about the mutations become scattered in the different publications and unpublished reports. Brian Hendrich and the author of this thesis have established the first freely available Rett syndrome mutation database on the Internet (http://homepages.ed.ac.uk/~skirmis/ which was later transferred to http://www.mecp2.org.uk) to concentrate data available in different sources.

The distribution of *MECP2* point mutations causing Rett syndrome, together with homology between different species suggested that apart from conserved and frequently mutated MBD and TRD domains, there is conserved C-terminal domain (Figure 1-4). Moreover, there are Rett syndrome causing point mutations which are at the very C-terminal end. This shows that C-terminal domain is important for the MeCP2 function, which have no molecular explanation yet.

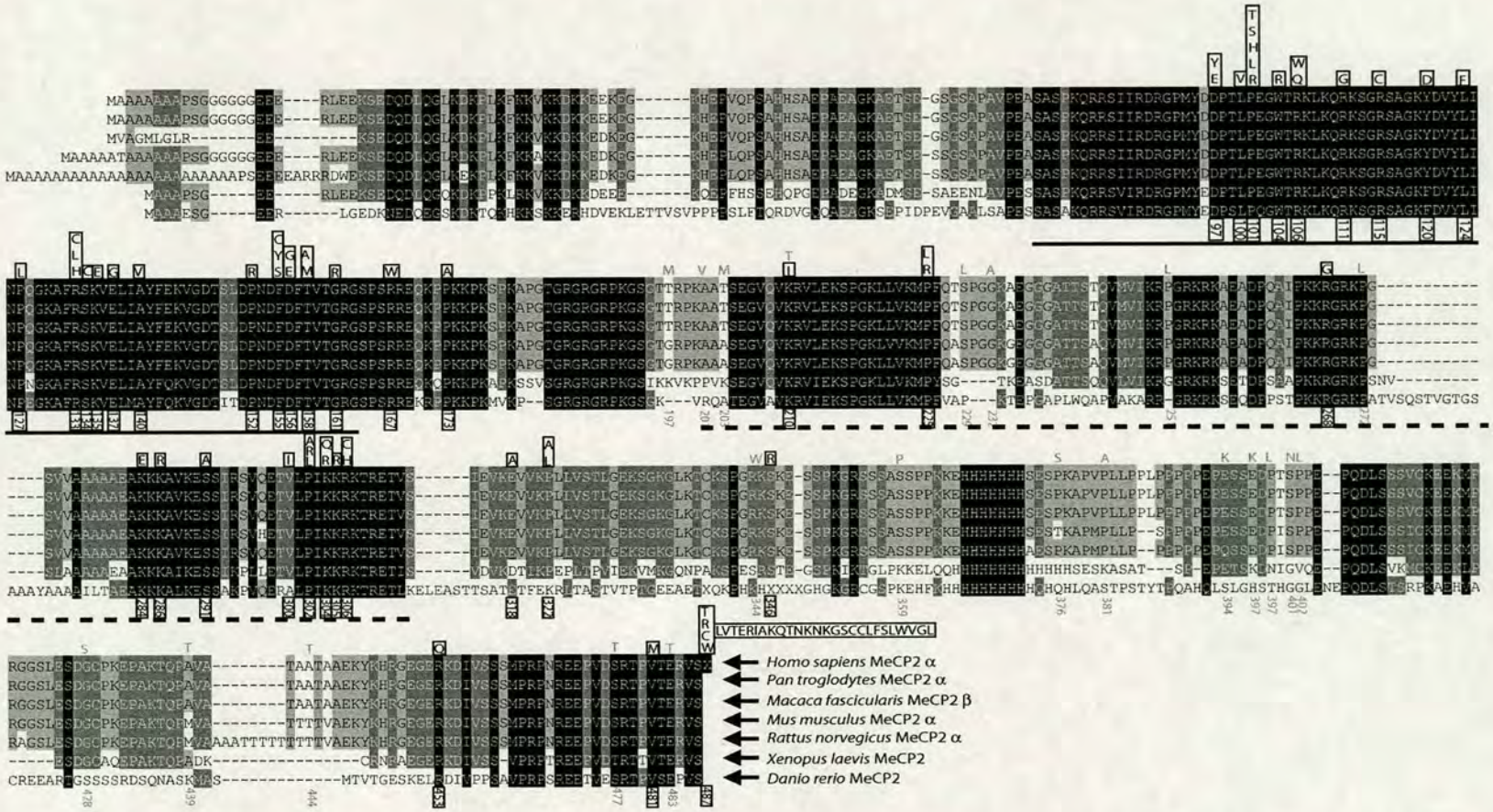

Figure 1-4. MECP2 alignment and sequence variations found in humans. Shading of the alignment represents different levels of conservation (the darkest shading represents the most conserved parts of the protein). On the top of alignment in black font and black boxes Rett syndrome causing mutations are shown. Grey font without any boxes marks sequence polymorphisms that are found in healthy individuals. Solid line delineates the MBD and dotted line the TRD.

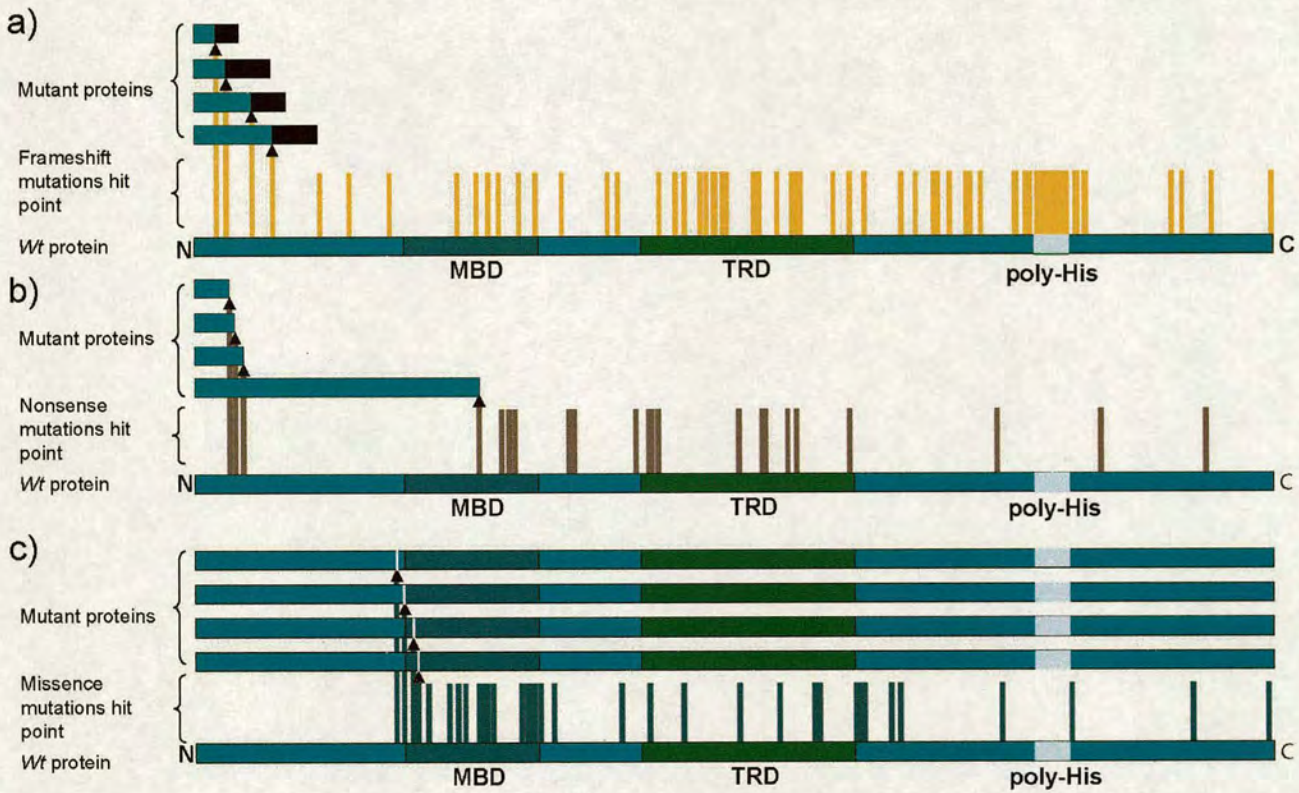

Figure 1-5. Distribution of different Rett syndrome causing mutations. Four examples of mutant proteins produced by specific mutation type are shown. The arrows and vertical lines indicate the point of a mutation. a) Frameshift mutations are usually nucleotide deletions or insertions, which cause a shift of the MECP2 coding frame and result in different amino acid composition from the point of mutation, followed by a premature STOP codon. b) Nonsense mutations are usually one nucleotide mutations that introduce a STOP codon at the point of mutation. This leads to the truncation of the protein in the place of mutation. c) Missense mutations are single nucleotide changes, which result in a single amino acid change (marked as a white line on a mutant protein).

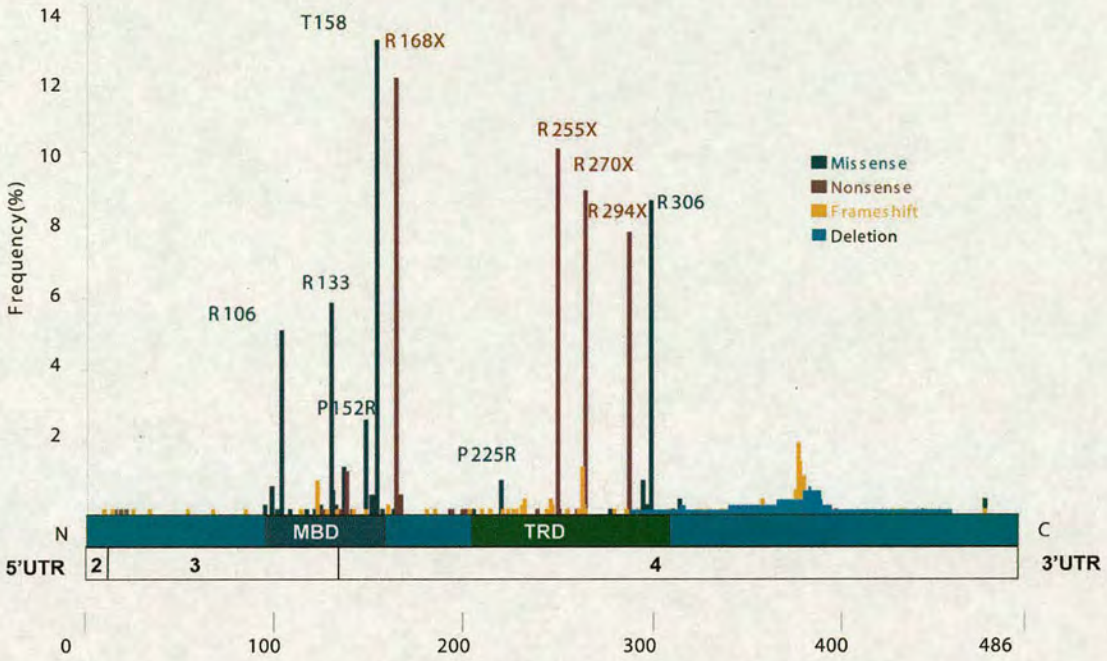

Figure 1-6. Frequencies of different Rett syndrome causing mutations in the MECP2 gene. The place of coding exons is denoted below the schematic structure of the protein. Numbers below indicate amino acids.

Most of the missense mutations in *MECP2* that cause Rett syndrome are tightly clustered at the methyl binding domain (MBD) (Figure 1-5). Deletion/insertion mutations leading to shifts of the open reading frame are clustered in the C-terminal part of the protein, which contains a poly-histidine repeat (Figure 1-5). Rett syndrome patients display a wide spectrum of mutations, but ~67 % of all mutations are in eight hot spots (R106, R133, T158, R168, R255, R270, R294 and R306) (Figure 1-6). Seven out of the eight major mutations affect arginine (R), which often has a CpG in its codon (four out of six arginine codons has got a CpG). In mammals, the majority of CpGs in the coding region of a gene are methylated and therefore can undergo deamination. As mentioned previously, if unrepaired methyl-CpG deamination leads to TpG transitions as a frequent event.

Several cases of mutations in *MECP2* were also reported in non-specific X-linked mental retardation (Couvert et al., 2001) and Angelman syndrome (Watson et al., 2001). Because one of the Rett syndrome symptoms is loss of communication, a

group of autistic patients were screened for MeCP2 mutation, with no MeCP2 mutations found (Lobo-Menendez et al., 2003; Zappella et al., 2003). In the latest study only two of sixty nine autism patients were shown to have a *de novo MECP2* mutations (Carney et al., 2003). However the significance of *MECP2* mutations in X-linked mental retardation, Angelman syndrome and autism is not clear because of low mutation frequency and possibility of disease misdiagnosis.

Because there is a population of Rett syndrome patients without *MECP2* mutations identified, a possibility exists that mutations in other genes are involved in Rett syndrome pathology as well. Mutation analysis was done for a group of candidate genes (*UBE1*, *GdX1*, *GABRA3* and *CDR2*) involved in the pathology of similar diseases (Angelman syndrome and X-linked mental retardation), however no mutations were found (Xiang et al., 2000). Expression analysis of several candidate genes (*GdX*, *L1CAM* and *GABRA3*) has not revealed any differences as well (Xiang et al., 2000).

Rett syndrome girls are heterozygous for the mutated *MECP2*, and as a result of random X chromosome inactivation, half of cells will have the wild type (*wt*) copy and the other half will have the mutated copy of *MECP2* inactivated. Therefore, the female cell population is mosaic for the mutated allele, whereas male with the mutated *MECP2* will have cells with a mutated allele only. Initially, it was thought that males with *MECP2* mutation die prenatally, but later, some live born boys carrying the mutant MeCP2 have been described. These boys have a different and more severe phenotype than Rett syndrome. The same mutations, which are common among female Rett patients, usually causes severe congenital encephalopathy in males (Ravn et al., 2003).

Numerous Rett syndrome studies failed to find a correlation between the location of different *MECP2* mutations and severity of the disease. Some studies claimed to find that truncations are more severe than point mutations, but others do not observe this (Colvin et al., 2003; Nielsen et al., 2001; Amir and Zoghbi, 2000; Cheadle et al., 2000; Ravn et al., 2003; Hoffbuhr et al., 2002). The complicating parameter in genotype phenotype correlation is the pattern of X chromosome inactivation. Shift

towards silencing of the mutated copy usually causes milder version of the disease and *vice versa.*

Linkage analysis of MECP2 mutations in Rett syndrome patients revealed that mutations almost exclusively arise in the paternal copy of X chromosome (Trappe et al., 2001; Girard et al., 2001). This finding helps to explain why MECP2 mutations are much more common in females.

1.6. Mecp2 mutations in mouse

The first attempt to make *Mecp2*-nulls by insertion mutation of promoterless *lacZ/neomycin* cassette into *Mecp2* locus was unsuccessful (Tate et al., 1996). Embryos with a high level of mutant ES cell contribution had developmental defects and died in mid-gestation. However, an *Mecp2*-null mouse was successfully produced using cre/lox recombination technology (Guy et al., 2001; Chen et al., 2001). The discrepancy between these results might be explained by *Mecp2* status in ES cells. Cre/lox recombination allows generation of ES cells with the protein still present, while insertion mutation disrupts the coding locus leading to null ES cells. These findings left an open question of MeCP2 significance in pluripotency during *in vitro* culturing of mouse ES cell lines.

Mecp2-null allele was made by crossing mice having MeCP2-loxP allele to mice expressing cre recombinase under ubiquitous viral promoter (Guy et al., 2001; Chen et al., 2001). *Mecp2*-null male ($Mecp2^{-/y}$) and female ($Mecp2^{-/-}$) mice have no apparent phenotype until around 6 weeks when a period of rapid regression starts, resulting in reduced spontaneous movement, clumsy gait, irregular breathing, hindlimb clasping and tremors. Rapid progression of symptoms leads to death at approximately 8 weeks of age (Guy et al., 2001; Chen et al., 2001). Interestingly, pathological examination revealed reduced brain and neuron cell sizes (Chen et al., 2001), which have been noted in Rett syndrome girls. The onset of symptoms can vary with littermates displaying symptoms and dying over different time periods. Crossing mice with intronic *loxP* sites flanking *Mecp2* to mice expressing cre

recombinase under the *nestin* promoter, allowed tissue/time specific *Mecp2* deletion. Nestin is expressed mainly in neuronal progenitors from around embryonic day 12 (Zimmerman et al., 1994). Mice with nestin-cre mediated *Mecp2* deletion showed the same phenotype as whole body nulls (Guy et al., 2001; Chen et al., 2001). This finding led to two important conclusions: a) *Mecp2* deletion in the brain is sufficient to produce the same phenotype as a whole body nulls; b) the presence of *wt* protein until embryonic day 12 is not enough to rescue or even relieve the phenotype. Further investigations used the same mouse genetics approach to delete *Mecp2* at a later developmental time. Under *CamKII* promoter, cre recombinase expresses in post-mitotic neurons (Tsien et al., 1996). After *CamKII*-cre mediated deletion, symptoms were delayed up to three months (Chen et al., 2001). Interestingly, the time between deletion of the gene and manifestation of symptoms remains approximately the same as nestin mediated nulls - around 60 days. In these mice, the onset of symptoms becomes more variable, than in germline inherited or nestin mediated deletions. An alternative explanation is that *CamKII-cre* is not expressed in the cerebellum, restricting the cre mediated deletion pattern. Therefore the delayed and variable symptoms could be due to presence of *wt* MeCP2 in cerebellum.

A lack of correlation between mutations and symptoms suggests that Rett syndrome is caused by loss of MeCP2 function regardless of what region of the gene is mutated. Therefore, the genetic mouse model for Rett syndrome is a female mouse heterozygous for *Mecp2*-null allele. The heterozygous mice are normal till around nine months old at which point they start showing breathing irregularities and hind limb clasping. Reduced mobility was confirmed by an open field test (Guy et al., 2001). There is a striking similarity between time of symptom onset in heterozygous mice and Rett patients despite the fact that a one year old human is still in its period of development and a nine month old mice has already been mature for 3 months.

Around 80 % of all Rett-causing mutations lie in the described functional MeCP2 domains: the methyl-CpG binding domain and transcriptional repression domain. As mentioned previously, currently no function has been mapped to the C-terminus, but mutations which disrupt C-terminus in humans cause Rett syndrome (Figure 1-5). Mice with C-terminally truncated MeCP2 reveal some interesting findings. The

symptom onset window in hemizygous mutants is increased with slight tremors at 6 weeks to kyphosis, visible tremors and seizures at around 5 months of age (Shahbazian et al., 2002a). Survival of these mice is only slightly affected. In mice, the C-terminal deletion of *Mecp2* shows less severe phenotype than the null mutation (Shahbazian et al., 2002a). The difference between the null mutation and the C-terminal truncation also suggests that mice, in contrast to humans, could have a more pronounced genotype – phenotype correlation for other mutations as well.

The X inactivation profile was examined in detail in mice carrying the truncated *Mecp2* mutation. The results showed that in two thirds of investigated female mouse brains, 70% of cells expressed *wt* MeCP2 (Young and Zoghbi, 2004). No mice were observed with fewer than 54% of neurons expressing *wt* MeCP2. Moreover, after 3 to 7 days in culture, neurons expressing *wt* MeCP2 had a better selective survival even when the initial number of *wt* and *Mecp2* mutant cells were equal (Young and Zoghbi, 2004).

Clear genetic confirmation that MeCP2 deficiency in neurons causes Rett-like phenotype in mouse was demonstrated by the rescue experiment, in which MeCP2 expression from the neuronal *Mapt* (*tau*) promoter was able to rescue *Mecp2*-null mouse (Luikenhuis et al., 2004). Interestingly, the same study showed that over-expression of MeCP2 in homozygous for *Mapt* (*tau*)-*Mecp2* transgene mice resulted in a motor dysfunction phenotype. Two to three times more MeCP2 can be tolerated, but 10 times more protein gives phenotypic defects.

1.7. MeCP2 studies in brain

Tissue-specific *Mecp2* gene knock-outs revealed the brain as a tissue of interest. Therefore now we can question the role of MeCP2 in the tissue that is responsible for the pathology of Rett syndrome.

Expression of MeCP2 mRNA is ubiquitous in mouse, rat and humans. In brain, MeCP2 is preferentially expressed in neurons but is not detected in glia. Laser scanning cytometry revealed an increase in the number of high MECP2 expressing

neurons during postnatal development in humans, and this expression correlated with alternative polyadenylation (Balmer et al., 2003). *In situ* hybridization showed that MeCP2 up-regulation starts in the postnatal brain in mouse, rat and humans (Shahbazian et al., 2002b; Jung et al., 2003; Akbarian et al., 2001; Cassel et al., 2004). MeCP2 expression studies in the olfactory epithelium, which contains both mature and immature olfactory receptor neurons, demonstrated that only mature olfactory receptor neurons up-regulate MeCP2 before synaptogenesis (Cohen et al., 2003). A recent study demonstrated that in different rat brain regions, MeCP2 is up-regulated at different times. For example, early generated Purkinje cells up-regulate MeCP2 by postnatal day 6, whilst late generated granule cells only become MeCP2 positive only at day 21 (Mullaney et al., 2004).

The time point of MeCP2 up-regulation helps to explain the symptom onset window in different *Mecp2* deletions. Nestin-cre mediated *Mecp2* deletion at around embryonic day 12 produces mice with the same symptom onset as the inherited *Mecp2*-null allele. However, when the protein is deleted at the same time as it is up-regulated (CamKII mediated deletion), the symptom onset is delayed.

Does MeCP2 bind methylated CpGs in the brain? Originally, MeCP2 activity was purified from rat brain, proposing that the brain "version" of MeCP2 *in vitro* preserves methylated CpG binding selectivity (Lewis et al., 1992). Later, *in situ* hybridization to mouse brain slices suggested that MeCP2 co-localizes with DAPI bright spots in mouse neurons (Payen et al., 1998). A more detailed compartmentalisation study in the nucleus showed co-localisation of 5-methyl cytosine, as well as γ-satellite DNA, with MeCP2 in large neurons (Akhmanova et al., 2000). However, MeCP2 did not localise to methylated ribosomal DNA loci (Akhmanova et al., 2000).

A microarray approach was used in search of transcriptional consequences of *Mecp2* loss in the mouse brain (Tudor et al., 2002). The experiment showed no significant changes in *Mecp2*-null mice brain, however, some gene expression variability was noticed. Statistical predictions, based on gene expression variability, could distinguish *Mecp2*-null brain samples from *wt* ones. Some of the genes were confirmed to show small (up to 35%) differences by RNase protection assay (Tudor

et al., 2002). One interpretation could be that the brain is a very heterogeneous tissue, therefore, when investigating a mixture of cells, it becomes difficult to see any transcriptional differences. In addition, microarray techniques have limitations, such as detection of low abundance transcripts and small differences in transcription (Nisenbaum, 2002).

As mentioned before, *Bdnf* gene was identified as the MeCP2 target gene in cultured mouse cortical neurons (Chen et al., 2003b; Martinowich et al., 2003). However it is still unclear how increase of basal *Bdnf* level could contribute to the pathophysiology of a mouse model for Rett syndrome.

A clue about the importance of MeCP2 in the brain function comes from studies in *Xenopus*. Morpholino MeCP2 down regulation in *Xenopus* embryos results in developmental arrest, which is likely a consequence of abnormal patterning of primary neurons (Stancheva et al., 2003).

The possibility was explored that MeCP2 has a transcription-independent role in the brain. One study suggests that MeCP2 could be localised in synapses (Aber et al., 2003). However, the result is not clear, because the lack of antibody controls in immuno-histochemistry experiment, and high MeCP2 abundance in brain that could allow contamination of the synaptic fraction.

1.8. Discussion

Recent data has highlighted that neurological defects occur when methyl-CpG binding proteins are mutated or deleted in mouse models. *Mbd2*-null females fail to nurse their offspring, with no known underlying neurological basis (Hendrich et al., 2001). *Mbd1*-null cells showed reduced neuronal differentiation and chromosome instability *in vitro,* and the mice had defected spatial learning and long-term potentiation in the hippocampus (Zhao et al., 2003). *Mecp2*-null mice have the most severe neurological symptoms and die at around 8 weeks of age (Guy et al., 2001; Chen et al., 2001). It is easy to notice that the most defects in MBD family nulls have the connection with a brain. One possibility is that the brain is the most intensively

studied tissue and the abnormalities in other tissues are waiting to be discovered. Another possibility is that the DNA methylation plays distinctive and important role in the brain, therefore removing any of the methyl CpG signal "readers" results defects in the brain. This possibility was investigated by attempts to eliminate the DNA methylation signal from brain. Removing *Dnmt1*, the maintenance DNA methyltransferase, has a very severe phenotype with failure of embryo development (Li et al., 1992). Tissue specific removal of *Dnmt1* in mouse CNS precursors using nestin-cre mediated deletion did not produce any viable offspring, however, embryos were recovered at all stages (Fan et al., 2001). After a Cesarean section, death occurred within 1 hr due to respiratory failure. Occasional gasping was seen, however there was no rhythmic breathing. Interestingly, *Mecp2*-null mice, as well as Rett patients, show breathing abnormalities. Post-natal *Dnmt1* deletion in neurons does not affect either animal viability or global methylation levels of endogenous retroviral repeats (Fan et al., 2001).

There are other functions for MBD proteins outside of the brain as *Hutchins et al* described in a helper T cell differentiation system in MBD2 null mice. Comprehensive experiments revealed that MBD2 null helper T cells fail to silence the *Il4* gene after induction of differentiation (Hutchins et al., 2002). Only when individual cells were assayed by cell sorting experiments, was a difference in *Il4* expression revealed, which could easily have been missed by global gene expression analysis tools such as microarrays. Maybe MeCP2 functions similarly in the post-natal brain? For example, at a time point when individual neurons acquire their late fate i.e. dopaminergic *versus* GABA-ergic function? These cells have a different role in signal interpretation producing different neurotransmitters and receptors, however, they are the closely related and share many properties as well.

The study by *Guan, Z.* demonstrated a link between different neurotransmitters and the chromatin state of the C/EBP promoter in *Aplysia* (Guan et al., 2002). Treating the synapse with the facilitatory transmitter 5-HT, recruited CREB1 with CBP histone acetylase, which caused histone acetylation and expression of C/EBP gene. While treatment with the inhibitory transmitter FMRFa brought CREB2 repressor with HDAC5 deacetylase, leading to deacetylation of promoter chromatin and

silencing of the gene (Guan et al., 2002). As there is a close interplay between chromatin modifications and DNA methylation, it might be possible that silencing of some genes relies on DNA methylation. The most attractive possibility is that closely related cell types that have just a few differentially expressed genes, might need more tight regulation to distinguish them in a specific manner.

It has also been proposed that the extensive DNA replication-independent replacement of histone H3 by a histone variant H3.3 in neurons may cause the loss of the information which is present in the modifications on the H3 histone tail. Therefore MeCP2 could use interactions with histone modifying enzymes (HDAC1,2 and Suv39h) to re-establish appropriate histone modifications at certain loci (Ahmad and Henikoff, 2002)

MeCP2 is the first MBD protein isolated and intensively studied in past years. However, the link with Rett syndrome created new questions to answer as well as pointing to the brain as a tissue of specific interest. Co-immuno precipitation studies have suggested some MeCP2 protein partners and chromatin IP studies point to promoters possibly regulated by MeCP2, however, the Holy Grail still remains to dissect the *in vivo* functions of MeCP2 and its relation to Rett syndrome.

1.9. Thesis objectives

The main objective of the work presented in this thesis is to find and investigate the molecular link between *MECP2* deficiency and Rett syndrome. After the discovery of *MECP2* mutations in Rett syndrome it became possible to merge the knowledge about molecular properties of MeCP2 and the clinical findings of Rett syndrome in order to understand both phenomena much better. On the one hand it was a big surprise, that mutations in a "global" repressor cause such a specific disease. Thus the "global" hypothesis had to be revisited in order to find specific target genes that MeCP2 represses. Consequently, the main part of the work presented here will be the search for genes that become deregulated by the absence of MeCP2. Finding target genes is crucial in understanding both MeCP2 function and Rett syndrome. From the

perspective of MeCP2 function, a target gene could serve as a tool to investigate its repression mechanism. What co-repressors are recruited for transcriptional repression? Is repression followed by local changes in chromatin modifications? What are the critical regions of MeCP2 required for *in vivo* repression? From the Rett syndrome point of view, a target gene could give a pathological insight. Which process is the target gene involved in? How does it relate with already known symptoms? What medicines could be used to intervene in the disease-specific pathway? One of the best examples of how a target gene could help to understand the biology, is the MeCP2 regulation of *Hairy2a* gene in *Xenopus laevis* development (discussed in 1.4.2). Therefore one of the major projects in this thesis was to find genes which are mis-expressed in *Mecp2*-null mouse brain (Chapter 3).

Growing EST and genome sequencing projects, especially sequencing of 5' enriched EST libraries such as the RIKEN consortium, allowed us to revisit gene structure. Examination of available EST clones encoding human and mouse MeCP2 aided in identification of a new MeCP2 splice isoform (Chapter 4).

There are a few theories about the role of MECP2 in originating Rett syndrome symptoms. The neurodevelopmental theory says that MECP2 is required for proper brain development and therefore the *MECP2* mutations cause developmental arrest. Alternatively MeCP2 may be required for proper maintenance of neuronal function. We have used mouse genetic approaches which are able to distinguish between these two possibilities to provide some potential hope for future therapies (Chapter 5)

2. Chapter Two.

Materials and methods

2.1. Materials

2.1.1. Common solutions and reagents

TAE electrophoresis buffer (10x): 0.4 M Tris-acetate, 100 mM EDTA, pH 8.5.
TBE electrophoresis buffer (10x): 890 mM Tris, 890 mM boric acid, 20 mM EDTA, pH 8.0.

MOPS electrophoresis buffer (10x): 400 mM MOPS; 100 mM sodium acetate; 1mM EDTA; pH 7.0; made with DEPC treated water.

Orange DNA loading buffer (10x): 0.33% (w/v) Orange G; 0.1 M EDTA; 30% (v/v) glycerol; pH 8.0

Blue DNA loading buffer (10x): 0.25% (w/v) bromphenol blue, 0.25% xylene cyanol, 0.1 M EDTA, 30% (v/v) glycerol, pH 8.0.

Formamide gel-loading buffer (2x): 80% formamide (v/v), 10 mM NaOH, 10 mM EDTA, 0.1% bromphenol blue, 0.1% xylene cyanol.

RNA loading buffer (10x): 0.25% (w/v) bromphenol blue, 0.25% xylene cyanol, 1mM EDTA, 50% (v/v) glycerol, pH 8.0, made with DEPC treated water.

DEPC treatment of water: 0.2% of DEPC was added, mixed well and autoclaved.

Nucleic acid transfer buffer (SSC 20x): 3 M NaCl, 0.3 M Na citrate, pH 7.0.

Phosphate buffer (1M, pH=7.4): Solution A: 276 g of $NaH_2PO_4 \cdot H_2O$ was dissolved in 1 l of water (2 M); Solution B: 536.5 g of $Na_2HPO_4 \cdot 7H_2O$ was dissolved in 1 l of water (2 M); to get 200 ml of 1 M phosphate buffer pH=7.4, 19.0 ml of solution A was mixed with 81.0 ml of solution B and diluted to total volume of 200 ml with water.

Modified Church and Gilbert buffer for hybridization: 0.5 M phosphate buffer, 7% SDS, 10 mM EDTA, 50 μg salmon sperm DNA.

Depurination solution: 0.125 M HCl.

Denaturation solution: 1.5 M NaCl, 0.5 M NaOH.

Denhardt's solution (50x): 1% v/v Ficoll 400, 1% w/v polyvinyl pyrolidone, 1% bovine serum albumine (BSA).

TE: 10 mM Tris-HCl, 1 mM EDTA pH=8.

TENT: 10 mM Tris-HCl, 0.1 M EDTA, 1 M NaCl, 0.1% (v/v) Triton X-100.

TB buffer: 10 mM Hepes, 55 mM $MnCl_2$, 15 mM $CaCl_2$, 250 mM KCl.

2.1.2. Protein manipulation solutions

TBS: 20 mM Tris-HCl, 100 mM NaCl pH=8.

5x tris-glycine electrophoresis buffer: 125 mM Tris, 1.25 M glycine, 1% SDS.

2x SDS-PAGE loading buffer: 6% β-mercaptoethanol, 6% SDS, 0.6 % bromophenol blue, 20% glycerol.

ECL (Enhanced Chemiluminescence) solution 1: 250 mM luminol, 90 mM p-coumaric acid, 1 mM Tris-HCl pH=8.5.

ECL solution 2: 0.015% H_2O_2, 1 mM Tris-HCl pH=8.5.

2.1.3. Cell culture solutions

PBS: 0.14 M NaCl, 3 mM KCl, 2 mM KH_2PO_4, 10 mM Na_2HPO_4.

ES cell medium: 500 ml Glasgow MEM (Invitrogen), 5.6 ml Sodium Pyruvate (100 mM, Gibco), 5.6 ml Non-essential Amino Acids (Gibco), 56 ml Foetal Calf Serum, 570 µl β-mercaptoethanol (50 mM), 570 µl LIF.

Mouse fibroblast medium: 500 ml Alpha-MEM (Gibco), 56 ml Calf Serum, 5.6 ml penicillin/streptomycin (Gibco).

Freezing medium: 15.6 ml complete medium, 2.4 ml Foetal Calf Serum, 2 ml DMSO.

100x Modified N2 supplement: bovine insulin (Sigma I-1882) 2.5 mg/ml, human apo-transferrin (Sigma T-1147) 10 mg/ml, progesterone (Sigma P-8783) 600 ng/ml, putrescine (Sigma P-5780) 1.6 mg/ml, selenium chloride (Sigma S-5261) 3 µM and BSA (Gibco/BRL 15260-011) 5 mg/ml.

HBS: HEPES 20 mM, 150 mM NaCl.

10x Trypsin/EDTA: 0.5% Trypsin, 5.3 mM EDTA (Gibco).

2.1.4. Microbiological solutions and reagents

LB broth: 10 g/l NaCl; 10 g/l Difco bacto-tryptone; 5 g/l Difco yeast extract.

***E. coli* freezing solution:** 65% glycerol; 0.1 M $MgSO_4$; 0.025 M Tris-HCl pH=8.

2.2. Specific Reagents

2.2.1. Antibodies

Table 2-1. Antibodies used in the different experiments presented in this thesis.

Primary antibodies:

Name	Manufacturer or reference	Dilution used for Western blot / immunohistochemistry	Antibody type
Anti-MeCP2	Upstate #07-013	1:1000 / 1:200	Rabbit polyclonal IgG
674, anti-MeCP2	(Nan et al., 1998)	1:1000 / not used	Rabbit anti-sera
anti H3 di-methyl	Abcam, #ab7312	ChIP 1:300	Rabbit polyclonal

K9 antibody			
Tuj1, anti-Neuronal Class III β-Tubulin	Covance, #MMS-435P	not used / 1:500	mouse monoclonal IgG_{2a}

Secondary antibodies:

Anti-Rabbit fluorescein conjugated	Vector Laboratories, #FI-1000	not used / 1:100	goat IgG (H+L)
Anti-Sheep fluorescein conjugated	Vector Laboratories, #FI-6000	not used / 1:100	rabbit IgG (H+L)
Anti-digoxigenin fluorescein conjugated	Roche, #1207741	not used / 1:15	sheep Fab fragments
Anti-rabbit peroxidase conjugated	Amersham, #NA 934	1:5000 / not used	donkey IgG
Anti-mouse peroxidase conjugated	Amersham, #NA 931	1:5000 / not used	sheep IgG

2.2.2. Primers

Table 2-2. Primers used for ADDER differential display.

Upstream primers (5'-3')		**Downstream primers (5'-3')**	
U1	CCAACGGATCGG	D1	AGCTTTTTTTTTTTTGG
U2	AACCGATCGA	D2	AGCTTTTTTTTTTTTAA
U3	AACCGATCGT	D3	AGCTTTTTTTTTTTTCT

U4	AACCGATCGC	D4	AGCTTTTTTTTTTTGC
U5	AACCGATCAG	D5	AGCTTTTTTTTTTTAG
U6	AACCGATCAA	D6	AGCTTTTTTTTTTTCA
U7	AACCGATCAT	D7	AGCTTTTTTTTTTTGT
U8	AACCGATCAC	D8	AGCTTTTTTTTTTTAC
U9	AACCGATCTG	D9	AGCTTTTTTTTTTTCG
U10	AACCGATCTA	D10	AGCTTTTTTTTTTTGA
U11	AACCGATCTT	D11	AGCTTTTTTTTTTTAT
U12	AACCGATCTC	D12	AGCTTTTTTTTTTTCC
U13	CCAACCGATCCG		
U14	CCAACCGATCCA		
U15	AACCGATCCT		
U16	AACCGATCCC		

Table 2-3. Primers used for the Real Time PCR.

Gene accession No.	Symbol, Name/ /Homology	Forward primer (5'-3')	Reverse primer (5'-3')
XM_146892	Gapdh, glyceraldehyde-3 phosphate dehydrogenase	tacccccaatgtgtccgtcg	cctgcttcaccaccttcttg
NM_011361	Sgk, serum/glucocorticoid regulated kinase	cgccaagtccctctcaacaa	tgcccttccgatcactttc

NM_213149	Fkbp5, FK506 binding protein 5	gctggcaaacaacacgagag	gaggagggccgagttcatt
AK009231	Prkaa2, the 5'-AMP-activated protein kinase	tggcatagttctgacttctcc	ttgtggatgctgttattagagg
XM_147936	Unknown	agaaggctggaagggctgtg	agtcggttattgtgctgcttagt
NM_025407	Uqcrc1, ubiquinol-cytochrome c reductase core protein 1	acggtgggagtgtggattgac	cattgccaggccgattctttg
NM_008946	Psmb6, proteasome (prosome, macropain) subunit, beta type 6	acacagccgccagtctcttt	agtacacctgccctccttcttg
AK075675	Spnb2, spectrin beta 2	gtttcctgcgctactacttgtc	catattgttgcttctctttagg
E130120	Unknown, contains SAM domain	gcatatcaagtgcatatcaagtg	cttaaattagtttgctttgcttg
NM_144828	Ppp1r1b, Protein phosphatase 1 regulatory (inhibitor) subunit 1B	ccagaaggccataaacaaccatt	ctcagtacctcctttccccagat
BC028971	Gtl2/Meg3, imprinted maternally expressed untranslated mRNA	tgcagcggagagccataaataac	acatcgcctccctccctcgtg
AK011516	Hist1h2bc, histone 1 H2bc	gatactagcagattaaccaccat	ttcttatcacaaatttctacagt
AK036751	Tbc1d20, TBC1 domain family member 20	tttggcaggaaccgcacacc	caaagccatcctaggaagaccaa
BC002028	Tarbp2, TAR (HIV) RNA binding protein 2	catttttccattggcgtgagc	gagcaacttcgaagggatagg
NM_011029	Lamr1, laminin receptor 1 (ribosomal protein SA)	gcaccagctcctgagttcactg	agtcttccgtggggaactgctg
AK034339	Unknown, similar to Esterase/lipase/thioesterase	gcctatcatgcagaccacag	gctcgcaggtaaggatgtag

	family members		
AK006990	Unknown	gcgtcctcataccttagtgc	gaagccattcagttaactcgg
AU018611	mt-Nd2, NADH dehydrogenase 2	gggcatgaggaggacttaaccaaac	tgaggttgagtagagtgagggatgg
AK049058	Unknown	ccagctagaaagaacgcagagg	gcaggggacagactgaaatagag
NM_016959	Rps3a, ribosomal protein S3a (tnf)	cagcaagtccgccagatc	atggagaggataaatggactgg
NM_175092	Rhof, ras homolog gene family, member f	gtcccaagcccactgtttctg	ttgatgcctgtgttctcctgatag
AK002412	Asb11, ankyrin repeat and SOCS box-containing protein 11 containing protein 11	cagagagttgattgtgtgaagaag	acagtgagcagattgatgacc
AK003881	Unknown, similar to ubiquinol cytochrome-c reductase	gaacttccacctttgccctcac	gtttccacagtttcccctcgt
BB266235	Unknown	atccttgggtgtattttatgg	gcttttctttctgttacctctca
AK049648	Unknown	agttccagaataaccgctctcc	ctctctcacccatctgataccttag
XM_127854	Akap11, A kinase (PRKA) anchor protein 11	tcaccgaagtcactggctaagc	gcactggggcacctgtagag
AK029199	Cdon, cell adhesion molecule-related/down-regulated by oncogenes	tcccagtggtagcctcttatcc	attggtgccacactgtccttg
AK079922	Add1, adducin 1 (alpha)	ggaacttccagatatgtactc	ccggtctaatggcaaaacgatg
BC025130	Ccl19, chemokine (C-C motif) ligand 19	gagccctgtgtcttgagtaaag	acttggctgggttaggtctg
NM_009941	Cox4i1, cytochrome c oxidase subunit IV isoform	agagcgctgagcctgattg	gtaagtggggaaagcatagtct

	1		
BC004742	Pja2, praja 2, RING-H2 motif containing	gcagcagcgatgaagggaatgag	acaggctccagtccacatccaag
BB634200	Unknown	ggagtcagtacaccctgagttg	gggcctacagaatagctcagc
NM_018753	Ywhab, tyrosine 3-monooxygenase/tryptophan 5-monooxygenase activation protein, beta polypeptide	aggtgcccgccgctcttcc	tgcagctccgcctcgatcttctc
AV021813	Unknown, similar to human AUTS2	gcagtcagacccacacaag	accagcggcagagaataaag
XM_127738	Unknown, similar to disrupter of silencing SAS10	cacgcttggttccagtacattac	ttcctctggggcgtctgag
BC058513	Snrp70, U1 small nuclear ribonucleoprotein polypeptide A	gctgactggtgggagtgtgag	tgccatctgcgtgcttgtaag
BC062180	Unknown, similar to tio-redox domain	cagatcgcaccctggaaacac	caccagcaaccaatccacagtc
BC006914	Lzf, leucine zipper domain protein	caagcacctgcctgactcctc	tgccatcagtaccacagggaatg
X63615	Camk2b, calcium/calmodulin-dependent protein kinase II, beta	actcaacaagaaagcagatggag	cagggcagcaggagggag

Table 2-4. PCR primers used for the genotyping of mice. Primers were designed by Jacky Guy.

Allele – expected fragment size	**Forward primer (5' - 3')**	**Reverse primer (5' - 3')**
Mecp2 wt – 420 bp	tggtaaagacccatgtgacccaag	tccacctagcctgcctgtactttg
Mecp2-null – 450 bp	tggtaaagacccatgtgacccaag	ggcttgccacatgacaagac
Mecp2-loxP – 490 bp	tggtaaagacccatgtgacccaag	tccacctagcctgcctgtactttg
Cre – 450 bp	gaccgtacaccaaaatttgcctgc	ttacgtatatcctggcagcgatc

2.3. Protocols

2.3.1. RNA and genomic DNA extraction

RNA was purified using TRI-Reagent (Sigma) according to the manufacturer's recommendations. Briefly, dissected tissues were snap frozen in liquid nitrogen and stored at -80°C until RNA purification. Frozen tissue was added to required volume of TRI-Reagent (1 ml per 50 - 100 mg of tissue) and homogenised in a dounce. For monolayer cultured cells, the cells were washed once with PBS, required volume (1 ml per 10 cm^2) of TRI-Reagent was added and cells were harvested by scraping with cell scraper. For complete lysis, the samples were incubated for 5 min at room temperature. After the addition of 0.2 ml of chloroform per 1 ml of TRI-Reagent, the samples were shaken vigorously and left to settle for 10 min at room temperature. The resulting mixture was centrifuged at 10 000 g for 20 min at 4°C. The top aqueous layer was removed to a separate tube and 0.5 ml of isopropanol was added per 1 ml of TRI-Reagent. Samples were mixed and left to stand for 10 min. RNA

was precipitated by centrifugation at 10 000 g for 15 min at 4°C. The RNA precipitate was washed by addition of 1 ml of 75% ethanol per 1 ml of TRI-Reagent used and a 7500 g spin for 5 min at 4°C. The RNA pellet was briefly dried at 37°C and re-suspended in the required volume of DEPC treated water.

DNA was purified by a standard method. Briefly, tissues were cut into small pieces, added to the lysis buffer (50 mM Tris-HCl pH=7.5, 100 mM NaCl, 100 mM EDTA, 1% SDS) with 0.5 mg/ml proteinase K and incubated overnight at 55°C. Next day RNase (final 10 μg/ml) was added and the incubation was continued for additional 1h at 37°C. For the protein extraction equal volume of phenol-chloroform-isoamyl alcohol (25:24:1) was added, samples were well mixed, centrifuged for 5 min at 16000 g (tabletop centrifuge) and top aqueous phase was removed to a separate tube. The DNA was precipitated by addition of 2.5 volumes of ethanol or 0.7 volumes of isopropanol and centrifugation at 16000 g for 10 min. The pellet was washed from salts by the additional incubation with 70% ethanol and centrifugation step. Finally, the precipitate was dried at 37°C for 10 min and re-suspended in required volume of water or TE buffer.

2.3.2. Crude genomic DNA extraction for the genotyping of mice

Mice were genotyped from ear punch biopsies. The ear punch was transferred to 25 μl of solution I (25 mM NaOH, 0.2 mM EDTA) and heated at 95°C for 20 min. The solution was then cooled down on ice and 25 μl of solution II (40 mM Tris pH=5) was added. The resulting solution was vortexed and 1 μl was used as a template for PCR reactions.

2.3.3. Preparation of frozen competent *E.coli*

2-3 fresh colonies were transferred into 5 ml of LB with antibiotics appropriate to the bacterial strain and grown overnight at 37°C. The next day 250 ml of LB was inoculated with 250 μl of the overnight culture. The cells were grown until they reached A_{600}=0.5 - 0.6. Then the cells were cooled down for 10 min on ice and

centrifuged for 10 min at 1400 g at 4°C. The supernatant was discarded and the bacterial pellet was re-suspended in 80 ml of ice cold TB and gently mixed. The mix was left on ice for 10 min and centrifuged for 10 min at 1400 g at 4°C. The supernatant was discarded and the bacterial pellet re-suspended in 20 ml of TB and 1.5 ml DMSO was then added. The bacteria were aliquoted in 1.5 ml tubes, 200 µl in each, and snap frozen in liquid nitrogen. Aliquots were transferred to a -70°C freezer for storage.

2.3.4. Restriction digestion of DNA

For restriction digestion the required amount of DNA was incubated with 5 U of a restriction endonuclease (NEB, Roche) per 1 µg of DNA in reaction mix containing required reaction buffer. For some reactions BSA was added to final concentration of 100 µg/ml.

2.3.5. DNA electrophoresis and gel purification

DNA electrophoresis was done on 0.8 – 3% (w/v) agarose gels containing 0.1 µg/ml ethidium bromide in 1x TAE or TBE running buffer. DNA loading buffer was added to one tenth of the total sample volume. Depending on the expected sample size distribution, various DNA ladders (NEB, Invitrogen) were loaded besides the sample. Electrophoresis was carried out at 30 – 200 V for required time. DNA was visualised by UV illumination. If the DNA fragments were going to be purified, the UV damage was avoided by minimizing the exposure time to UV and using glass plate as a protection. For DNA purification the gel piece was excised with sterile scalpel. Recovery of the DNA fragments was carried out using QIAquick Gel Extraction Kit (Qiagen) following manufacturers recommendations.

2.3.6. DNA ligation

Prior to a ligation reaction, if necessary according to a cloning strategy, DNA was treated with Calf Intestine Phosphatase (NEB) to prevent vector self-ligation, T4 DNA polymerase (NEB) to fill in overhangs or poly-nucleotide kinase (NEB) for the phosphorylation of the DNA ends according the manufacturers recommendations. For the ligation reaction, DNA vector and insert sequences were mixed in equa-molar amounts (total 50 – 500 ng) and incubated with 6 – 12 Weiss Units of T4 DNA ligase (NEB) in the supplied buffer for 2 – 24 h at 20 - 4°C. After the ligation, whole reaction mixture was used for the transformation of bacteria.

2.3.7. Plasmid DNA transformation of competent *E.coli*

A frozen competent bacteria stock was defrosted on ice. Approximately 10 ng of bacterial plasmid or whole ligation reaction was cooled on ice and added to 200 µl of the bacterial stock. The mixture was left on ice for 20 min. Then the tube was transferred to a 42°C bath for 1 min and placed on ice again for a few minutes to cool down. Subsequently 1.2 ml of LB was added and the tube was incubated at 37°C for 1h. 100 µl of the transformation mix was plated on a selective agar plate. If a low transformation efficiency was expected (i.e. blunt end ligation) then the transformed cells were pelleted, most of supernatant is discarded leaving approximately 100 µl and all of the bacterial pellet was then plated onto the selective agar plate.

2.3.8. Small scale crude plasmid DNA preparation

Small scale crude DNA purification was often used for a restriction digest based screening of plasmid DNA constructs. Single bacterial colonies were streaked on around 3 - 4 cm^2 spots in Petri dish and incubated at 37°C overnight. Next day, some of the culture from the spot was scraped with a sterile tooth stick and re-suspended in 50 µl of TE with 100 µg/ml RNase A. Then 50 µl of 0.2 M NaOH, 1% SDS was added and the solution was gently mixed. Neutralisation was done by addition of 75 µl of 3M NaOAc (pH=5) and the liquid was again mixed gently by inverting the

tube. Insoluble proteins were then precipitated by 5 min centrifugation at 16 000 g in a benchtop centrifuge. The supernatant was transferred to a new tube, 130 µl of iso-propanol was added, solutions were mixed and precipitated by 10 min centrifugation at 16 000 g. The supernatant was discarded and the precipitate dissolved in 50 µl of water. Then 45 µl of 10 M LiCl was added, solutions were mixed and incubated at -80°C for 20 min. Proteins were precipitated with an additional 5 min centrifugation at 16 000 g and the supernatant was transferred to a tube containing 75 µl of isopropanol. Solutions were mixed and centrifuged for 10 min at 16 000 g. The DNA pellet was then washed once with 70% ethanol, briefly dried and re-suspended in 30 µl of water. 10 µl was usually used for a restriction digest.

2.3.9. Large, medium and small scale plasmid DNA purification

Plasmid DNA purification is a common technique and was done using the Qiagen Maxi, Midi and Mini prep kits, according to the manufacturer's instructions.

2.3.10. DNA labelling by direct incorporation of radioactive nucleotides

The protocol presented here is a general protocol used for radioactive labelling of DNA probes for Southern and Northern hybridisations. The protocol is adapted from Roche. 25 – 50 ng of DNA (usually sufficient for 1 - 2 hybridisations) was denatured by heating for 10 min at 100°C and snap cooled on ice. Then dDTP (final 72 µM each), hexanucleotide mix (containing random hexanucleotides and reaction buffer, Roche), P^{32}-αdCTP (40 µCi, ~3000 Ci/mmol, Amersham) and Klenow enzyme (2 U, Roche) were added. The reaction was incubated at 37°C for 30 min – 1 h. The probe was purified from unincorporated radio-nucleotides using a home made G50 sepharose (Amersham Biosciences) column. Before addition to the hybridisation solution, the probe was denatured (10 min at 100°C) and cooled on ice (5 min).

2.3.11. DNA end labelling by phosphate group transfer

DNA end labelling was used to label the 30 - 330 AFLP DNA Ladder (GibcoBRL). The labelling reaction was performed according to the manufacturer's recommendations. Briefly the reaction mix was prepared by mixing 4 µl of AFLP DNA Ladder, 2 µl of 5x kinase buffer (NEB), 2 µl of γ^{32}P-ATP (~3000 Ci/mmol; 10 µCi/µl) and 2 µl of (10 U/µl) T4 polynucleotide kinase (NEB). The reaction was incubated for 10 min at 37°C and stopped by heating for 15 min at 65°C. For the electrophoresis, 10 µl of TE buffer and 50 µl denaturing DNA loading buffer were additionally added. 7 µl of the labelled ladder was loaded onto each sequencing gel.

2.3.12. Southern blot using alkali transfer

Southern blots were done using standard procedures and recommendations from the Hybond-N+ (Amersham Biosciences) users manual. Briefly, DNA was digested overnight with the appropriate restriction endonuclease. Digested DNA was separated on 0.8 – 2.0 % (w/v) agarose gel containing 0.1 µg/ml ethidium bromide. After taking a photograph under UV for size evaluation purposes, the gel was incubated in depurination solution for 10 min on a gently shaking platform. The gel was then washed with water and incubated with denaturation solution for 30 min on a gently shaking platform. DNA was transferred onto Hybond-N+ membrane by capillary action using denaturation solution as the transfer buffer. The nucleic acid transfer was left to proceed overnight. After the transfer the membrane was pre-wetted in 0.5 M phosphate buffer and transferred into a hybridisation tube containing Church and Gilbert hybridisation buffer. Pre-hybridisation was done for at least 30 min in a 65°C oven. Later the solution was replaced with fresh hybridisation solution containing a radioactively labelled probe. The hybridisation was carried out overnight in a 65°C oven. After the hybridisation the blot was briefly rinsed with pre-heated 65°C 2x SSC 0.1% SDS. The washes are performed in 65°C as follows: 5 min twice with 2x SSC 0.1% SDS; 15 min with 1x SSC 0.1% SDS; 10 min twice 0.1x SSC 0.1% SDS. The membrane was then covered with Saran wrap and exposed to a phosphor cassette overnight. The next day the phosphor screen was scanned

using a Storm phosphor-imager (Molecular Dynamics). Signals were visualised and quantified with ImageQuant software v3.3 (Amersham).

2.3.13. Northern blot

Northern blots were done using standard procedures and recommendations from the Hybond-N+ (Amersham Biosciences) users manual. Electrophoresis was performed in a denaturing MOPS agarose gel (with 0.7 M formaldehyde) using MOPS as the electrophoresis buffer. Typically 30 µg of total RNA was denatured in RNA loading buffer at 55°C for 15 min. The sample was then placed on ice, and DNA loading buffer with ethidium bromide was added just prior to loading. The samples subjected to electrophoresis at 50 V in a 4°C room for 3 – 4 h. After electrophoresis, a photograph of the gel was taken in a UV chamber. Soon after, the gel was placed on a shaking platform in a box with distilled water for 15 min. The water was then replaced with 10x SSC, followed by a second incubation for 15 min. Later the RNA was transferred to Hybond-N+ membrane by capillary transfer using 20x SSC as the transfer buffer. After overnight transfer the RNA was crosslinked to the membrane using a Stratalinker 1800 (Stratagene) UV crosslinker (120 mJ). The blot was then pre-wetted in 0.5 M phosphate buffer. Hybridisation and washes were done as described in the Southern blot protocol (section 2.3.12 above).

2.3.14. Nascent RNA fluorescent in situ hybridization (FISH) on mouse brain tissue sections

The nascent RNA FISH protocol was adapted from the Nonradioactive In Situ Hybridisation Manual (Roche).

Generation of the RNA probe

The probe for nascent RNA FISH has to be located within an intron. The nascent RNA probe was PCR cloned into the pBSIIKS+ vector containing multiple cloning sites in between the T3 and T7 promoters. T3 and T7 promoters allow transcribing in sense and antisense directions. It was important to be able to synthesise either RNA

strand, because the probe transcribed from sense direction was used as a control for specific RNA hybridisation. The RNA probe was generated by *in vitro* transcription using UTP with covalently attached digoxigenin (Dig RNA labelling Mix; Roche). To increase permeability of long probes (longer than 1 kB) the probe was partially hydrolysed in 80 mM $NaHCO_3$, 120 mM Na_2CO_3 at 60°C for the required period of time. The incubation time depends on the length of the probe (L) to be hydrolysed and is calculated using formula $\frac{L-0.5}{0.055L}$. Probe was then precipitated with the addition of ethanol (75% final), 0.3 M sodium acetate and then examined by agarose electrophoresis. Finally, the probe was quantified using a dot blot and comparing intensities with a standard provided with the DIG labelling kit (Roche).

Preparation of cryopreserved brain sections for RNA FISH

5-15 μm thickness sections were cut with a CM1900 (Leica) cryostat and mounted on Super Frost Plus Gold (Erie Scientific Company) slides. The RNA was fixed in the tissue by heating the slides for 2 min at 50°C. After drying for 30 min at room temperature the sections were fixed in 4% paraformaldehyde in PBS for 10 min. The slides were then washed three times for 5 min in PBS. An excess of proteins was removed by overlaying the slides with 10 μg/ml proteinase K (RNase free, Sigma) solution for 10 min at room temperature. After an additional round of fixation in paraformaldehyde the slides were washed once with PBS and twice with 2x SSC. Sections were then used immediately for hybridisation.

FISH hybridisation and signal detection

Mounted sections were pre-hybridised for 1 h at 37°C in 100 μl of hybridisation buffer (4x SSC; 10% dextran sulfate; 1x Denhardt's solution; 2 mM EDTA; 50% formamide; 500 μg/ml herring sperm DNA; made with DEPC treated water) in a humidified sealed chamber (a box with tissues soaked with 50% formamide and 5x SSC). No coverslips were used. For the hybridisation, the solution was replaced with hybridisation solution containing 200 ng/ml of a DIG labelled RNA probe and incubated at 37°C for 16 h. After the hybridisation the sections were washed once for 5 min with 2x SSC at 37°C; three times for 5 min with 60% formamide 0.2x SSC at

37°C; twice for 5 min with 2x SSC at room temperature and once with 100 mM Tris-HCl (pH=7.5) 150 mM NaCl at room temperature. The sections were then blocked with blocking solution (100 mM Tris-HCl, 150 mM NaCl, 1% w/v blocking powder [Roche]) for 30 min at room temperature. The blocking solution was then replaced with primary anti-digoxigenin antibody (Roche) diluted 1:15 in blocking solution. The slides were incubated with the primary antibody for 2 h at room temperature. Antibodies were washed three times for 5 min with 100 mM Tris-HCl 150 mM NaCl at room temperature. The slides were then incubated with fluorescein anti-sheep IgG (Vector Laboratories) labelled secondary antibody (1:100 dilution) for 1 h at room temperature. Washes were performed the same as after the incubation with the primary antibody. The slides were then mounted with Vectashield + DAPI (Vector Laboratories) and examined with a Zeiss axioscope. Images were captured with IPLab v3.2 (Scanalytic) software.

2.3.15. Immuno-staining of monolayer cells

Cells were grown on a coverglass (BDH, 20x22 mm) in 6 well tissue culture plates. After an initial wash with PBS, the cells were fixed in 4% paraformaldehyde (in PBS) for 20 min. Subsequently, the cells were washed twice with PBS and permeabilised in 0.2% Triton X-100 (BDH) for 10 min. The cells were then washed 2x with PBS and blocked with 3% bovine serum albumine (Sigma). The primary antibody was diluted in blocking solution. 100 µl of diluted antibody was applied on a piece of Parafilm M (Sigma) and the coverglass was placed on the drop, upside down. The incubation was continued for 60 min. Primary antibodies were washed 3 times for 3 min in PBS. The incubation with an appropriate secondary antibody and subsequent washes were done the same way as with the primary antibody. The slides were then mounted with Vectashield + DAPI (Vector Laboratories) and examined using a Zeiss axioscope. Images were captured with IPLab v3.2 (Scanalytic) software.

2.3.16. cDNA synthesis

Prior to cDNA synthesis RNA was treated with RQ1 RNase-Free DNase (Promega) to avoid the contamination of sample with genomic DNA. cDNA was synthesised by annealing 5 μg of total RNA and 5 μg random hexanucleotides (Amersham) at 70°C for 5 min. Then the RT mix (final 1x reaction buffer, 40 U RNasin Ribonuclease Inhibitor (Promega), 1 mM dNTP) was added and the solution was incubated for 5 min at 25°C. After addition of M-MLV reverse transcriptase (RNase H Minus; Promega) the 25 μl reaction mix was incubated for 10 min at 25°C and 1 h at 37°C. The reverse transcriptase was inactivated by incubating for 10 min at 70°C. The reaction mixture was diluted to 500 μl and 2.5 μl used for PCR reactions. The control experiments (reactions without the reverse trascriptase) were always done and evaluated by PCR to ensure that there is no contamination or genomic DNA.

2.3.17. Western blotting

Proteins were separated using SDS denaturing poly-acrylamide gel electrophoresis (SDS-PAGE). After electrophoresis proteins were transferred to a Protran nitrocellulose (Schleicher & Schuell Bioscience GmBH) membrane using semi dry transfer apparatus Trans-Blot SD (BioRad). The membrane was then shifted to blocking solution (5 % milk powder in 1x TBS) and left to block overnight at 4°C. The next day the membrane was incubated with a primary antibody for 2 h at room temperature in a tube on a rolling platform. The unbound antibodies were washed 3 times (10 – 15 min each wash) with blocking buffer. Incubation with horseradish peroxidase (HRP) conjugated secondary antibody (1:5000 dilution in blocking solution) was done for 1 h at room temperature. Then the antibodies were washed once with blocking solution and twice with 1x TBS. After the last wash the membrane was incubated with ECL solution (mix of equal volumes of ECL solutions 1 and 2) for 1 min, wrapped in Saran wrap and exposed to ECL-grade film (Hyperfilm ECL, Amersham) for various lengths of time (usually 10 s, 1 min, 5 min). The films were then developed using a SCX-101A (Konica) medical film processor.

2.3.18. DNA sequencing

DNA sequencing was performed with Big Dye v3.1 (ABI PRISM) according to the manufacturer's recommendations. Briefly, the required amount of DNA (5 – 20 ng PCR product; 150 – 300 ng double stranded plasmid DNA) was mixed with 2 µl of Big Dye reaction mix and the required amount of primers (final concentration 3.2 pmol) in a 10 µl reaction volume. The reaction was then transferred into a thermo cycler (MJ Research). The cycling conditions were as follows:

Initial denaturation 96 °C for 1 min, then

25 cycles of

96 °C for 10 s,

50 °C for 5 s,

60 °C for 4 min.

DNA electrophoresis and fluorescence detection were performed by the sequencing service in the department of Biological sciences. Analysis of received DNA sequence trace was performed with Seqman (DNAStar).

2.3.19. Site-directed mutagenesis

Site directed mutagenesis was done with QuikChange XL Site-Directed Mutagenesis Kit (Stratagene) according to the manufacturer's recommendations. Briefly, primers with the target mutation were annealed to the plasmid, where the mutation had to be introduced. PCR was performed using high fidelity *Pfu* DNA polymerase resulting in nicked circular strands. Parental non-mutated plasmid was digested with *Dpn*I restriction endonuclease, which cuts methylated DNA (the parental plasmid is methylated by *dcm* from the host *E. coli*). Nicked plasmid was then transformed into the competent *E.coli,* where the nicks were repaired. Plating bacteria on selective

plates allowed growth of only the clones with the repaired plasmid. The mutation was then confirmed by DNA sequencing.

2.3.20. Real Time PCR

All Real-time PCR was performed using SYBR Green I chemistry. Fluorescent dye SYBR Green I binding to the minor groove of double stranded DNA helix enhances its fluorescence. During the PCR reaction, the amount of double stranded product increases resulting in an increase in fluorescence.

Real-time PCR analysis was done using the iCycler (Bio-Rad) Real Time PCR machine. Four reactions were done for each cDNA pool with IQ SYBR Green supermix (Bio-Rad) or a home-made mix consisting of 0.5x SYBR Green I (Molecular Probes); 10 nm fluorescein (Sigma); 1x PCR buffer with $MgCl_2$ (Roche); 200 μM dNTP (ABgene) and 1U FastStart *Taq* polymerase (Roche). The dilutions of cDNA (2x or 10x) were always made to ensure that fluorescence readings correlated with the amount of template used and to evaluate PCR efficiency (Figure 2-1 a,b). Standard PCR cycling conditions were as follows:

Initial denaturation and hot start *Taq* polymerase activation 95 °C for 3 min, then 40 cycles of

95 °C for 45 s,

T_a °C for 45 s,

T_a is the primers specific annealing temperature. There was no need for an additional extension step as products are usually very short (90 – 150 bp), therefore there was sufficient time for synthesis while thermal cycler was increasing the temperature of the block.

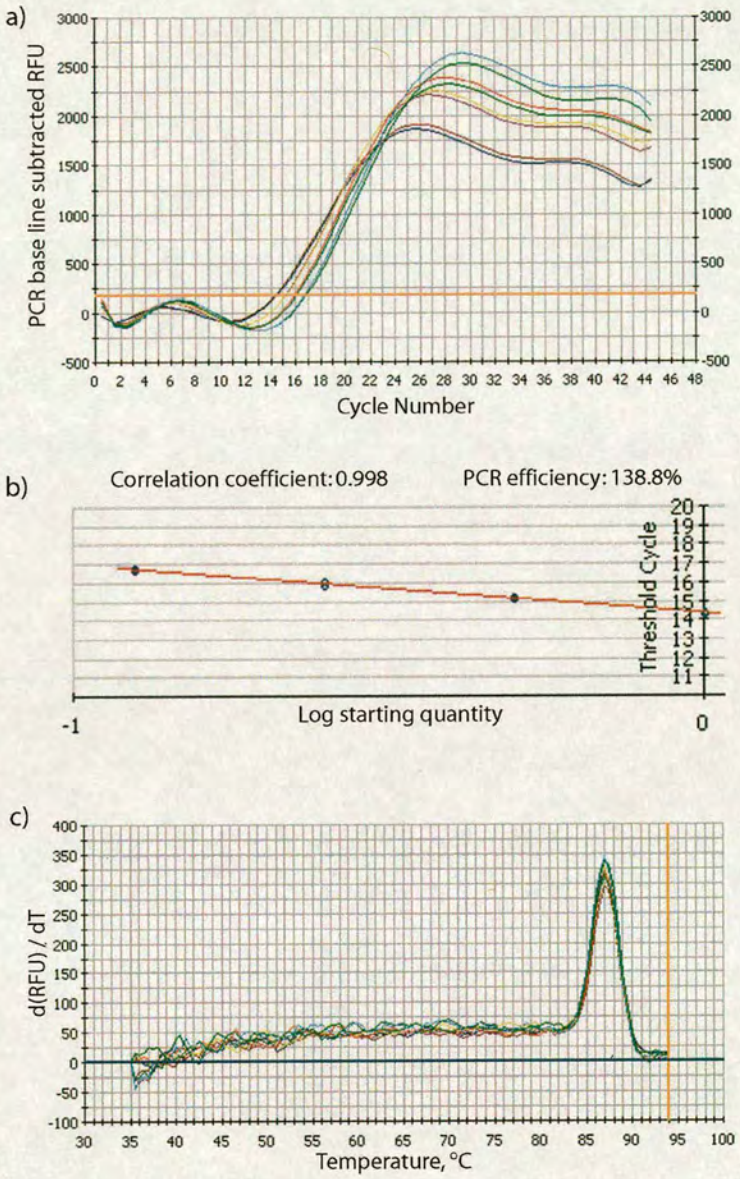

Figure 2-1. Evaluation of the Real Time PCR assay. *Gapdh* gene was amplified from mouse brain cDNA template. For each cDNA dilution the PCR was done in duplicate. a) The figure shows relative fluorescence change during PCR reaction (from blue to green cDNA is diluted twice: 1x, 0.5x, 0.25x, 0.125x). For more diluted DNA, more cycles are required to achieve the same fluorescence (the red line). b) Correlation between cycle number and the amount of template. The line is derived from data in panel a. c) Melt curve analysis shows one peak, which means that only one product was amplified during PCR reaction.

PCR was followed by melting curve analysis:

95 °C for 60 s, denaturation of product

35 °C for 10 s,

0.5 °C increase and 10 s incubation for 120 cycles.

The melting curve was used to determine, if the result of the PCR reaction was a single PCR product (Figure 2-1 c).

A constant fluorescence value was picked (usually 10 δ values above the baseline) from the linear phase of PCR amplification (Figure 2-1). To calculate the relative amounts of a transcript represented by cDNA (Q), following formula was used:

$$Q = 2^{-(Ct_{gene} - Ct_{gapdh})}$$

C_t (threshold cycle) is the fractional cycle number at which fluorescence of a sample passes the fixed threshold in the linear amplification range. Q values were calculated for each replica reaction. The mean, standard error of the mean and standard deviation were calculated and displayed with statistical software packages (SPSS, Sigma Plot). Comparison of the values was done using the Student t-test method.

2.3.21. Mammalian monolayer cell culture

Monolayer cells were grown in the required medium (listed in paragraph 2.1.3). To passage cells, the medium was aspirated, the flask was rinsed-aspirated with trypsin solution (1 ml per 25 cm^2 flask), then additional trypsin was added and cells were incubated 1 - 2 min in a 37°C incubator until cells have detached. Trypsinisation was stopped by addition of 5 volumes of complete medium and the suspension was transferred into a conical bottomed tube. Cells were pelleted by 5 min centrifugation at 1300 rpm. The supernatant was discarded and the cells were re-suspended in an appropriate volume of fresh medium.

For long term storage, the cells were usually kept in liquid nitrogen. Cultures to be frozen were passaged using the same protocol as above. In the last step of trypsinisation the cells were re-suspended in cold (+4°C) freezing medium and aliquoted into cryo-vials. The aliquots were then transferred to -20°C freezer for 2 h and to -80°C overnight. Then the vials were transferred to liquid nitrogen for long term storage. To defrost cells from frozen stocks, the cells were thawed rapidly at 37°C and diluted in the appropriate medium, before plating out.

Mouse embryonic stem cells were cultured in tissue culture plastic-ware pre coated with gelatine.

2.3.22. Monolayer cell transient transfection

Mouse fibroblasts were transfected using Lipofectamine Reagent (Invitrogen), according to the manufacturer's recommendations. Briefly, the day before transfection the cells were seeded at ~10^6 per well of a 6 well plate. When the cells had reached the required density, the medium was replaced with serum free Opti-MEM (Invitrogen). For each transfection 3 µg of DNA was diluted into 100 µl (final volume) of Opti-MEM and mixed with 15 µl Lipofectamine reagent diluted in 100 µl (final volume) of Opti-MEM. The resulting 200 µl mixture was incubated at room temperature for 45 min to form DNA-lipid complexes. The resulting mixture was then added to the well. Complete culture medium was usually added after 5 h. Cells were harvested 48 h after transfection.

2.3.23. Embryonic stem (ES) cell differentiation into neurons

Coating plastics for neuronal adhesion:

Poly-D-lysine (PDL) was diluted to 10 µg/ml with PBS. Enough PDL was applied to cover the surface and incubated at room temperature for 20 min. The PDL solution was then aspirated off and the plastics were washed twice with PBS. Laminin solution was applied (2 – 10 µg/ml) and left at room temperature for at least 20 min. The laminin was aspirated just before plating dissociated EB.

ES differentiation:

E14TG2a mouse ES cells were differentiated into neurons as described elsewhere (Li et al., 1998). ES cells were dissociated by trypsinisation and washed with ES cell medium without LIF. 10 ml of the cell suspension (5-7 x 10^5 cells/ml) was plated on a 90 mm bacterial grade plate (to prevent adhesion). Under these conditions, ES cells form embryoid bodies (EB), which contain different cell lineage progenitors. On the second day the media was replaced after letting the EB to sediment in a conical tube. On the fourth day media was again replaced and all-trans retinoic acid (Sigma) was added to a final concentration of 10 μM. The medium was again replaced with retinoic acid containing medium on the sixth day. On the eight day EB were collected into conical tubes and washed twice with PBS. The EB were dissociated by 5 min incubation with 500 μl of 4x trypsin-EDTA in a 37°C bath. Trypsinisation was stopped by the addition of 5 ml of the complete medium and the EB were pelleted by 5 min centrifugation at 1300 rpm. The pellet was re-suspended in complete medium and gently dissociated by pipetting with a glass pipette. Undigested EB were left to sediment for 5 min and upper portion, containing the single cells, was transferred to a fresh tube. The cells were then counted and pelleted by centrifugation. The pellet was re-suspended in DMEM/F12 with 1x N2 and the cells were plated 1-2 x 10^5 cells/cm^2 on a laminin pre-coated surface. One to two days later, half of the medium was replaced by Neurobasal medium supplemented with B27 (Gibco). Every three days, half of the medium was replaced with Neurobasal+B27 medium. The cells were used for experiments 1 - 2 weeks after plating. Most of the cells displayed a neuronal phenotype and stained positively with β-tubulin type III antibody (Figure 2-2).

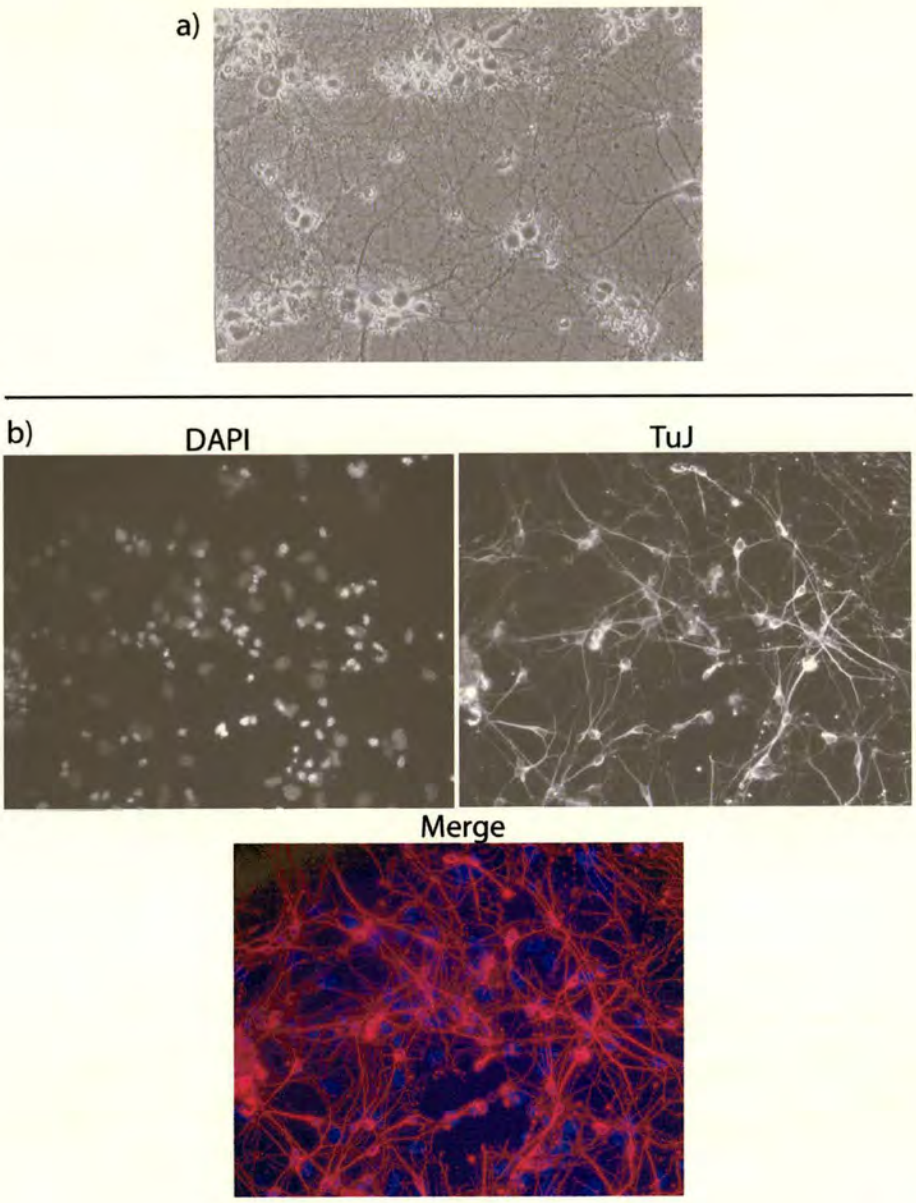

Figure 2-2. Neurons derived by *in vitro* differentiation of ES cells. a) Cell morphology through a light microscope after the differentiation procedure. Multiple outgrowths reminiscent of neuronal morphology. b) Cells stained with neuron specific β-tubulin type III antibody (TuJ). Many cells display strong staining.

2.3.24. ADDER differential display

Amplification of Double-stranded cDNA End Restriction Fragments (ADDER) has been described previously (Kornmann et al., 2001) and is presented here with minor modifications. Briefly, pooled total RNA samples were used for cDNA synthesis. Prior to cDNA synthesis the RNA samples were treated with RQ1 RNase free DNase (Promega). cDNA was synthesised using a polyA annealing oligonucleotide with a biotin label at 5' end (Figure 2-3). The cDNA was then adsorbed on magnetic streptavidin beads and cut with *Mbo*I (NEB) restriction endonuclease. The resulting DNA ends were ligated to oligonucleotide adaptors and then released from the beads by *Asc*I (NEB) digestion. These cDNA fragments were amplified and used as templates for differential display PCR using primers with different terminal nucleotides (total of 196 combinations, Table 2-2). Bands with different intensities in all three pools were cut from the gel, and eluted DNA was PCR amplified.

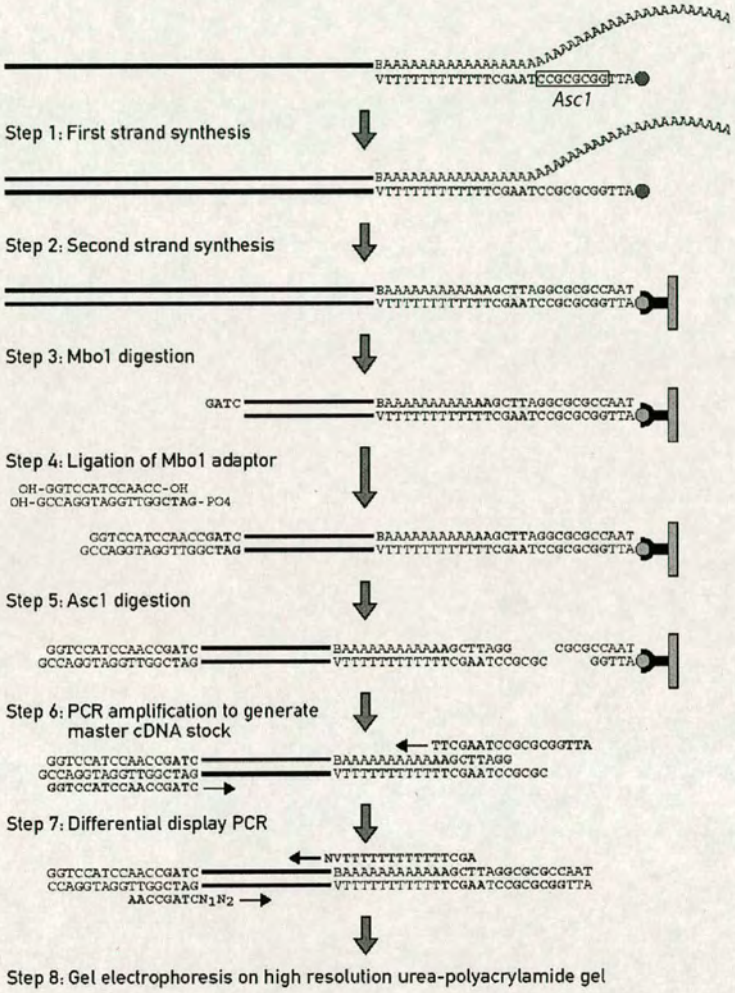

Figure 2-3 Schematic diagram shows steps involved in ADDER differential display. Diagram was taken from (Kornmann et al., 2001).

Instead of a general long primer containing NV at the 3' end, a specific primer e.g. ending with CA was used to amplify DNA eluted from gel bands (resulted in a better recovery). The re-amplified DNA was cloned into a plasmid vector. Restriction digest analysis of 24 picked clones allowed identification of the mis-expressed fragment.

2.3.25. Bisulfite DNA modification

1 μg of genomic DNA was digested with a restriction enzyme outside the region of interest. When digestion was complete the DNA was denatured by 5 min incubation at 100°C and 20 min incubation with fresh 0.3 M NaOH at 37°C. Then 10 volumes of bisulfite/hydroquinone mix (0.51 g/ml sodium hydrogensulfite (Aldrich 24 397-3), 0.11 g/ml hydroquinone (Sigma H9003) and 0.4 M NaOH) were added, the solution was overlayed with mineral oil and incubated for 5 h at 55°C. Bisulfite treated DNA was precipitated with isopropanol (with 50 μg of glycogen carrier) and washed with 70% ethanol. DNA was desulfonated by the addition of NaOH (0.3 M final) and 15 min incubation at 37°C. The DNA was then purified using a PCR purification kit (Qiagen). Primers for amplification of *Uqcrc1* promoter region were designed with Methprimer (Li and Dahiya, 2002): ubisd (AAATTATTTTTATATTGTTTTTTTT) and ubisr (AAACCCTTCATCTAATCCC ATCTA).

PCR amplified DNA was cloned using a TOPO cloning kit (Invitrogen), transformed into competent *E.coli* and plated on agar plates with X-gal for blue-white selection. Cloned inserts from white colonies were PCR amplified directly from the bacterial colony (bacterial colony was touched with sterile pipetman tip and then the tip was washed in 20 μl of water, which was used as the template for the PCR reaction). Half of the PCR reaction (usually 25 μl) was examined by agarose gel electrophoresis. Samples which migrated at the expected size were then used as the template for sequencing (5 μl from the other half of the PCR reaction was incubated with 5 U of Exonuclease I and 1 U of Shrimp alkaline phosphatase at 37°C for 15 min, followed by incubation at 80°C for 15 min; 2 μl were used as the template for the sequencing reaction).

2.3.26. Chromatin Immunoprecipitation

3 whole brains were used as input material (enough for 6-7 immunoprecipitations). Brains were ground in liquid nitrogen and the powder was poured into fixation solution (1 % formaldehyde in PBS). Fixation was continued for 15 min at room temperature and was quenched with 0.125 M (final) glycine solution. Pelleted cells were washed with PBS and homogenized in a dounce. After centrifugation cells were re-suspended in 9 ml of cell lysis buffer (0.2% NP40, 10 mM NaCl, 10 mM Tris-HCl pH=8, Complete [Roche] protease inhibitors). Lysate was triturated through a 25G needle until no lumps were left and incubated for 15 min in with added additional 6 ml of lysis buffer. Nuclei were then harvested by spinning at 4000 g for 5 min. and re-suspended in 3.6 ml of nuclei lysis buffer (50 mM Tris-HCl, 10 mM EDTA, 1% SDS, protease inhibitors). Nuclei were lysed for 10 min at room temperature and diluted with 2.2 ml of IP dilution buffer (1% Triton X-100, 2 mM EDTA, 150 mM NaCl, 20 mM Tris HCl pH=8, protease inhibitors). Chromatin was then sonicated twice for 4 min with a Branson Sonifier 250 (Duty cycle 60; Output 6), to obtain chromatin DNA fragments of about 200 bp on average. Chromatin was cleared by centrifugation, diluted five times, pre-cleared with protein A sepharose (Amersham) and subjected to overnight immunoprecipitation with the following antibodies: rabbit polyclonal antibody 674 against MeCP2 (Nan et al., 1998); rabbit polyclonal histone H3 di-methyl K9 antibody (Abcam) and un-relevant rabbit serum. Antibody precipitates were bound to protein A sepharose for 1 h. Washes were performed once with TSEI (0.1% SDS, 1% Triton X-100, 2 mM EDTA, 150 mM NaCl, 20 mM Tris-HCl pH=8), four times with TSEII (0.1% SDS, 1% Triton X-100, 2 mM EDTA, 500 mM NaCl, 20 mM Tris-HCl pH=8), once with buffer III (0.25 M LiCl, 1% NP40, 1% deoxycholate, 1 mM EDTA, 10 mM Tris-HCl pH=8) and three times with TE. Antibody precipitates were then extracted twice with extraction solution (1% SDS, 0.1 M sodium hydrocarbonate) and crosslinks were reversed overnight at 65°C. DNA was purified with Qiagen PCR purification kit and eluted in 50 µl of elution buffer (Qiagen). 2 µl of final eluate was used for PCR reactions. Uqcrc1 promoter PCR was done with primers uq1pd (CTTCTGTGTCTCCATTTCCCAAG) and uq1pr

(TCTGTGCAAGAAGGTGTCCAC). Bdnf pIII primers were the same as described previously (Chen et al., 2003b).

Sgk1 promoter primers were:

Sgkp1d	(ACGGACGGGGTTTAAGGCAGTG),
Sgkp1r	(CGTGAGGAGGTGGCGAGTTAGAG).

Fkbp5 promoter primers are:

Fkp1d	(TGCTCCCTTAGATTCATCCCACAC),
Fkp1r	(CCACTGGCTCCGATACACATTCTC).
Fkpd	(AGCCACGGTCCTAGATGAGAGC),
Fkpr	(GTGTGTGAAGGAGAGTGGCAGAAC).

2.3.27. TUNEL staining

TUNEL staining detects apoptotic cells by their DNA fragmentation characteristics. Fragmented (either by nicks or double stranded breaks) DNA can be labelled by 3'OH incorporation of a labelled nucleotide using terminal deoxynucleotidyl transferase (TdT).

TUNEL labelling was done using Roche *in situ* cell death detection kit, TMR red (# 2156792) according to the manufacturer's recommendations. Briefly, mouse brain 10 μm thickness cryostat sections were cut and adhered onto slides. The tissue sections were fixed in 4% paraformaldehyde in PBS (pH=7.4) for 20 min. After a 30 min wash in PBS, the sections were incubated with permeabilisation solution (0.1% Triton X-100, 0.1 % sodium citrate) for 2 min on ice. After two washes with PBS, 50 μl of TUNEL reaction mixture was added on top of the section and incubated for 1 h at 37°C in the dark. Subsequently the slides were washed three times with PBS and mounted using mounting medium with DAPI (Vector laboratories). Slides then were examined with a Zeiss axioscope.

For the negative control, a mixture was prepared without TdT. For the positive control a section was incubated with 30 U/ml of DNase I (in 50 mM Tris-HCl, 1 mg/ml BSA) for 10 min at room temperature.

2.3.28. Screening for mutations in exon 1 of the *Mecp2* gene in Rett syndrome patients

The human DNA samples were obtained from John Warner. 1 µl of genomic DNA was used in a 50 µl PCR mix, which had the following composition (Roche Fast Start Taq DNA Polymerase #2 032 902):

10x Reaction buffer with $MgCl_2$ (20 mM)	5 µl
2 mM (each) dNTP	5 µl
primer hME1d (50 ng/µl)	2.5 µl
primer hME1r (50 ng/µl)	2.5 µl
GC rich solution (Roche)	10 µl
H_2O	24.7 µl
Fast Start DNA Polymerase	0.3 µl

Cycling conditions:

Initial denaturation	4 min at 95°C
Denaturation	1 min at 95°C
Annealing	1 min at 63°C
Synthesis	1 min at 72°C

Primer sequences were hME1d (cagcccggccatcacagc) and hME1r (gacgggccgaggggagagt). The size of PCR product was examined by gel electrophoresis (10 µl of PCR product) and was expected to be 450 bp long. 20 µl of

PCR product was purified with a QIAGEN PCR purification kit and eluted in a final volume of 30 µl. 1 µl of this was used for the sequencing reaction with hME1d and hME1r primers (Big Dye version 3.1).

2.3.29. Generation of a mouse with a targeted mutation

Gene targeting enables the making of mutations in mice by using homologous recombination and the pluripotency of mouse embryonic stem cells (Thompson et al., 1989).

General description

Initially the mutation is engineered in the plasmid, which would have homologous arms to the target locus and resistance marker. The plasmid is then linearised and electroporated into mouse ES cells. Subsequently the ES cells are incubated in the presence of a selection drug which allows survival of the cells with the resistance marker. The ES colonies are then expanded and assayed by PCR or Southern blot to find the ones in which homologous recombination have occurred. The correctly targeted ES cells are injected into the mouse blastocysts, which are surgically transferred into pseudopregnant females.

The ES cells are derived from a mouse with agouti (129/Ola) coat colour and blastocysts are from a mouse with black coat colour (C57/BL), therefore the level of the ES cells contribution to the organism can be evaluated by the chimerism of coat colour. Coat colour as well helps to evaluate if the engineered mutation can be transmited from the chimera to the progeny. Because agouti colour is dominant, if crossing the agouti/black chimera with black partner produces an agouti progeny, then the progeny is going to be heterozygous for the engineered mutation too. And this is an end for the successful targeting experiment, because the mutated allele can further be propagated by maintaining the mutant mouse line.

Gene targeting was done according to published reports (Thompson et al., 1989; Hogan et al., 1994) and personal recommendations of Jim Selfridge and Jacky Guy.

ES cell electroporation

For gene targeting 50 x 10^6 cells were electroporated (BioRad Gene Pulser, 0.4 cm electrode gap cuvettes, 800 V, 3 μF) with 250 μg of linearised plasmid in 0.8 ml of HBS. After electroporation, the cells were left at room temperature for 10 min. Subsequently 8 x 10^6 cells were plated per 90 mm gelatinised dish. Selection with G418 (350 μg/ml) was applied 24 hours after plating. Cells were grown under selection until resistant colonies became visible (around 10 days).

Colony picking

ES cell colonies were picked into 96 or 24 well tissue culture plates. The following protocol is for a 96 well plate.

Ninety six well plates were prepared by the addition of 10 μl of PBS to each well. The medium was aspirated from dishes containing ES cell colonies, followed by washing them twice with 10 ml of PBS. After the last wash, some PBS was left in the dish, to prevent colony drying. The colony, together with 5 μl of PBS, was picked with a pipette tip and transferred to the 96 well plate containing 10 μl of PBS. After the transfer of 48 colonies, 20 μl of trypsin/EDTA was added to each well and the plate was incubated at 37°C for 3 - 5 min. Subsequently, the cells were pipetted to help dis-aggregation and incubated for an additional 3 - 5 min at 37°C. During the incubation a flat-bottomed gelatine coated 96 well plate was prepared by filling the wells with 100 μl of growth medium. After the trypsin incubation was finished, 120 μl of growth medium was added and all the contents of the wells transferred to the gelatine coated plate with 100 μl medium in it. Cells were grown until medium turned yellow (usually 2 days after picking). Then selection medium was replaced with 150 μl of fresh one.

When the cells in most wells became confluent, they were then split into other 96 or 24 well plates. One half was frozen down and the other half used for genomic DNA purification. After clones with the correctly targeted mutation were identified, the replicas were defrosted and expanded for injection into blastocysts.

ES cell microinjection into blastocysts and embryo transfer

ES cells were trypsinised and pipetted thoroughly to obtain a single cell suspension. Blastocycts were collected from C57BL/6 pregnant mice at 3.5 days p.c. by flushing uteri with M2 (Sigma) medium. After collection, the embryos were stored in M16 (Sigma) medium at 37°C until injection. Injections were done using Narashige micromanipulator in M2 medium. Under high power magnification, 10 – 15 cells were taken up into the injection needle and injected into the blastocysts. Ten injected blastocysts were then transferred into a drop containing M16 medium until the embryo transfer. Subsequently injected embryos were surgically transferred to the uteri of pseudopregnant (2.5 days p.c.) recipient females via a unilateral transfer of 10 embryos per recipient mouse.

2.3.30. Luciferase activity measurements

Luciferase activity was measured with a TD-20/20 Luminometer (Turber designs). The protocol and the reagents used for the measurements were from the Dual-Luciferase Reporter Assay System (Promega). Cells were washed with PBS once and lysed in a passive lysis buffer by incubation for 15 min at room temperature and then scraping cell lysates into a tube. Un-lysed cells were pelleted by spinning briefly. 100 µl of LAR II reagent (Promega) was added to a glass tube followed by addition of 20 µl of cell lysate. The tube was then transferred into the luminometer, which, after a pre-programmed 2 s delay, performed 10 s measurement of luminescence. Readings were repeated five times and normalised to the total protein concentration.

2.3.31. Generation of amino acid sequence alignments

Amino acid sequence alignmens were done using AlignX program (Informax). AlignX uses Clustal W algorithm (Thompson et al., 1994). Settings were as follows: gap opening penalty 15, gap extension penalty 6.66 and gap separation penalty 8. Visual enhancements (shading and etc) were done using GeneDoc software (http://www.psc.edu/biomed/genedoc).

2.3.32. BLAST searches

NCBI BLAST server was used to identify genes from ADDER differential display screen. 3' cDNA end sequences obtained by sequencing of clonned ADDER products were queried (using Mega BLAST) against nr (all GenBank, RefSeq Nucleotides, EMBL, DDBJ, PDB sequences) database. mRNA hit with highest score (usually >98% identity) was assigned as a candidate mis-regulated gene. If BLAST against nr database produced only genomic hits, then mouse EST database was queried.

2.3.33. Examination of condition of *Mecp2*-null mice

Gene expression studies were done using *Mecp2*-null mice which were backcrossed 6 times onto C57Bl/6 background. *Mecp2*-null mice were grouped into pre, early or late symptomatic groups according the phenotype at the time of brain dissection. Mice were selected by investigating clasping, inertia, tremor, weight loss and coat condition (Table 2-5). Examination of hindlimb clasping involved picking a mouse by the tail and visually assessing the hindlimbs. A *wt* mouse spreads its hindlimbs (-) whilst a *Mecp2*-null mouse at late stage of sickness clasps its hindlimbs (+). When evaluating inertia a mouse was transferred on the flat surface. Inertic mouse was sitting in one place (+), opposite to a normal mouse, which was running around investigating new area (-). Presence (+) or absence (-) of tremors was investigated by placing mouse on the hand. The assessment of weight loss was made by visually comparing wether a mouse was significantly smaller then it's siblings (+). Normal mouse usually has a shiny coat (-) contrary to a sick mouse which coat is dull and sticking (+).

Phenotype	Clasping	Inertia	Tremor	Weight loss	LOC*	Average Age
Pre-symptomatic	-	-	-	-	-	~30d
Early symptomatic	-/+	+	+	-	-	~55d
Late symptomatic	+	+	+	+	+	~ 70d

Table 2-5. Classification of *Mecp2*-null mice according to the manifestation of phenotype. The last column shows the average age of mice displaying the symptoms. The age was not considered in the classification. *LOC – loss of coat condition. Jacky Guy designed the main table categories.

3. Chapter three.

Gene expression analysis in *Mecp2*-null mouse brain

3.1. Introduction

Multiple observations show that methylation of a gene promoter restricts its expression in mammals. As a methyl CpG binding protein, MeCP2 was therefore tested for its transcriptional repression activity. Transient transfection experiments with methylated or GAL4 reporters demonstrated MeCP2's ability to repress transcription (Nan et al., 1997). The transcriptional repression hypothesis was even more strengthened by findings that MeCP2 interacts with the already known Sin3a / HDAC1,2 co-repressor complex (Nan et al., 1998; Jones et al., 1998).

Due to the low complexity of the MeCP2 binding site, it was postulated that MeCP2 might be a global transcriptional repressor. It was thus expected that many genes will be deregulated in the absence of MeCP2. However, it has been difficult to find global differences in gene expression between wild-type and *Mecp2*-nulls mice brains (Tudor et al., 2002) or clonal cell lines from the human Rett syndrome patients (Traynor et al., 2002). A key point in the field then became to find endogenous target genes, which would confirm or reject the idea of an *in vivo* role of the MeCP2 in transcriptional repression and could serve as a tool for the investigation of its transcriptional repression mechanism.

Another important purpose of MeCP2 target gene identification is to understand the pathology of Rett syndrome. The discovery of *MECP2* mutations as the cause of this neurological disorder was rather surprising, because MECP2 had no previously known connections with a specific role in brain. One potential possibility is that MeCP2 is involved in regulation of certain genes, which are important in normal brain function. Finding target genes would help to clarify what is happening when MeCP2 is damaged due to a mutation.

This gene expression analysis chapter is divided into seven sections. The introduction will review the currently published achievements in finding "candidate" genes and previous attempts in identifying mis-regulated genes by global analysis of gene expression. The following results section will address mis-regulation of several candidate genes (*Bdnf*, *Ss18l1* and *Hes1*) in mouse brain. Subsequently verification of genes obtained by microarray analysis together with promoter occupancy will

follow. ADDER, a variant of differential display, was completed, and a dozen genes were found to be mis-regulated in late symptomatic *Mecp2*-null brain. The final, section explains the experiments addressing the biological meaning of several mis-regulated genes (*Meg3/gtl2* and *Uqcrc1*). Investigation of *Meg3/gtl2* imprinting status revealed no bi-allelic expression, and the mitochondrial respiration measurements showed performance defects in certain components of respiration chain.

3.2. Literature overview of previously identified MeCP2 target genes by a candidate approach

The expression of imprinted genes correlates with the methylation status of differentially methylated regions (DMR), suggesting the involvement of members of MBD family. *Fuks et al* tested the role of MeCP2 on the imprinted non-coding *h19* gene in tissue culture cells (Fuks et al., 2003). In *Mecp2*-null mouse fibroblasts *h19* expression was found to be up-regulated compared to *wt* cells. MeCP2 was associated with the methylated DMR, suggesting that *h19* could be a direct target of repression by MeCP2. Over-expression of MeCP2 in *wt* cells lead to increased occupancy of MeCP2 at the *h19* locus and increased level of histone H3 lysine 9 methylation in the *h19* DMR (Fuks et al., 2003). Together with MeCP2-GST pull-downs of methyltransferase activity, occupancy studies by chromatin IP suggested that MeCP2 recruits H3K9 methyltransferase to the *h19* locus, which would result in methylation of histones and facilitate silencing of transcription (Fuks et al., 2003).

In frogs inhibition of MeCP2 translation by morpholino oligonucleotide injection resulted in developmental arrest (Stancheva et al., 2003). *Stancheva et al* then examined the expression of genes involved in early neurogenesis. Morpholino MeCP2 down-regulation have not resulted in mis-regulation of proneural genes (*neurogenin*, *NeuroD* and *Notch/Delta*), but affected downstream targets (*Hairy2a, N-tubulin and NCAM*) (Stancheva et al., 2003). In more detail, MeCP2 morpholino frogs had *Hairy2a* up-regulated, while other genes (*N-tubulin* and *NCAM*) were down-regulated (Stancheva et al., 2003). *Hairy2a* encodes a basic-helix-loop-helix

transcription factor, which in turn represses a group of neural genes. Because it acts up-stream of the other mis-regulated genes and it is up-regulated in the absence of the transcriptional repressor, it was thought to be a primary target for MeCP2. This assumption was confirmed by chromatin IP, which showed the presence of MeCP2 at the *Hairy2a* promoter in frog embryos. Interestingly, after the *Notch/Delta* signaling, MeCP2 was removed from the *Hairy2a* promoter by the intracellular domain of Notch (Stancheva et al., 2003).

Recent studies have identified *Bdnf* as a target gene of MeCP2 (Martinowich et al., 2003; Chen et al., 2003b). The *Bdnf* promoter 3 is highly induced by calcium influx in cultured neurons. By introduction of point mutations in the different minimal promoter sites, several factors required for calcium mediated *Bdnf* induction were identified, such us calcium response factor (CaRF), upstream stimulatory factors (USFs) and calcium/cAMP responsive element binding protein (CREB) (Tao et al., 1998). There are several CpGs in the promoter 3 region, therefore authors have examined the possibility of MeCP2 presence by chromatin IP (Martinowich et al., 2003; Chen et al., 2003b). Interestingly, several CpGs in that locus were methylated and MeCP2 was found binding to the promoter region. Upon calcium influx MeCP2 was shown to become phosphorylated and leave the *Bdnf* promoter (Chen et al., 2003b). The other group however observed significant de-methylation of *Bdnf* promoter 3, which was suggested as a reason why MeCP2 leaves the promoter (Martinowich et al., 2003). Possibly both de-methylation and phosphorylation contributes to MeCP2 leaving the *Bdnf* promoter. Interestingly, MeCP2 disappearance correlates with local changes in chromatin structure such as decrease in histone H3 lysine 9 methylation, increase in H3 lysine 4 methylation and H4/H3 acetylation (Martinowich et al., 2003). Absence of MeCP2 in cultured cortical neurons resulted in almost two fold higher basal level of *Bdnf*. When induced by calcium, which increases *Bdnf* expression up to 100 fold, the difference between *Mecp2*-null and *wt* neurons disappears (Chen et al., 2003b).

3.3. Previously described attempts to identify MeCP2 target genes by global analysis of gene expression

Mis-regulation of gene expression in Rett syndrome patients has been examined using post-mortem brains and microarray analysis (Colantuoni et al., 2001). Multiple microarray experiments allowed identification of many mis-regulated genes. Glial GFAP and α B-crystallin were confirmed to be up-regulated using several different methods, but not in all patient samples examined (Colantuoni et al., 2001). Other group have failed to confirm mis-regulation of these genes in mouse model of Rett syndrome (Tudor et al., 2002).

Global gene expression analysis was performed on clonal fibroblast cell lines derived from Rett syndrome patients (Traynor et al., 2002). Affymetrix microarrays identified mis-regulated genes, but Real Time PCR analysis showed significant variability between different clones rather than genotypes. The study concluded that there is no global deregulation of gene expression, which could be detectable in the cell lines (Traynor et al., 2002). However the cell lines used in the study express *MECP2* at a much lower level than brain (Traynor et al., 2002), thus the transcriptional consequences of the mutations in MECP2 may be reduced in these cells.

Affymetrix microarrays were used to investigate global gene expression changes in different brain regions of *Mecp2*-null mice (Tudor et al., 2002). Multiple experiments revealed no significant gene mis-expression. However when the advanced gene expression classifiers were used, predictions could correctly distinguish between *wt* and *Mecp2*-null mice brains. The best candidates for prediction were serum glucocorticoid kinase (SGK), Cam kinase II, prostaglandin D2 synthase, Rho GDP dissociation inhibitor γ and parvalbumin. (Tudor et al., 2002).

Recently, another method was used to identify MeCP2 target genes. Chromatin IP was used to make a library enriched in fragments bound to MeCP2 in the human cell line, MCF7 (Koch and Stratling, 2004). Sequencing of the library clones identified different repeat families, most of them being Alu repeats, SINEs and LINEs.

3.4. MeCP2 target genes identified by candidate approach

3.4.1. Bdnf mRNA is down-regulated in *Mecp2*-null mouse brain

As described in the section above, during resting state *Bdnf* mRNA was found present in a two fold excess in *Mecp2*-null cultured cortical neurons (Chen and Weber, 2004). Because *Bdnf* expression was compared in a cultured neuronal cell system, we decided to examine *Bdnf* expression in *Mecp2*-null mouse brain tissue. For the analysis mice were classified according the manifestation of symptoms into three groups – pre-symptomatic, early symptomatic and late symptomatic (Table 2-5 in page 88). The grouping of mouse according the phenotype presentation rather than the age was decided because of observations that even in the same litter *Mecp2*-nulls start to display symptoms at different ages. A pre-symptomatic mouse looks undistinguishable from a *wt* littermate. According our criteria, an early symptomatic mouse has a tremor which can be felt when a mouse is held on the hand, reduced movement in the cage and sometimes clasps its hindlimbs if picked by the tail. It is easy to find a late symptomatic mouse in the cage, because it sits in one place, it is smaller than littermates and has a dull coat as well as other symptoms listed at Table 2-5.

For the each group and genotype we pooled mouse brain RNA from nine mice into three pools of three. cDNA was made from these pools and used for Real Time PCR analysis. Because *Bdnf* is transcribed from four different promoters, we initially asked if the total coding *Bdnf* mRNA level is different between *wt* and *Mecp2*-null mice samples. Surprisingly, the quantitative Real Time PCR analysis demonstrated that *Bdnf* mRNA is significantly down-regulated in *Mecp2*-null mouse brain (Figure 3-1). Furthermore, *Bdnf* was found to be down-regulated at all three different stages of disease progression, from 35% in late symptomatic mice to 23% in pre-symptomatic mice (Figure 3-1). This finding with whole brain cDNA is opposite to the previously published observations in *Mecp2* deficient neuronal cultures, where basal *Bdnf* mRNA level was found to be two fold up-regulated (Chen et al., 2003b).

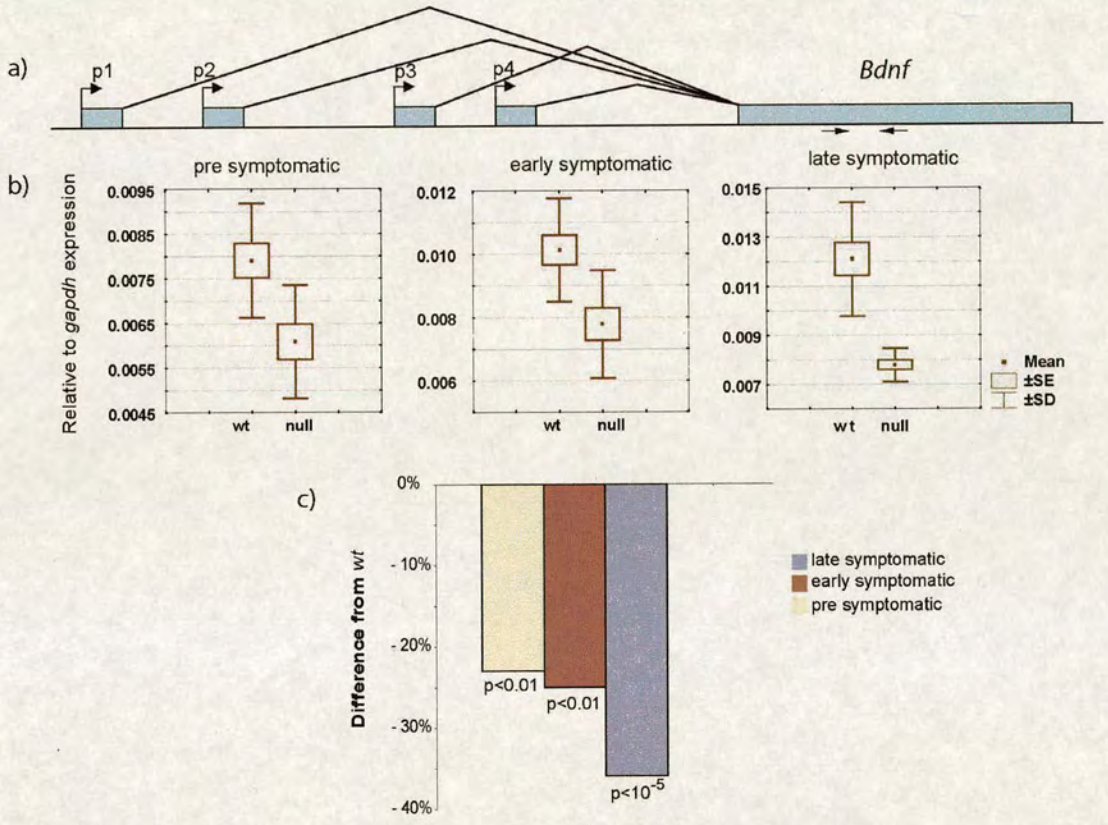

Figure 3-1. *Bdnf* expression is significantly down-regulated in the *Mecp2*-null mouse brain during progression of symptoms. a) Schematic structure of the *Bdnf* gene. Boxes represent exons. p1, p2, p3 and p4 are different *Bdnf* promoters and the long box contains coding DNA region. The two arrows underneath the box show the position of primer pairs used for the Real Time PCR analysis. b) Primary Real Time PCR data of *Bdnf* expression. The dot in a box represents the mean of Real Time PCR values, a box outlines the standard error of the mean and the whisker is standard deviation. c) Statistical analysis of Real Time PCR data. Columns represent the difference from the corresponding *wt* value and the statistical significance of the difference is displayed as a p value (Student t test).

The discrepancy between these observations raised several possibilities. Firstly, the study of *Chen et al.* examined the transcription from *Bdnf* promoter 3 only, whereas here the total *Bdnf* expression was assayed, which starts at all promoters (see primers in Figure 3-1). Therefore, there was a possibility that a different *Bdnf* promoter is responsible for the down-regulation of total *Bdnf*. To test this hypothesis we examined transcripts from the different *Bdnf* promoters using promoter-specific Real Time PCR primers in pre-symptomatic mice (Figure 3-2). The data revealed that there is no significant contribution from any one promoter, however promoter 3 showed the lowest p value ($p=0.07$) and the highest down regulation (22%). Further we examined possibility of potential feedback mechanism, which could act through the high affinity Bdnf receptor Ntrk2 (trkB). It has been reported that external application of Bdnf results in a decrease of full length Ntrk2 receptor in retina (Chen and Weber, 2004). Therefore, we have compared Ntrk2 mRNA levels in *wt* and *Mecp2*-null mouse brain (Figure 3-3 a). There was no statistically significant difference in Ntrk2 mRNA levels, suggesting that up-regulation of Bdnf mRNA does not alter expression of its receptor.

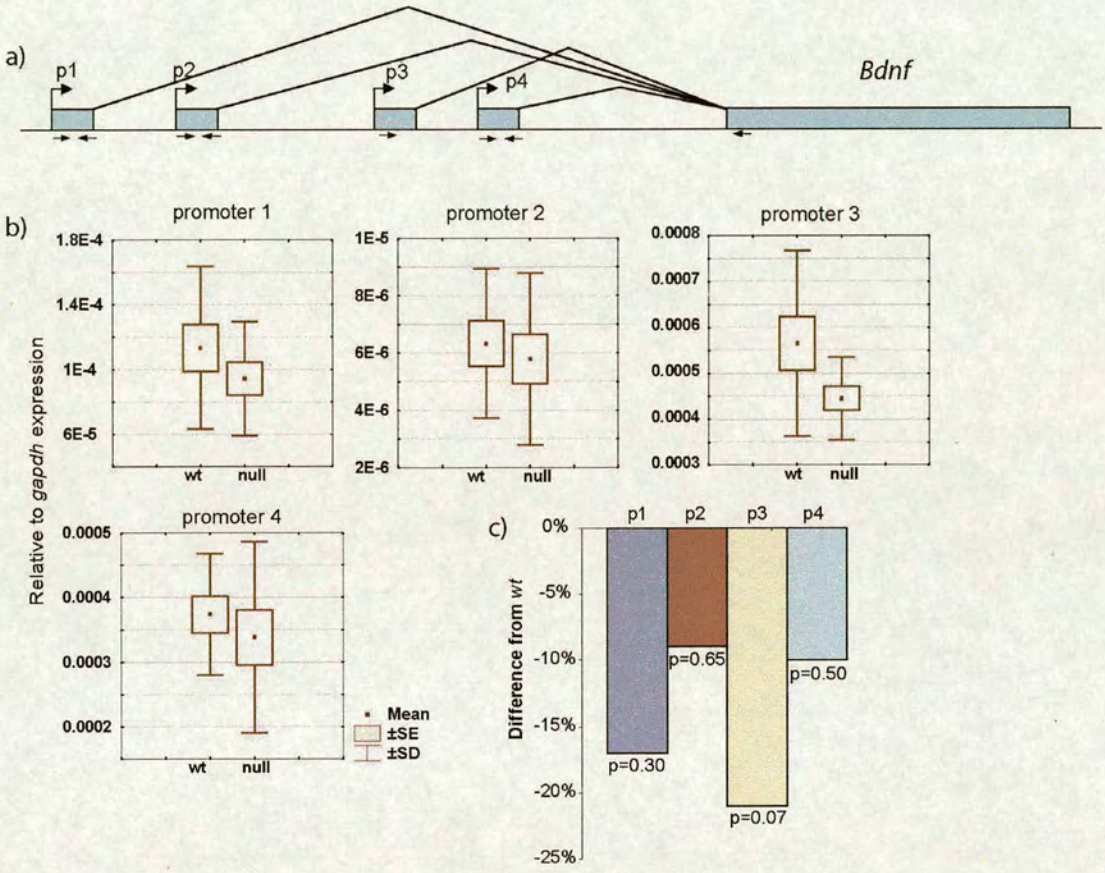

Figure 3-2. Contribution of different *Bdnf* promoters to the total Bdnf mRNA under-representation in pre-symptomatic *Mecp2*-null mouse brain. a) Structure of the *Bdnf* gene. p1, p2, p3 and p4 are different promoters that generate alternative first exons that are spliced onto exon 2. Specific primers, used for detection of each transcript are shown below. For promoter 3 one primer was used from p3 region and other was from exon 2 of *Bdnf*. b) Data from Real Time PCR analysis of different promoter activity. c) Statistical analysis of Real Time PCR data. No single promoter is significantly down-regulated. Significance of difference between expression in *wt* and *Mecp2*-null mouse brain is displayed by p value.

3.4.2. Ss18l1 (Crest) mRNA is not mis-regulated in *Mecp2*-null mouse brain

Ss18l1 was selected as a candidate gene for examination because of the phenotypic and pathological overlap between *Mecp2*-null and *Ss18l1*-null mouse. *Ss18l1*-null mice look normal at birth, but later develop coordination defects and are smaller than littermates (Aizawa et al., 2004). Most of the mutant mice die between post-natal day 14 and 28. The pathological analysis done by *Aizawa et al* revealed that *Ss18l1*-null mice have smaller cortex and cerebellum. There was also a marked decrease in dendritic branching and growth (Aizawa et al., 2004). Because above mentioned pathological findings observed in *Ss18l1*-null mice are similar to ones in the *Mecp2*-null mice (described in section 1.6 in the literature review chapter), we thought of a possibility that a similar molecular pathway could be affected. A simple hypothesis is that MeCP2 is involved in the regulation of *Ss18l1* expression. We have compared *Ss18l1* expression between the late symptomatic *Mecp2*-null mice and *wt* littermates. Real Time PCR data showed no mis-regulation of *Ss18l1* expression in late symptomatic mice (Figure 3-3 b).

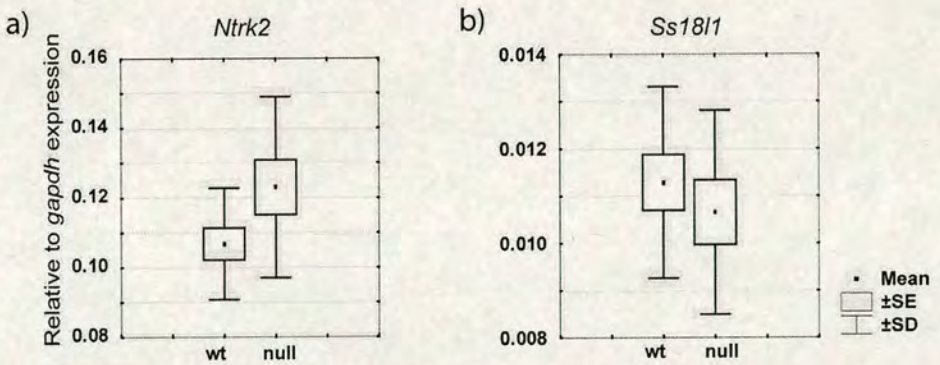

Figure 3-3. *Ntrk2* and *Ss18l1* are not mis-regulated in late symptomatic *Mecp2*-null mouse brain. a) Real Time PCR data of *Ntrk2* expression. Statistical analysis revealed that there is no significant mis-regulation (p=0.08) of *Ntrk2* in *Mecp2*-null mouse brain. b) Real Time PCR data of *Ss18l1* expression. There is no significant mis-regulation (p=0.49).

3.4.3. Mammalian homolog of *Hairy2a* is up-regulated in the *Mecp2*-null mouse brain

Section 3.2 describes the findings by *Stancheva et al* showing that in frog embryos lacking MeCP2, *Hairy2a* expression is up-regulated. Even though *Mecp2* deletion in a mouse does not give as severe phenotype as the morpholino knock-down in frogs, the possibility was considered that MeCP2 might be involved in the regulation of the mammalian homolog of *Hairy2a*. *Hes1* is the closest *Hairy2a* homolog in mammals. Therefore the expression of *Hes1* was examined in *Mecp2*-null mouse brain. Interestingly, *Hes1* was found to be significantly up-regulated in pre, early and late symptomatic mice (Figure 3-4). The level of up-regulation is moderate and reaches its maximum of 80 % in late-symptomatic *Mecp2*-null mice.

3.4.4. Verification and syptom-course analysis of *Sgk* and *Fkbp5* expression

In collaboration with Ulrike A. Nuber and Jacky Guy microarray analysis was carried out on the late symptomatic *Mecp2*-null mouse brain. Eleven genes were identified mis-regulated and four of these genes (*Fkbp5*, *Sgk*, *Pomc1* and *Hsp105*) are known to be regulated by stress hormones, glucocorticoids. *Fkbp5* encodes a peptidyl-prolyl cis-trans-isomerase which was shown to interact with glucocorticoid receptor in cell-free receptor assembly assay (Barent et al., 1998). Serum glucocorticoid induced kinase (SGK1) is up-regulated immediately when cells are exposed to glucocorticoids (Lang and Cohen, 2001). Real Time PCR analysis was performed to verify mis-regulation of *Sgk* and *Fkbp5* genes. Consistent with microarray results, *Sgk* and *Fkbp5* expression was found to be up regulated to around 2.6 fold in late symptomatic *Mecp2*-null mice (Figure 3-5). Additionally, expression analysis in early and late symptomatic mice demonstrated significant up-regulation at these stages as well. Interestingly, the standard deviation was increased significantly (F-test, $p<0.001$) in early and late symptomatic *Mecp2*-null mice for both *Fkbp5* and *Sgk* genes (Figure 3-5 a).

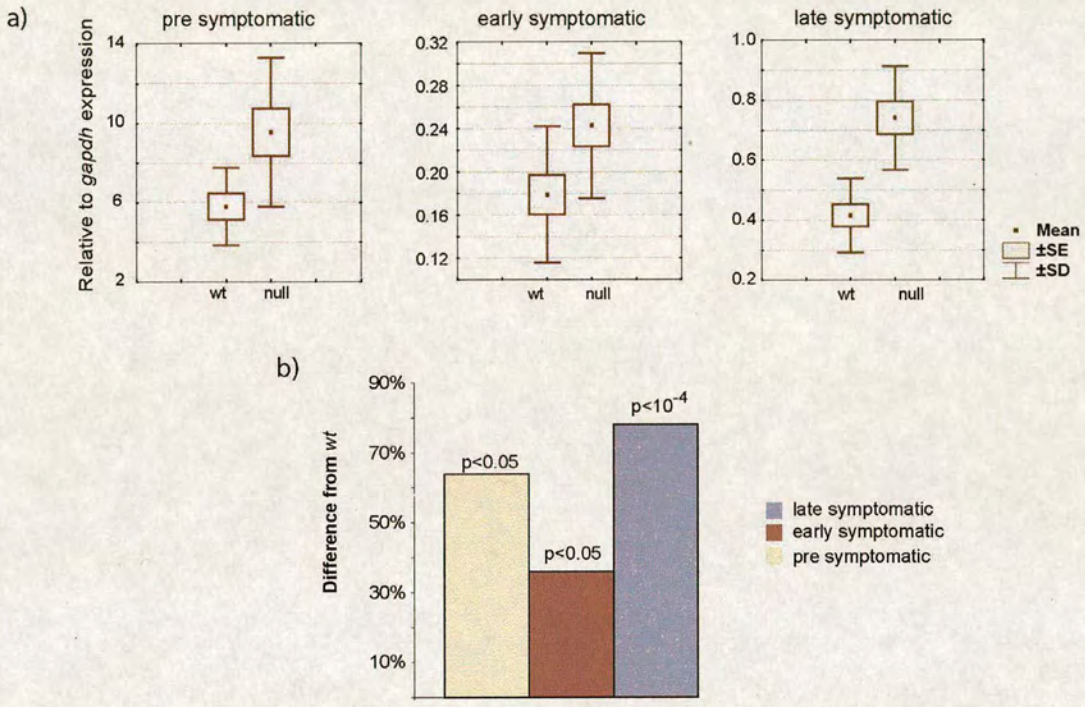

Figure 3-4. *Hes1* is significantly up-regulated at all stages of disease examined. a) Real Time PCR data shows significantly increased *Hes1* mRNA abundance in pre, early and late symptomatic *Mecp2*-null mice brain. b) Statistical analysis and the level of up-regulation in *Mecp2*-null mouse brain.

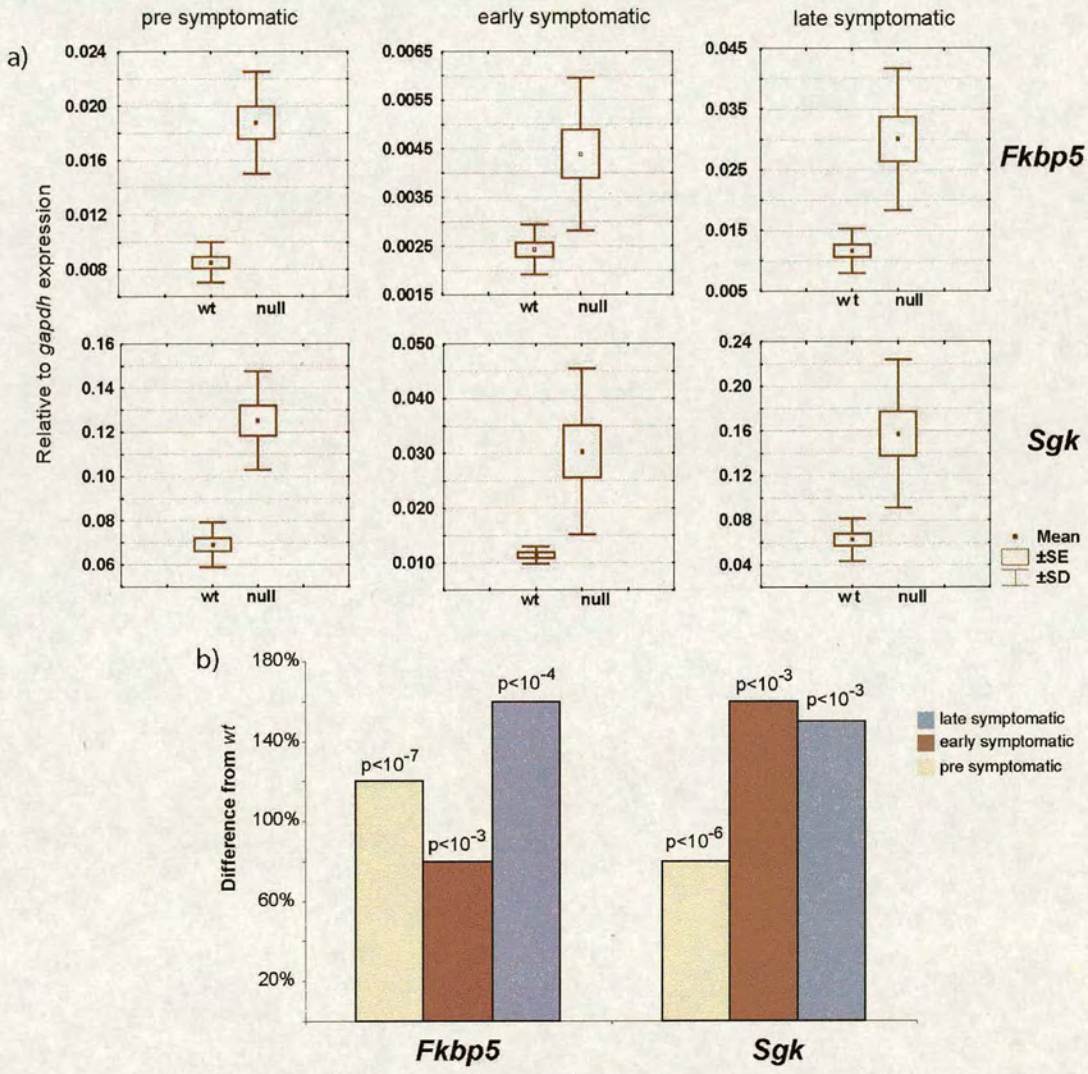

Figure 3-5. *Fkbp5* and *Sgk* are significantly up-regulated in pre, early and late symptomatic mice. a) Real Time PCR analysis of *Fkbp5* and *Sgk* expression. Note highly increased standard deviations in early and late symptomatic mice *Mecp2*-null mice. b) T-test statistical analysis and the level of up-regulation, compared with *wt* littermates. Both genes are significantly up-regulated in all stages examined.

Because both *Sgk* and *Fkbp5* are regulated in the response to stress hormones, the possibility was considered that the hormone levels are elevated in these mice. Therefore the circulating glucocorticoid levels were measured in *Mecp2*-null mice (work done by Jim Selfridge and Megan C. Holmes). There was no significant difference of basal and stressed levels of circulating glucocorticoids between *Mecp2*-null mouse and *wt* littermates. If not the hormones induce *Sgk* and *Fkbp5* up-regulation in *Mecp2*-null mice, then it could be that MeCP2 directly regulates expression of these genes. In this case it was expected that MeCP2 would bind promoter regions of *Sgk* and *Fkbp5* genes. The presence of MeCP2 was examined by chromatin IP and MeCP2 was found to bind in the vicinity of both *Sgk* and *Fkbp5* promoters (Figure 3-6 c, placebo).

It was previously demonstrated that MeCP2 leaves the promoter III of *Bdnf* after *Bdnf* induction by membrane depolarization (Chen et al., 2003b; Martinowich et al., 2003). We thought that MeCP2 could behave in the similar manner on the *Sgk* and *Fkbp5* promoters, when these genes are induced by glucocorticoids. For this experiment mice were implanted with corticosterone and placebo pumps for 2 days and sacrificed 3 days later (experiment done by Megan C. Holmes). The plasma corticosterone level was increased approximately 7.4 folds (measured by Megan C. Holmes). Comparison of *Sgk* and *Fkbp5* promoter occupancy by MeCP2 between vehicle and hormone treated mice brain revealed the absence of any obvious changes (Figure 3-6).

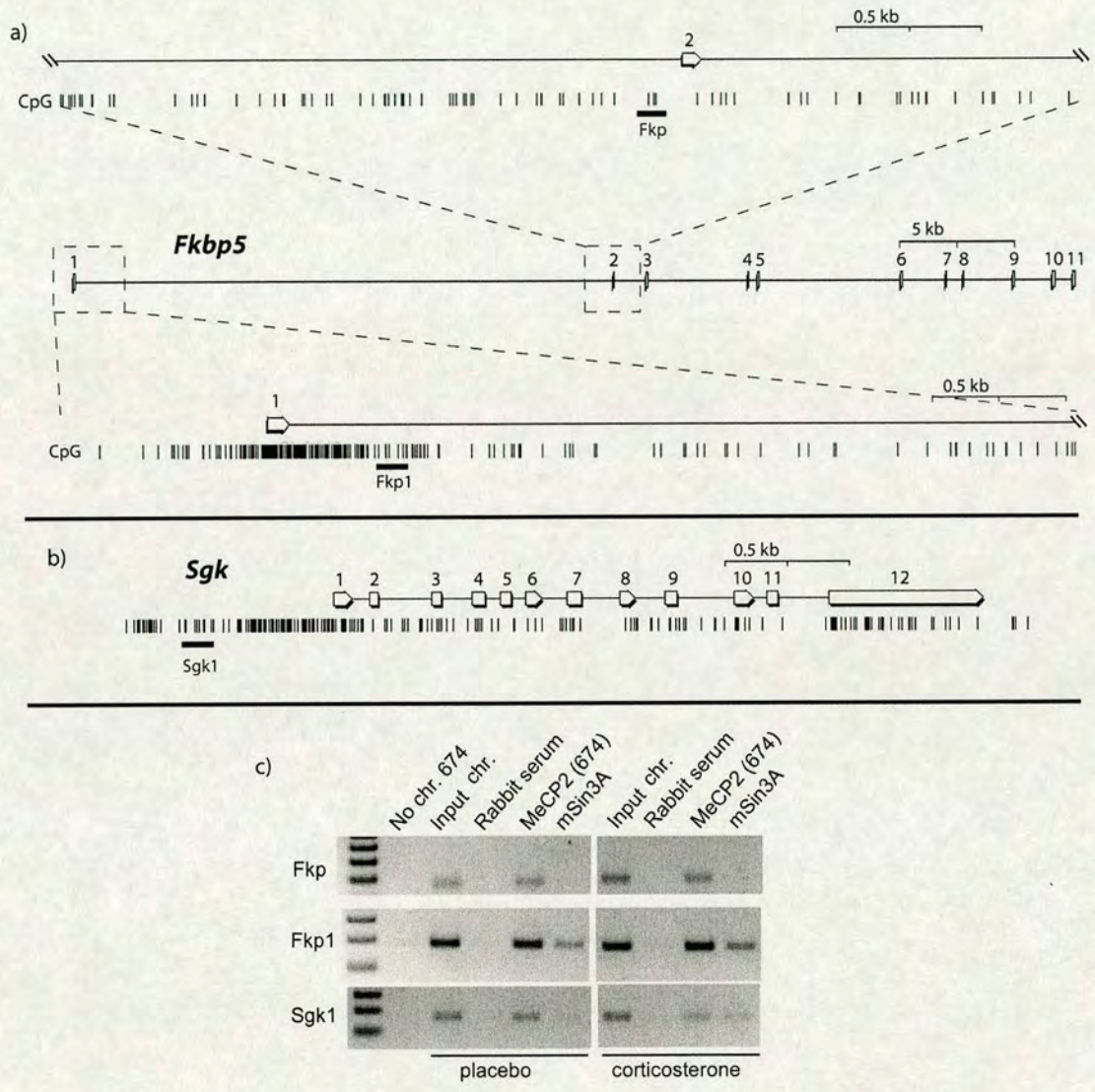

Figure 3-6. MeCP2 presence at the two different regions of *Fkbp5* and one region of *Sgk* is not abolished after the infusion of corticosterone. a) Genomic organisation of *Fkbp5* gene. The regions which were used for the amplification after chromatin IP are marked as solid lines. Two regions of *Fkbp5* were assayed because the current information is limited in distinguishing which is the real promoter (Exon 1 is non-coding). b) Genomic organisation of *Sgk* gene with the highlighted region of PCR amplification. c) PCR analysis of chromatin IP DNA fragments from hormone treated and control mice brains. Similar amounts of Fkp, Fkp1 and Sgk1 DNA fragments were precipitated with MeCP2 antibody after corticosterone treatment. MeCP2 (674) antibody is raised against N-terminal part of MeCP2 and it recognises both MeCP2 isoforms.

3.5. Global analysis of gene expression

3.5.1. Gene expression analysis in *Mecp2*-null mouse brain by a variant of differential display

Conventional differential display is based on cDNA synthesis and PCR amplification using different primer sets, which will amplify different set of genes. The labelled PCR products are then resolved on high resolution gels and intensities of PCR products can be compared between the samples.

The benefits of differential display are that the method is not dependent on the knowledge about expressed genes and PCR amplification allows detection of low abundance transcripts. The same benefit provides the hitch as well. Thus the band of interest needs to be extracted, cloned and identified before it is possible know which gene it represents. Another problem with conventional differential display is that it suffers from reproducibility difficulties. Reproducibility and sensitivity issues were improved by *Kornmann et al* in developing a new variant of different display termed ADDER (Kornmann et al., 2001). Instead of using arbitrary 10-mers for cDNA synthesis and differential display PCR, ADDER uses adaptor sequences with all possible combinations of two 3' nucleotides, which allow selective amplification of different cDNA sub-populations (Figure 3-7 and more detail description in the second chapter of materials and methods).

ADDER and other differential display techniques were reported to suffer from the presence of polymorphisms in the genome, which could be found even in the genome of inbred mouse strains. Even one nucleotide difference in a primer binding site could change the efficiency by which the product is amplified. Additionally insertions or deletions would change the amplified fragment size. To avoid false positives, which could appear due to polymorphisms, in the differential dispaly screen we used RNA from nine mouse brains pooled into three pools, 3 brains in each. For the analysis we carefully grouped *Mecp2*-null mice according the presentation of symptoms (Table 2-5) and used late symptomatic mice for ADDER experiment, with the expectation to see more differentially expressed genes.

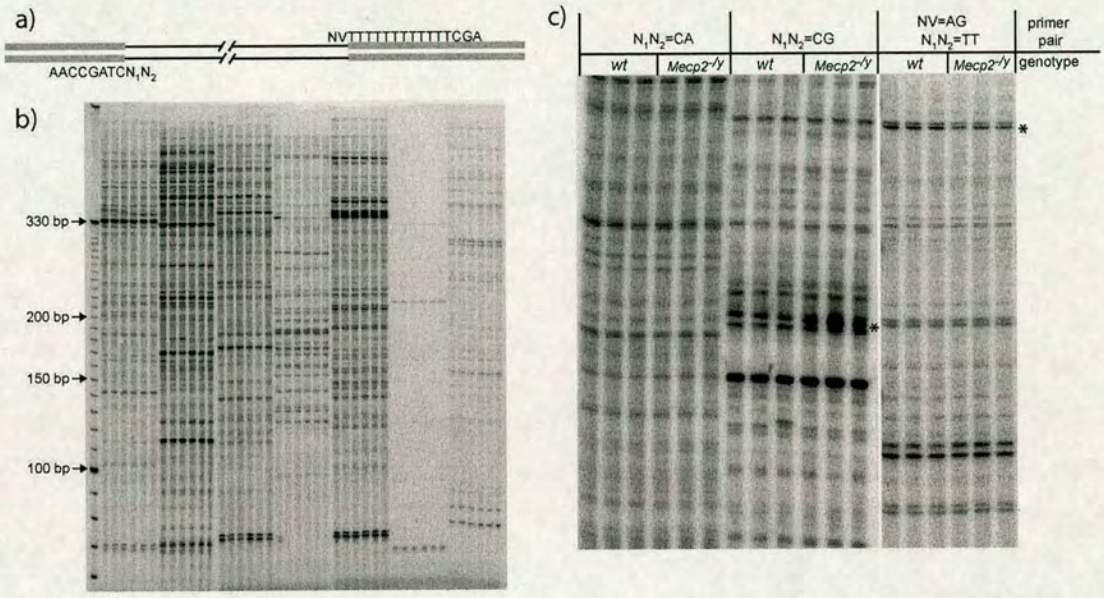

Figure 3-7. ADDER differential display analysis from *Mecp2*-null and *wt* mice brains. a) Schematics of differential display PCR. Shaded bars are the known poly-A and adaptor sequences common for all cDNAs, and the line in between represents unknown cDNA. b) A typical differential display gel. Each column of similar pattern (containing 6 smaller columns) contains resolved products of the differential display PCR amplification using different primer combination. The first three small columns are derived from *wt* and next three from *Mecp2*-null mice brains (the same loading order as in b). b) The part of differential display gel, which has two mis-regulated bands marked with *. Bands showing different intensity in all three lanes were considered as mis-regulated candidates.

Thus we performed ADDER on nine *Mecp2*-null late symptomatic mice (in three pools) and nine *wt* littermates (in three pools). A total of 196 primer combinations were used for differential display PCR, whose products were resolved on high resolution electrophoresis gels (Figure 3-7). The intensity of bands was examined visually by phosphor screen derived image and exposure with film. Only when a band showed increased or decreased intensity in all three lanes it was considered as a potential candidate for a differentially expressed gene (Figure 3-7).

On average, differential display PCR with one primer pair produced 50 bands. Thus, all 196 primer pair combinations allowed examination of approximately 10 000 bands. If the assumption is made that a single gene is represented by only one band on the gel, then the total number of examined genes is 10 000 approximately. In practice the number of transcription units analysed is probably less than this number and more difficult to estimate, since we have observed that one gene can be represented by more than one band on the gel. This happens when the cDNA synthesis primer anneals not only to the poly-A tail, but to the tracks of five As or more present in the middle of a transcription unit.

After examining all 196 differential display primer combinations, 39 bands were observed to be more intense in *Mecp2*-null samples and 11 were less intense. Following the previous estimations, mis-regulated genes accounted for only ~0.5 % of total 10 000 bands examined.

Potential candidate genes were then cloned and identified (Figure 3-8). As one band was found often to contain more than one PCR fragment, fingerprinting using restriction enzyme digests was used to identify the fragment showing differential expression between the genotypes. For identification of differentially expressed transcription unit, the restriction digest pattern was compared between high and low intensity bands (Figure 3-8). In some cases it was difficult to identify the correct band. In these cases two or three of the most frequently represented clones were picked as potential candidates for the mis-regulated transcript.

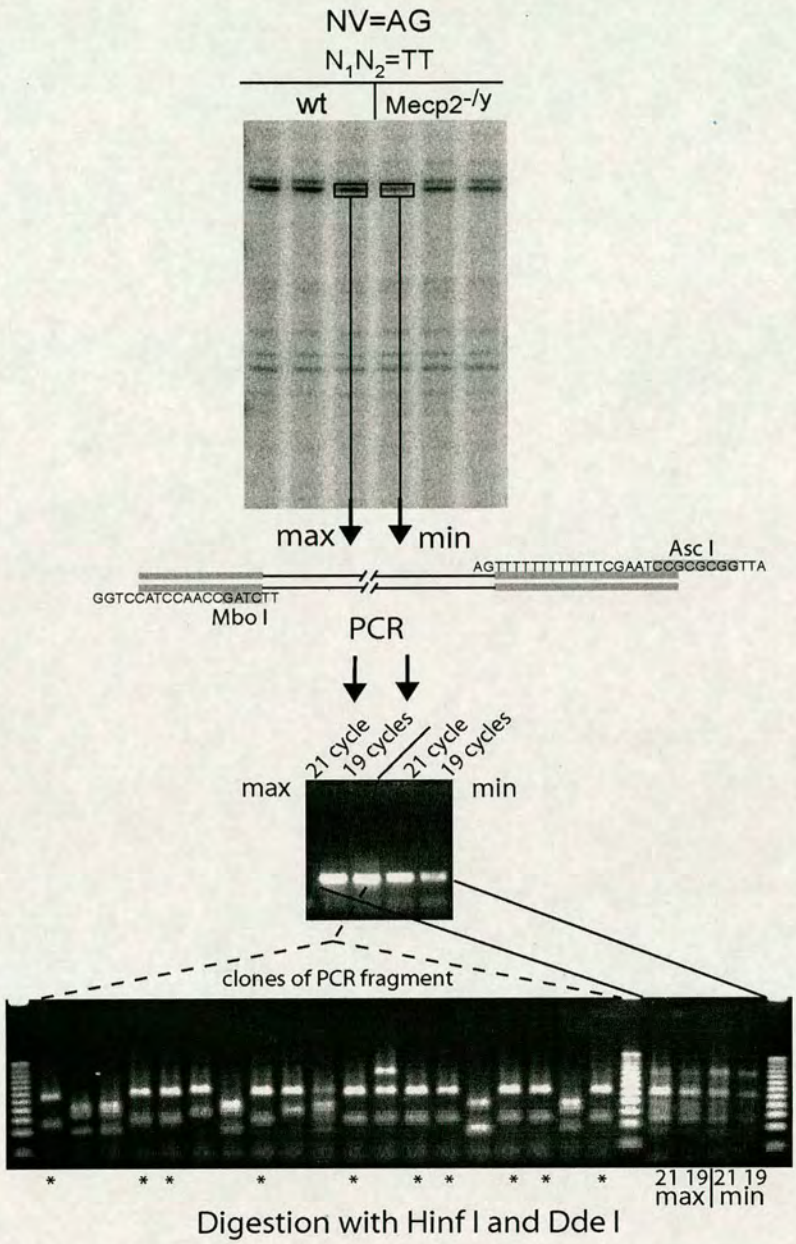

Figure 3-8. An example of a standart procedure used for the identification of genes from differential display screen. Bands which display maximum (max) and minimum (min) intensity were excised from the gel and re-amplified using specific primers, which contain MboI and AscI restriction sites. Different cycle numbers were used for PCR amplification to ensure that the band used for cloning is in the linear phase of amplification (19 cycles). To identify the clone, which contains the differentially expressed band, inserts from 24 clones were amplified and digested with frequently cutting restriction endonucleases and compared with the digestion pattern of the source "max" and "min" PCR products. Patterns that show the difference between "max" and "min" were compared with digestions from clones and the representing clones were then identified (*). Sequencing of one identified clone allowed identification of the mis-regulated gene (in this example *Uqcrc1* gene).

The selected clones were then sequenced to identify mis-regulated genes. Subsequently Real Time PCR analysis was done to confirm the mis-regulation. Real Time PCR quantification was done on the same cDNA pools of late symptomatic *Mecp2*-null mice used for ADDER. From 36 isolated genes (listed in Table 2-3, from row 4 onwards) mis-regulation was confirmed for 11 genes (Table 3-1, $p<0.05$). Because multiple Real Time PCR experiments were done to identify mis-regulated genes (36 in total for late symptomatic samples), the probability of false positives increases if $p<0.05$ is used as a cut-off of significance. The Bonferroni significance correction for the multiple tests could be used to exlude the possibility of random positives. After Bonferroni correction p value becomes $p<0.0014$. Because there is a dispute that Bonferroni correction as well increases the probability of the true positive exlusion, both $p<0.05$ (grey shaded) and $p<0.0014$ (* marked) values are shown in the table 3-1.

Subsequently, the expression of the genes (which are below $p<0.05$ significance in late symptomatic samples) was examined at earlier stages of disease progression (pre- and early symptomatic mice). Real time PCR analysis showed that out of 11 mis-regulated genes in late symptomatic mice only 3 genes were significantly mis-regulated in early symptomatic mice and none were mis-regulated in pre-symptomatic mice (Table 3-1).

The list of 11 mis-regulated genes was then examined to see if it could tell something about MeCP2 function or Rett syndrome. Interestingly, ubiquinol-cytochrome c reductase core protein I (Uqcrc1) and Nadh dehydrogenase subunit 2 (mt-Nd2) are proteins involved in mitochondrial respiration (described in paragraph 3.6.2 below). The maternally expressed gene 3 (*Meg3/gtl2*) is an imprinted gene (described in paragraph 3.6 below). Other genes are less well described in the literature, but have similarity to known domains of certain proteins such as a sterile alpha motif (SAM), histone core or rho protein. From the early mis-regulated genes, embryo spinal cord cDNA is present in different tissues and does not have an open reading frame. Esterase/lipase/thioesterase family member is an unknown protein, which has a homology to arylacetamide deacetylases known to be involved in lipid metabolism.

Gene accession No.	Gene name	Late symptomatic					Early symptomatic					Pre-symptomatic				
		wt		*Mecp2*-null			*wt*		*Mecp2*-null			*wt*		*Mecp2*-null		
		Mean	SD	Mean	SD	p	Mean	SD	Mean	SD	p	Mean	SD	Mean	SD	p
NM_025407	Uqcrc1, ubiquinol-cytochrome c reductase core protein 1	1.00	0.28	1.73	0.56	$<10^{-3}$*	1.00	0.12	1.22	0.09	$<10^{-3}$	1.00	0.15	1.10	0.30	0.32
E130120	Unknown, contains SAM domain	1.00	0.28	0.69	0.10	<0.01	1.00	0.16	0.96	0.12	0.28	-	-	-	-	-
BC028971	Gtl2/Meg3, imprinted maternally expressed	1.00	0.22	1.69	0.33	$<10^{-5}$*	1.00	0.42	1.14	0.37	0.42	-	-	-	-	-
AK011516	Hist1h2bc, histone 1 H2bc	1.00	0.34	0.44	0.16	$<10^{-4}$*	1.00	0.37	0.82	0.25	0.17	1.00	0.37	1.00	0.21	0.95
AK034339	Unknown, similar to esterase/lipase/thioesterase family members	1.00	0.26	1.35	0.47	<0.05	1.00	0.23	1.37	0.50	<0.05	1.00	0.25	1.05	0.20	0.49
AU018611	mt-Nd2, NADH dehydrogenase 2	1.00	0.17	0.6	0.08	$<10^{-6}$*	1.00	0.44	0.73	0.25	0.08	1.00	0.16	1.14	0.30	0.16
NM_175092	Rhof, ras homolog gene family, member f	1.00	0.33	0.67	0.29	<0.05	1.00	0.65	1.44	0.64	0.12	-	-	-	-	-
AK049648	Unknown	1.00	0.34	1.39	0.34	<0.02	1.00	0.46	2.07	0.96	<0.01	1.00	0.15	1.13	0.32	0.26
AK029199	Cdon, cell adhesion molecule-related/down-regulated by oncogenes	1.00	0.16	1.39	0.23	$<10^{-3}$*	1.00	0.25	0.89	0.23	0.31	-	-	-	-	-
BC025130	Ccl19, chemokine (C-C motif) ligand 19	1.00	0.21	2.69	0.71	$<10^{-7}$*	1.00	0.40	1.00	0.30	0.96	-	-	-	-	-
BC058513	Snrp70, U1 small nuclear ribonucleoprotein polypeptide A	1.00	0.38	1.44	0.57	<0.05	1.00	0.42	1.40	0.59	0.08	-	-	-	-	-

Table 3-1. List of genes found to be mis-regulated in *Mecp2*-null mouse brain by ADDER and confirmed by Real Time PCR. Mean values (the column under the name of genotype) are normalised against *Gapdh* signal and displayed relatively to *wt*. Alongside the mean there is corresponding value of standart deviation (SD). The statistical significance of the expression difference was calculated using the Student t test and is shown in column p. Grey shaded genes has $p<0.05$ and * marked ones $p<0.0014$ (Bonferroni correction, only for the late symptomatic ones).

3.6. Biological causes and consequences of gene mis-regulation in *Mecp2-null* mouse brain

3.6.1. *Meg3/gtl2* up-regulation is not due to bi-allelic expression

Initially, the *Gtl2* locus was characterized in a gene trap integration site screen, for parental origin-dependent phenotypes in mouse (Schuster-Gossler et al., 1998). When the gene trap transgene was inherited from the father, mice showed the dwarfism phenotype. The penetrance and expressivity of the phenotype were greatly reduced if the transgene was inherited from the mother (Schuster-Gossler et al., 1998). Later independently, the *Meg3* (*gtl2*) imprinted gene was identified by subtraction-hybridisation screen using androgenetic and normally fertilized embryos (Miyoshi et al., 2000). Further investigations revealed a reciprocally imprinted gene *Dlk1* and a differentially methylated region, with characteristics of *Igf2/h19* locus (Schmidt et al., 2000; Takada et al., 2000; Wylie et al., 2000).

Identification of up-regulation of the *Meg3/gtl2* gene in *Mecp2*-null mouse brain by the ADDER technique raised the possibility that MeCP2 might be involved in repressing the silent, paternal copy of the gene. The possibility was considered that over-expression of *Meg3/gtl2* is due to bi-allelic expression. Few approaches can be used to address the question. Often, parental origin-dependent expression is examined by identifying polymorphisms in the gene of interest in different mouse lines (such as *Mus musculus molossinus* and *Mus musculus domesticus*), crossing the mouse lines and examining which allele is being expressed. Another approach uses fluorescent *in situ* hybridization (FISH) with an intronic probe, which detects nascent RNA transcripts. Because nascent transcripts are present only at the site of transcription, it is therefore seen as a dot after hybridization with a labelled probe. If two alleles are transcribed, two dots are observed (Figure 3-9 b). To investigate the allelic expression of *Meg3/gtl2* gene the last approach was chosen, because the absence of a different mouse line in the laboratory.

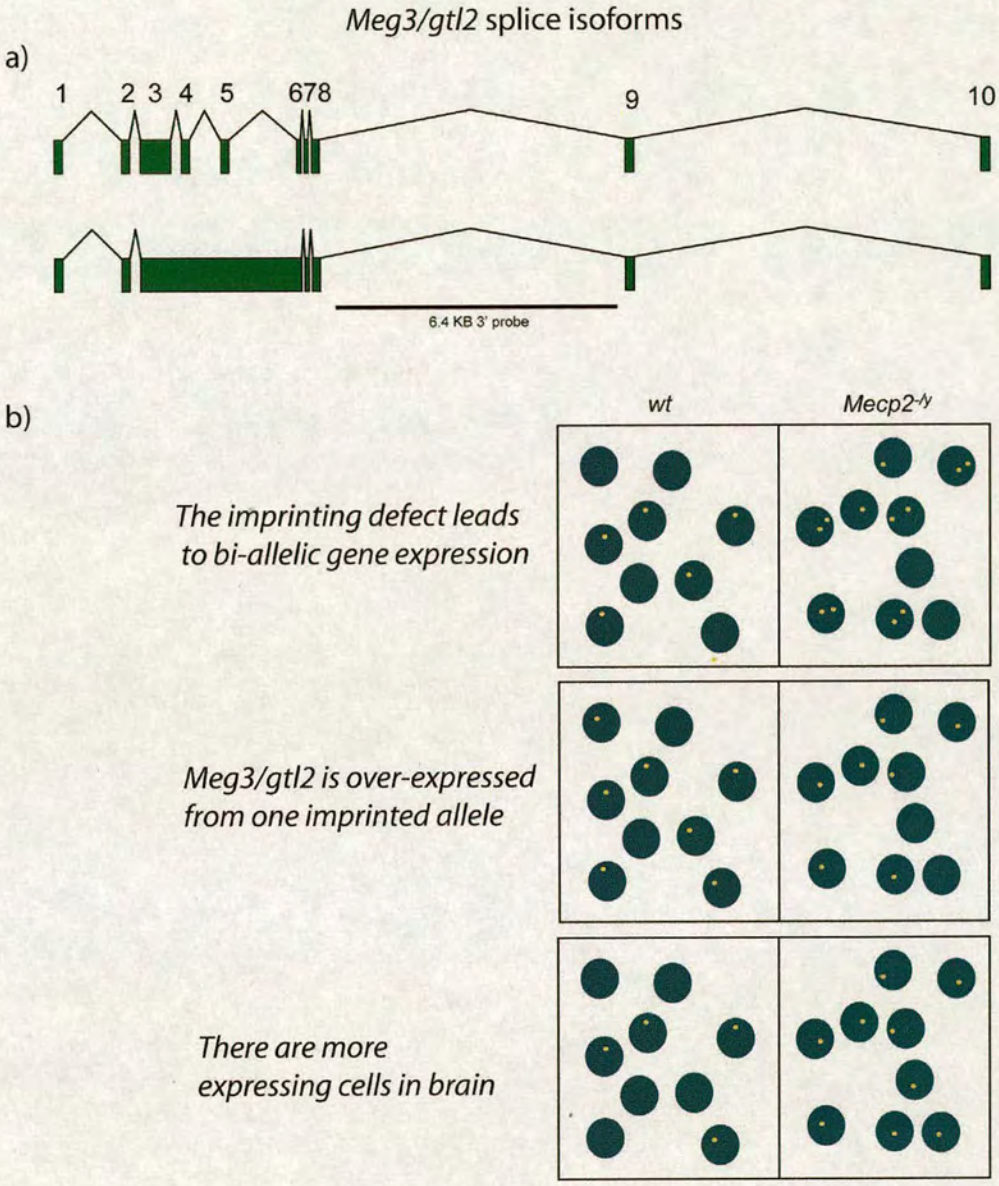

Figure 3-9. Nascent RNA FISH experiment scheme. a) Two possible splice isoforms of the *Meg3/gtl2* gene. The line underneath intron 8 shows the position of the probe, which was used for the FISH experiment. b) Prediction of the results from the FISH experiment that would explain the *Meg3/gtl2* up-regulation observed in *Mecp2*-null mice brain. The top panel shows more cells with two dots in *Mecp2*-null mouse brain, which would suggest bi-allelic expression. In the middle panel no difference is observed, because if over-expression is from a single allele, then nascent RNA FISH is not sensitive enough in quantifying the brightness of a dot. In the bottom panel, more cells express the *Meg3/gtl2* mono-allelicly in *Mecp2*-null mouse brain.

Using nascent RNA FISH is advantageous because it would be possible to discriminate between two possibilities of over expression of *Meg3/gtl2* due to bi-allelic expression or due to an increased number of expressing cells (Figure 3-9).

Nascent RNA FISH was never reported before in adult mouse tissue sections. Therefore the protocols were adapted from nascent RNA FISH done in cell culture systems and regular RNA FISH in tissue sections.

The bacterial artificial chromosome, containing mouse *Meg3/gtl2* genomic locus was obtained (Invitrogen, RPCI-23-394E14) and the 6.4 kb intron 8 (Figure 3-9 a) was sub-cloned between T3 and T7 promoters. The T3 and T7 promoters permitted *in vitro* transcription of sense and anti-sense RNA strands. Hybridisation to the sense strand serves a negative control for the experiment.

For the nascent RNA FISH experiment a *Mecp2*-null late symptomatic mouse and a *wt* littermate were selected, the brains were harvested and divided into two halves. One half was used for purification of RNA to determine if *Meg3/gtl2* is significantly up-regulated in this animal. As expected, Real Time PCR showed significant up-regulation of *Meg3/gtl2* in this late symptomatic mouse (Figure 3-10). Hence the other brain half was used to prepare cryo-sections for the FISH experiment. When the sense probe was used for the experiment no signal was observed, therefore the conditions were stringent enough to eliminate unspecific binding (Figure 3-11 d). Hybridisation with the antisense probe mostly showed one dot per nucleus. However there were some instances of two dots per nucleus (Figure 3-11 a,c). These could be due to bi-allelic expression in certain cell types, or to dividing or partially overlapping cells.

In order to avoid subjectivity in the experiment, samples from *wt* and *Mecp2*-null mouse were coded. Cells in fifty fields were analysed and scored by the presence of one or two dots. Surprisingly, the *wt* sample scored highest in both categories - the opposite to the expectation considering *Meg3/gtl2* up-regulation in *Mecp2*-null brains (Figure 3-10). Most of the cells were still expressing one, rather then two copies of the gene.

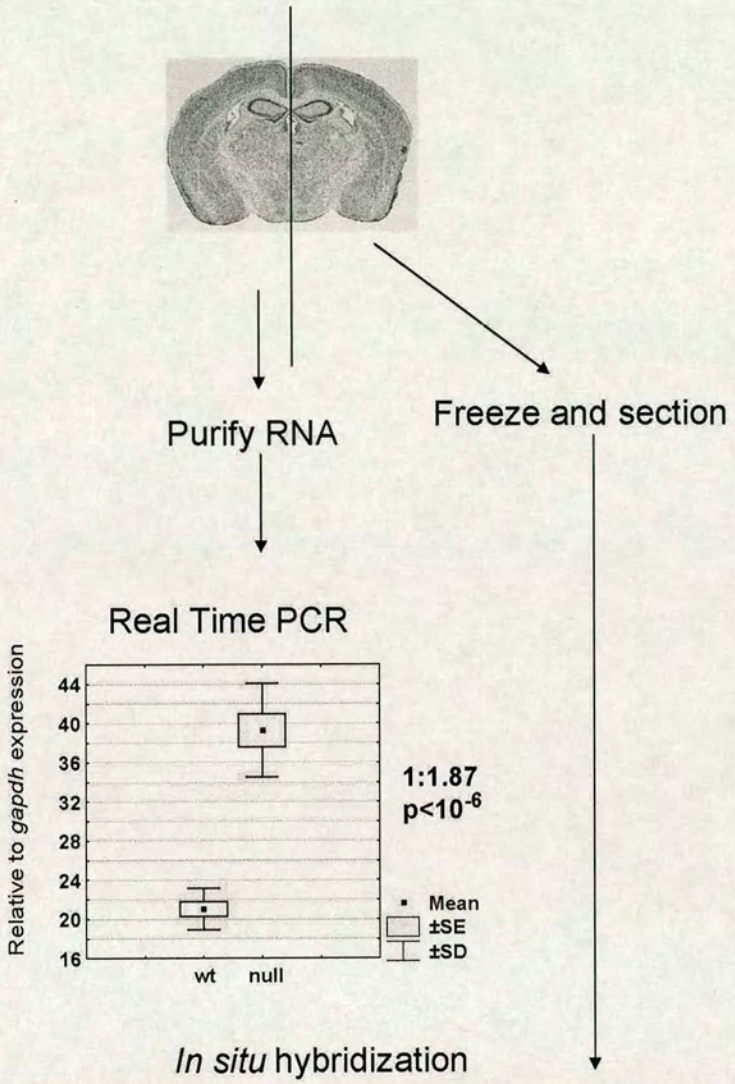

Code name	Number of fields counted	Number of nuclei with 1 dot	Number of nuclei with 2 dots	*Mecp2* genotype
1	50	302	9	-/y
2	50	340	26	+/y

Figure 3-10. Results from the nascent RNA FISH experiment. Brains from *Mecp2*-null late symptomatic mouse and *wt* littermate were divided into two halves. One half was used for *Meg3/gtl2* expression analysis (quantitative PCR was done in 8 replicas) and shows that the gene is up-regulated in the selected *Mecp2*-null mouse (quantitative PCR analysis). The table shows results from the nascent RNA FISH experiment. Slides were given code names and fifty fields were analysed before the genotypes were uncovered.

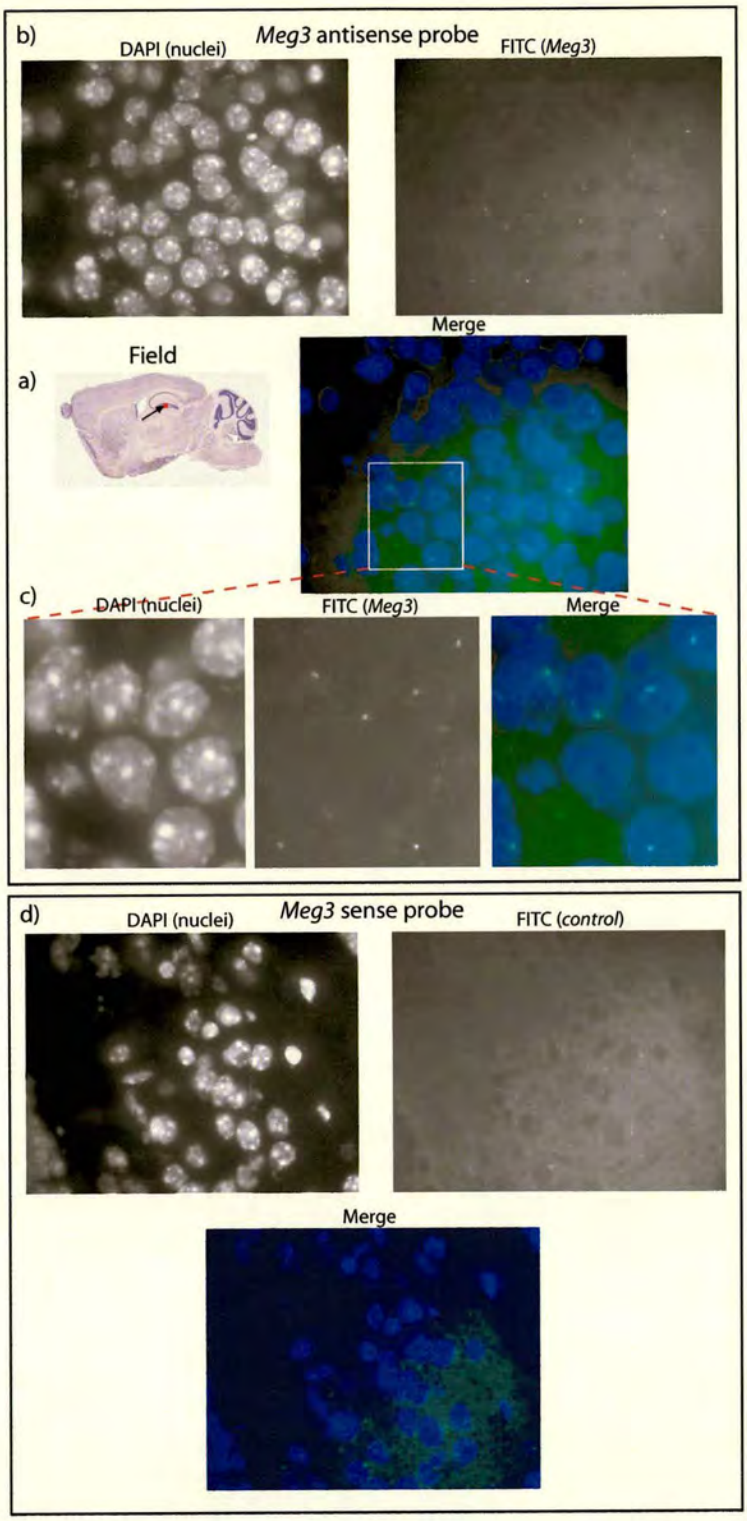

Figure 3-11. Nascent RNA FISH images. a) An arrow points to the brain region (picture was taken from the mouse brain atlas), which is showed in b, c and d. b) Hybridization of the antisense *Meg3/gtl2* intron probe. Dots visualise sites of transcription, where nascent RNA is still present. c) Magnification of the indicated region from a. d) Hybridization of the sense probe serves as a negative control.

Therefore, the conclusion was made that *Meg3/gtl2* up-regulation is not due to biallelic expression in *Mecp2*-null mouse brain. The likely explanation is that *Meg3/gtl2* is over-expressed from one allele (Figure 3-9 b).

3.6.2. Mis-regulation of *Uqcrc1* correlates with mitochondrial respiration defect in *Mecp2*-null mouse brain

As mentioned previously, two mis-regulated genes *Uqcrc1,* and *mt-Nd2,* are localised to mitochondria. Uqcrc1 and mt-Nd2 are components of the mitochondrial electron transport chain that maintains a proton gradient across the mitochondrial inner membrane and drives synthesis of ATP (Figure 3-12). Uqcrc1 is a core structural component of Complex III, whereas NADH dehydrogenase subunit 2 (mt-Nd2) is a part of Complex I in the mitochondrial respiratory chain.

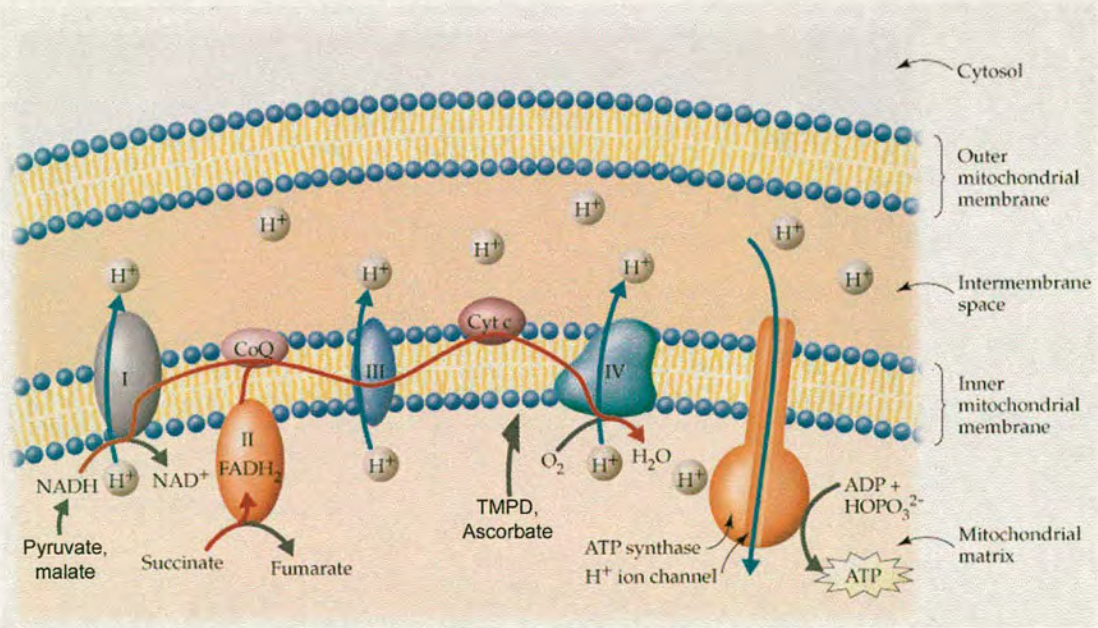

Figure 3-12. The mitochondrial respiration chain consists of four complexes, which pump protons to maintain a proton gradient across the inner mitochondrial membrane. Complex V or ATP synthase uses the proton gradient to synthesise ATP. Different substrates (pyruvate/malate, succinate or TMPD/ascorbate) can provide electrons for electron transport chain at different stages permitting an examination of the activity of different complexes. The figure is from Internet (http://wps.prenhall.com/wps/media/objects/376/385232/Media-Portfolio/index.html)

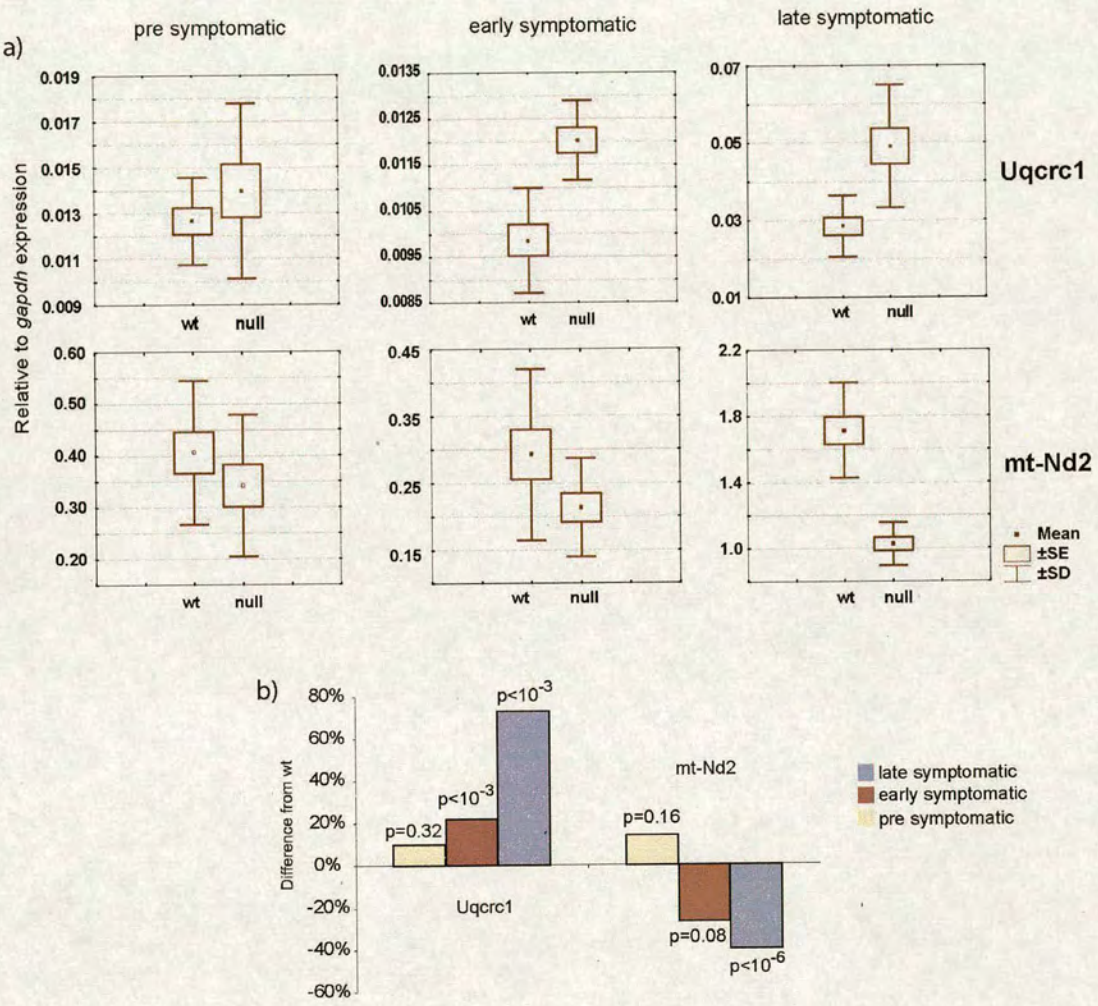

Figure 3-13. Real Time PCR data showing *Uqcrc1* and *mt-Nd2* mis-regulation in *Mecp2*-null mouse brain. a) Real Time PCR data of *Uqcrc1* and *mt-Nd2* expression in pre, early and late symptomatic mouse brain. b) Summary of the real Time PCR data with statistical analysis, showing that *Uqcrc1* is significantly up-regulated in early and late symptomatic mice and that *mt-Nd2* is significantly down-regulated only in late symptomatic mice.

Uqcrc1, a nuclear-encoded gene, was significantly up-regulated in early and late symptomatic brain, whereas mitochondrially encoded *mt-Nd2* was significantly down-regulated in late, but not early, symptomatic brains. Neither gene was mis-expressed in pre-symptomatic animals (Figure 3-13).

Because the *mt-Nd2* gene is not nuclear and is only mis-regulated in late symptomatic mice, the *Uqcrc1* gene was considered as a potential direct target for MeCP2. If *Uqcrc1* is a direct target, MeCP2 should bind in the vicinity of its promoter. This prediction was verified by chromatin immunoprecipitation, which showed that an anti-MeCP2 antibody, but not random rabbit serum, could precipitate a DNA region near the *Uqcrc1* transcriptional start site (Figure 3-14). This region was not detected when *Mecp2*-null brain nuclei were subjected to anti-MeCP2 chromatin immunoprecipitation, which eliminates the possibility of non-specific cross-reaction of the antibody with other nuclear components (Figure 3-14 b). An antibody against di-methylated lysine 9 of histone H3 gave identical recovery of the *Uqcrc1* promoter region in *Mecp2*-null and *wt* brain nuclei showing equivalent quality of chromatin in these preparations. A known MeCP2 binding site, promoter III of the *Bdnf* gene (Chen et al., 2003b; Martinowich et al., 2003), served as a positive control for the immunoprecipitation reaction. Because chromatin IP precipitates different length DNA fragments (usually ranging from 200 - 800 bp) it is impossible to say which CpG could be occupied by MeCP2. To narrow down the MeCP2 binding site DNA methylation status was examined in the region. The presence of methylated CpG sites in the region that binds MeCP2 was determined using bisulfite sequencing. The region is generally non methylated but one CpG site in the *Uqcrc1* promoter was found to be 33% methylated in total brain DNA. This data permit the conclusion that MeCP2 is associated with the *Uqcrc1* gene in brain and that *Uqcrc1* up-regulation might therefore be a direct consequence of MeCP2 deficiency.

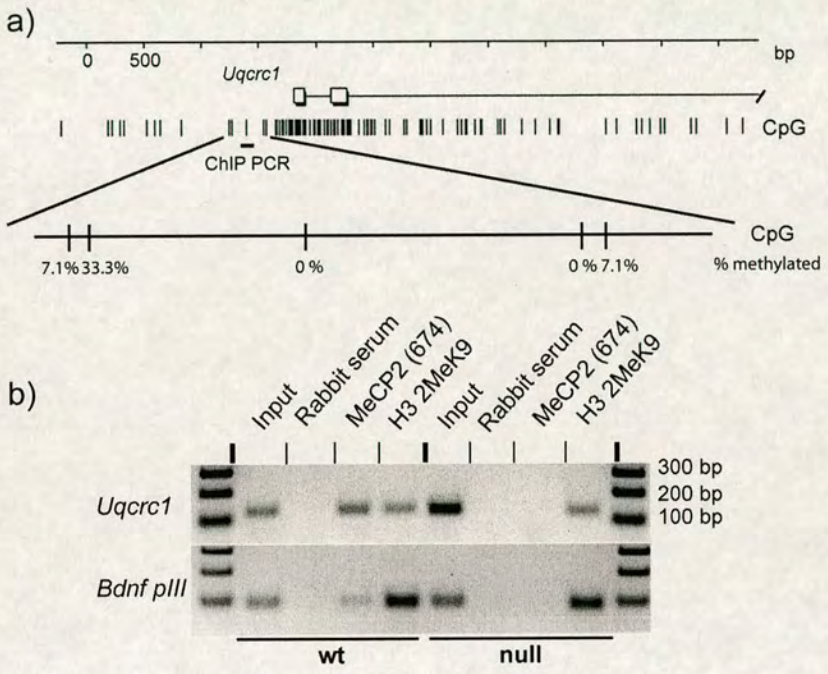

Figure 3-14. MeCP2 binds the promoter region of *Uqcrc1* gene. a) *Uqcrc1* promoter map showing CpG frequency and the region used for PCR amplification of immunoprecipitated chromatin. Below the methylation status of the investigated region is shown (determined by the bisulfide sequencing analysis). b) Chromatin immunoprecipitation reveals binding of MeCP2 to the *Uqcrc1* promoter in *wt* mouse brain, but not in *Mecp2*-null mouse brain. The *Bdnf* promoter III is a positive control. DNA is specifically immunoprecipitated with MeCP2 antibody, but not with rabbit serum. Chromatin corresponding to neither *Bdnf* pIII nor *Uqcrc1* is precipitated from *Mecp2*-null mouse brain using anti-MeCP2 antibody. Anti di-methyl H3 K9 antibody is able to precipitate similar amounts of DNA showing that chromatin amount and quality is similar in *wt* and *Mecp2*-null mouse brain.

The possibility was considered that the abnormal expression of *Uqcrc1* in symptomatic *Mecp2*-null mice might affect mitochondrial morphology and/or physiology. Initial examination of purified mitochondria by transmission electron microscopy (TEM) did not reveal gross structural differences between *wt* and *Mecp2*-null mice (Figure 3-15 a). The mitochondrial purification procedure changes the normal appearance of some mitochondria. Therefore *in situ* TEM of brain sections is an important follow-up experiment.

Polarographic oxygen electrode studies were done to evaluate the activity of the different complexes within the electron transport chain (as noted in Figure 3-15 these experiments were done by A.P., J.C. and N.M.). The protonophore FCCP was added to uncouple the activity of complexes I-IV from the rate-limiting electrochemical proton gradient, thereby permitting analysis of maximal activity. Symptomatic *Mecp2*-null mitochondrial samples consistently showed increased uncoupled respiration rates when substrates that fed in upstream of complex III were used (Figure 3-15c P/M, Succ.), but not with a substrate that enters downstream of complex III (Figure 3-15c, TMPD). This difference was not seen in brain mitochondria from pre-symptomatic mice. The data suggests that in the symptomatic *Mecp2*-nulls the maximal capacity of the respiratory chain upstream of complex IV, but probably downstream of complexes I and II, is increased. Enhancement of complex III activity is consistent with the observed over-expression of the complex III component *Uqcrc1* in *Mecp2*-null mice.

Under physiological conditions, proton translocation associated with complexes I, III and IV works against an electrochemical proton gradient, providing a mechanism for respiratory control. The states 2 and 4 represent this condition. Increases in oxygen consumption at state 2 and 4 were observed in symptomatic *Mecp2*-null versus *wt* mitochondria when substrates fed in at complex I and II, but not when these were by-passed by addition of a complex IV substrate (Figure 3-15 d and e). Differences in state 3 respiration rates between symptomatic *Mecp2*-null and *wt* mouse brain mitochondria were also observed only for substrates that feed electrons to the chain before complex IV (Figure 3-15 f).

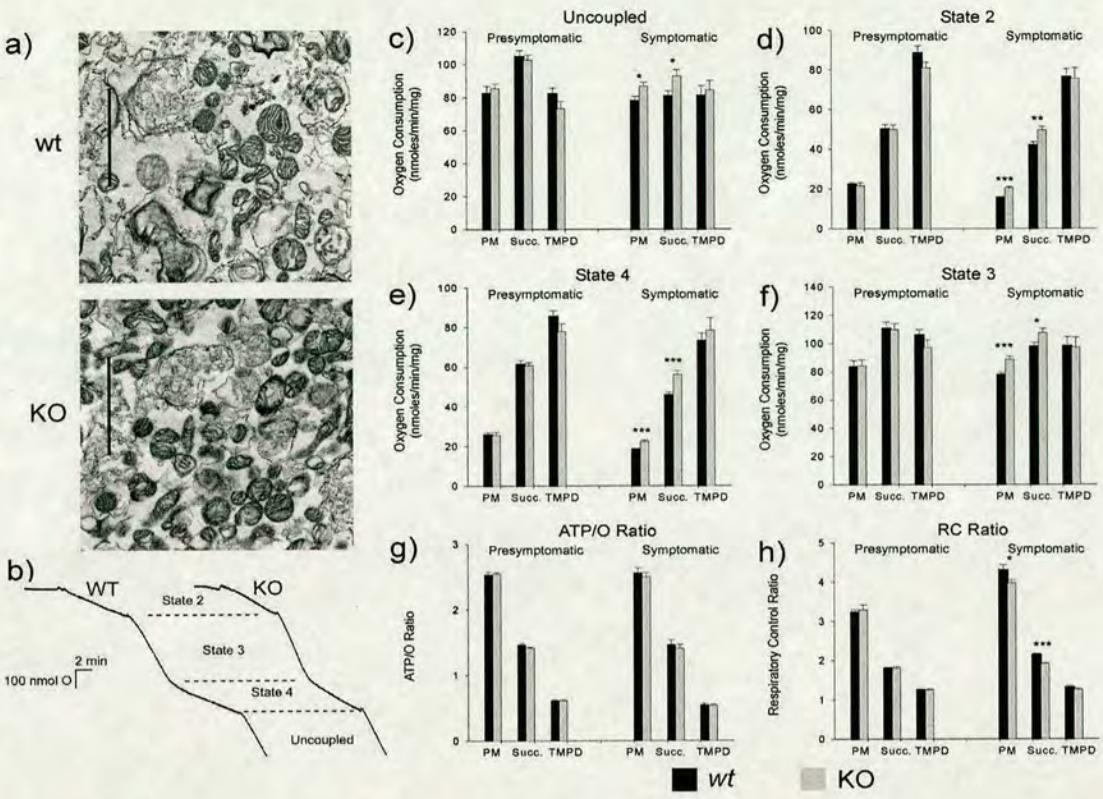

Figure 3-15. Investigation of the respiratory chain in mitochondria isolated from whole brain of *wt* and *Mecp2*-null mice. a) Electron micrographs showing isolated mitochondria from a symptomatic *Mecp2*-null (KO) mouse and an age-matched *wt* littermate. Scale bar is 2 μm. b) Typical output traces from a polarographic oxygen electrode. Initially, mitochondria consume very little oxygen, but following the addition of substrates, oxygen consumption is moderately increased (State 2). Addition of ADP (State 3) permits rapid respiration during which the proton gradient is relieved by ATP synthase. Following phosphorylation of all the ADP present, respiration slows again (State 4). At this point, mitochondria were directly uncoupled by the addition of the protonophore FCCP allowing the proton pumps to run freely. Panels c-h: each pair of columns shows data using one of three different substrates: pyruvate and malate (PM), succinate (succ) or TMPD. Panels c,d,e, and f compare respiration rates during the different respiratory states from brain mitochondria isolated from *Mecp2*-null animals (light bars; n = 8 runs with separate mitochondrial preparations derived from 4 animals) compared to age-matched *wt* litter-mate controls (dark bars). Data from symptomatic *Mecp2*-null mouse mitochondria (n = 16 runs with preparations from 8 animals), compared to *wt* controls are shown to the right of each panel. All comparisons were tested with one-way ANOVA's. One star (*) indicates $p<0.05$; two stars (**) $p<0.01$; three stars (***) represent $p<0.001$ Panel g, shows the calculated ATP:O ratios for pre-symptomatic and symptomatic *Mecp2*-null animals and *wt* controls. Panel h, shows the calculated respiratory control ratios (RCRs). Mitochondrial isolation, respiration measurements and data analysis were done by Andrew Paterson, John Curtis and Nikki MacLeod. TEM technical work was done by John Findlay and image analysis was done by the author of this thesis.

Measurement of the amount of oxygen consumed during the conversion of a known amount of ADP (during state 3), allows the calculation of the ATP:O ratio. This relates the stoichiometries of protons translocated to the number of protons flowing through the ATP synthase per ATP molecule produced. There were no significant differences observed in any of the measured ATP:O ratios (Figure 3-15 g), implying that the significant differences reported above were not the result of a change in the respiratory chain proton pumps or the efficiency of the ATP synthase. In none of the above experiments we have observed difference between pre-symptomatic *Mecp2*-nulls and *wt* controls.

Our data show that respiration rates for symptomatic *Mecp2*-null animals are significantly increased relative to *wt* controls for all substrates that feed in upstream of complex IV. Calculation of the respiratory control ratios (RCR) shows how the coupled respiration has increased proportionally than the uncoupled respiration rate (Figure 3-15 h). This may indicate an increase in the proton conductance across the mitochondrial inner membrane (Nicholls and Ferguson, 2002). Therefore, to maintain the proton gradient against this background "leak", the electron transport chain works faster and therefore consumes more oxygen. Thus mitochondria from symptomatic mutants appear to have an overall greater respiratory capacity (Figure 3-15 c), but also appear to work less efficiently (Figure 3-15 e & h).

3.6.3. Mitochondrial respiration dysfunction does not lead to increased apoptosis in *Mecp2*-null mouse brain

Mitochondria are important players in programmed cell death - apoptosis. They store important factors for the apoptotic signalling cascade such as cytochrome c and caspases (Gorman et al., 2000). Cytochrome c release from the intermembrane space either by rupture of the outer membrane or by transport through channel, activates various caspases, which degrade cellular proteins. Apoptosis inducing factor (AIF) and endonuclease G release from mitochondria contributes to nuclear DNA

fragmentation (Saelens et al., 2004). Nuclear DNA breaks are often used to detect apoptosis.

Mitochondrial respiration abnormality was observed in late symptomatic *Mecp2*-null mouse brain. Hence there was a possibility that cells in the brain die by apoptosis. As mentioned before, the decrease in RCR suggested that there might be a leak of protons through inner membrane (Figure 3-15 h). The leak might be caused by the rupture of the outer membrane, which could also release apoptosis signals.

One of the characteristic signs of apoptosis is fragmentation of DNA either by double stranded breaks or by nicks. The resulting 3'OH termini can be labelled by the fill in reaction with labelled nucleotides using nucleotide terminal transferase (TdT). The TUNEL (TdT-mediated dUTP nick end labelling) procedure was used to compare the cell death frequencies between late symptomatic *Mecp2*-null mouse brain and healthy control littermate. As a result in both *wt* and *Mecp2*-null mice we observed less than ten labelled cells per brain section, suggesting that there is no increased apoptosis (Figure 3-16). Because only two diagonal brain sections were analysed per genotype, it is still possible that in certain areas of the brain, there might be increased cell death rate in *Mecp2*-null mice.

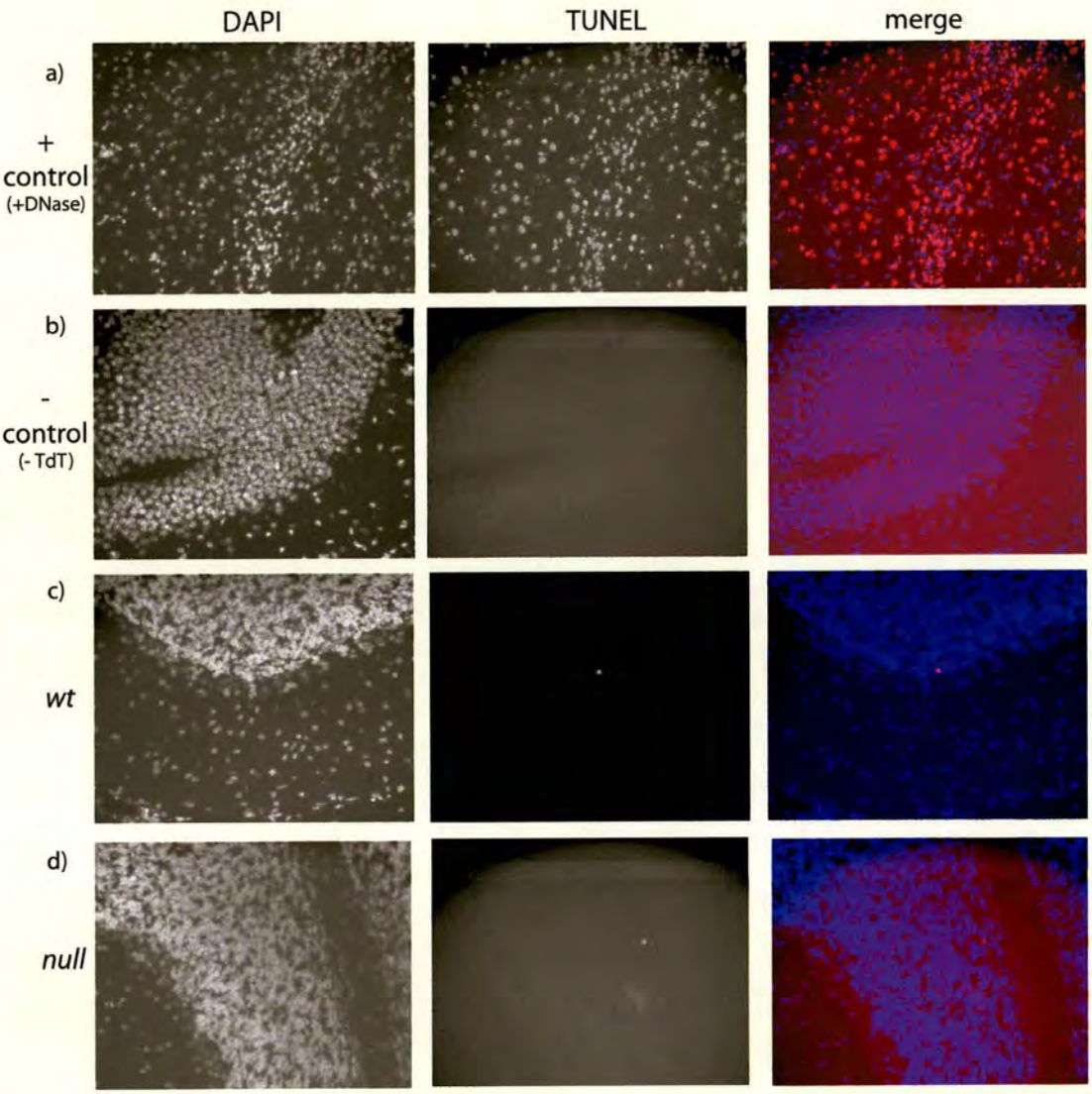

Figure 3-16. TUNEL staining on late symptomatic *Mecp2*-null mouse and *wt* litter mate brain section. a) A brain section treated with DNase I serves a positive control for TUNEL labelling. b) As a negative control for unspecific labelling serves a brain section, which has gone trough the TUNEL procedure without TdT. No unspecific labelling was observed. TUNEL assay of *wt* (c) and late symptomatic *Mecp2*-null (d) mouse brain sections display only few apoptosis dying cell in the brain. DAPI stain marks cell nuclei.

3.7. Summary and conclusions

In this chapter a thorough analysis of gene expression in *Mecp2*-null mouse brain is described. Candidate approaches surprisingly revealed that *Bdnf* is down regulated in *Mecp2*-null mouse brain. This is the opposite of the observed up-regulation in cultured neurons. The discrepancy might be due to feedback loops in living animal which are dependent on the different cell types in the brain or even different organs. From the perspective of Rett syndrome, the findings about the *Bdnf* gene raised several issues. Firstly, *Bdnf* is a neurotrophic factor, which promotes neuronal growth and survival (Bonni et al., 1999). Therefore the expectation is that neurons would be larger in cells over-expressing *Bdnf*. It is documented, that *Bdnf* overexpressing transgenic mice has no gross abnormalities (Croll et al., 1999) and that dendritic branching in these mice is increased (Tolwani et al., 2002). However, in Rett syndrome girls one of the best documented findings is that neurons have reduced dendritic branching and brains are smaller. In mouse models for Rett syndrome the findings are rather similar – brain and neuronal soma size are reduced (Chen et al., 2001). As mentioned before, the finding presented in this thesis shows that *Bdnf* is in fact down regulated in total *Mecp2*-null mouse brains. This finding better relates with the mouse phenotype of smaller brain size and reduced neuronal branching in humans. Reduced neuronal branching, smaller brains and delayed symptoms onset were seen as well in the *Ss18l1*-null mouse (Aizawa et al., 2004). Real Time PCR analysis, however, did not reveal any mis-expression of *Ss18l1* gene in late symptomatic *Mecp2*-null mice.

The *Hes1* gene was found to be up-regulated in *Mecp2*-null mice at pre, early and late stages of the disease. This is an interesting gene for future work for the following reasons. Firstly, it is up-regulated in the absence of MeCP2, therefore it is more likely to be a primary target for a transcriptional repressor. Secondly, the gene is mis-regulated in pre-symptomatic mice and it could be involved in the development of symptoms.

Microarray and Real Time PCR analysis revealed constitutively up-regulated *Sgk* and *Fkbp5* genes, even though glucocorticoid levels are not affected. Interestingly in Rett syndrome patients cortisol levels appear to be normal (Huppke et al., 2001;

Echenne et al., 1991), but over-alertness, agitation an periods of scream may result from absence of functional MeCP2, which affect downstream members of stress signalling pathway. Reduced head size, lower IQ scores and poor motor coordination were noted in children, who had early post-natal administration of the glucocorticoids (Yeh et al., 2004). Reduced neuronal branching observed in Rett syndrome (Armstrong, 2002) was also seen after chronic administration of the glucocorticoids (Wellman, 2001). Osteopenia is known side side-effect of glucocorticoid administration (Patschan et al., 2001), occurs in Rett syndrome as well (Haas et al., 1997; Leonard et al., 1999). These phenotypic similarities suggest that disturbance in glucocorticoid signalling may be responsible for some symptoms in Rett syndrome.

By global analysis of gene expression about dozen genes were found to be mis-regulated in late symptomatic mice. Of these only a few were mis-regulated in early symptomatic mice as well. This suggests that either more genes become targets of MeCP2 when MeCP2 becomes progressively up-regulated in the brain, or that disease progression causes secondary responses, which are reflected as changes in transcription. One of the genes up-regulated in late symptomatic mice was *Meg3/gtl2* gene which was known to be maternally expressed. The possibility was raised, that MeCP2 could be important in silencing of the paternal copy of the gene. A closer examination of the imprinted status of up-regulated *Meg3/gtl2* revealed that *Meg3/gtl2* is mostly expressed monoallelicly in late-symptomatic *Mecp2*-null mice. The option remains that the expression is up-regulated from the one expressed allele.

Up-regulation of *Uqcrc1* expression in early and late symptomatic mice and down regulation of *mt-Nd2* only in late symptomatic mice suggested examination of the mitochondrial respiration in *Mecp2*-null mouse brain. Investigation of the activity of different respiration complexes showed no difference in respiration, when complex IV substrates were used. However complex I or II substrates both resulted in an increase in the respiration of mitochondria purified from symptomatic *Mecp2*-null mice. These results suggested that either both complex I and II or only the downstream complex III are affected. Given the evidence that the complex III member *Uqcrc1* is up-regulated, it is possible that complex III might be responsible

for the observed increase in mitochondrial respiration. Additionally, reduced respiratory control ratio suggested that membrane leakage might be contributing to the mitochondrial defect as well. However, at this stage, it is still un-clear how the transcriptional up-regulation of one of the complex III components could perturb the mitochondrial respiration. Future experiments will have to determine if there is any change in Uqcrc1 protein amounts and in complex III assembly in *Mecp2*-null mouse. Over-expression of *Uqcrc1* in cells or mice would help to find out if the observed respiration defects are the only dependent on increased Uqcrc1 amounts. Another interesting question is if the increased mitochondrial respiration causes any symptoms in mice and in humans. The possible experiment that could answer this question is examination if over-expression of *Uqcrc1* gives rise to any of the symptoms in mice.

The delayed onset of *Uqcrc1* up-regulation may mean that mis-expression is an indirect consequence of the absence of MeCP2. However, the amount of MeCP2 in neurons is known to increase dramatically as neurons mature (Mullaney et al., 2004; Jung et al., 2003) and therefore some genes that are not initially affected by MeCP2 may come under its regulatory influence as MeCP2 becomes more abundant. The increase in the concentration in brain MeCP2 occurs progressively during postnatal life as synaptogenesis proceeds and neurons mature, continuing well beyond 6 weeks of age in the rat (Mullaney et al., 2004).

The presented data revive the idea that mitochondrial abnormality may contribute to pathogenesis of Rett syndrome. Structural abnormalities in mitochondria from skin and muscle biopsies of RTT patients have been sporadically reported (Armstrong, 1992; Dotti et al., 1993; Eeg-Olofsson et al., 1989; Ruch et al., 1989) and there is limited evidence of defects in the electron transport chain in these samples (Coker and Melnyk, 1991; Dotti et al., 1993). Small stature and hypotonia are typical features of mitochondrial disorders that are shared with RTT. Additional circumstantial support for this link comes from the observation that in about half of RTT patients elevated levels of circulatory lactic or pyruvic acid were measured (Lappalainen and Riikonen, 1994; Matsuishi et al., 1992). This might be caused by defects in the respiratory chain and urea cycle complexes, both of which are

mitochondrial. Finally, breathing abnormalities are a key feature of RTT and may conceivably reflect an underlying weakness in oxidative respiration.

There are several reasons to expect increased apoptosis in the *Mecp2*-null mouse brain. Observed mitochondrial respiration abnormalities potentially could lead to apoptosis. Other suggestions for the increased apoptosis come from experiment, in which *in vitro* cultured *wt* neurons were found to have a better survival rate than *Mecp2* mutant ones (Young and Zoghbi, 2004). The examination of *Mecp2*-null late symptomatic mouse by the TUNEL assay leads to the conclusion that there is no dramatic increase in apoptosis. However, because only few sections were analysed there is still a possibility that certain regions of brain has increased cell death.

4. Chapter four.

MeCP2 isoforms

4.1. Introduction

Initially, MeCP2 protein was purified from rat brain as a single 84 kD protein based on it's binding to methylated CpG (Lewis et al., 1992). The results of Edman degradation allowed the design of a degenerate probe which was then used to screen a cDNA library and isolate full length MeCP2 cDNA (Lewis et al., 1992). Later, the mouse *Mecp2* gene was mapped to Xq28 and shown to be subject to X-inactivation (Quaderi et al., 1994). Further analysis of the *Mecp2* transcript identified alternative polyadenylation sites, that give rise to two main mRNA variants with different 3'UTRs (10KB and 2KB) (Coy et al., 1999). At this time *Mecp2* was annotated as a three-exon gene, with all exons contributing to the protein (Coy et al., 1999). Sequencing of the *Mecp2* genomic locus in mouse and human combined with more detailed bioinformatic analysis revealed an additional upstream non-coding exon (Reichwald et al., 2000). *Mecp2* is therefore currently recognized as a four-exon gene.

This results chapter describes the identification of a new MeCP2 splice isoform. By searching EST databases a novel MeCP2 splice isoform (MeCP2α) was found, which encodes a distinct N-terminus. MeCP2α mRNA splice variant is more abundant than the previously annotated MeCP2 mRNA (MeCP2β) in mouse tissues and human brain. Furthermore, MeCP2β mRNA has an upstream open reading frame that inhibits its translation. As a result of these differences, more than 90% of MeCP2 in mouse brain is MeCP2α. Both protein isoforms are nuclear and co-localise with densely methylated heterochromatic foci in mouse cells. To investigate if newly discovered coding exon1 is a hot spot for Rett syndrome causing mutations a further mutation screen in Rett syndrome patients was performed. Characterisation of the generated isoform-specific antibodies finishes the chapter.

Other group (Mnatzakanian et al., 2004) at the same time identified the new MeCP2 isoform as well. However they named the previously known MeCP2 isoform as MeCP2A and newly discovered one as MeCP2B. To avoid different nomenclature for the same isoforms, in the 5th Annual Rett syndrome Symposium it was commonly agreed to call the known MeCP2 isoform as MeCP2e2 (previously described as

MeCP2β or MeCP2A), because it starts at exon 2. The newly discovered isoform was accordingly called MeCP2e1 (previously described as MeCP2α or MeCP2B). In this thesis further on MeCP2e1 and MeCP2e2 nomenclature will be used.

4.2. Identification of MeCP2 splice variant in EST databases

Mouse expressed sequence tag (EST) databases were searched for cDNA sequences encoding MeCP2. Alignments revealed that ESTs can be grouped into two categories depending on the presence (BY107013, BI409371) or absence (CA980031, BY244111) of exon 2. Human MECP2 cDNAs with (BC11612, BM923600) and without exon 2 (BG706068, BI458175) also exist in human EST database. As exon 2 contains the ATG for the initiation of translation, the possibility was considered that the transcript lacking exon 2 is a non-coding RNA. However exon 1 contains an ATG that in the absence of exon 2 initiates a potential open reading frame (ORF) of 501 amino acids (a.a.) in mice and a 498 a.a. in humans (Table 4-1). The new exon 2-minus isoform was designated as "MeCP2e1" and the previously described isoform containing exon 2 as "MeCP2e2". Alignment of e1 and e2 predicted protein sequences demonstrate identity except at the extreme N-terminus (Figure 4-1). The MeCP2e1 N-terminus contains poly-alanine and poly-glycine repeat tracts encoded by GCC and GGA trinucleotides. Comparison of these isoforms with other vertebrate MeCP2 sequences showed that MeCP2e1 shares a poly-alanine tract, serine-glycine residues and EERL motifs with frog and zebrafish MeCP2 sequences, whereas MeCP2e2 lacks these features. The alignment suggested that MeCP2e1 more closely resembles the ancestral form of MeCP2 than does MeCP2e2 (Figure 4-1c).

	MW, kDa	Length, a.a.	pI	Charge at pH 7
mMeCP2e1	53.6	501	9.89	34.9
hMeCP2e1	53.3	498	9.88	34.8
mMeCP2e2	52.3	484	9.96	37.8
hMeCP2e2	52.4	486	9.95	37.8

Table 4-1. Physical characteristics of human and mouse MeCP2 isoforms.

4.3. MeCP2e1 is the major mRNA splice variant in vivo

To confirm *in silico* evidence and assess the relative abundance of the different MeCP2 isoforms *in vivo*, semi-quantitative RT-PCR analysis of cDNA derived from different mouse tissues was performed. The two primers were designed to anneal to exon 1 and exon 3 respectively (Figure 4-2 a). Control amplification of mixed MeCP2e1 and MeCP2e2 encoding plasmids showed no significant amplification bias towards the shorter product (Figure 4-2 a). RT-PCR analysis demonstrated that MeCP2e1 is more abundant than MeCP2e2 in most tissues. Relative abundance of MeCP2e1 was highest in the brain, thymus and lung, whereas an approximately 1:1 isoform ratio was seen in testis and liver. Semi-quantitative RT-PCR provided evidence that both splice variants exist in human brain; again the predominant form of mRNA encodes MECP2e1 (Figure 4-2 b).

To analyse the abundance of the two isoforms during cellular differentiation, we differentiated mouse embryonic stem (ES) cells into neurons. Samples from stages of differentiation were assayed for the different isoforms. Semi-quantitative RT-PCR showed that MeCP2e1 mRNA is more abundant than MeCP2e2 mRNA in ES cells and the proportion of e1 mRNA appeared to increase during neuronal differentiation (Figure 4-2 c).

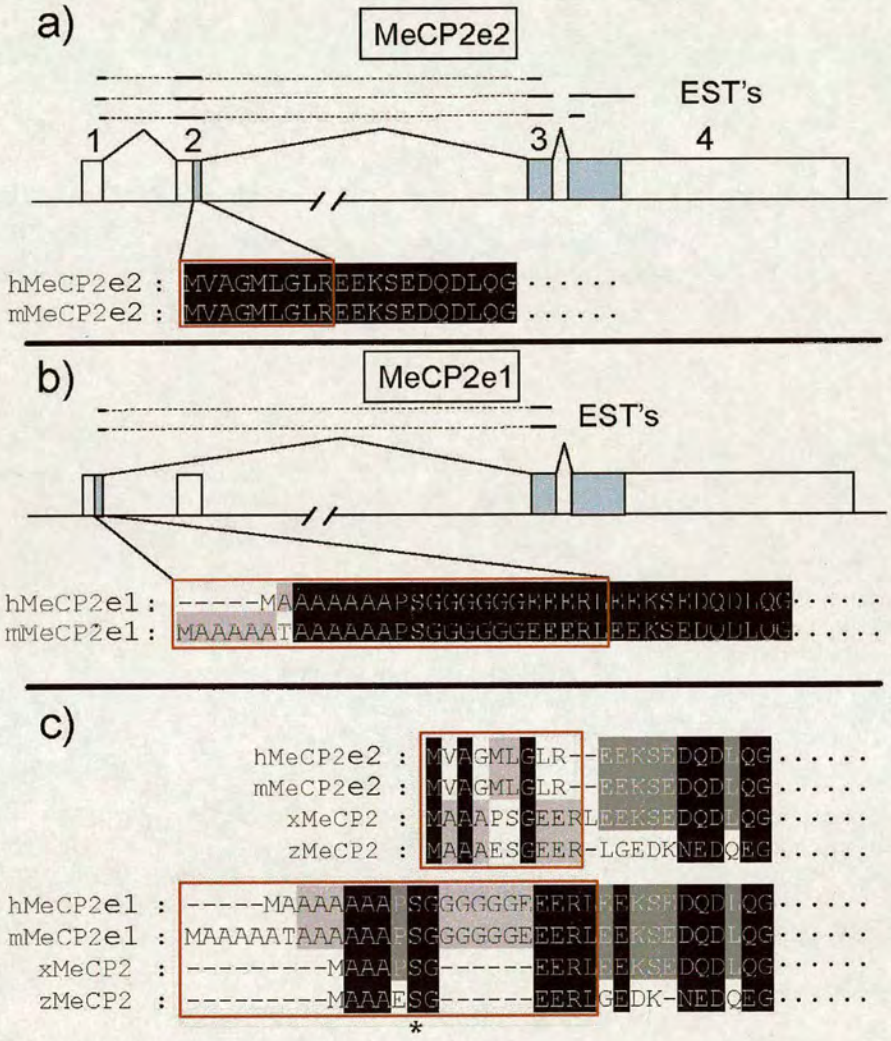

Figure 4-1. Alternative splicing of MeCP2 mRNA. a) Previously described MeCP2e2 is encoded when all known exons are sequentially spliced. b) The novel MeCP2e1 isoform arises when exon 1 is spliced onto exon 3, skipping exon 2. Shaded boxes are protein coding and open boxes are non-coding. ESTs suggesting the occurence of each isoform *in vivo* are mapped as lines above the genomic DNA. c) Alignment of mouse and human MeCP2e1 and MeCP2e2 N-termini with zebrafish and frog MeCP2. MeCP2e1 is more similar to zebrafish and frog orthologs than is MeCP2e2. * indicates a putative serine phosphorylation site.

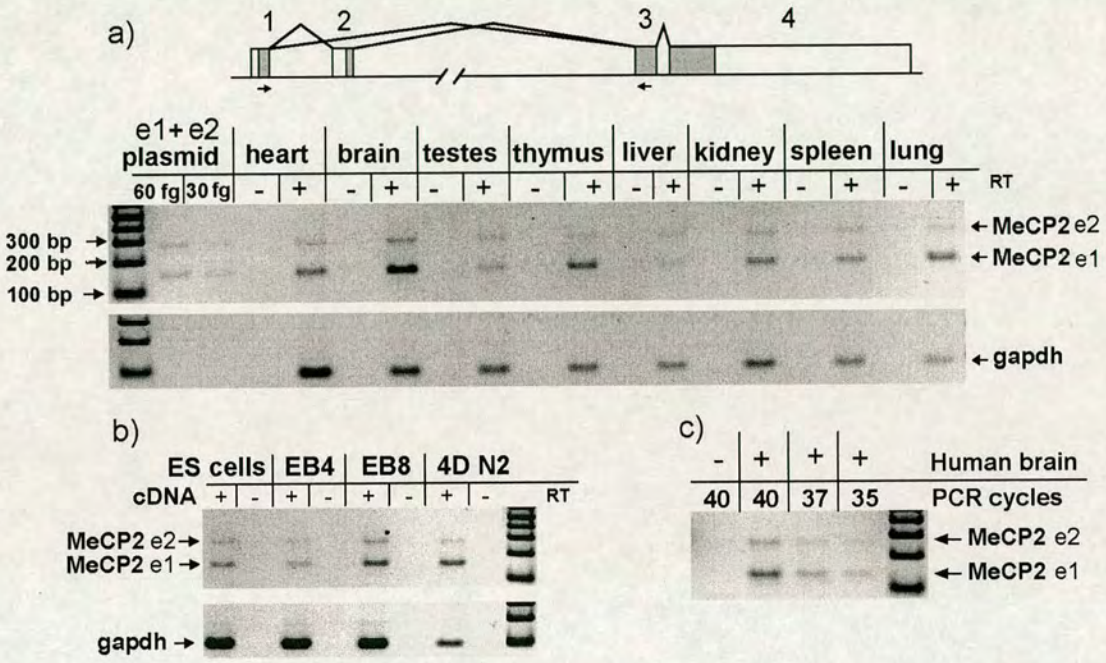

Figure 4-2. Relative abundance of splice variant mRNAs in mouse tissues, human brain and differentiating ES cells. a) A mouse tissue cDNA panel was analysed by semi-quantitative PCR with primers that anneal to exon 1 and 3 (short arrows on the map). The e1 isoform was found more abundant in lung, thymus, brain and heart. Amplification of an equimolar mixture of e1- and e2-encoding plasmids indicated no preference for amplification of either PCR band. b) Mouse ES cells were differentiated to give embryoid bodies and neuronal cells in culture. EB4 and EB8 refer to embryoid bodies on day 4 and day 8 of differentiation. 4DN2 refers to day 4 after embryoid bodies were dissociated and plated on serum-free neurobasal medium. c) PCR with human brain cDNA showed dominance of the e1 splice isoform.

4.4. The MeCP2e1 splice variant is more efficiently translated in vivo

Having established that the MeCP2e1 mRNA splice isoform is abundant in mouse tissues and human brain, we next asked if MeCP2e1 mRNA is translated *in vivo*. To address this, mouse cDNAs coding both isoforms were obtained from IMAGE consortium and sub-cloned into mammalian expression vectors (pRL-SV40, Promega) under SV40 viral promoter. Tail fibroblasts from *Mecp2*-null mice (Guy et al., 2001) were transfected with plasmid constructs containing e1 or e2 isoform cDNA (Figure 4-3). Western blotting with a C-terminal MeCP2 antibody showed that MeCP2e1 is successfully translated, but we consistently observed only very low amounts of MeCP2e2 in independent transfections. As a potential explanation, a short ORF (39 a.a.) within the 5'UTR region of MeCP2e2 was noted that could possibly interfere with its translation. The short ORF starts from the ATG that initiates translation of the MeCP2e1 isoform, but in MeCP2e2 mRNA this ORF terminates due to alternative splicing 55 bp (in mouse) upstream of the *bona fide* MeCP2e2 translation start site. To test for interference of the upstream ORF, a point mutation that changed the upstream ATG to AAG (Figure 4-4 a) was introduced and the wild-type and mutant versions of MeCP2e2 were expressed in fibroblasts. Northern blots probed with MeCP2 cDNA showed that similar amounts of mRNA were produced from transfected wildtype MeCP2e1, MeCP2e2 and mutant MeCP2e2 plasmids (Figure 4-4 b, lanes 1,2 and 3). As before, MeCP2e1 was efficiently synthesised, but a negligible amount of MeCP2e2 protein was translated from the wildtype cDNA construct. Mutation of the upstream ATG, however, led to a dramatic increase in the amount of translated MeCP2e2 (Figure 4-4 b lanes 1, 2 and 3). The results indicate that the MeCP2e1 mRNA is more abundant than MeCP2e2 mRNA, but also that MeCP2e2 mRNA is inefficiently translated. Together, these findings suggest that MeCP2e1 protein will be much more abundant than MeCP2e2 *in vivo*. To test this prediction, advantage was taken of the different predicted sizes of the e1 and e2 protein isoforms (Table 4-1).

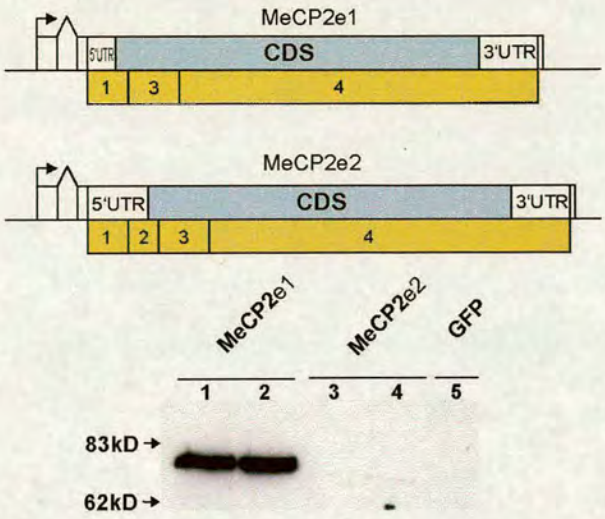

Figure 4-3. Western blot analysis of mouse cells transfected with MeCP2e1 and MeCP2e2. Top panel shows the part of the constructs used for transfections. An SV-40 promoter and artificial intron is followed by MeCP2 5'UTR, coding sequence, 3'UTR, MeCP2 polyadenylation signal and SV40 polyadenylation signal (polyadenylation signals are not shown). MeCP2 exons are shown below each map. Two independent plasmid purification baches were used for each type of transfection (MeCP2e1, lanes 1 and 2; MeCP2e2, lanes 3 and 4). The MeCP2e1 plasmid gave high protein levels, whereas the product of the MeCP2e2 plasmid was barely visible in lane 4 only. MeCP2 was detected using Upstate antibody, which was raised agains the common part of both proteins.

A high resolution SDS-PAGE gel of *in vivo* translated e1 and e2 forms confirmed that they migrate differently (Figure 4-4 b). Co-transfection of equal amounts of e1 and e2 isoform expression constructs showed that MeCP2e1 is greatly over-represented among the translation products (Figure 4-4 b lanes 4 and 5). Even when the first ATG is mutated co-transfection shows preference in the expression of e1 isoform (Figure 4-4 b lane 4). To ask whether endogenous brain MeCP2 also contains predominantly MeCP2e1, we loaded different amounts of mouse brain nuclear extract on the same gel (Figure 4-4 b lanes 8, 9 and 10). MeCP2e2 protein could be detected only with higher amounts of nuclear extract loaded. The estimate was made that the MeCP2e1 protein is at least 10 fold more abundant than MeCP2e2 in mouse brain. Observations showing the dominance of MeCP2e1 isoform in the mouse brain were also made with isoform specific antibodies (see section 4.7 below).

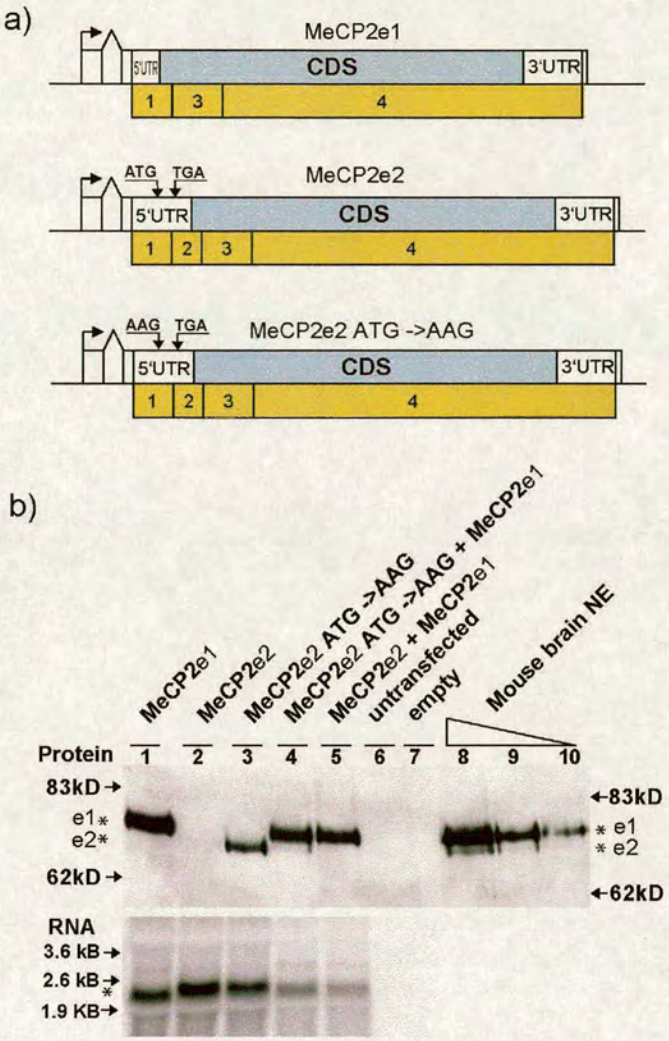

Figure 4-4. Reduced abundance of MeCP2e2 due to translational interference by an upstream ORF. a) Diagrams of MeCP2 constructs used for transfections. The MeCP2e1 expressing construct is shown on top. The start codon of the wildtype upstream ORF is labeled as ATG (middle diagram) and is mutated to AAG in the lower construct (MeCP2e2 ATG->AAG). b) Western blot analysis of transfected *Mecp2*-null mouse fibroblasts and native MeCP2 from mouse brain nuclear extracts. MeCP2 protein isoforms (*) migrated at different sizes on this 8% PAGE gel (compare lanes 1, 3 and 4). The upstream ORF inhibited the translation of MeCP2e2 (lanes 2 and 3). MeCP2e1 is the predominant isoform in mouse brain nuclear extract (lanes 8, 9 and 10). The Northern blot (lower panel) showed that different levels of translated MeCP2 protein are not due to differential transcription of the constructs, as similar amounts of MeCP2 mRNA were seen in lanes 1, 2 and 3. In the absence of transfection, no endogenous MeCP2 RNA seen in these *Mecp2*-null cells (lane 6).

4.5. Localisation of different MeCP2 isoforms in mouse cells

The majority of methylated DNA in mouse cell nuclei is in repeated major satellite sequences, which exhibit punctate staining with DAPI. In mouse cells MeCP2e2 has previously been shown to co-localise with DAPI bright spots in a DNA methylation-dependent manner (Nan et al., 1996). To compare localisation of the different MeCP2 isoforms in mouse cells, *Mecp2*-null tail fibroblasts were transfected with plasmids expressing the e1 or e2 isoforms and stained with an MeCP2 antibody that recognises the invariant C-terminal domain (Upstate). Both isoforms were nuclear and colocalised with DAPI bright spots (Figure 4-5). Therefore no functional difference was detected between e1 and e2 isoforms at the level of cellular localisation.

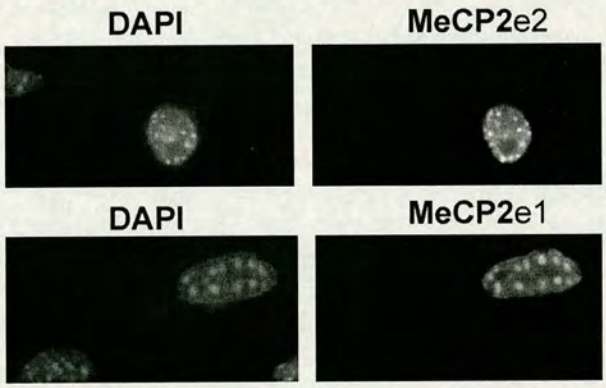

Figure 4-5. Both MeCP2 isoforms co-localise with methyl-CpG-rich DAPI bright spots when MeCP2e1 and MeCP2e2 expression constructs are transfected to *Mecp2*-null fibroblasts. Cells showing strong staining were less frequently observed in MeCP2e2 transfection.

4.6. Screening of isoform specific sequence variations in humans

The existence of the new isoform has implications for the study of Rett syndrome. Exon 1 was previously thought to be non-coding and has therefore been excluded from many mutational screening programmes. To investigate the possibility of

mutations in the exon 1, mutation screening strategy was developed. Rett syndrome patient DNA samples were kindly provided by John Warner.

Primers were designed to amplify a 450 bp region of exon 1. PCR amplified fragment was then cleaned and used for direct sequencing using the same primers. The PCR fragment was sequenced from both directions in order to have better coverage and reproducibility. The DNA samples from 60 healthy individuals (30 male and 30 female) and 100 individuals (all female) with Rett syndrome were obtained and sequenced. From these 100 individuals with Rett syndrome there were 9 samples without known MeCP2 mutations. The screen revealed no sequence variations in healthy individuals and no mutations in Rett syndrome. Failure to find any mutations could be explained by the fact that we had a very small group of patients without known *MECP2* mutation. The other group, which in parallel described MECP2e1 isoform was successful in identifying 11 nucleotide deletion in the exon 1 (Mnatzakanian et al., 2004). However to identify a mutation they screened 19 Rett syndrome girls, which were tested negative for a *MECP2* mutation in other exons.

4.7. Generation of MeCP2 isoform specific antibodies

Previous results showed that MeCP2e1 isoform on the PAGE gel migrates at higher molecular size than MeCP2e2 (Figure 4-4 b). Following this observation it was suggested that the bottom band from brain nuclear extract represents the MeCP2e2 isoform. However it is possible that the bottom band is other protein or degradation product of MeCP2e1, which is recognized by the antibody. In order to investigate the distribution of different isoforms and possible functional differences anti-peptide antibodies were raised, which would specifically recognize one or the other MeCP2 isoform.

Because there is only a very short amino acid stretch different between the two isoforms there was no good choice of possible peptides. Therefore, peptides were chosen AAPSGGGGGGEEERLC and MVAGMLGLREEKSC for MeCP2e1 and

MeCP2e2 respectively. Cysteine residues at the end of each peptide are for conjugation purposes. Genosphere Biotechnologies synthesised the peptides, conjugated them with an antigen, immunised two rabbits for each peptide and carried out ELISA tests. Pre-immune serum was taken before the immunisations were done. Ten weeks after immunisation, anti-serum was collected and ELISAs showed good chance of antibody affinity for the peptide substrates. Because Genosphere Biotechnologies has mixed the antisera, we had to find out the specificity of antisera ourselfes. To test specificity for MeCP2 protein, *Mecp2*-null cells were transfected with constructs expressing MeCP2e1 or MeCP2e2 isoforms followed by Western blot analysis. Initially transfections were tested using Upstate anti-MeCP2 antibody. Then all four pre-immune and anti sera were Western blot tested using 1:500 dilution (Figure 4-6). Based on the Western blot analysis probed with Upstate antibodies (Figure 4-3 and Figure 4-4) the expectation was to see an MeCP2 band below the 83 kDa marker. Neither of the pre- immune sera had any immunoreactivity, suggesting that all signals which were seen in the anti-sera were due to the immunisations of rabbits (Figure 4-6). Western blot with 1958 anti-serum has a predicted size band in cells transfected with e1 and e2 isoforms with slightly stronger band in the e2 transfected lane (Figure 4-6). Considering that e1 transfected cells have slightly more protein, 1958 anti-serum has better affinity to e2 isoform, however it cross-reacts with e1 isoform as well. In the brain nuclear extract mostly e1 isoform is visible, because it is much more abundant. Additionally the strong band of around 100 kDa size is been recognised in the brain. Overall we concluded that 1958 is not very specific antibody. When probed with 1959 anti-serum, there is a strong predicted size band visible in the e1 transfected cell lane but no right size band are in the e2 lane (Figure 4-6). There is one band just above 62 kDa marker, however it is wrong size. Untransfected lane is clean and the brain nuclear extract has a single predicted size signal. Therefore it is a very specific MeCP2e1 antibody, which does not cross-react with many other proteins. Probing with 1960 anti-serum gives several strong cross-reacting bands above 83 kDa marker in transfected, untransfected and brain nuclear extract lanes (Figure 4-6). Predicted size band is also observed for e2 transfected cells, which is absent in e1 or untransfected lanes. The weak band of the same size is present in the brain nuclear extract, were e2 was shown to be under-represented.

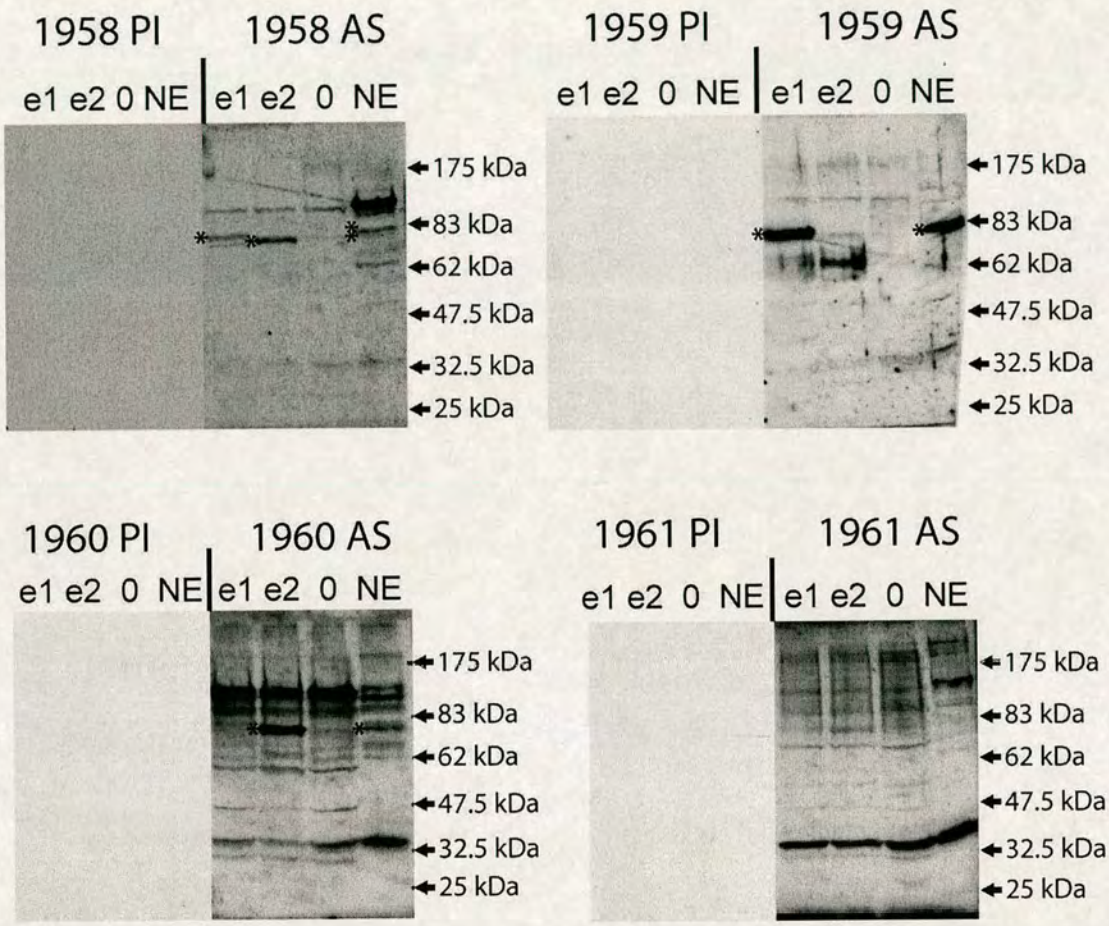

Figure 4-6. Western blot analysis of isoform specific anti-sera. Each panel has two sections: one is probed with the pre-immune serum (PI) and other with serum harvested 10 weeks after immunisation (AS). The first lane in each blot is loaded with the whole cell extract of *Mecp2*-null fibroblasts transfected with MeCP2e1 expressing plasmid (e1), the second is transfection with MeCP2e2 expressing plasmid with mutated first ATG (e2), the third is untransfected cells (0) and the last is *wt* mouse brain nuclear extract. The expected size band is 75 - 80 kDa and marked with an asterisk (*). Equal amounts of protein were loaded. Antisera were used at 1:500 dilution.

In the region of interest (between 83 and 62 kDa) 1960 anti-serum shows clear signal and is able to discriminate between e1 and e2 isoforms. This anti-serum is going to be a good tool for Western blot, but probably not for immuno-precipitations. Western blot with 1961 anti-serum was the least successful, because no strong predicted size bands were observed in any of the lanes (Figure 4-6).

4.8. Discussion

MeCP2e1 is more similar to frog and zebrafish MeCP2 sequences than the currently known isoform, MeCP2e2. These findings suggest that MeCP2e1 is more closely related to the ancestral form of MeCP2 and that the appearance of exon 2 may be a relatively recent event in the evolution of the mammalian gene. The differing size and charge of e1 and e2 isoforms permit their separation by gel electrophoresis. Subsequently it was demonstrated that both isoforms exist in mouse brain, but MeCP2e1 is by far the dominant form. The higher abundance of MeCP2e1 in mouse brain was later confirmed by protein detection with specific antibodies. The predominance of MeCP2e1 can be partly accounted for by the greater abundance of its transcript. In addition, translational interference occurs by an upstream ORF in mRNA of the e2 isoform. Translational interference by upstream ORFs is well established and has been shown to depend on the distance between the upstream ORF and the ATG of the downstream ORF and also on the structure of 5'UTR RNA (Kozak, 2001; Child et al., 1999; Xu et al., 2001; Arrick et al., 1991). It is not known whether translational interference of this kind can be modulated in vertebrates as a means of regulating protein synthesis.

New isoform specific antisera investigated in this study have shown to be a promising tool in the future investigations of the specific role of MeCP2 isoforms. More experiments are still required to proper characterise antisera. Dot-blot with peptides would be useful in determining the affinity of antibodies; affinity purification would be useful in reducing background noise (especially for the 1960 antiserum) and competition experiments could strengthen the results showing antibody specificity.

The discovery of a new coding exon emphasises the need for routine inclusion of exon 1 in Rett syndrome screens. Because MECP2e1 is the predominant MeCP2 isoform, introduction of a nonsense or frameshift mutation would remove over 90% of total MeCP2. Indeed, a disease-causing frameshift mutation (11 nucleotide insertion) was found in the patient of Rett syndrome (Mnatzakanian et al., 2004).

MeCP2e1 N-terminus contains poly-alanine and poly-glycine sequences that are encoded by repeated GCC and GGA codons respectively. Expansion of a GCC trinucleotide sequence in the FMR2 gene is reported to cause FRAXE mental retardation (Knight et al., 1993). It is noteworthy that no Rett syndrome mutations in the exon 2 have been described. It is possible that exon 2 mutations, which would only affect MeCP2e2, are compensated by the more abundant MECP2e1 isoform and would therefore have a much less severe or no phenotypic consequence. Alternatively there is no CpGs in the exon 2 therefore it has a no chance to get mutations due to methyl-CpG deamination.

A similar characterisation of the new MeCP2 isoform was published by another group (Mnatzakanian et al., 2004). They named the new isoform as MeCP2B, while the old isoform MeCP2A (following historical discovery order). Similarly they have found that in human and mouse brain the MeCP2e1 is the dominant isoform. Interestingly, RT-PCR suggested that MECP2e1 dominance was only seen in the human brain, while MECP2e2 is dominant in other human tissues (Mnatzakanian et al., 2004). Contrary to the observations in humans, MeCP2e1 was found to be a dominant isoform in different mouse tissues.

Most previous research on MeCP2 function has utilised the MeCP2e2 isoform, which we now report to be a minor form *in vivo*. MeCP2 localisation in mouse cells is the same for both isoforms, at least in cultured cells. Also, the alternative N-terminus is located outside the previously described functional domains – MBD and TRD. It is therefore unlikely that MBD or TRD function is affected by the N-terminus. Indeed, human MECP2e2 alone was able to successfully rescue MeCP2 deficiency in frog embryos, whose endogenous protein more closely resembles MeCP2e1 (Stancheva et al., 2003). Consequently it is expected that the functions of e1 and e2 isoforms may overlap significantly. On the other hand, it cannot be ruled

out that the two isoforms exert somewhat distinct functions *in vivo*. For example, the MeCP2e1 N-terminus contains a conserved serine residue that is absent in MeCP2e2 and which could be a target of phosphorylation. Recently, MeCP2 phosphorylation has been shown to accompany induction of *Bdnf* transcription in cultured mouse neurons (Martinowich et al., 2003; Chen et al., 2003b). It may be of future interest to determine the functional significance of different MeCP2 N-termini by creation of isoform-specific gene disruptions in mice.

5. Chapter five.
Inducible MeCP2 expression in a mouse

5.1. Introduction

A mouse transgene, in which expression can be regulated by drug administration, is a powerful tool for the investigation of the function of a gene. Several systems are now commonly used to produce inducible gene expression. One of them is derived from the *E.coli* tetracycline operon (tetO). The tetracycline repressor (tetR) binds tetO and represses transcription, when tetracycline is absent. In the presence of tetracycline, tetR associates with the drug and loses its DNA binding affinity. To make a tetracycline inducible activator, tetR was fused with the herpes simplex virus virion protein activation domain (VP16). The resulting protein (tTA) was able to induce transcription from a minimal cytomegalovirus promoter containing several tetO sites in the absence of tetracycline (Gossen and Bujard, 1992). The tetracycline inducible system has since had many modifications and is widely used. The tetracycline system was successfully used to investigate different brain functions in mice, such as memory formation through a regulated CaMKII transgene (Mayford et al., 1996), adenoviral brain infection with regulated EGFP (Harding et al., 1998) and reversal of neuropathology of Huntington's disease with regulated huntingtin (Yamamoto et al., 2000).

Another approach to achieve non reversible gene induction or silencing uses the combination of conventional ligand mediated induction of Cre recombinase, which in turn is able to mediate specific recombination at *loxP* sites present in the gene of interest. The positioning of *loxP* sites then determines the nature of the mutation, which could result in a gene knock-out (i.e. when *loxP* flanks coding exons) or knock-in (i.e. when *loxP* flanks an engineered artificial exon with STOP signals). To reduce the number of steps for gene targeting, required for generation of mice, *Cre* recombinase was fused with the ligand binding domain of the estrogen receptor (ER) (Metzger et al., 1995). A mutation in the binding site prevents binding of the natural ligand estradiol, but binding of synthetic ligands such as tamoxifen (TAM) or 4-hydroxytamoxifen remains the same (Danielian et al., 1993). The mutated fusion protein (Cre-ER^T) was shown to induce recombination of *loxP* sites in cell cultures and mice after the administration of the ligand (Feil et al., 1996). TAM is able to penetrate blood-brain barrier as the Cre-ER^T expressed from the brain specific prion

protein (PrP) promoter was able to produce recombination of a lacZ transgene in mouse brain, after the administration of TAM (Weber et al., 2001).

Inducible MeCP2 expression in mice would help to answer several important questions. Induction of MeCP2 after a *Mecp2*-null mouse has developed symptoms would help to determine whether Rett syndrome is a reversible disease. This could open the prospect for gene therapy based treatments. If it is not possible to reverse or relieve the Rett-like phenotype in the mouse (by MeCP2 induction after commencement of symptoms) then MeCP2 expression could be induced at different ages before the onset of symptom to permit the identification of the critical period at which the non reversible pathological events in the brain occur.

In the first part of the results section, the strategy and the attempts to create a tetracycline-inducible MeCP2 mouse will be described. In the second part, a mouse with Cre-ER^T transgene was used to delete *Mecp2* in the adult animal.

5.2. Construction of the inducible MeCP2 allele in mice

To make a MeCP2 inducible mouse line, the tetracycline inducible system was chosen because of its flexibility and history of successful applications in mice. The "Tet-on" system has a modified tetracycline trans-activator termed "reverse tetracycline trans-activator (rtTA)", which in the absence of tetracycline or its analog doxycycline (Dox) is unable to bind to DNA (Figure 5-1). Opposite to tTA, the addition of doxycyline results in the binding of rtTA to the promoter (with tetO sites) followed by target gene activation. As a target gene, the *Mecp2* cDNA was cloned into a bi-directional expression cassette, which upon activation allows simultaneous transcription of two genes. The second gene in the expression vector was *Luciferase*. Once the Luciferase activity ratio with the amount of MeCP2 is established, then only Luciferase activity can be measured to evaluate the level of induction in different animals harbouring the same transgene.

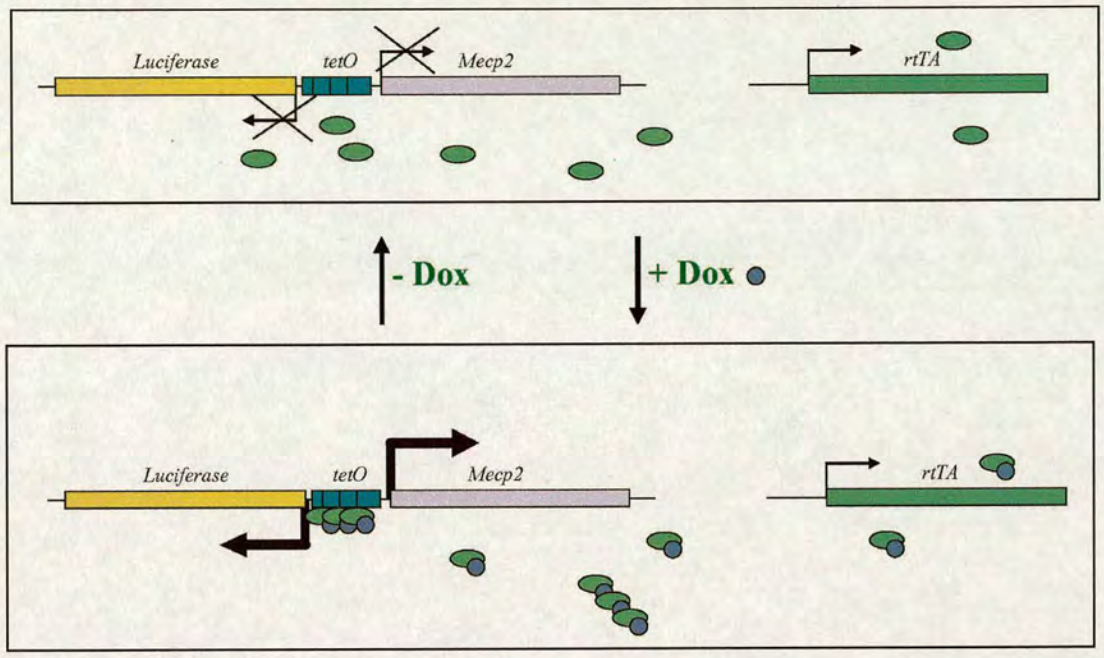

Figure 5-1. Mechanism of "Tet-on" inducible gene expression for induction of *Mecp2*. In the absence of doxycycline, transcription from the bi-directional vector expressing both luciferase and MeCP2 is silent. After addition of doxycyline, it binds rtTA. Subsequently complex associates with *tetO* sequences and activates transcription from both promoters. Doxycyline withdrawal results in silencing of the *Luciferase* and *Mecp2* genes again.

To accomplish the described experiment in mice (Figure 5-1), three genetic modifications have to be present in the one mouse: constant and ubiquitous expression of rtTA, a bi-directional vector allowing MeCP2/Luciferase expression and the mutation inactivating the endogenous *Mecp2* gene. These mutations can be engineered in one animal according to the scheme proposed in the Figure 5-2. The modified version of rtTA has a nuclear localisation signal fused to the N-terminal part of the protein (N-nlsrtTA) (Gossen et al., 1995). For the ubiquitous expression of N-nlsrtTA, the construct was chosen to be targeted to the ROSA26 locus, which was demonstrated to provide high ubiquitous expression and it is easily targeted by homologous recombination (Soriano, 1999; Zambrowicz et al., 1997).

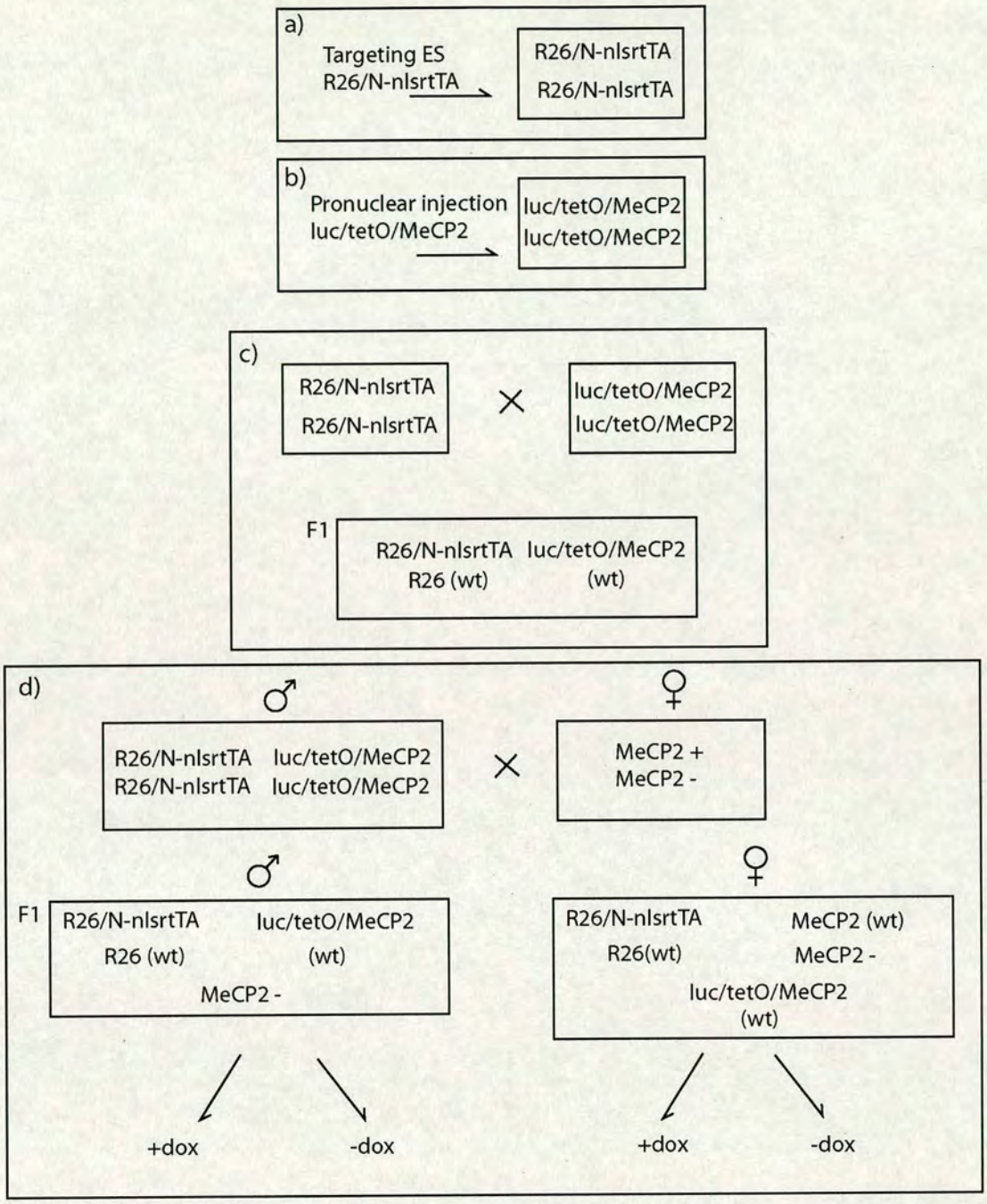

Figure 5-2. Strategy for the production of an inducible MeCP2 in mouse. a) In the first step *N-nlsrtTA* (rtTA with N terminal nuclear localisation signal) is targeted to the ubiquitously expressing ROSA26 locus in ES cells and correctly targeted clones are used to generate mice. b) The bi-directional vector with *Mecp2* and *Luciferase* is used to generate a transgenic mouse by pronuclear injection. c) A homozygous *N-nlsrtTA* mouse is then crossed with a transgenic *luc/tetO/Mecp2* mouse and F1 progeny can then be assayed for MeCP2 inducibility. d) A homozygous mouse carrying all of the described modifications could be then crossed with a *Mecp2* heterozygous female and the progeny used for the MeCP2 restoration experiments.

The ROSA26 N-nlsrtTA targeting construct together with screening probe was previously used by Anton Wutz who provided us with the materials (Wutz and Jaenisch, 2000). According to the experimental strategy, to generate rtTA expression from the ROSA26 locus in mouse, E14TG2a embryonic stem cells were targeted with the R26/N-nlsrtTA vector. Correct targeting was confirmed by Southern blot analysis (Figure 5-3). The targeting efficiency was calculated as 5.6 % (from 54 successfully screened clones). Three correctly targeted ES cell lines were generated: R26A6, R26E3 and R26G6. Subsequently, to test if a functional tetracycline trans-activator was produced, the targeted R26G6 ES cell line was electroporated with a *Luciferase* reporter construct and incubated with doxycycline (1 μg/ml) or without doxycyline. Luciferase measurements revealed that in the presence doxycyline, Luciferase activity is induced almost 100 fold (Figure 5-4).

ES cells were then injected into the blastocysts derived from C57BL/6 mice and transplanted into pseudopregnant recipient females. Chimaeric mice were identified by the presence of their patchy agouti coat colour. From ES cell lines R26E3, R26A6 and R26G6, 0, 4 and 27 chimaeras were generated, respectively. The chimaeric mice were then crossed with C57BL/6 mates to test for germline transmision. Three litters (producing 10 – 25 pups) were examined from each chimera, however no germline transmission was observed from any of the chimeras generated. It is possible that ES cells were compromised during gene targeting manipulations and lost their totipotency.

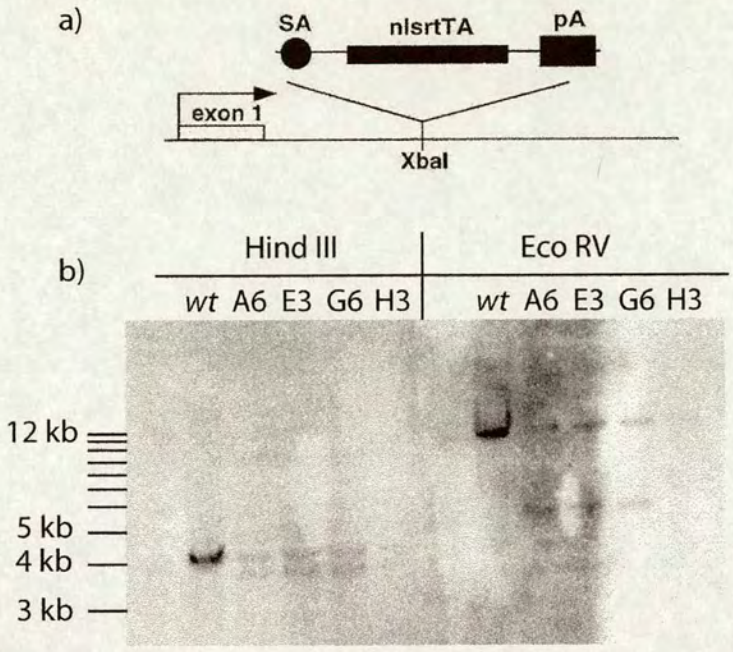

Figure 5-3. The targeting of ROSA26 locus with the tetracycline trans-acivator. a) ROSA26 locus targeting scheme. SA – splice acceptor. Figure taken is from (Wutz and Jaenisch, 2000). b) Southern blot analysis of correctly targeted clones. Expected band sizes are: for *Hind*III digestion *wt* allele - 4.4 kb, targeted - 3.8 kb; for *Eco*RV digestion *wt* allele - 14 kb, tartgeted - 5 kb.

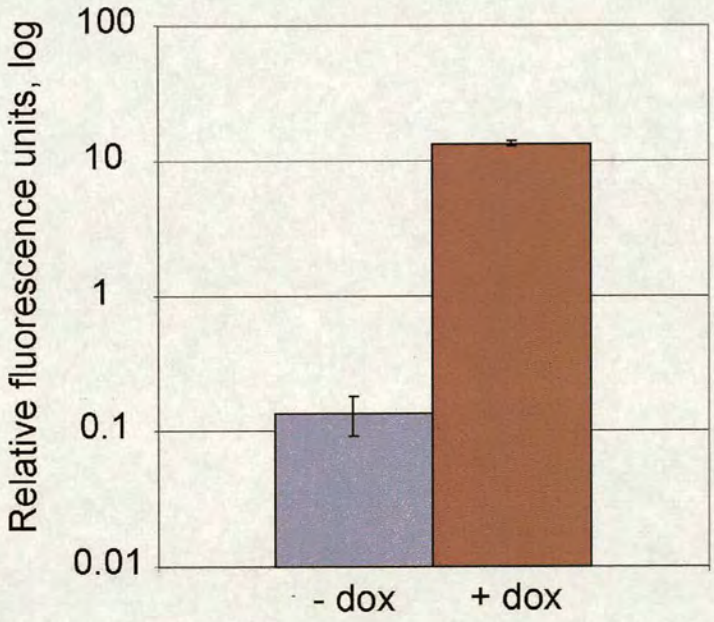

Figure 5-4. N-nlsrtTA targeted ES cells were electroporated with a *Luciferase* reporter construct under control of the tetO promoter. In the presence of doxycycline (+dox) luciferase activity is induced approximately 100 fold.

5.3. Cre-ER^T mediated MeCP2 knock-out in adult mice

There are two theories about the nature of Rett syndrome. One says that MECP2 is required for a particular developmental event in the brain. Therefore at the time of early post-natal development the presence of mutated MECP2 leads to the failure of normal brain development. Another possibility is that MECP2 is required for the proper maintenance of neuronal function and, in the absence of MECP2, brain function can be maintained for some time after which it becames compromised. An experiment in which MeCP2 mutation could be introduced at different ages in the mouse could help to distinguish between these two possibilities.

The previously discussed Cre-ER^T system was used to introduce a Cre-*loxP* mediated MeCP2 deletion in the adult mouse (Figure 5-5). A homozygous mouse line carrying *Cre-ER^T* transgene was available in the laboratory. The *Mecp2 loxP* mouse line was used to generate the original MeCP2 knock-out was also available (Guy et al., 2001). After a single cross of a homozygous *Mecp2$^{lox/lox}$* female with a *Cre-ER^T* male, all the F1 progeny had one *Cre-ER^T* allele and were hemizygous (*Mecp2$^{lox/y}$*) or heterozygous (*Mecp2$^{lox/+}$*) for *Mecp2-loxP* allele. All progeny were genotyped using PCR with *Cre* and *Mecp2 loxP* specific primers.

To induce deletion of the *Mecp2* gene in adult mice, the animals were aged until 7 weeks old and then tamoxifen (TAM) was injected intra-peritoneally at a dose of 1 mg/day (dissolved in corn oil) for 5 consecutive days. To monitor the possible negative effects of TAM, the same number of *wt* mice underwent identical injections. Five days after the last injection, the animals were sacrificed and genomic DNA was purified from different tissues. Genomic DNA was digested with *Bam*HI and a Southern blot was probed with *Nco*I-*Bam*HI 3' MeCP2 cDNA probe as described previously (Guy et al., 2001). The Southern blot results demonstrated low amounts of recombination were present (Figure 5-6). The highest recombination rate was seen in the tail and the lower rates in kidney and liver.

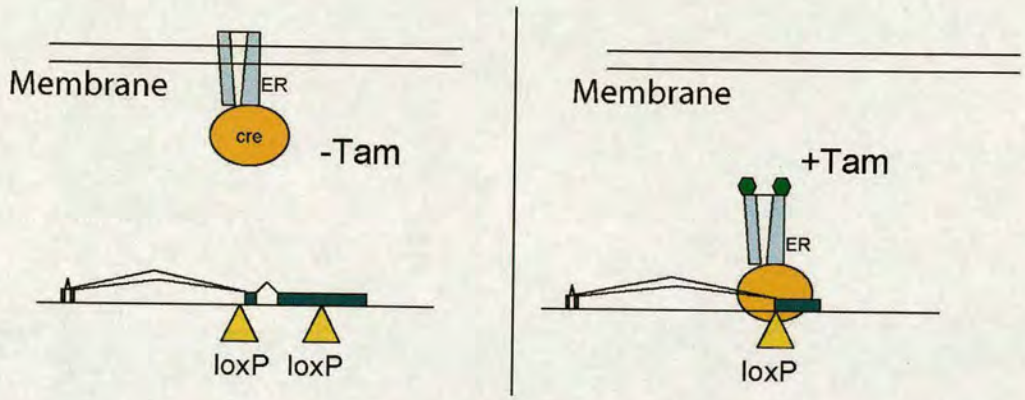

Figure 5-5. Generation of ligand inducible mutation in the *Mecp2* gene using Cre-ER^T technology. In the absence of the inducer tamoxifen (TAM) the Cre-ER^T protein is immobilised in the membrane. After administration of TAM, the protein leaves the membrane and in the nucleus recombines the *loxP* sites, resulting in a null mutation in the *Mecp2* gene.

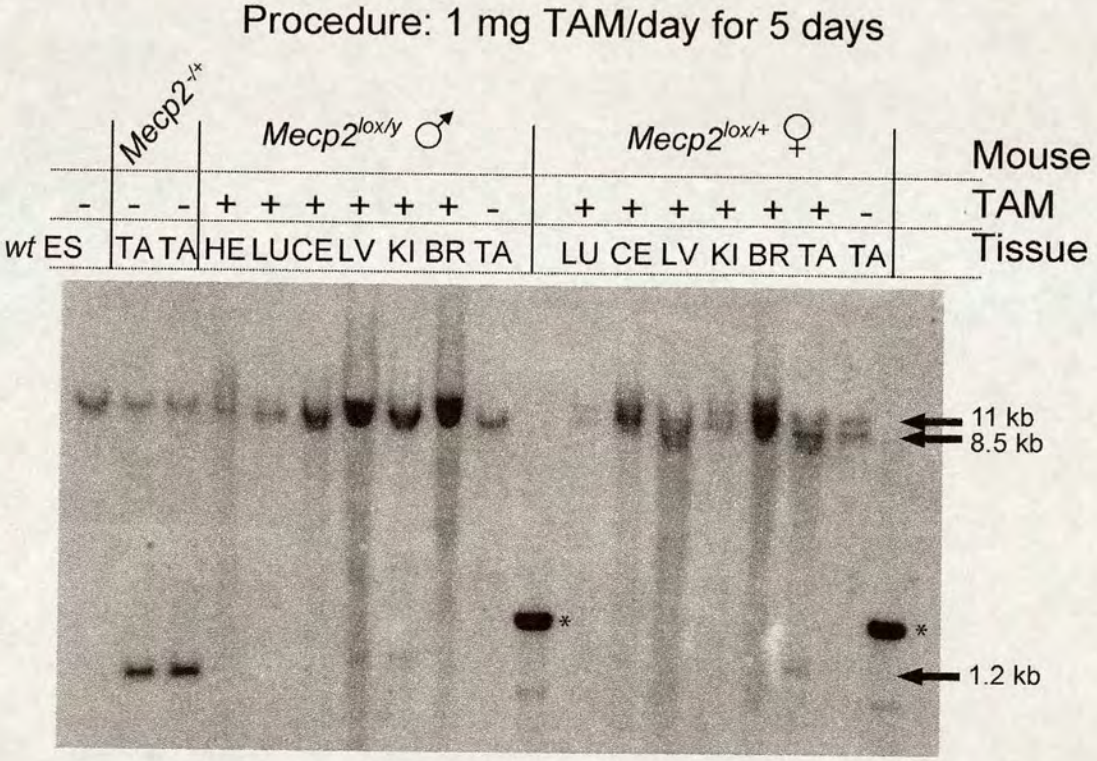

Figure 5-6. Southern blot analysis of *loxP* recombination at the *Mecp2* locus after administration of 1 mg of TAM per day. *Wt* ES – *wt* embryonic stem cell DNA; TA – tail, HE – heart, LU – lungs, CE – cerebellum, LV – liver, KI – kidney, BR – brain. *Wt* allele gives an 11 kb band, loxP allele – 8.5 kb and the deleted *Mecp2* allele – 1.2 kb. A strong band marked with * is cross-hybridisation with a size marker.

Some published reports used a higher dose of tamoxifen for adult animals such as 3 or 9 mg of TAM per day (Hayashi and McMahon, 2002). The dose of TAM used here was then increased in an attempt to get a higher recombination rate in brain (Figure 5-7). Still a low recombination rate was observed in all tissues except tail tip. The low recombination rate observed in different tissues could be due to tissue specific expression of Cre-ER^{T} transgene. Epithelial cells and connective tissue, which significantly contribute to the tail tip, showed consistently moderate recombination rate.

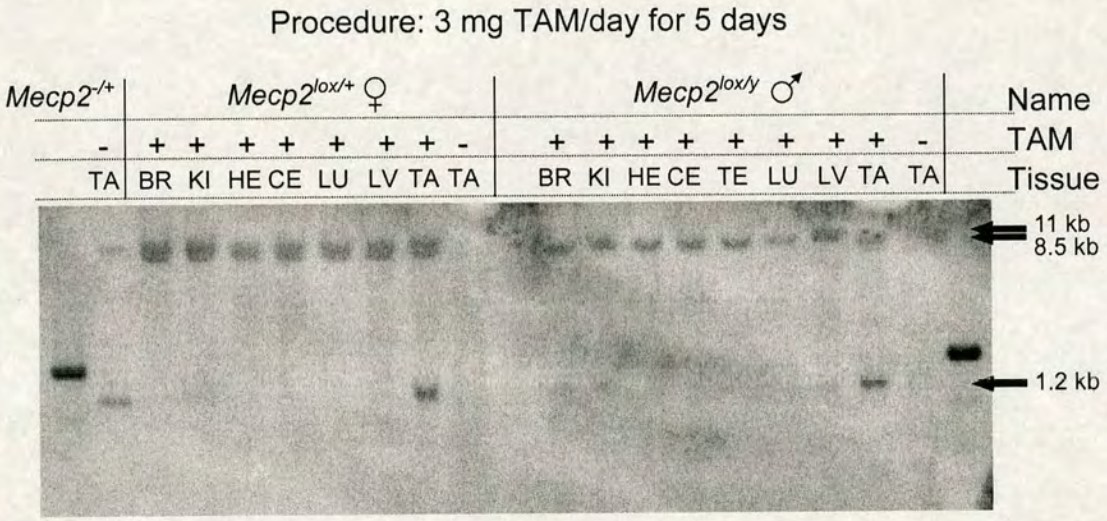

Figure 5-7. Southern blot of *Mecp2* loxP recombination following administration of 3 mg of TAM per day for 5 consecutive days. TA – tail, HE – heart, LU – lungs, CE – cerebellum, LV – liver, KI – kidney, BR – brain, TE - testis. *Wt* allele gives an 11 kb band, *loxP* allele – 8.5 kb and the deleted *Mecp2* allele – 1.2 kb.

5.4. Summary and discussion

This chapter describes attempts to generate mice with inducible MeCP2 expression. In the initial experiment a tetracycline inducible gene expression system was used for the regulation MeCP2 expression. This system is considered to be the most flexible,

because administration of doxycycline would allow induction of the *Mecp2* transgene expression and withdrawal would silence it. Therefore bi-directional temporal control of MeCP2 expression could be achieved. In addition, different amounts of doxycycline would allow different levels of MeCP2 induction. This is a very important feature, because in the transgenic model it was shown that over-expression of MeCP2 causes a neurological phenotype (Luikenhuis et al., 2004). However 2 to 3 fold MeCP2 over-expression is tolerated in mice (Luikenhuis et al., 2004). Three ES cell lines with a tetracycline trans-activator were generated. There were very low numbers of chimaeric mice born from two of the cell lines R26A6 and R26E3. The R26G6 ES cell line produced a high number of chimeras, however the chimeras were unable to transmit the mutation to the offspring. It is therefore possible, that the cells were defective or were damaged during the procedure of targeting.

Knock-out of the *Mecp2* gene using a Cre-ER^T inducible cassette was unsuccessful. The Cre-ER^T mouse line used was not suitable for experimental purposes. The only tissue with a significant amount of recombination present was the tail.

For follow up experiments using the Cre-ER^T system, mice with a high recombination rate in the brain should be acquired. A few suitable mouse strains have since been published. The CAGGCre-ER^{TM} mouse strain was shown to have a high recombination rate using a β-galactosidase reporter, which is activated after Cre-loxP recombination (Hayashi and McMahon, 2002). PrP-Cre-ER^T mice were shown to have a very high recombination rate in cerebellum and intermediate recombination in the brain cortex (Weber et al., 2001). These lines are good candidate lines to be obtained for Cre-ER^T mediated gene knock-out or knock-in strategies in mouse.

6. Chapter six.

Final conclusions

6.1. Final summary and discussion

The studies in this thesis are focused on the investigation of MeCP2 function in relevance to Rett syndrome. As highlighted in the introduction chapter, the key issue in understanding the role of the MeCP2 is identification of its target genes. When the global analysis of gene expression by ADDER was initiated, no MeCP2 target genes were known in the brain. Only in the recent years were *Hairy2a* and *Bdnf* shown to be mis-regulated in the absence of MeCP2 (Stancheva et al., 2003; Chen et al., 2003b; Martinowich et al., 2003). However, it was difficult to relate the mis-expression of these genes to Rett syndrome, because the expression status of *Hairy2a* and *Bdnf* genes was not known in the brain. *Hairy2a* was shown to be mis-regulated in frog embryos lacking MeCP2 (Stancheva et al., 2003) and *Bdnf* in primary mouse neuronal cultures from the *Mecp2*-null mice (Chen et al., 2003b). *Bdnf* and *Hairy2a* mammalian homolog *Hes1* expression in mouse brain were investigated in this thesis. Comparing the expression of *Hes1* between *wt* and *Mecp2*-null brains confirmed that it is significantly up-regulated in the nulls. However, surprisingly, in this work *Bdnf* was shown to be down-regulated in whole mouse brains instead of expected up-regulation, which was observed in cultured neurons (Chen et al., 2003b). There are few explanations of the different results obtained from mouse brain and neuronal cultures. One possibility is that cortical neurons isolated from embryonic mice brain behave differentially from the ones present in brain. An alternative explanation could be that brain is a very heterogeneous tissue with multiple cell types which could have unknown *Bdnf* regulatory feedback mechanisms.

The findings of *Bdnf* and *Hes1* being mis-regulated in the *Mecp2*-null mouse brain opened new research prospects. Subsequently it is important to investigate further the possibility of the primary MeCP2 involvement in the regulation of *Hes1* expression. The presence of MeCP2 at the promoter region would strengthen the hypothesis of its primary involvement; however it would not reject the statement that secondary factors are contributing to the up-regulation of the gene as well. Therefore, at this stage it would be beneficial to establish a simplified model system, such as mammalian tissue culture, where the genetic manipulations can be more easily done.

The down-regulation of total *Bdnf* in *Mecp2*-null mouse whole brains was observed at different stages of the disease progression, including healthy looking pre-symptomatic mice. Because the *Bdnf* gene is transcribed from different promoters, it was important to know which promoter causes the observed down-regulation. After examination of different promoters, a statistically significant difference between the samples was not obtained. It is possible, that several promoters contribute to the total down-regulation of *Bdnf* in pre-symptomatic mice. Another explanation can be based on the sensitivity issues of the Real Time PCR technique. Real Time PCR is more sensitive in comparing the expression of the higher abundance transcripts rather than the lower abundance ones. Therefore, the division of total *Bdnf* expression into activities of four specific promoters may have reduced the sensitivity of the assay. Further research should determine how the basal up-regulation of *Bdnf* expression in cultured *Mecp2*-null neurons relates with the observed decrease of *Bdnf* messages in *Mecp2*-null brains. RNA FISH or *in situ* hybridisation with specific Bdnf antibodies would be helpful in finding the specific cell types and brain regions, responsible for the down-regulation of total *Bdnf* expression.

Further gene expression study by microarray suggested that the stress response regulation may be perturbed in the mouse model for Rett syndrome. Expression analysis clearly showed up-regulation of *Sgk* and *Fkbp5* expression in pre-, early and late symptomatic mice. None of the other examined mis-regulated genes showed as high as 2.6 fold induction observed for *Sgk* in the absence of MeCP2. The relation between Rett syndrome and symptoms caused by therapeutic glucocorticoid administration suggests that the patho-physiological side of Rett syndrome may partially caused by the defects in the hormone regulation. Therapeutically, the use of glucocorticoid antagonists may provide a potential relief for certain symptoms.

The global gene expression analysis by ADDER revealed 11 genes that were mis-regulated in late symptomatic mice, 3 in the early symptomatic mice and no mis-regulated genes in the pre-symptomatic mice. The previous study of gene expression by microarray failed to find any mis-regulated genes (Tudor et al., 2002). The above described microarray study identified several genes related to the stress regulation pathway. The difficulties in finding many MeCP2 target genes raise few possibilities.

One possibility is that there are not many genes mis-regulated in the absence of MeCP2. Another possibility is that the microarray technique is not sensitive enough to find genes that are subtly mis-regulated and transcribed at a low level. Additionally, mice in the study by Tudor *et al.* were grouped by the age and not by symptoms, providing more heterogeneity to the sample. In this thesis, an attempt was made both to improve sensitivity by using a variant of differential display and to ensure homogeneity of samples by grouping mice according to the presentation of symptoms. The third possibility which could explain difficulties in finding mis-regulated genes by global approaches is that brain contains a lot of cell types with different gene expression profiles (Nisenbaum, 2002). Therefore even a hypothetical large difference in mRNA abundance in a certain cell type will be diluted by the equal expression in others.

Another important consideration in investigating gene expression changes in the relation to the symptom progression is to understand which event triggers the appearance of the symptoms. In classical Rett syndrome the disease starts very dramatically with a period of rapid regression. Until this period it is difficult to distinguish a normal child from the child which will develop the disease. Therefore, an expectation is that a physiological event happens at this period, when the rapid regression is initiated. The gene expression studies performed in this thesis suggest that such event might be related with mis-expression of mitochondrial gene *Uqcrc1*. *Uqcrc1* is normally expressed in the *Mecp2*-null mice without symptoms and it starts to be mis-expressed with appearance of the first symptoms in mice. Furthermore, similar observations are made for the mitochondrial respiration, where the Uqcrc1 protein is functioning. Mitochondrial respiration is normal in the healthy *Mecp2*-null mice and it becomes abnormal with the appearance of symptoms. The time course conjunction of *Uqcrc1* expression, abnormal mitochondrial respiration and appearance of the symptoms suggest that these events might be related.

The molecular basis of the observed mitochondrial respiration abnormalities is not clear. Future experiments could address if the Uqcrc1 protein amounts are affected, if mis-regulation of one component affects the assembly of the whole complex and if MeCP2 primarily regulates the expression of the *Uqcrc1* gene.

Genes found to be mis-regulated in *Mecp2*-null mouse brain in the research presented in this thesis opened several different prospects of investigation. First strand could focus on molecular biology of MeCP2 action. *Bdnf*, *Sgk*, *Fkbp5* are all inducible genes. *Bdnf* is induced by Ca^{2+} induced depolarisation. *Sgk* and *Fkbp5* are glucocorticoid inducible genes. This raises the possibility that MeCP2 regulates inducible gene expression in a dynamic way, which was suggested for the *Bdnf* case (Chen et al., 2003b). Data presented in the thesis show no any obvious MeCP2 occupancy changes in the *Sgk* and *Fkbp5* promoters after corticosterone treatment. However it is still possible that heterogeneity of brain samples masks some small changes. The promoter occupancy could still be envisited in more homogeneous populations of cells such as primary cortical neurons or neuronal cell lines. In addition new target genes could serve as a model to test what is the mechanism of repression. What co-repressors are recruited and how the local chromatin modifications are changed?

Another big strand of investigations could be involved in exploring the relevance of newly discovered mis-regulated genes to Rett syndrome. Creating transgenic mouse models mimicking the mis-expression of *Bdnf*, *Sgk*, *Fkbp5* and *Uqcrc1* genes could help to find out how much these genes are contributing to the phenotype observed in *Mecp2*-null mice. Therefore the real relevance of mis-expressed genes to Rett syndrome could be evaluated. However there is a possibility that Rett syndrome is a very complicated disease, which develops as a consequence of mis-expression of many genes in specific regions of the brain.

This thesis described a new MeCP2 isoform. Both data presented here and parallel data published by another group (Mnatzakanian et al., 2004) indicated that the newly discovered isoform represents the majority of MeCP2 present in mouse and human brain. The lower splicing rate and the inhibition of translation of MeCP2e2 provide an explanation for MeCP2e1 dominance. The new coding exon 1 has been shown to harbour Rett syndrome-causing mutations (Mnatzakanian et al., 2004). However the recent mutation screen of 97 Rett patients negative for mutations in exons 2, 3 and 4, revealed no mutations in exon 1 (Evans et al., 2005). Several sequence variations were identified, which also were found to be present in healthy individuals. One

interesting variation was a $(GCC)_2$ insertion, suggesting that trinucleotide expansions can occur in *MECP2* exon 1 (Evans et al., 2005). In future it will be important to find out if two MeCP2 isoforms have different functions. Isoform specific knock-out will be helpful in indicating the possible importance of an alternative MeCP2 splicing.

Finally, attempts to create a mouse with inducible MeCP2 expression were not successful. The lack of a mouse harbouring the transgene (either Cre-ER^T or rtTA), which would allow creation of inducible *Mecp2* gene, was the main restriction. The question of whether the restoration of MeCP2 expression relieves Rett syndrome-like symptoms in mice is still un-answered and important for the prospects of possible treatment. Gene therapy based treatments could help in delivering functional MeCP2 to the cells, which have the mutated copy of *Mecp2* gene. However it will be still important to find out whether there is any dominant negative effect of the presence of mutated *Mecp2* copy in the same cell, and how the overexpression of MeCP2 (in the case of expression vector delivery to the cell expressing *wt* MeCP2) is going to affect the physiology of a cell.

Reference List

Aber,K.M., Nori,P., MacDonald,S.M., Bibat,G., Jarrar,M.H., and Kaufmann,W.E. (2003). Methyl-CpG-binding protein 2 is localized in the postsynaptic compartment: an immunochemical study of subcellular fractions. Neuroscience *116*, 77-80.

Ahmad,K. and Henikoff,S. (2002). Epigenetic consequences of nucleosome dynamics. Cell *111*, 281-284.

Aizawa,H., Hu,S.C., Bobb,K., Balakrishnan,K., Ince,G., Gurevich,I., Cowan,M., and Ghosh,A. (2004). Dendrite development regulated by CREST, a calcium-regulated transcriptional activator. Science *303*, 197-202.

Akbarian,S., Chen,R.Z., Gribnau,J., Rasmussen,T.P., Fong,H., Jaenisch,R., and Jones,E.G. (2001). Expression pattern of the Rett syndrome gene MeCP2 in primate prefrontal cortex. Neurobiol. Dis. *8*, 784-791.

Akhmanova,A., Verkerk,T., Langeveld,A., Grosveld,F., and Galjart,N. (2000). Characterisation of transcriptionally active and inactive chromatin domains in neurons. J. Cell Sci. *113 Pt 24*, 4463-4474.

Amir,R.E., Van,d.V., I, Wan,M., Tran,C.Q., Francke,U., and Zoghbi,H.Y. (1999). Rett syndrome is caused by mutations in X-linked MECP2, encoding methyl-CpG-binding protein 2. Nat. Genet. *23*, 185-188.

Amir,R.E. and Zoghbi,H.Y. (2000). Rett syndrome: methyl-CpG-binding protein 2 mutations and phenotype-genotype correlations. Am. J. Med. Genet. *97*, 147-152.

Antequera,F. and Bird,A. (1993). Number of CpG islands and genes in human and mouse. Proc. Natl. Acad. Sci. U. S. A *90*, 11995-11999.

Armstrong,D.D. (1992). The neuropathology of the Rett syndrome. Brain Dev. *14 Suppl*, S89-S98.

Armstrong,D.D. (2001). Rett syndrome neuropathology review 2000. Brain Dev. *23 Suppl 1*, S72-S76.

Armstrong,D.D. (2002). Neuropathology of Rett syndrome. Ment. Retard. Dev. Disabil. Res. Rev. *8*, 72-76.

Armstrong,D.D. (1995). The neuropathology of Rett syndrome--overview 1994. Neuropediatrics *26*, 100-104.

Arrick,B.A., Lee,A.L., Grendell,R.L., and Derynck,R. (1991). Inhibition of translation of transforming growth factor-beta 3 mRNA by its 5' untranslated region. Mol. Cell Biol. *11*, 4306-4313.

Bale,A., d'Alarcao,M., and Marinus,M.G. (1979). Characterization of DNA adenine methylation mutants of Escherichia coli K12. Mutat. Res. *59*, 157-165.

Balmer,D., Goldstine,J., Rao,Y.M., and LaSalle,J.M. (2003). Elevated methyl-CpG-binding protein 2 expression is acquired during postnatal human brain development and is correlated with alternative polyadenylation. J. Mol. Med. *81*, 61-68.

Barent,R.L., Nair,S.C., Carr,D.C., Ruan,Y., Rimerman,R.A., Fulton,J., Zhang,Y., and Smith,D.F. (1998). Analysis of FKBP51/FKBP52 chimeras and mutants for Hsp90 binding and association with progesterone receptor complexes. Mol. Endocrinol. *12*, 342-354.

Bauman,M.L., Kemper,T.L., and Arin,D.M. (1995). Microscopic observations of the brain in Rett syndrome. Neuropediatrics *26*, 105-108.

Baylin,S.B. and Herman,J.G. (2000). DNA hypermethylation in tumorigenesis: epigenetics joins genetics. Trends Genet. *16*, 168-174.

Beard,C., Li,E., and Jaenisch,R. (1995). Loss of methylation activates Xist in somatic but not in embryonic cells. Genes Dev. *9*, 2325-2334.

Bell,A.C. and Felsenfeld,G. (2000). Methylation of a CTCF-dependent boundary controls imprinted expression of the Igf2 gene. Nature *405*, 482-485.

Bestor,T.H. (1990). DNA methylation: evolution of a bacterial immune function into a regulator of gene expression and genome structure in higher eukaryotes. Philos. Trans. R. Soc. Lond B Biol. Sci. *326*, 179-187.

Bestor,T.H. (1988). Cloning of a mammalian DNA methyltransferase. Gene *74*, 9-12.

Bestor,T.H. (2000). The DNA methyltransferases of mammals. Hum. Mol. Genet. *9*, 2395-2402.

Bird,A. (2002). DNA methylation patterns and epigenetic memory. Genes Dev. *16*, 6-21.

Bird,A. and Tweedie,S. (1995). Transcriptional noise and the evolution of gene number. Philos. Trans. R. Soc. Lond B Biol. Sci. *349*, 249-253.

Bird,A.P. and Wolffe,A.P. (1999). Methylation-induced repression--belts, braces, and chromatin. Cell *99*, 451-454.

Bonni,A., Brunet,A., West,A.E., Datta,S.R., Takasu,M.A., and Greenberg,M.E. (1999). Cell survival promoted by the Ras-MAPK signaling pathway by transcription-dependent and -independent mechanisms. Science *286*, 1358-1362.

Bourc'his,D., Xu,G.L., Lin,C.S., Bollman,B., and Bestor,T.H. (2001). Dnmt3L and the establishment of maternal genomic imprints. Science *294*, 2536-2539.

Brockdorff,N. (2002). X-chromosome inactivation: closing in on proteins that bind Xist RNA. Trends Genet. *18*, 352-358.

Brown,C.J., Ballabio,A., Rupert,J.L., Lafreniere,R.G., Grompe,M., Tonlorenzi,R., and Willard,H.F. (1991a). A gene from the region of the human X inactivation centre is expressed exclusively from the inactive X chromosome. Nature *349*, 38-44.

Brown,C.J., Lafreniere,R.G., Powers,V.E., Sebastio,G., Ballabio,A., Pettigrew,A.L., Ledbetter,D.H., Levy,E., Craig,I.W., and Willard,H.F. (1991b). Localization of the X inactivation centre on the human X chromosome in Xq13. Nature *349*, 82-84.

Carney,R.M., Wolpert,C.M., Ravan,S.A., Shahbazian,M., Ashley-Koch,A., Cuccaro,M.L., Vance,J.M., and Pericak-Vance,M.A. (2003). Identification of MeCP2 mutations in a series of females with autistic disorder. Pediatr. Neurol. *28*, 205-211.

Cass,H., Reilly,S., Owen,L., Wisbeach,A., Weekes,L., Slonims,V., Wigram,T., and Charman,T. (2003). Findings from a multidisciplinary clinical case series of females with Rett syndrome. Dev. Med. Child Neurol. *45*, 325-337.

Cassel,S., Revel,M.O., Kelche,C., and Zwiller,J. (2004). Expression of the methyl-CpG-binding protein MeCP2 in rat brain. An ontogenetic study. Neurobiol. Dis. *15*, 206-211.

Chan,M.F., van,A.R., Nijjar,T., Cuppen,E., Jones,P.A., and Laird,P.W. (2001). Reduced rates of gene loss, gene silencing, and gene mutation in Dnmt1-deficient embryonic stem cells. Mol. Cell Biol. *21*, 7587-7600.

Chandler,S.P., Guschin,D., Landsberger,N., and Wolffe,A.P. (1999). The methyl-CpG binding transcriptional repressor MeCP2 stably associates with nucleosomal DNA. Biochemistry *38*, 7008-7018.

Cheadle,J.P., Gill,H., Fleming,N., Maynard,J., Kerr,A., Leonard,H., Krawczak,M., Cooper,D.N., Lynch,S., Thomas,N., Hughes,H., Hulten,M., Ravine,D., Sampson,J.R., and Clarke,A. (2000). Long-read sequence analysis of the MECP2 gene in Rett syndrome patients: correlation of disease severity with mutation type and location. Hum. Mol. Genet. *9*, 1119-1129.

Chen,H. and Weber,A.J. (2004). Brain-derived neurotrophic factor reduces TrkB protein and mRNA in the normal retina and following optic nerve crush in adult rats. Brain Res. *1011*, 99-106.

Chen,R.Z., Akbarian,S., Tudor,M., and Jaenisch,R. (2001). Deficiency of methyl-CpG binding protein-2 in CNS neurons results in a Rett-like phenotype in mice. Nat. Genet. *27*, 327-331.

Chen,R.Z., Pettersson,U., Beard,C., Jackson-Grusby,L., and Jaenisch,R. (1998). DNA hypomethylation leads to elevated mutation rates. Nature *395*, 89-93.

Chen,T., Ueda,Y., Dodge,J.E., Wang,Z., and Li,E. (2003a). Establishment and maintenance of genomic methylation patterns in mouse embryonic stem cells by Dnmt3a and Dnmt3b. Mol. Cell Biol. *23*, 5594-5605.

Chen,W.G., Chang,Q., Lin,Y., Meissner,A., West,A.E., Griffith,E.C., Jaenisch,R., and Greenberg,M.E. (2003b). Derepression of BDNF transcription involves calcium-dependent phosphorylation of MeCP2. Science *302*, 885-889.

Cheng,X. and Roberts,R.J. (2001). AdoMet-dependent methylation, DNA methyltransferases and base flipping. Nucleic Acids Res. *29*, 3784-3795.

Child,S.J., Miller,M.K., and Geballe,A.P. (1999). Translational control by an upstream open reading frame in the HER-2/neu transcript. J. Biol. Chem. *274*, 24335-24341.

Cohen,D.R., Matarazzo,V., Palmer,A.M., Tu,Y., Jeon,O.H., Pevsner,J., and Ronnett,G.V. (2003). Expression of MeCP2 in olfactory receptor neurons is developmentally regulated and occurs before synaptogenesis. Mol. Cell Neurosci. *22*, 417-429.

Coker,S.B. and Melnyk,A.R. (1991). Rett syndrome and mitochondrial enzyme deficiencies. J. Child Neurol. *6*, 164-166.

Colantuoni,C., Jeon,O.H., Hyder,K., Chenchik,A., Khimani,A.H., Narayanan,V., Hoffman,E.P., Kaufmann,W.E., Naidu,S., and Pevsner,J. (2001). Gene expression profiling in postmortem Rett Syndrome brain: differential gene expression and patient classification. Neurobiol. Dis. *8*, 847-865.

Colvin,L., Fyfe,S., Leonard,S., Schiavello,T., Ellaway,C., De Klerk,N., Christodoulou,J., Msall,M., and Leonard,H. (2003). Describing the phenotype in Rett syndrome using a population database. Arch. Dis. Child *88*, 38-43.

Constancia,M., Pickard,B., Kelsey,G., and Reik,W. (1998). Imprinting mechanisms. Genome Res. *8*, 881-900.

Cooper,D.N., Taggart,M.H., and Bird,A.P. (1983). Unmethylated domains in vertebrate DNA. Nucleic Acids Res. *11*, 647-658.

Cooper,D.N. and Youssoufian,H. (1988). The CpG dinucleotide and human genetic disease. Hum. Genet. *78*, 151-155.

Couvert,P., Bienvenu,T., Aquaviva,C., Poirier,K., Moraine,C., Gendrot,C., Verloes,A., Andres,C., Le Fevre,A.C., Souville,I., Steffann,J., des,P., V, Ropers,H.H., Yntema,H.G., Fryns,J.P., Briault,S., Chelly,J., and Cherif,B. (2001). MECP2 is highly mutated in X-linked mental retardation. Hum. Mol. Genet. *10*, 941-946.

Coy,J.F., Sedlacek,Z., Bachner,D., Delius,H., and Poustka,A. (1999). A complex pattern of evolutionary conservation and alternative polyadenylation within the long 3"-untranslated region of the methyl-CpG-binding protein 2 gene (MeCP2) suggests a regulatory role in gene expression. Hum. Mol. Genet. *8*, 1253-1262.

Croll,S.D., Suri,C., Compton,D.L., Simmons,M.V., Yancopoulos,G.D., Lindsay,R.M., Wiegand,S.J., Rudge,J.S., and Scharfman,H.E. (1999). Brain-derived neurotrophic factor transgenic mice exhibit passive avoidance deficits, increased seizure severity and in vitro hyperexcitability in the hippocampus and entorhinal cortex. Neuroscience *93*, 1491-1506.

Daniel,J.M., Spring,C.M., Crawford,H.C., Reynolds,A.B., and Baig,A. (2002). The p120(ctn)-binding partner Kaiso is a bi-modal DNA-binding protein that recognizes both a sequence-specific consensus and methylated CpG dinucleotides. Nucleic Acids Res. *30*, 2911-2919.

Danielian,P.S., White,R., Hoare,S.A., Fawell,S.E., and Parker,M.G. (1993). Identification of residues in the estrogen receptor that confer differential sensitivity to estrogen and hydroxytamoxifen. Mol. Endocrinol. *7*, 232-240.

Dodge,J.E., Ramsahoye,B.H., Wo,Z.G., Okano,M., and Li,E. (2002). De novo methylation of MMLV provirus in embryonic stem cells: CpG versus non-CpG methylation. Gene *289*, 41-48.

Dong,A., Yoder,J.A., Zhang,X., Zhou,L., Bestor,T.H., and Cheng,X. (2001). Structure of human DNMT2, an enigmatic DNA methyltransferase homolog that displays denaturant-resistant binding to DNA. Nucleic Acids Res. *29*, 439-448.

Dotti,M.T., Manneschi,L., Malandrini,A., De Stefano,N., Caznerale,F., and Federico,A. (1993). Mitochondrial dysfunction in Rett syndrome. An ultrastructural and biochemical study. Brain Dev. *15*, 103-106.

DUNN,D.B. and SMITH,J.D. (1955). Occurrence of a new base in the deoxyribonucleic acid of a strain of Bacterium coli. Nature *175*, 336-337.

Dunn,H.G. and MacLeod,P.M. (2001). Rett syndrome: review of biological abnormalities. Can. J. Neurol. Sci. *28*, 16-29.

Echenne,B., Bressot,N., Bassir,M., Daures,J.P., and Rabinowitz,A. (1991). Cerebrospinal fluid beta-endorphin and cortisol study in Rett syndrome. J. Child Neurol. *6*, 257-262.

Eden,A., Gaudet,F., Waghmare,A., and Jaenisch,R. (2003). Chromosomal instability and tumors promoted by DNA hypomethylation. Science *300*, 455.

Eeg-Olofsson,O., al Zuhair,A.G., Teebi,A.S., and al Essa,M.M. (1989). Rett syndrome: genetic clues based on mitochondrial changes in muscle. Am. J. Med. Genet. *32*, 142-144.

El Osta,A., Kantharidis,P., Zalcberg,J.R., and Wolffe,A.P. (2002). Precipitous release of methyl-CpG binding protein 2 and histone deacetylase 1 from the methylated human multidrug resistance gene (MDR1) on activation. Mol. Cell Biol. *22*, 1844-1857.

Evans,J.C., Archer,H.L., Whatley,S.D., Kerr,A., Clarke,A., and Butler,R. (2005). Variation in exon 1 coding region and promoter of MECP2 in Rett syndrome and controls. Eur. J. Hum. Genet. *13*, 124-126.

Fan,G., Beard,C., Chen,R.Z., Csankovszki,G., Sun,Y., Siniaia,M., Biniszkiewicz,D., Bates,B., Lee,P.P., Kuhn,R., Trumpp,A., Poon,C., Wilson,C.B., and Jaenisch,R. (2001). DNA hypomethylation perturbs the function and survival of CNS neurons in postnatal animals. J. Neurosci. *21*, 788-797.

Feil,R., Brocard,J., Mascrez,B., LeMeur,M., Metzger,D., and Chambon,P. (1996). Ligand-activated site-specific recombination in mice. Proc. Natl. Acad. Sci. U. S. A *93*, 10887-10890.

Feng,Q. and Zhang,Y. (2001). The MeCP1 complex represses transcription through preferential binding, remodeling, and deacetylating methylated nucleosomes. Genes Dev. *15*, 827-832.

Field,L.M., Lyko,F., Mandrioli,M., and Prantera,G. (2004). DNA methylation in insects. Insect Mol. Biol. *13*, 109-115.

Finnegan,E.J., Peacock,W.J., and Dennis,E.S. (1996). Reduced DNA methylation in Arabidopsis thaliana results in abnormal plant development. Proc. Natl. Acad. Sci. U. S. A *93*, 8449-8454.

Fischle,W., Wang,Y., and Allis,C.D. (2003). Histone and chromatin cross-talk. Curr. Opin. Cell Biol. *15*, 172-183.

Fisscher,U., Weisbeek,P., and Smeekens,S. (1996). A tobacco nuclear protein that preferentially binds to unmethylated CpG-rich DNA. Eur. J. Biochem. *235*, 585-592.

Fournier,C., Goto,Y., Ballestar,E., Delaval,K., Hever,A.M., Esteller,M., and Feil,R. (2002). Allele-specific histone lysine methylation marks regulatory regions at imprinted mouse genes. EMBO J. *21*, 6560-6570.

Fujita,N., Takebayashi,S., Okumura,K., Kudo,S., Chiba,T., Saya,H., and Nakao,M. (1999). Methylation-mediated transcriptional silencing in euchromatin by methyl-CpG binding protein MBD1 isoforms. Mol. Cell Biol. *19*, 6415-6426.

Fujita,N., Watanabe,S., Ichimura,T., Ohkuma,Y., Chiba,T., Saya,H., and Nakao,M. (2003a). MCAF mediates MBD1-dependent transcriptional repression. Mol. Cell Biol. *23*, 2834-2843.

Fujita,N., Watanabe,S., Ichimura,T., Tsuruzoe,S., Shinkai,Y., Tachibana,M., Chiba,T., and Nakao,M. (2003b). Methyl-CpG binding domain 1 (MBD1) interacts with the Suv39h1-HP1 heterochromatic complex for DNA methylation-based transcriptional repression. J. Biol. Chem. *278*, 24132-24138.

Fuks,F., Hurd,P.J., Wolf,D., Nan,X., Bird,A.P., and Kouzarides,T. (2003). The methyl-CpG-binding protein MeCP2 links DNA methylation to histone methylation. J. Biol. Chem. *278*, 4035-4040.

Gaudet,F., Hodgson,J.G., Eden,A., Jackson-Grusby,L., Dausman,J., Gray,J.W., Leonhardt,H., and Jaenisch,R. (2003). Induction of tumors in mice by genomic hypomethylation. Science *300*, 489-492.

Georgel,P.T., Horowitz-Scherer,R.A., Adkins,N., Woodcock,C.L., Wade,P.A., and Hansen,J.C. (2003). Chromatin compaction by human MeCP2. Assembly of novel secondary chromatin structures in the absence of DNA methylation. J. Biol. Chem. *278*, 32181-32188.

Ghoshal,K., Datta,J., Majumder,S., Bai,S., Dong,X., Parthun,M., and Jacob,S.T. (2002). Inhibitors of histone deacetylase and DNA methyltransferase synergistically activate the methylated metallothionein I promoter by activating the transcription factor MTF-1 and forming an open chromatin structure. Mol. Cell Biol. *22*, 8302-8319.

Girard,M., Couvert,P., Carrie,A., Tardieu,M., Chelly,J., Beldjord,C., and Bienvenu,T. (2001). Parental origin of de novo MECP2 mutations in Rett syndrome. Eur. J. Hum. Genet. *9*, 231-236.

Glaze,D.G. (2002). Neurophysiology of Rett syndrome. Ment. Retard. Dev. Disabil. Res. Rev. *8*, 66-71.

Gorman,A.M., Ceccatelli,S., and Orrenius,S. (2000). Role of mitochondria in neuronal apoptosis. Dev. Neurosci. *22*, 348-358.

Gossen,M. and Bujard,H. (1992). Tight control of gene expression in mammalian cells by tetracycline-responsive promoters. Proc. Natl. Acad. Sci. U. S. A *89*, 5547-5551.

Gossen,M., Freundlieb,S., Bender,G., Muller,G., Hillen,W., and Bujard,H. (1995). Transcriptional activation by tetracyclines in mammalian cells. Science *268*, 1766-1769.

Guan,Z., Giustetto,M., Lomvardas,S., Kim,J.H., Miniaci,M.C., Schwartz,J.H., Thanos,D., and Kandel,E.R. (2002). Integration of long-term-memory-related synaptic plasticity involves bidirectional regulation of gene expression and chromatin structure. Cell *111*, 483-493.

Guy,J., Hendrich,B., Holmes,M., Martin,J.E., and Bird,A. (2001). A mouse Mecp2-null mutation causes neurological symptoms that mimic Rett syndrome. Nat. Genet. *27*, 322-326.

Haas,R.H., Dixon,S.D., Sartoris,D.J., and Hennessy,M.J. (1997). Osteopenia in Rett syndrome. J. Pediatr. *131*, 771-774.

Hagberg,B. (2002). Clinical manifestations and stages of Rett syndrome. Ment. Retard. Dev. Disabil. Res. Rev. *8*, 61-65.

Haines,T.R., Rodenhiser,D.I., and Ainsworth,P.J. (2001). Allele-specific non-CpG methylation of the Nf1 gene during early mouse development. Dev. Biol. *240*, 585-598.

Harding,T.C., Geddes,B.J., Murphy,D., Knight,D., and Uney,J.B. (1998). Switching transgene expression in the brain using an adenoviral tetracycline-regulatable system. Nat. Biotechnol. *16*, 553-555.

Hark,A.T., Schoenherr,C.J., Katz,D.J., Ingram,R.S., Levorse,J.M., and Tilghman,S.M. (2000). CTCF mediates methylation-sensitive enhancer-blocking activity at the H19/Igf2 locus. Nature *405*, 486-489.

Hayashi,S. and McMahon,A.P. (2002). Efficient recombination in diverse tissues by a tamoxifen-inducible form of Cre: a tool for temporally regulated gene activation/inactivation in the mouse. Dev. Biol. *244*, 305-318.

Hendrich,B. and Bickmore,W. (2001). Human diseases with underlying defects in chromatin structure and modification. Hum. Mol. Genet. *10*, 2233-2242.

Hendrich,B. and Bird,A. (1998). Identification and characterization of a family of mammalian methyl-CpG binding proteins. Mol. Cell Biol. *18*, 6538-6547.

Hendrich,B., Guy,J., Ramsahoye,B., Wilson,V.A., and Bird,A. (2001). Closely related proteins MBD2 and MBD3 play distinctive but interacting roles in mouse development. Genes Dev. *15*, 710-723.

Hendrich,B. and Tweedie,S. (2003). The methyl-CpG binding domain and the evolving role of DNA methylation in animals. Trends Genet. *19*, 269-277.

Hermann,A., Schmitt,S., and Jeltsch,A. (2003). The human Dnmt2 has residual DNA-(cytosine-C5) methyltransferase activity. J. Biol. Chem. *278*, 31717-31721.

Hoffbuhr,K.C., Moses,L.M., Jerdonek,M.A., Naidu,S., and Hoffman,E.P. (2002). Associations between MeCP2 mutations, X-chromosome inactivation, and phenotype. Ment. Retard. Dev. Disabil. Res. Rev. *8*, 99-105.

Hogan,B., Beddington,R., Costantini,F., and Lacy,E. (1994). Manipulating the Mouse Embryo. Cold Spring Harbor Laboratory Press).

Hotchkiss,R.D. (1948). THE QUANTITATIVE SEPARATION OF PURINES, PYRIMIDINES, AND NUCLEOSIDES BY PAPER CHROMATOGRAPHY. J. Biol. Chem. *175*, 315-332.

Howell,C.Y., Bestor,T.H., Ding,F., Latham,K.E., Mertineit,C., Trasler,J.M., and Chaillet,J.R. (2001). Genomic imprinting disrupted by a maternal effect mutation in the Dnmt1 gene. Cell *104*, 829-838.

Huppke,P., Roth,C., Christen,H.J., Brockmann,K., and Hanefeld,F. (2001). Endocrinological study on growth retardation in Rett syndrome. Acta Paediatr. *90*, 1257-1261.

Hutchins,A.S., Mullen,A.C., Lee,H.W., Sykes,K.J., High,F.A., Hendrich,B.D., Bird,A.P., and Reiner,S.L. (2002). Gene silencing quantitatively controls the function of a developmental trans-activator. Mol. Cell *10*, 81-91.

Iida,T., Suetake,I., Tajima,S., Morioka,H., Ohta,S., Obuse,C., and Tsurimoto,T. (2002). PCNA clamp facilitates action of DNA cytosine methyltransferase 1 on hemimethylated DNA. Genes Cells *7*, 997-1007.

Issa,J.P., Ottaviano,Y.L., Celano,P., Hamilton,S.R., Davidson,N.E., and Baylin,S.B. (1994). Methylation of the oestrogen receptor CpG island links ageing and neoplasia in human colon. Nat. Genet. *7*, 536-540.

Issa,J.P., Vertino,P.M., Boehm,C.D., Newsham,I.F., and Baylin,S.B. (1996). Switch from monoallelic to biallelic human IGF2 promoter methylation during aging and carcinogenesis. Proc. Natl. Acad. Sci. U. S. A *93*, 11757-11762.

Jackson,J.P., Lindroth,A.M., Cao,X., and Jacobsen,S.E. (2002). Control of CpNpG DNA methylation by the KRYPTONITE histone H3 methyltransferase. Nature *416*, 556-560.

Jaenisch,R. and Bird,A. (2003). Epigenetic regulation of gene expression: how the genome integrates intrinsic and environmental signals. Nat. Genet. *33 Suppl*, 245-254.

Jahner,D., Stuhlmann,H., Stewart,C.L., Harbers,K., Lohler,J., Simon,I., and Jaenisch,R. (1982). De novo methylation and expression of retroviral genomes during mouse embryogenesis. Nature *298*, 623-628.

Janulaitis,A., Klimasauskas,S., Petrusyte,M., and Butkus,V. (1983). Cytosine modification in DNA by BcnI methylase yields N4-methylcytosine. FEBS Lett. *161*, 131-134.

Jellinger,K., Armstrong,D., Zoghbi,H.Y., and Percy,A.K. (1988). Neuropathology of Rett syndrome. Acta Neuropathol. (Berl) *76*, 142-158.

Jellinger,K.A. (2003). Rett Syndrome - an update. J. Neural Transm. *110*, 681-701.

Jones,P.A. (2002). DNA methylation and cancer. Oncogene *21*, 5358-5360.

Jones,P.L., Veenstra,G.J., Wade,P.A., Vermaak,D., Kass,S.U., Landsberger,N., Strouboulis,J., and Wolffe,A.P. (1998). Methylated DNA and MeCP2 recruit histone deacetylase to repress transcription. Nat. Genet. *19*, 187-191.

Jorgensen,H.F., Ben-Porath,I., and Bird,A.P. (2004). Mbd1 is recruited to both methylated and nonmethylated CpGs via distinct DNA binding domains. Mol. Cell Biol. *24*, 3387-3395.

Jung,B.P., Jugloff,D.G., Zhang,G., Logan,R., Brown,S., and Eubanks,J.H. (2003). The expression of methyl CpG binding factor MeCP2 correlates with cellular differentiation in the developing rat brain and in cultured cells. J. Neurobiol. *55*, 86-96.

Kaludov,N.K. and Wolffe,A.P. (2000). MeCP2 driven transcriptional repression in vitro: selectivity for methylated DNA, action at a distance and contacts with the basal transcription machinery. Nucleic Acids Res. *28*, 1921-1928.

Kanduri,C., Pant,V., Loukinov,D., Pugacheva,E., Qi,C.F., Wolffe,A., Ohlsson,R., and Lobanenkov,V.V. (2000). Functional association of CTCF with the insulator upstream of the H19 gene is parent of origin-specific and methylation-sensitive. Curr. Biol. *10*, 853-856.

Kaneda,M., Okano,M., Hata,K., Sado,T., Tsujimoto,N., Li,E., and Sasaki,H. (2004). Essential role for de novo DNA methyltransferase Dnmt3a in paternal and maternal imprinting. Nature *429*, 900-903.

Kankel,M.W., Ramsey,D.E., Stokes,T.L., Flowers,S.K., Haag,J.R., Jeddeloh,J.A., Riddle,N.C., Verbsky,M.L., and Richards,E.J. (2003). Arabidopsis MET1 cytosine methyltransferase mutants. Genetics *163*, 1109-1122.

Kerr,A. (2002). Annotation: Rett syndrome: recent progress and implications for research and clinical practice. J. Child Psychol. Psychiatry *43*, 277-287.

Kimura,H. and Shiota,K. (2003). Methyl-CpG-binding Protein, MeCP2, Is a Target Molecule for Maintenance DNA Methyltransferase, Dnmt1. J. Biol. Chem. *278*, 4806-4812.

Klimasauskas,S., Gerasimaite,R., Vilkaitis,G., and Kulakauskas,S. (2002). N4,5-dimethylcytosine, a novel hypermodified base in DNA. Nucleic Acids Res. Suppl 73-74.

Klimasauskas,S., Kumar,S., Roberts,R.J., and Cheng,X. (1994). HhaI methyltransferase flips its target base out of the DNA helix. Cell *76*, 357-369.

Klimasauskas,S., Timinskas,A., Menkevicius,S., Butkiene,D., Butkus,V., and Janulaitis,A. (1989). Sequence motifs characteristic of DNA[cytosine-N4]methyltransferases: similarity to adenine and cytosine-C5 DNA-methylases. Nucleic Acids Res. *17*, 9823-9832.

Klose,R.J. and Bird,A.P. (2004). MeCP2 behaves as an elongated monomer that does not stably associate with the Sin3a chromatin remodeling complex. J. Biol. Chem. *279*, 46490-46496.

Knight,S.J., Flannery,A.V., Hirst,M.C., Campbell,L., Christodoulou,Z., Phelps,S.R., Pointon,J., Middleton-Price,H.R., Barnicoat,A., Pembrey,M.E., and . (1993). Trinucleotide repeat amplification and hypermethylation of a CpG island in FRAXE mental retardation. Cell *74*, 127-134.

Koch,C. and Stratling,W.H. (2004). DNA binding of methyl-CpG-binding protein MeCP2 in human MCF7 cells. Biochemistry *43*, 5011-5021.

Koizume,S., Tachibana,K., Sekiya,T., Hirohashi,S., and Shiraishi,M. (2002). Heterogeneity in the modification and involvement of chromatin components of the CpG island of the silenced human CDH1 gene in cancer cells. Nucleic Acids Res. *30*, 4770-4780.

Kokura,K., Kaul,S.C., Wadhwa,R., Nomura,T., Khan,M.M., Shinagawa,T., Yasukawa,T., Colmenares,C., and Ishii,S. (2001). The Ski protein family is required for MeCP2-mediated transcriptional repression. J. Biol. Chem. *276*, 34115-34121.

Kondo,T., Bobek,M.P., Kuick,R., Lamb,B., Zhu,X., Narayan,A., Bourc'his,D., Viegas-Pequignot,E., Ehrlich,M., and Hanash,S.M. (2000). Whole-genome methylation scan in ICF syndrome: hypomethylation of non-satellite DNA repeats D4Z4 and NBL2. Hum. Mol. Genet. *9*, 597-604.

Kornmann,B., Preitner,N., Rifat,D., Fleury-Olela,F., and Schibler,U. (2001). Analysis of circadian liver gene expression by ADDER, a highly sensitive method for the display of differentially expressed mRNAs. Nucleic Acids Res. *29*, E51.

Kouzminova,E. and Selker,E.U. (2001). dim-2 encodes a DNA methyltransferase responsible for all known cytosine methylation in Neurospora. EMBO J. *20*, 4309-4323.

Kozak,M. (2001). Constraints on reinitiation of translation in mammals. Nucleic Acids Res. *29*, 5226-5232.

Kumar,S., Cheng,X., Klimasauskas,S., Mi,S., Posfai,J., Roberts,R.J., and Wilson,G.G. (1994). The DNA (cytosine-5) methyltransferases. Nucleic Acids Res. *22*, 1-10.

Kunert,N., Marhold,J., Stanke,J., Stach,D., and Lyko,F. (2003). A Dnmt2-like protein mediates DNA methylation in Drosophila. Development *130*, 5083-5090.

Laird,P.W. (2003). The power and the promise of DNA methylation markers. Nat. Rev. Cancer *3*, 253-266.

Laird,P.W., Jackson-Grusby,L., Fazeli,A., Dickinson,S.L., Jung,W.E., Li,E., Weinberg,R.A., and Jaenisch,R. (1995). Suppression of intestinal neoplasia by DNA hypomethylation. Cell *81*, 197-205.

Lang,F. and Cohen,P. (2001). Regulation and physiological roles of serum- and glucocorticoid-induced protein kinase isoforms. Sci. STKE. *2001*, RE17.

Lappalainen,R. and Riikonen,R.S. (1994). Elevated CSF lactate in the Rett syndrome: cause or consequence? Brain Dev. *16*, 399-401.

Lee,J.T. (2003). Molecular links between X-inactivation and autosomal imprinting: X-inactivation as a driving force for the evolution of imprinting? Curr. Biol. *13*, R242-R254.

Lehnertz,B., Ueda,Y., Derijck,A.A., Braunschweig,U., Perez-Burgos,L., Kubicek,S., Chen,T., Li,E., Jenuwein,T., and Peters,A.H. (2003). Suv39h-mediated histone H3 lysine 9 methylation directs DNA methylation to major satellite repeats at pericentric heterochromatin. Curr. Biol. *13*, 1192-1200.

Leonard,H., Thomson,M.R., Glasson,E.J., Fyfe,S., Leonard,S., Bower,C., Christodoulou,J., and Ellaway,C. (1999). A population-based approach to the investigation of osteopenia in Rett syndrome. Dev. Med. Child Neurol. *41*, 323-328.

Leonhardt,H., Page,A.W., Weier,H.U., and Bestor,T.H. (1992). A targeting sequence directs DNA methyltransferase to sites of DNA replication in mammalian nuclei. Cell *71*, 865-873.

Lerchner,W. and Barlow,D.P. (1997). Paternal repression of the imprinted mouse Igf2r locus occurs during implantation and is stable in all tissues of the post-implantation mouse embryo. Mech. Dev. *61*, 141-149.

Lewis,J.D., Meehan,R.R., Henzel,W.J., Maurer-Fogy,I., Jeppesen,P., Klein,F., and Bird,A. (1992). Purification, sequence, and cellular localization of a novel chromosomal protein that binds to methylated DNA. Cell *69*, 905-914.

Li,E. (2002). Chromatin modification and epigenetic reprogramming in mammalian development. Nat. Rev. Genet. *3*, 662-673.

Li,E., Beard,C., and Jaenisch,R. (1993). Role for DNA methylation in genomic imprinting. Nature *366*, 362-365.

Li,E., Bestor,T.H., and Jaenisch,R. (1992). Targeted mutation of the DNA methyltransferase gene results in embryonic lethality. Cell *69*, 915-926.

Li,L.C. and Dahiya,R. (2002). MethPrimer: designing primers for methylation PCRs. Bioinformatics. *18*, 1427-1431.

Li,M., Pevny,L., Lovell-Badge,R., and Smith,A. (1998). Generation of purified neural precursors from embryonic stem cells by lineage selection. Curr. Biol. *8*, 971-974.

Litt,M.D., Simpson,M., Gaszner,M., Allis,C.D., and Felsenfeld,G. (2001). Correlation between histone lysine methylation and developmental changes at the chicken beta-globin locus. Science *293*, 2453-2455.

Lobo-Menendez,F., Sossey-Alaoui,K., Bell,J.M., Copeland-Yates,S.A., Plank,S.M., Sanford,S.O., Skinner,C., Simensen,R.J., Schroer,R.J., and Michaelis,R.C. (2003). Absence of MeCP2 mutations in patients from the South Carolina autism project. Am. J. Med. Genet. *117B*, 97-101.

Luikenhuis,S., Giacometti,E., Beard,C.F., and Jaenisch,R. (2004). Expression of MeCP2 in postmitotic neurons rescues Rett syndrome in mice. Proc. Natl. Acad. Sci. U. S. A *101*, 6033-6038.

Lunyak,V.V., Burgess,R., Prefontaine,G.G., Nelson,C., Sze,S.H., Chenoweth,J., Schwartz,P., Pevzner,P.A., Glass,C., Mandel,G., and Rosenfeld,M.G. (2002). Corepressor-dependent silencing of chromosomal regions encoding neuronal genes. Science *298*, 1747-1752.

Lyko,F. (2001). DNA methylation learns to fly. Trends Genet. *17*, 169-172.

Lyko,F., Ramsahoye,B.H., and Jaenisch,R. (2000). DNA methylation in Drosophila melanogaster. Nature *408*, 538-540.

Maier,H., Colbert,J., Fitzsimmons,D., Clark,D.R., and Hagman,J. (2003). Activation of the early B-cell-specific mb-1 (Ig-alpha) gene by Pax-5 is dependent on an unmethylated Ets binding site. Mol. Cell Biol. *23*, 1946-1960.

Makar,K.W., Perez-Melgosa,M., Shnyreva,M., Weaver,W.M., Fitzpatrick,D.R., and Wilson,C.B. (2003). Active recruitment of DNA methyltransferases regulates interleukin 4 in thymocytes and T cells. Nat. Immunol. *4*, 1183-1190.

Malagnac,F., Bartee,L., and Bender,J. (2002). An Arabidopsis SET domain protein required for maintenance but not establishment of DNA methylation. EMBO J. *21*, 6842-6852.

Mandrioli,M. and Volpi,N. (2003). The genome of the lepidopteran Mamestra brassicae has a vertebrate-like content of methyl-cytosine. Genetica *119*, 187-191.

Martinowich,K., Hattori,D., Wu,H., Fouse,S., He,F., Hu,Y., Fan,G., and Sun,Y.E. (2003). DNA methylation-related chromatin remodeling in activity-dependent BDNF gene regulation. Science *302*, 890-893.

Matsuishi,T., Urabe,F., Komori,H., Yamashita,Y., Naito,E., Kuroda,Y., Horikawa,M., and Ohtaki,E. (1992). The Rett syndrome and CSF lactic acid patterns. Brain Dev. *14*, 68-70.

Mayford,M., Bach,M.E., Huang,Y.Y., Wang,L., Hawkins,R.D., and Kandel,E.R. (1996). Control of memory formation through regulated expression of a CaMKII transgene. Science *274*, 1678-1683.

Meehan,R.R., Lewis,J.D., and Bird,A.P. (1992). Characterization of MeCP2, a vertebrate DNA binding protein with affinity for methylated DNA. Nucleic Acids Res. *20*, 5085-5092.

Meehan,R.R., Lewis,J.D., McKay,S., Kleiner,E.L., and Bird,A.P. (1989). Identification of a mammalian protein that binds specifically to DNA containing methylated CpGs. Cell *58*, 499-507.

Mertineit,C., Yoder,J.A., Taketo,T., Laird,D.W., Trasler,J.M., and Bestor,T.H. (1998). Sex-specific exons control DNA methyltransferase in mammalian germ cells. Development *125*, 889-897.

Metzger,D., Clifford,J., Chiba,H., and Chambon,P. (1995). Conditional site-specific recombination in mammalian cells using a ligand-dependent chimeric Cre recombinase. Proc. Natl. Acad. Sci. U. S. A *92*, 6991-6995.

Millar,C.B., Guy,J., Sansom,O.J., Selfridge,J., MacDougall,E., Hendrich,B., Keightley,P.D., Bishop,S.M., Clarke,A.R., and Bird,A. (2002). Enhanced CpG mutability and tumorigenesis in MBD4-deficient mice. Science *297*, 403-405.

Miyoshi,N., Wagatsuma,H., Wakana,S., Shiroishi,T., Nomura,M., Aisaka,K., Kohda,T., Surani,M.A., Kaneko-Ishino,T., and Ishino,F. (2000). Identification of an imprinted gene, Meg3/Gtl2 and its human homologue MEG3, first mapped on mouse distal chromosome 12 and human chromosome 14q. Genes Cells *5*, 211-220.

Mnatzakanian,G.N., Lohi,H., Munteanu,I., Alfred,S.E., Yamada,T., MacLeod,P.J., Jones,J.R., Scherer,S.W., Schanen,N.C., Friez,M.J., Vincent,J.B., and Minassian,B.A. (2004). A previously unidentified MECP2 open reading frame defines a new protein isoform relevant to Rett syndrome. Nat. Genet. *36*, 339-341.

Mullaney,B.C., Johnston,M.V., and Blue,M.E. (2004). Developmental expression of methyl-CpG binding protein 2 is dynamically regulated in the rodent brain. Neuroscience *123*, 939-949.

Mund,C., Musch,T., Strodicke,M., Assmann,B., Li,E., and Lyko,F. (2004). Comparative analysis of DNA methylation patterns in transgenic Drosophila overexpressing mouse DNA methyltransferases. Biochem. J. *378*, 763-768.

Nan,X., Campoy,F.J., and Bird,A. (1997). MeCP2 is a transcriptional repressor with abundant binding sites in genomic chromatin. Cell *88*, 471-481.

Nan,X., Meehan,R.R., and Bird,A. (1993). Dissection of the methyl-CpG binding domain from the chromosomal protein MeCP2. Nucleic Acids Res. *21*, 4886-4892.

Nan,X., Ng,H.H., Johnson,C.A., Laherty,C.D., Turner,B.M., Eisenman,R.N., and Bird,A. (1998). Transcriptional repression by the methyl-CpG-binding protein MeCP2 involves a histone deacetylase complex. Nature *393*, 386-389.

Nan,X., Tate,P., Li,E., and Bird,A. (1996). DNA methylation specifies chromosomal localization of MeCP2. Mol. Cell Biol. *16*, 414-421.

Ng,H.H., Jeppesen,P., and Bird,A. (2000). Active repression of methylated genes by the chromosomal protein MBD1. Mol. Cell Biol. *20*, 1394-1406.

Nguyen,C.T., Gonzales,F.A., and Jones,P.A. (2001). Altered chromatin structure associated with methylation-induced gene silencing in cancer cells: correlation of accessibility, methylation, MeCP2 binding and acetylation. Nucleic Acids Res. *29*, 4598-4606.

Nicholls,D.G. and Ferguson,S.J. (2002). Bioenergetics 3. (San Diego, Calif: Academic Press).

Nielsen,J.B., Henriksen,K.F., Hansen,C., Silahtaroglu,A., Schwartz,M., and Tommerup,N. (2001). MECP2 mutations in Danish patients with Rett syndrome: high frequency of mutations but no consistent correlations with clinical severity or with the X chromosome inactivation pattern. Eur. J. Hum. Genet. *9*, 178-184.

Nisenbaum,L.K. (2002). The ultimate chip shot: can microarray technology deliver for neuroscience? Genes, Brain and Behavior *1*, 27-34.

Ohki,I., Shimotake,N., Fujita,N., Jee,J., Ikegami,T., Nakao,M., and Shirakawa,M. (2001). Solution structure of the methyl-CpG binding domain of human MBD1 in complex with methylated DNA. Cell *105*, 487-497.

Okano,M., Bell,D.W., Haber,D.A., and Li,E. (1999). DNA methyltransferases Dnmt3a and Dnmt3b are essential for de novo methylation and mammalian development. Cell *99*, 247-257.

Okano,M., Xie,S., and Li,E. (1998b). Dnmt2 is not required for de novo and maintenance methylation of viral DNA in embryonic stem cells. Nucleic Acids Res. *26*, 2536-2540.

Okano,M., Xie,S., and Li,E. (1998a). Cloning and characterization of a family of novel mammalian DNA (cytosine-5) methyltransferases. Nat. Genet. *19*, 219-220.

Palmer,B.R. and Marinus,M.G. (1994). The dam and dcm strains of Escherichia coli--a review. Gene *143*, 1-12.

Patschan,D., Loddenkemper,K., and Buttgereit,F. (2001). Molecular mechanisms of glucocorticoid-induced osteoporosis. Bone *29*, 498-505.

Payen,E., Verkerk,T., Michalovich,D., Dreyer,S.D., Winterpacht,A., Lee,B., De Zeeuw,C.I., Grosveld,F., and Galjart,N. (1998). The centromeric/nucleolar chromatin protein ZFP-37 may function to specify neuronal nuclear domains. J. Biol. Chem. *273*, 9099-9109.

Petronzelli,F., Riccio,A., Markham,G.D., Seeholzer,S.H., Genuardi,M., Karbowski,M., Yeung,A.T., Matsumoto,Y., and Bellacosa,A. (2000). Investigation of the substrate spectrum of the human mismatch-specific DNA N-glycosylase MED1 (MBD4): fundamental role of the catalytic domain. J. Cell Physiol *185*, 473-480.

Plass,C. (2002). Cancer epigenomics. Hum. Mol. Genet. *11*, 2479-2488.

Prokhortchouk,A., Hendrich,B., Jorgensen,H., Ruzov,A., Wilm,M., Georgiev,G., Bird,A., and Prokhortchouk,E. (2001). The p120 catenin partner Kaiso is a DNA methylation-dependent transcriptional repressor. Genes Dev. *15*, 1613-1618.

Prokhortchouk,E. and Hendrich,B. (2002). Methyl-CpG binding proteins and cancer: are MeCpGs more important than MBDs? Oncogene *21*, 5394-5399.

Quaderi,N.A., Meehan,R.R., Tate,P.H., Cross,S.H., Bird,A.P., Chatterjee,A., Herman,G.E., and Brown,S.D. (1994). Genetic and physical mapping of a gene encoding a methyl CpG binding protein, Mecp2, to the mouse X chromosome. Genomics *22*, 648-651.

Ramsahoye,B.H., Biniszkiewicz,D., Lyko,F., Clark,V., Bird,A.P., and Jaenisch,R. (2000). Non-CpG methylation is prevalent in embryonic stem cells and may be mediated by DNA methyltransferase 3a. Proc. Natl. Acad. Sci. U. S. A *97*, 5237-5242.

Ravn,K., Nielsen,J.B., Uldall,P., Hansen,F.J., and Schwartz,M. (2003). No correlation between phenotype and genotype in boys with a truncating MECP2 mutation. J. Med. Genet. *40*, e5.

Reichwald,K., Thiesen,J., Wiehe,T., Weitzel,J., Poustka,W.A., Rosenthal,A., Platzer,M., Stratling,W.H., and Kioschis,P. (2000). Comparative sequence analysis of the MECP2-locus in human and mouse reveals new transcribed regions. Mamm. Genome *11*, 182-190.

Reik,W., Dean,W., and Walter,J. (2001). Epigenetic reprogramming in mammalian development. Science *293*, 1089-1093.

Rietveld,L.E., Caldenhoven,E., and Stunnenberg,H.G. (2002). In vivo repression of an erythroid-specific gene by distinct corepressor complexes. EMBO J. *21*, 1389-1397.

Ronemus,M.J., Galbiati,M., Ticknor,C., Chen,J., and Dellaporta,S.L. (1996). Demethylation-induced developmental pleiotropy in Arabidopsis. Science *273*, 654-657.

Ruch,A., Kurczynski,T.W., and Velasco,M.E. (1989). Mitochondrial alterations in Rett syndrome. Pediatr. Neurol. *5*, 320-323.

Saelens,X., Festjens,N., Walle,L.V., van,G.M., van,L.G., and Vandenabeele,P. (2004). Toxic proteins released from mitochondria in cell death. Oncogene *23*, 2861-2874.

Sansom,O.J., Berger,J., Bishop,S.M., Hendrich,B., Bird,A., and Clarke,A.R. (2003). Deficiency of Mbd2 suppresses intestinal tumorigenesis. Nat. Genet. *34*, 145-147.

Saze,H., Scheid,O.M., and Paszkowski,J. (2003). Maintenance of CpG methylation is essential for epigenetic inheritance during plant gametogenesis. Nat. Genet. *34*, 65-69.

Schmidt,J.V., Matteson,P.G., Jones,B.K., Guan,X.J., and Tilghman,S.M. (2000). The Dlk1 and Gtl2 genes are linked and reciprocally imprinted. Genes Dev. *14*, 1997-2002.

Schuster-Gossler,K., Bilinski,P., Sado,T., Ferguson-Smith,A., and Gossler,A. (1998). The mouse Gtl2 gene is differentially expressed during embryonic development,

encodes multiple alternatively spliced transcripts, and may act as an RNA. Dev. Dyn. *212*, 214-228.

Segawa,M. (2001). Guidelines for reporting clinical features in cases with MECP2 mutations, by Allison Kerr and an international group. Brain Dev. *23*, 269.

Shahbazian,M., Young,J., Yuva-Paylor,L., Spencer,C., Antalffy,B., Noebels,J., Armstrong,D., Paylor,R., and Zoghbi,H. (2002a). Mice with truncated MeCP2 recapitulate many Rett syndrome features and display hyperacetylation of histone H3. Neuron *35*, 243-254.

Shahbazian,M.D., Antalffy,B., Armstrong,D.L., and Zoghbi,H.Y. (2002b). Insight into Rett syndrome: MeCP2 levels display tissue- and cell-specific differences and correlate with neuronal maturation. Hum. Mol. Genet. *11*, 115-124.

Singer,M.J., Marcotte,B.A., and Selker,E.U. (1995). DNA methylation associated with repeat-induced point mutation in Neurospora crassa. Mol. Cell Biol. *15*, 5586-5597.

Soriano,P. (1999). Generalized lacZ expression with the ROSA26 Cre reporter strain. Nat. Genet. *21*, 70-71.

Stancheva,I., Collins,A.L., Van,d.V., I, Zoghbi,H., and Meehan,R.R. (2003). A mutant form of MeCP2 protein associated with human Rett syndrome cannot be displaced from methylated DNA by notch in Xenopus embryos. Mol. Cell *12*, 425-435.

Stein,D.C., Gunn,J.S., Radlinska,M., and Piekarowicz,A. (1995). Restriction and modification systems of Neisseria gonorrhoeae. Gene *157*, 19-22.

Suzuki,M., Yamada,T., Kihara-Negishi,F., Sakurai,T., and Oikawa,T. (2003). Direct association between PU.1 and MeCP2 that recruits mSin3A-HDAC complex for PU.1-mediated transcriptional repression. Oncogene *22*, 8688-8698.

Takada,S., Tevendale,M., Baker,J., Georgiades,P., Campbell,E., Freeman,T., Johnson,M.H., Paulsen,M., and Ferguson-Smith,A.C. (2000). Delta-like and gtl2 are reciprocally expressed, differentially methylated linked imprinted genes on mouse chromosome 12. Curr. Biol. *10*, 1135-1138.

Tamaru,H. and Selker,E.U. (2001). A histone H3 methyltransferase controls DNA methylation in Neurospora crassa. Nature *414*, 277-283.

Tang,L.Y., Reddy,M.N., Rasheva,V., Lee,T.L., Lin,M.J., Hung,M.S., and Shen,C.K. (2003). The eukaryotic DNMT2 genes encode a new class of cytosine-5 DNA methyltransferases. J. Biol. Chem. *278*, 33613-33616.

Tao,X., Finkbeiner,S., Arnold,D.B., Shaywitz,A.J., and Greenberg,M.E. (1998). Ca2+ influx regulates BDNF transcription by a CREB family transcription factor-dependent mechanism. Neuron *20*, 709-726.

Tariq,M. and Paszkowski,J. (2004). DNA and histone methylation in plants. Trends Genet. *20*, 244-251.

Tariq,M., Saze,H., Probst,A.V., Lichota,J., Habu,Y., and Paszkowski,J. (2003). Erasure of CpG methylation in Arabidopsis alters patterns of histone H3 methylation in heterochromatin. Proc. Natl. Acad. Sci. U. S. A *100*, 8823-8827.

Tate,P., Skarnes,W., and Bird,A. (1996). The methyl-CpG binding protein MeCP2 is essential for embryonic development in the mouse. Nat. Genet. *12*, 205-208.

Thompson,J.D., Higgins,D.G., and Gibson,T.J. (1994). CLUSTAL W: improving the sensitivity of progressive multiple sequence alignment through sequence weighting, position-specific gap penalties and weight matrix choice. Nucleic Acids Res. *22*, 4673-4680.

Thompson,S., Clarke,A.R., Pow,A.M., Hooper,M.L., and Melton,D.W. (1989). Germ line transmission and expression of a corrected HPRT gene produced by gene targeting in embryonic stem cells. Cell *56*, 313-321.

Tolwani,R.J., Buckmaster,P.S., Varma,S., Cosgaya,J.M., Wu,Y., Suri,C., and Shooter,E.M. (2002). BDNF overexpression increases dendrite complexity in hippocampal dentate gyrus. Neuroscience *114*, 795-805.

Trappe,R., Laccone,F., Cobilanschi,J., Meins,M., Huppke,P., Hanefeld,F., and Engel,W. (2001). MECP2 mutations in sporadic cases of Rett syndrome are almost exclusively of paternal origin. Am. J. Hum. Genet. *68*, 1093-1101.

Traynor,J., Agarwal,P., Lazzeroni,L., and Francke,U. (2002). Gene expression patterns vary in clonal cell cultures from Rett syndrome females with eight different MECP2 mutations. BMC. Med. Genet. *3*, 12.

Tsien,J.Z., Chen,D.F., Gerber,D., Tom,C., Mercer,E.H., Anderson,D.J., Mayford,M., Kandel,E.R., and Tonegawa,S. (1996). Subregion- and cell type-restricted gene knockout in mouse brain. Cell *87*, 1317-1326.

Tudor,M., Akbarian,S., Chen,R.Z., and Jaenisch,R. (2002). Transcriptional profiling of a mouse model for Rett syndrome reveals subtle transcriptional changes in the brain. Proc. Natl. Acad. Sci. U. S. A *99*, 15536-15541.

Vertino,P.M., Sekowski,J.A., Coll,J.M., Applegren,N., Han,S., Hickey,R.J., and Malkas,L.H. (2002). DNMT1 is a component of a multiprotein DNA replication complex. Cell Cycle *1*, 416-423.

Wade,P.A., Gegonne,A., Jones,P.L., Ballestar,E., Aubry,F., and Wolffe,A.P. (1999). Mi-2 complex couples DNA methylation to chromatin remodelling and histone deacetylation. Nat. Genet. *23*, 62-66.

Waterston,R.H., Lindblad-Toh,K., Birney,E., Rogers,J., Abril,J.F., Agarwal,P., Agarwala,R., Ainscough,R., Alexandersson,M., An,P., and et al (2002). Initial sequencing and comparative analysis of the mouse genome. Nature *420*, 520-562.

Watson,P., Black,G., Ramsden,S., Barrow,M., Super,M., Kerr,B., and Clayton-Smith,J. (2001). Angelman syndrome phenotype associated with mutations in MECP2, a gene encoding a methyl CpG binding protein. J. Med. Genet. *38*, 224-228.

Weber,P., Metzger,D., and Chambon,P. (2001). Temporally controlled targeted somatic mutagenesis in the mouse brain. Eur. J. Neurosci. *14*, 1777-1783.

Wellman,C.L. (2001). Dendritic reorganization in pyramidal neurons in medial prefrontal cortex after chronic corticosterone administration. J. Neurobiol. *49*, 245-253.

White,G.P., Watt,P.M., Holt,B.J., and Holt,P.G. (2002). Differential patterns of methylation of the IFN-gamma promoter at CpG and non-CpG sites underlie differences in IFN-gamma gene expression between human neonatal and adult CD. J. Immunol. *168*, 2820-2827.

Wijmenga,C., van den Heuvel,L.P., Strengman,E., Luyten,J.A., van,d.B., I, de,G.R., Smeets,D.F., Draaisma,J.M., van Dongen,J.J., De Abreu,R.A., Pearson,P.L., Sandkuijl,L.A., and Weemaes,C.M. (1998). Localization of the ICF syndrome to chromosome 20 by homozygosity mapping. Am. J. Hum. Genet. *63*, 803-809.

Wilson,G.G. and Murray,N.E. (1991). Restriction and modification systems. Annu. Rev. Genet. *25*, 585-627.

Wutz,A. and Jaenisch,R. (2000). A shift from reversible to irreversible X inactivation is triggered during ES cell differentiation. Mol. Cell *5*, 695-705.

Wylie,A.A., Murphy,S.K., Orton,T.C., and Jirtle,R.L. (2000). Novel imprinted DLK1/GTL2 domain on human chromosome 14 contains motifs that mimic those implicated in IGF2/H19 regulation. Genome Res. *10*, 1711-1718.

Xiang,F., Buervenich,S., Nicolao,P., Bailey,M.E., Zhang,Z., and Anvret,M. (2000). Mutation screening in Rett syndrome patients. J. Med. Genet. *37*, 250-255.

Xu,G., Rabadan-Diehl,C., Nikodemova,M., Wynn,P., Spiess,J., and Aguilera,G. (2001). Inhibition of corticotropin releasing hormone type-1 receptor translation by an upstream AUG triplet in the 5' untranslated region. Mol. Pharmacol. *59*, 485-492.

Yamamoto,A., Lucas,J.J., and Hen,R. (2000). Reversal of neuropathology and motor dysfunction in a conditional model of Huntington's disease. Cell *101*, 57-66.

Yeh,T.F., Lin,Y.J., Lin,H.C., Huang,C.C., Hsieh,W.S., Lin,C.H., and Tsai,C.H. (2004). Outcomes at school age after postnatal dexamethasone therapy for lung disease of prematurity. N. Engl. J. Med. *350*, 1304-1313.

Yoder,J.A., Soman,N.S., Verdine,G.L., and Bestor,T.H. (1997). DNA (cytosine-5)-methyltransferases in mouse cells and tissues. Studies with a mechanism-based probe. J. Mol. Biol. *270*, 385-395.

Yoon,H.G., Chan,D.W., Reynolds,A.B., Qin,J., and Wong,J. (2003). N-CoR mediates DNA methylation-dependent repression through a methyl CpG binding protein Kaiso. Mol. Cell *12*, 723-734.

Young,J.I. and Zoghbi,H.Y. (2004). X-chromosome inactivation patterns are unbalanced and affect the phenotypic outcome in a mouse model of rett syndrome. Am. J. Hum. Genet. *74*, 511-520.

Zambrowicz,B.P., Imamoto,A., Fiering,S., Herzenberg,L.A., Kerr,W.G., and Soriano,P. (1997). Disruption of overlapping transcripts in the ROSA beta geo 26 gene trap strain leads to widespread expression of beta-galactosidase in mouse embryos and hematopoietic cells. Proc. Natl. Acad. Sci. U. S. A *94*, 3789-3794.

Zappella,M., Meloni,I., Longo,I., Canitano,R., Hayek,G., Rosaia,L., Mari,F., and Renieri,A. (2003). Study of MECP2 gene in Rett syndrome variants and autistic girls. Am. J. Med. Genet. *119B*, 102-107.

Zhang,Y., Ng,H.H., Erdjument-Bromage,H., Tempst,P., Bird,A., and Reinberg,D. (1999). Analysis of the NuRD subunits reveals a histone deacetylase core complex and a connection with DNA methylation. Genes Dev. *13*, 1924-1935.

Zhao,X., Ueba,T., Christie,B.R., Barkho,B., McConnell,M.J., Nakashima,K., Lein,E.S., Eadie,B.D., Willhoite,A.R., Muotri,A.R., Summers,R.G., Chun,J., Lee,K.F., and Gage,F.H. (2003). Mice lacking methyl-CpG binding protein 1 have deficits in adult neurogenesis and hippocampal function. Proc. Natl. Acad. Sci. U. S. A.

Zimmerman,L., Parr,B., Lendahl,U., Cunningham,M., McKay,R., Gavin,B., Mann,J., Vassileva,G., and McMahon,A. (1994). Independent regulatory elements in the

nestin gene direct transgene expression to neural stem cells or muscle precursors. Neuron *12*, 11-24.

Human Molecular Genetics, 2003, Vol. 12, Review Issue 2 **R221–R227**
DOI: 10.1093/hmg/ddg286

DNA methylation and Rett syndrome

Skirmantas Kriaucionis and Adrian Bird*

Wellcome Trust Centre for Cell Biology, University of Edinburgh, The King's Buildings, Edinburgh EH9 3JR, Scotland, UK

Received August 8, 2003; Accepted August 13, 2003

Methylation of cytosine in human DNA has been studied for over 60 years, but has only recently been confirmed as an important player in human disease. Rett syndrome is a neurological disorder caused by mutations in the MeCP2 protein, which has been shown to bind methylated DNA and repress transcription. This review will focus on experiments addressing the basic properties of MeCP2 and on mouse models of Rett syndrome that are starting to yield insights into this condition.

DNA METHYLATION

DNA methylation is probably universal in vertebrates. In humans, approximately 1% of DNA bases are modified postsynthetically by addition of a methyl group to carbon-5 of the cytosine pyrimidine ring, predominantly at CpG dinucleotides. In mammalian cells, methylated CpGs are dispersed throughout the genome, but the majority are located in transcribed regions and intergenic DNA. Exceptions to this generalization are CpG islands, which are mostly methylation-free. CpG islands contain high densities of the CpG dinucleotide and are found at the promoter regions of about 60% of human genes that are transcribed by RNA polymerase II (1,2). In atypical cases, where CpG islands become methylated during development, modification is important for stable silencing of the associated gene. For example, failure to methylate CpG islands on the inactive X chromosome (X_i) leads to leaky repression of X_i-linked genes (3,4).

The methylation mark can affect gene expression in two ways. The first mechanism involves direct interference of methyl-CpG with the DNA binding of transcription factors. For example, the transcription factor Ets-1 or the boundary element factor CTCF, bind non-methylated but not methylated sites (5,6). The second mechanism involves a group of proteins which bind methylated CpGs independent of their DNA sequence context. Currently there are five known mammalian proteins which bind methylated CpG. Four of these, MeCP2, MBD1, MBD2 and MBD4, have related DNA binding domains (7). A fifth unrelated protein, Kaiso, requires two symmetrically methylated CpGs for binding (8). Four of the five proteins can repress transcription from methylated promoters in model experiments (the exception being MBD4 which is a DNA repair protein) (9).

Defects in the DNA methylation machinery are involved in human disease. Most directly, mutations in the *de novo* DNA methyltransferase DNMT3B result in reduced methylation of pericentromeric DNA sequences and cause a rare disorder called ICF syndrome. The symptoms of this condition are immunodeficiency, instability of pericentromeric heterochromatin, facial abnormalities and mental retardation (10). Most cancers also involve DNA methylation abnormalities, in particular unscheduled gene silencing via DNA methylation at CpG island promoters. This review concerns Rett syndrome, which is known to be caused by mutations in the gene for one of the methyl-CpG binding proteins, MeCP2 (11).

RETT SYNDROME

Rett syndrome is a relatively frequent form of mental retardation and occurs sporadically once every 10 000–22 000 female births. It is characterized by a period of normal development until around 1 year followed by a rapid regression that involves loss of acquired speech and motor skills, microcephaly, seizures, autism, ataxia, intermittent hyperventilation and stereotypic hand movements (12–15). Despite these symptoms, patients often survive into adulthood. Several recent studies show that, after the initial crisis associated with symptom onset, there is no further regression, suggesting that the condition does not involve progressive neurodegeneration (16,17).

Rare familial Rett syndrome cases allowed mapping of the disease region to Xq28 (18), and screening of candidate genes in the region identified mutations in the *MECP2* gene as frequent events in Rett patients (11). Later, extensive patient screening established that ~80% of Rett syndrome cases are associated with discernable mutations in the *MECP2* gene. These mutations are, beyond reasonable doubt, the cause of Rett syndrome, as they are almost always absent (see below) in parents of the affected child.

*To whom correspondence should be addressed. Tel: +44 1316505670; Fax: +44 1316505379; E-mail: a.bird@ed.ac.uk

Comprehensive databases of disease-causing *MECP2* mutations and some apparently benign *MECP2* polymorphisms have been compiled. A database at the University of Edinburgh (www.mecp2.org.uk) is primarily focused on collecting *MECP2* mutations with detailed information about symptoms provided by parents and caregivers. Another database, RettBASE (http://mecp2.chw.edu.au/), collects information from laboratories and from paediatricians who screen for *MECP2* mutations.

Most missense mutations in *MECP2* that cause Rett syndrome are tightly clustered at the methyl-CpG binding domain (MBD; Fig. 1). Deletion/insertion mutations leading to loss of the open reading frame occur throughout the protein, but are clustered in the C-terminal region, which contains a poly-histidine repeat. Rett syndrome patients display a wide spectrum of mutations, but ~67% of all mutations are in eight hot spots (R106, R133, T158, R168, R255, R270, R294 and R306). Seven out of eight major mutations affect arginine, which has a CpG in its codon. It is therefore likely that these mutations are due to unrepaired deamination of 5-methylcytosine which is responsible for about one-third of all point mutations that give rise to human genetic disease (19). It is striking that many mutations appear to exclusively affect the C-terminus of MeCP2, to which no biochemical function has yet been attributed. We clearly have much still to learn about this protein.

Besides Rett syndrome, mutations in *MECP2* are now thought to contribute to some cases of non-specific X-linked mental retardation (20) and Angelman syndrome (21). As Rett syndrome patients have some autistic features, autism patients have also been screened for *MECP2* mutations, with no *MECP2* mutations found (22). Another study found MeCP2 mutation in two autistic patients who meet Rett syndrome preserved speech variant criteria (23). In the latest study only two of 69 autism patients were shown to have *de novo MECP2* mutations (24). At present, the significance of *MECP2* mutations in X-linked mental retardation, Angelman syndrome and autism is not clear because of low mutation frequency and relatively wide variability of Rett syndrome symptoms.

Rett syndrome is almost exclusively a disease of females because *MECP2* is X-linked and patients are heterozygous for the mutated allele. Following random X chromosome inactivation, typically half of their cells express wild-type (*wt*) *MECP2* and the other half express the mutated *MECP2*. As a result, the female cell population is mosaic for expression of the mutant allele. This mixture of functionally $MECP2^{+}$ and $MECP2^{-}$ cells leads to Rett syndrome. Symptom-free female carriers of such *MECP2* mutations have only been seen in very rare cases where extreme skewing of X chromosome inactivation prevents expression of the mutated allele (25).

Males that are hemizygous for comparable *MECP2* mutations rarely live beyond 2 years and have a different and more severe phenotype than Rett syndrome, usually involving congenital encephalopathy (25,26). There are, however, very rare males with classical Rett syndrome (27). In these individuals, an *MECP2* mutation appears to have arisen early in development, giving rise to clones of mutant and *wt* cells in the same individual that mimic the mosaic expression of the mutant and *wt MECP2* genes in $MECP2^{+/-}$ females.

MeCP2–METHYL CpG BINDING PROTEIN 2

The original methyl-CpG binding activity known as MeCP1 was reported in crude nuclear extracts through its ability to bind a methylated DNA probe containing multiple methylated CpGs (28). Later, a second activity, MeCP2, was detected as an 80 kDa protein that could bind a single methylated CpG in a south-western assay (29). In mouse cells, MeCP2 is detectable throughout the metaphase chromosome arms, but is concentrated in the pericentromeric heterochromatin, which contains highly methylated satellite DNA (30). The methyl-CpG binding domain (MBD) of MeCP2 was mapped near the N-terminus by construction of deletion mutants (Fig. 1) and DNase I *in vitro* footprinting indicated that it could protect a 12 nucleotide region surrounding a methyl-CpG site. The approximate dissociation constant was 10^{-9} M. Symmetrically methylated CpG is required for *in vitro* binding, whereas hemi-methylated DNA is only weakly bound (31). The search for other MBD-like domains revealed another four proteins, which were assigned to the MBD family—MBD1, MBD2, MBD3 and MBD4 (7).

MeCP2 was suggested to bind methylated CpGs without major impediment from the nucleosome surface (32). This finding is compatible with the structure of an MBD (from MBD1) in complex with DNA, which indicates that access to methyl-CpG sites exposed in the major groove might occur without encountering steric interference from the core histones (33).

Early experiments suggested the MeCP2 was targeted to methyl CpG sites *in vivo*, as heterochromatic localization was lost in mouse cells lacking the DNA methyltransferase Dnmt1 (30). More directly, several chromatin immunoprecipitation (ChIP) experiments have shown that MeCP2 is bound to methylated DNA *in vivo*, but does not associate with non-methylated DNA. Examples include the 'differentially methylated regions' of the imprinted U2af1-rs1 and H19 genes in mouse, the silenced metallothionein I promoter and sodium channel II promoters in Rat-1 cells, and the methylated p14(ARF)/p16(INK4A) CpG islands in human cancer cells (34–40). These findings support the idea that MeCP2 functions by binding to methyl-CpG sites *in vivo*. Furthermore, the observations that missense mutations in Rett syndrome patients are highly clustered at the MBD of MeCP2 and cause decreased binding to methylated DNA (41–43) imply that methyl-CpG binding by MeCP2 is essential for brain function.

MeCP2 AS TRANSCRIPTIONAL REPRESSOR

Many genes are silenced when the promoter becomes methylated. Therefore, MeCP2 was initially hypothesized to be a transcriptional repressor. This was confirmed by transient transfection studies which showed that MeCP2 is able to repress transcription both in cells and *in vitro* (44,45). MeCP2's repression properties were investigated by monitoring reporter gene expression following fusion of the GAL4 DNA binding domain with various parts of the *Mecp2* gene (45). An ~100 amino acid domain in the middle of the protein was found to be responsible for transcriptional repression (TRD). Tethered MeCP2 was found to repress transcription from up to 2000 bp from the transcription initiation site (45).

Immunoprecipitation from HeLa nuclear extracts and partial MeCP2 complex purification from *Xenopus laevis* oocytes

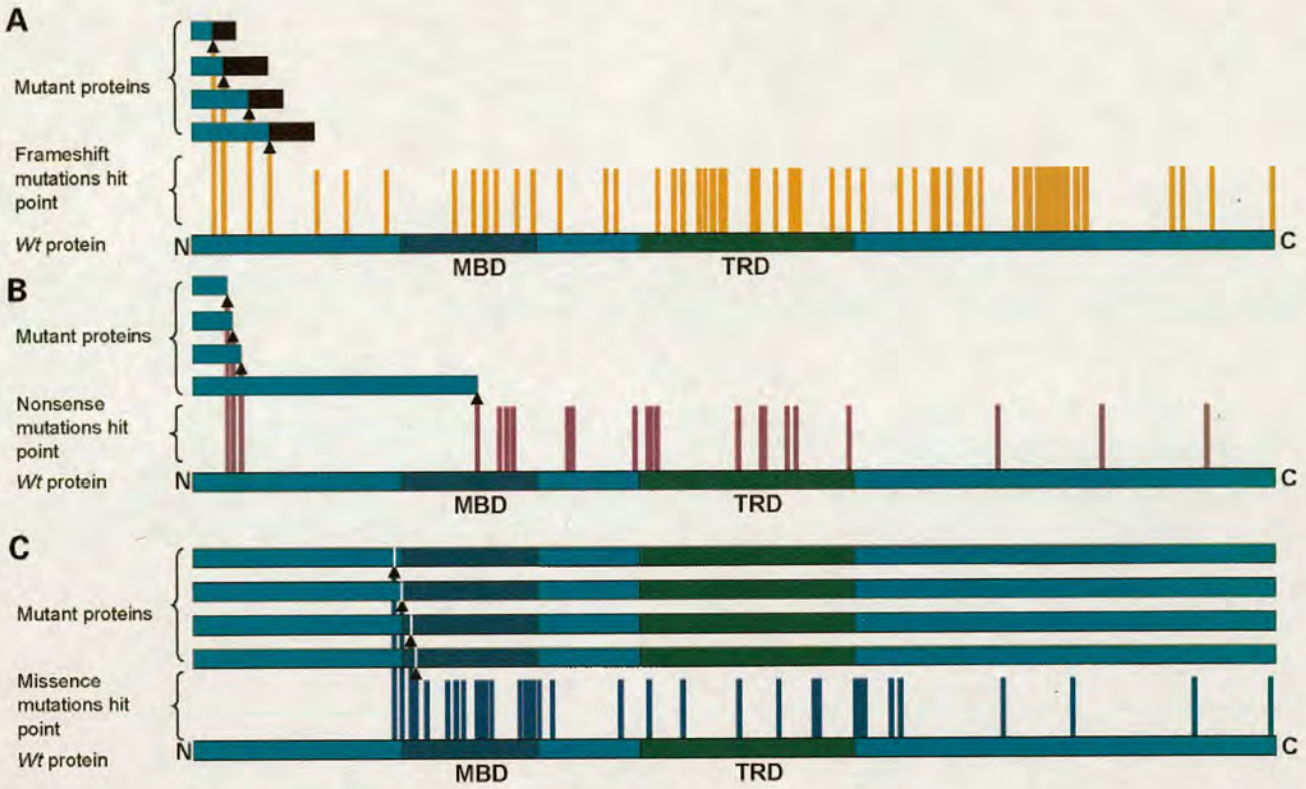

Figure 1. Distribution of human MeCP2 mutations along the protein sequence. (**A**) Frameshift mutations are nucleotide(s) insertions or deletions that lead to loss of the open reading frame. The protein amino acid sequence is different from the point of mutation and terminates at the first STOP signal (black shading). (**B**) Nonsense mutations are single nucleotide changes, which lead to a STOP signal and premature termination of the protein. (**C**) Missense mutations are single nucleotide changes, which change one codon into another producing a different amino acid at the point of mutation but leaving the rest of the protein intact. It is important point to consider that for most mutations there is no evidence that the altered protein is stably produced. Some mutations could affect mRNA or protein stability leading to absence of the protein. Four examples of expected proteins are shown above each map.

uncovered the mSin3A/HDAC1,2 corepressor complex as an interaction partner for MeCP2 (46,47). Treating cells with the HDAC inhibitor TSA partially relieves MeCP2 mediated repression, supporting HDAC involvement in transcriptional repression. Candidate approaches have since identified several other interacting proteins—including transcription factor TFIIB, the proto oncogene c-ski, the DNA methyltransferase DNMT1 and histone methyltransferase Suv39H1 (35,38,48–50). The lack of clear target genes as an *in vivo* assay for MeCP2 function has made it difficult to draw firm conclusions about the importance of these interactions, although there is evidence that the association of MeCP2 with Suv39H1 contributes to H19 silencing in mouse cells (35). The balance of evidence therefore suggests that MeCP2 can act as a transcriptional repressor *in vivo*. Whether this function has relevance to Rett syndrome now depends on progress in identification of *bona fide* target genes in the brain (see below).

THE *Mecp2*-NULL MOUSE

The first attempt to make *Mecp2*-null mice by insertion mutation of a promoterless *lacZ/neomycin* cassette into *Mecp2* locus was unsuccessful (51). Chimeric embryos with a high proportion of mutant ES cells had developmental defects and died in mid-gestation. *Mecp2*-null mice were, however, produced subsequently using cre/lox recombination technology (52,53). The discrepancy between these two sets of results could be explained if MeCP2-deficiency during *in vitro* culturing of mouse ES cell lines reduces their pluripotency, but this has yet to be tested. *Mecp2*-null male ($Mecp2^{-/y}$) and female ($Mecp2^{-/-}$) mice generated via cre/lox recombination have no apparent phenotype until around 6 weeks. There follows a period of rapid regression resulting in reduced spontaneous movement, clumsy gait, irregular breathing, hindlimb clasping and tremors. Rapid progression of symptoms leads to death at ~8 weeks of age (52,53). Detailed brain examination revealed reduced brain and neuron cell size (53). Conditional deletion of *Mecp2* in brain only was achieved by crossing mice with intronic *loxP* sites flanking *Mecp2* to mice expressing cre under the nestin promoter. Nestin is expressed mainly in neuronal progenitors from around embryonic day 12 (54). Mice with nestin–cre mediated *Mecp2* deletion showed the same phenotype as *Mecp2*-null mice (52,53). This finding led to two important conclusions: (a) the *Mecp2* mutation in the brain is sufficient to produce the same phenotype as a 'whole animal' nulls; (b) the presence of *wt* MeCP2 protein until embryonic day 12 is not enough to rescue or even relieve the phenotype. Deletion of Mecp2 in postmitotic neurons (i.e. still later in brain development) using the CamKII promoter to drive

cre recombinase (55) led to delayed onset of symptoms by up to 3 months (Fig. 2) (53). Interestingly the time between deletion of the gene and manifestation of symptoms remained approximately the same (~60 days).

Mecp2$^{+/-}$ FEMALES—A MOUSE MODEL FOR RETT SYNDROME?

Numerous Rett syndrome studies failed to find a strong correlation between the location of different *MECP2* mutations and severity of the disease. Some report that truncations are more severe than point mutations, but others do not observe this (26,56–60). The absence of a strong correlation between mutation type/location and symptoms suggests that Rett syndrome may be caused by loss of MeCP2 function regardless of the precise mutation involved. If so, the appropriate genetic mouse model for Rett syndrome may be a female mouse heterozygous for the *Mecp2*-null allele. These heterozygous mice are normal until they are around 9 months old, when they start showing breathing irregularities and hand limb clasping. Reduced mobility was confirmed by an open field test (52). There is a striking parallel between the time of symptom onset in heterozygous mice and in Rett patients, despite the vast developmental difference between a 1-year-old infant human and a 9-month-old mouse that has already raised several litters.

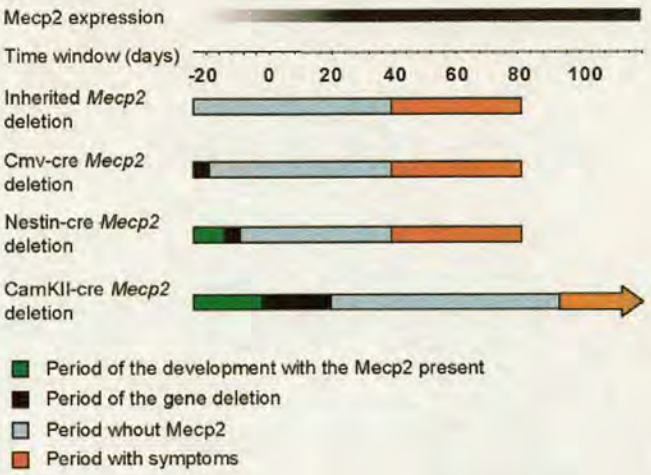

Figure 2. Comparison of the times of symptom onset in *Mecp2*-null mice that have lost the gene at different developmental stages and the correlation with the timing *Mecp2* gene expression in brain.

TRUNCATING MeCP2 MUTATION IN MICE

Around 80% of all Rett-causing mutations lie in characterized functional domains of MeCP2: the MBD and the TRD. Currently no function has been mapped to the C-terminus, but mutations which disrupt C-terminus in humans cause Rett syndrome. Mice with C-terminally truncated MeCP2 revealed some interesting findings. The symptom onset window in hemizygous mutants was increased from slight tremors at 6 weeks to kyphosis, visible tremors and seizures at around 5 months of age (61). Thus, in mice, the C-terminal deletion of *Mecp2* shows a significantly less severe phenotype than the null mutation (61). The difference between null mutation and C-terminal truncation also suggests that mice, in contrast to humans, may show a clear genotype–phenotype correlation for *Mecp2* mutations affecting different regions of the protein.

MeCP2 EXPRESSION IN BRAIN

Expression of MeCP2 is ubiquitous in mouse rat and humans, although levels vary widely between tissues. In brain, MeCP2 is preferentially expressed in neurons but not in glia. Laser scanning cytometry revealed an increase in the number of high MeCP2 expressing neurons at postnatal development in humans, and this expression correlated with alternative polyadenylation (62). *In situ* hybridization in mouse and rat brains also showed MeCP2 up-regulation postnatally (63–65). MeCP2 expression studies in olfactory epithelium, which contains both mature and immature olfactory receptor neurons, demonstrated that only mature olfactory receptor neurons up-regulate MeCP2 before synaptogenesis (66). Does MeCP2 bind methylated CpG in the brain? *In situ* hybridization to mouse brain slices suggested that MeCP2 is concentrated within DAPI bright spots of mouse neurons (67). More detailed compartmentalization studies showed co-localization of 5-methylcytosine as well as the major-satellite DNA with MeCP2 in large neurons (68).

THE SEARCH FOR MeCP2-REGULATED GENES

A microarray approach was used in search of transcriptional consequences of MeCP2 loss in mouse brain (69). Surprisingly the experiments showed no major changes in the transcriptome, although some gene expression variation was noticed. Statistical analysis, based on gene expression variability, could, however, distinguish *Mecp2*-null from *wt* brains. Some of the genes were confirmed to show small (up to 35%) differences by an RNase protection assay (69). One interpretation could be that brain is a very heterogeneous tissue, making it difficult to detect regional transcription differences due to MeCP2 loss. Alternatively, limitations to the sensitivity of microarray technology may prevent the accurate detection of low abundance transcripts and of small, but perhaps significant, changes in transcription (70). Another possible interpretation of this result is that MeCP2 has a transcription-independent role in the brain.

Recent progress in identifying MeCP2 target genes has relied on a candidate gene approach. Stancheva *et al.* (71) used *Xenopus laevis* as a model organism, taking advantage of antisense morpholino oligonucleotide injection to knock-out gene expression. MeCP2-deficient frog embryos had multiple developmental abnormalities in the head and dorsal axis. Developmental defects, together with the MeCP2 expression pattern suggested that lack of MeCP2 caused a problem in neurogenesis. The possibility of a gene mis-expression was therefore explored by investigating candidate genes in the Delta/Notch signalling pathway, which is known as a key pathway in early neuronal development. The *Hairy2a* gene was found to be up-regulated in MeCP2-deficient frog embryos. Further experiments showed that the *Hairy2a* promoter has methylated CpGs nearby with MeCP2 bound to them.

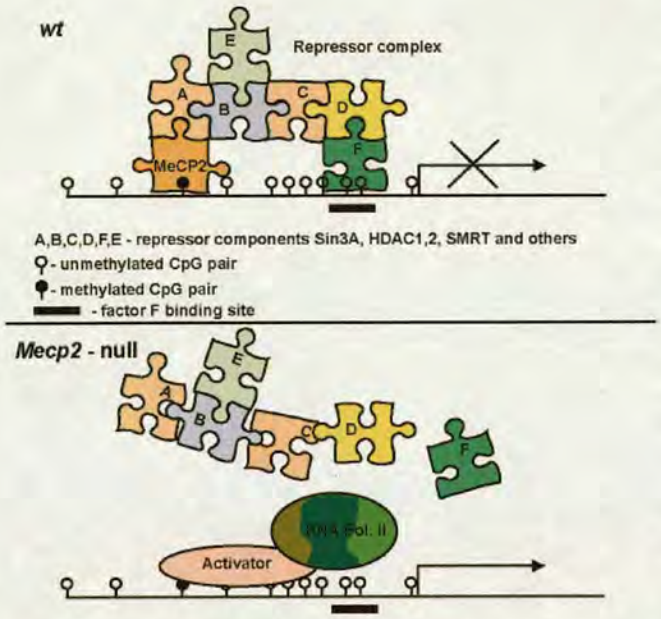

Figure 3. Model of transcription repression activity by MeCP2 protein based on the findings of Stancheva *et al.* (71). MeCP2 binds methylated CpG and interacts with the co-repressor complex, comprising components A, B, C etc. The specificity of repressor complex might be enhanced by other transcriptional factors, with DNA binding ability (e.g. F). In the absence of MeCP2, the repressor complex loses stability and the gene becomes subject to activation. Because the promoter is inducible, all other factors are already present to make it active. As a result the inducible promoter is more sensitive to de-repression.

Repression of the *Hairy2a* promoter depends on the MeCP2 interaction with SMRT complex via Sin3A. After *Notch*-mediated induction of *Hairy2a*, MeCP2 leaves the methylated CpGs, together with Sin3A, histone deacetylase and the SMRT complex. Thus *Xenopus Hairy2a* provides the first documented case of a gene that is normally repressed by MeCP2 (Fig. 3).

METHYL-CpG BINDING PROTEINS AND THE BRAIN

Recent data has highlighted that neurological defects occur when methyl-CpG binding proteins are mutated or deleted in mouse models. *Mbd2*-null females neglect their offspring, probably due to an unknown neurological lesion (72). Also, *Mbd1*-null mice show reduced neuronal differentiation and chromosome instability *in vitro* and the mice have defective spatial learning and long-term potentiation in hippocampus (73). As described earlier, *Mecp2*-null mice have more severe neurological symptoms and die at around 8 weeks of age (52,53). As MBD proteins share methyl-CpG binding domain, these findings raise the question: what role does DNA methylation play in the brain? Removing Dnmt1, the maintenance DNA methyltransferase, has a very severe phenotype resulting in failure of mouse embryo development (74), but post-natal deletion of *Dnmt1* in neurons does not affect animal viability, as might be expected in non-dividing cells (75). Tissue specific removal of *Dnmt1* in mouse central nervous system precursors using nestin–cre mediated deletion, however, led to absence of viable offspring, although embryos were recovered at all stages (75). After a Caesarean section, death occurred within 1 h due to respiratory failure. Occasional gasping was seen, but there was no rhythmic breathing. Interestingly both *Mecp2*-null mice and Rett patients show breathing abnormalities.

Functions for MBD proteins outside of the brain have recently been described. Helper T cell differentiation is abnormal in *MBD2* null mice due to faulty silencing of the *Il4* gene both before and during differentiation (76). It may be significant that the deregulation of *Il4* expression was only revealed when individual cells were assayed by cell sorting experiments. Changes of this magnitude could be easily missed by global gene expression analysis tools, such as those used to study gene expression changes in the *Mecp2*-null mouse brain.

A study by Guan *et al.* (77) demonstrated an intriguing link between different neurotransmitters and the chromatin state of the C/EBP promoter in the mollusc *Aplysia*. Treating the synapse with the facilitatory transmitter 5-HT recruited CREB1 with CBP histone acetylase, which causes histone acetylation and expression of the gene. On the other hand, treatment with inhibitory transmitter FMRFa brought CREB2 repressor with HDAC5 to the C/EBP promoter, leading to deacetylation of chromatin and silencing of the gene (77). As there is a close interplay between the chromatin modifications and DNA methylation, it is likely that silencing of certain neuronal genes relies on DNA methylation and recruitment of MeCP2, as already indicated for the *Hairy2a* gene in frog embryos (71) (Fig. 3). It has also been proposed that the extensive DNA replication-independent replacement of histone H3 in neurons may rely on MeCP2 to re-establish appropriate histone modifications (78). The study of chromatin structure in the brain is in its infancy, but we can look forward to rapid developments as we unravel the pathways that involve MeCP2 in neurological development and, with them, the reasons why MeCP2-loss leads to Rett syndrome.

ACKNOWLEDGEMENTS

We thank Helle Jørgensen, Rob Klose and Jacky Guy for critical reading and discussions, and Dr Alison Kerr (Glasgow University) for advice. S.K. holds a studentship from the Darwin Trust (Edinburgh). This work was supported by the Wellcome Trust.

REFERENCES

1. Antequera, F. and Bird, A. (1993) Number of CpG islands and genes in human and mouse. *Proc. Natl Acad. Sci. USA*, **90**, 11995–11999.
2. Waterston, R.H., Lindblad-Toh, K., Birney, E., Rogers, J., Abril, J.F., Agarwal, P., Agarwala, R., Ainscough, R., Alexandersson, M., An, P. *et al.* (2002) Initial sequencing and comparative analysis of the mouse genome. *Nature*, **420**, 520–562.
3. Bird, A.P. and Wolffe, A.P. (1999) Methylation-induced repression—belts, braces, and chromatin. *Cell*, **99**, 451–454.
4. Jaenisch, R. and Bird, A. (2003) Epigenetic regulation of gene expression: how the genome integrates intrinsic and environmental signals. *Nat. Genet.*, **33** (Suppl.), 245–254.
5. Maier, H., Colbert, J., Fitzsimmons, D., Clark, D.R. and Hagman, J. (2003) Activation of the early B-cell-specific mb-1 (Ig-alpha) gene by Pax-5 is dependent on an unmethylated Ets binding site. *Mol. Cell. Biol.*, **23**, 1946–1960.

6. Bell, A.C. and Felsenfeld, G. (2000) Methylation of a CTCF-dependent boundary controls imprinted expression of the Igf2 gene. *Nature*, **405**, 482–485.
7. Hendrich, B. and Bird, A. (1998) Identification and characterization of a family of mammalian methyl-CpG binding proteins. *Mol. Cell. Biol.*, **18**, 6538–6547.
8. Prokhortchouk, A., Hendrich, B., Jorgensen, H., Ruzov, A., Wilm, M., Georgiev, G., Bird, A. and Prokhortchouk, E. (2001) The p120 catenin partner Kaiso is a DNA methylation-dependent transcriptional repressor. *Genes Dev.*, **15**, 1613–1618.
9. Hendrich, B., Hardeland, U., Ng, H.H., Jiricny, J. and Bird, A. (1999) The thymine glycosylase MBD4 can bind to the product of deamination at methylated CpG sites. *Nature*, **401**, 301–304.
10. Hendrich, B. and Bickmore, W. (2001) Human diseases with underlying defects in chromatin structure and modification. *Hum. Mol. Genet.*, **10**, 2233–2242.
11. Amir, R.E., Van, d. V., I, Wan, M., Tran, C.Q., Francke, U. and Zoghbi, H.Y. (1999) Rett syndrome is caused by mutations in X-linked MECP2, encoding methyl-CpG-binding protein 2. *Nat. Genet.*, **23**, 185–188.
12. Armstrong, D.D. (2002) Neuropathology of Rett syndrome. *Ment. Retard. Dev. Disabil. Res. Rev.*, **8**, 72–76.
13. Glaze, D.G. (2002) Neurophysiology of Rett syndrome. *Ment. Retard. Dev. Disabil. Res. Rev.*, **8**, 66–71.
14. Hagberg, B. (2002) Clinical manifestations and stages of Rett syndrome. *Ment. Retard. Dev. Disabil. Res. Rev.*, **8**, 61–65.
15. Jellinger, K.A. (2003) Rett syndrome—an update. *J. Neural Transm.*, **110**, 681–701.
16. Cass, H., Reilly, S., Owen, L., Wisbeach, A., Weekes, L., Slonims, V., Wigram, T. and Charman, T. (2003) Findings from a multidisciplinary clinical case series of females with Rett syndrome. *Dev. Med. Child Neurol.*, **45**, 325–337.
17. Akbarian, S. (2003) The neurobiology of Rett syndrome. *Neuroscientist*, **9**, 57–63.
18. Amir, R., Dahle, E.J., Toriolo, D. and Zoghbi, H.Y. (2000) Candidate gene analysis in Rett syndrome and the identification of 21 SNPs in Xq. *Am. J. Med. Genet.*, **90**, 69–71.
19. Cooper, D.N. and Youssoufian, H. (1988) The CpG dinucleotide and human genetic disease. *Hum. Genet.*, **78**, 151–155.
20. Couvert, P., Bienvenu, T., Aquaviva, C., Poirier, K., Moraine, C., Gendrot, C., Verloes, A., Andres, C., Le Fevre, A.C., Souville, I. *et al.* (2001) MECP2 is highly mutated in X-linked mental retardation. *Hum. Mol. Genet.*, **10**, 941–946.
21. Watson, P., Black, G., Ramsden, S., Barrow, M., Super, M., Kerr, B. and Clayton-Smith, J. (2001) Angelman syndrome phenotype associated with mutations in MECP2, a gene encoding a methyl CpG binding protein. *J. Med. Genet.*, **38**, 224–228.
22. Lobo-Menendez, F., Sossey-Alaoui, K., Bell, J.M., Copeland-Yates, S.A., Plank, S.M., Sanford, S.O., Skinner, C., Simensen, R.J., Schroer, R.J. and Michaelis, R.C. (2003) Absence of MeCP2 mutations in patients from the South Carolina autism project. *Am. J. Med. Genet.*, **117B**, 97–101.
23. Zappella, M., Meloni, I., Longo, I., Canitano, R., Hayek, G., Rosaia, L., Mari, F. and Renieri, A. (2003) Study of MECP2 gene in Rett syndrome variants and autistic girls. *Am. J. Med. Genet.*, **119B**, 102–107.
24. Carney, R.M., Wolpert, C.M., Ravan, S.A., Shahbazian, M., Ashley-Koch, A., Cuccaro, M.L., Vance, J.M. and Pericak-Vance, M.A. (2003) Identification of MeCP2 mutations in a series of females with autistic disorder. *Pediatr. Neurol.*, **28**, 205–211.
25. Villard, L., Kpebe, A., Cardoso, C., Chelly, P.J., Tardieu, P.M. and Fontes, M. (2000) Two affected boys in a Rett syndrome family: clinical and molecular findings. *Neurology*, **55**, 1188–1193.
26. Ravn, K., Nielsen, J.B., Uldall, P., Hansen, F.J. and Schwartz, M. (2003) No correlation between phenotype and genotype in boys with a truncating MECP2 mutation. *J. Med. Genet.*, **40**, e5.
27. Topcu, M., Akyerli, C., Sayi, A., Toruner, G.A., Kocoglu, S.R., Cimbis, M. and Ozcelik, T. (2002) Somatic mosaicism for a MECP2 mutation associated with classic Rett syndrome in a boy. *Eur. J. Hum. Genet.*, **10**, 77–81.
28. Meehan, R.R., Lewis, J.D., McKay, S., Kleiner, E.L. and Bird, A.P. (1989) Identification of a mammalian protein that binds specifically to DNA containing methylated CpGs. *Cell*, **58**, 499–507.
29. Lewis, J.D., Meehan, R.R., Henzel, W.J., Maurer-Fogy, I., Jeppesen, P., Klein, F. and Bird, A. (1992) Purification, sequence, and cellular localization of a novel chromosomal protein that binds to methylated DNA. *Cell*, **69**, 905–914.
30. Nan, X., Tate, P., Li, E. and Bird, A. (1996) DNA methylation specifies chromosomal localization of MeCP2. *Mol. Cell Biol.*, **16**, 414–421.
31. Nan, X., Meehan, R.R. and Bird, A. (1993) Dissection of the methyl-CpG binding domain from the chromosomal protein MeCP2. *Nucl. Acids Res.*, **21**, 4886–4892.
32. Chandler, S.P., Guschin, D., Landsberger, N. and Wolffe, A.P. (1999) The methyl-CpG binding transcriptional repressor MeCP2 stably associates with nucleosomal DNA. *Biochemistry*, **38**, 7008–7018.
33. Ohki, I., Shimotake, N., Fujita, N., Jee, J., Ikegami, T., Nakao, M. and Shirakawa, M. (2001) Solution structure of the methyl-CpG binding domain of human MBD1 in complex with methylated DNA. *Cell*, **105**, 487–497.
34. Fournier, C., Goto, Y., Ballestar, E., Delaval, K., Hever, A.M., Esteller, M. and Feil, R. (2002) Allele-specific histone lysine methylation marks regulatory regions at imprinted mouse genes. *EMBO J.*, **21**, 6560–6570.
35. Fuks, F., Hurd, P.J., Wolf, D., Nan, X., Bird, A.P. and Kouzarides, T. (2003) The methyl-CpG-binding protein MeCP2 links DNA methylation to histone methylation. *J. Biol. Chem.*, **278**, 4035–4040.
36. Ghoshal, K., Datta, J., Majumder, S., Bai, S., Dong, X., Parthun, M. and Jacob, S.T. (2002) Inhibitors of histone deacetylase and DNA methyltransferase synergistically activate the methylated metallothionein I promoter by activating the transcription factor MTF-1 and forming an open chromatin structure. *Mol. Cell. Biol.*, **22**, 8302–8319.
37. Koizume, S., Tachibana, K., Sekiya, T., Hirohashi, S. and Shiraishi, M. (2002) Heterogeneity in the modification and involvement of chromatin components of the CpG island of the silenced human CDH1 gene in cancer cells. *Nucl. Acids Res.*, **30**, 4770–4780.
38. Lunyak, V.V., Burgess, R., Prefontaine, G.G., Nelson, C., Sze, S.H., Chenoweth, J., Schwartz, P., Pevzner, P.A., Glass, C., Mandel, G. and Rosenfeld, M.G. (2002) Corepressor-dependent silencing of chromosomal regions encoding neuronal genes. *Science*, **298**, 1747–1752.
39. El Osta, A., Kantharidis, P., Zalcberg, J.R. and Wolffe, A.P. (2002) Precipitous release of methyl-CpG binding protein 2 and histone deacetylase 1 from the methylated human multidrug resistance gene (MDR1) on activation. *Mol. Cell. Biol.*, **22**, 1844–1857.
40. Nguyen, C.T., Gonzales, F.A. and Jones, P.A. (2001) Altered chromatin structure associated with methylation-induced gene silencing in cancer cells: correlation of accessibility, methylation, MeCP2 binding and acetylation. *Nucl. Acids Res.*, **29**, 4598–4606.
41. Ballestar, E., Yusufzai, T.M. and Wolffe, A.P. (2000) Effects of Rett syndrome mutations of the methyl-CpG binding domain of the transcriptional repressor MeCP2 on selectivity for association with methylated DNA. *Biochemistry*, **39**, 7100–7106.
42. Yusufzai, T.M. and Wolffe, A.P. (2000) Functional consequences of Rett syndrome mutations on human MeCP2. *Nucl. Acids Res.*, **28**, 4172–4179.
43. Free, A., Wakefield, R.I., Smith, B.O., Dryden, D.T., Barlow, P.N. and Bird, A.P. (2001) DNA recognition by the methyl-CpG binding domain of MeCP2. *J. Biol. Chem.*, **276**, 3353–3360.
44. Meehan, R.R., Lewis, J.D. and Bird, A.P. (1992) Characterization of MeCP2, a vertebrate DNA binding protein with affinity for methylated DNA. *Nucl. Acids Res.*, **20**, 5085–5092.
45. Nan, X., Campoy, F.J. and Bird, A. (1997) MeCP2 is a transcriptional repressor with abundant binding sites in genomic chromatin. *Cell*, **88**, 471–481.
46. Nan, X., Ng, H.H., Johnson, C.A., Laherty, C.D., Turner, B.M., Eisenman, R.N. and Bird, A. (1998) Transcriptional repression by the methyl-CpG-binding protein MeCP2 involves a histone deacetylase complex. *Nature*, **393**, 386–389.
47. Jones, P.L., Veenstra, G.J., Wade, P.A., Vermaak, D., Kass, S.U., Landsberger, N., Strouboulis, J. and Wolffe, A.P. (1998) Methylated DNA and MeCP2 recruit histone deacetylase to repress transcription. *Nat. Genet.*, **19**, 187–191.
48. Kaludov, N.K. and Wolffe, A.P. (2000) MeCP2 driven transcriptional repression in vitro: selectivity for methylated DNA, action at a distance and contacts with the basal transcription machinery. *Nucl. Acids Res.*, **28**, 1921–1928.
49. Kimura, H. and Shiota, K. (2003) Methyl-CpG-binding protein, MeCP2, is a target molecule for maintenance DNA methyltransferase, Dnmt1. *J. Biol. Chem.*, **278**, 4806–4812.
50. Kokura, K., Kaul, S.C., Wadhwa, R., Nomura, T., Khan, M.M., Shinagawa, T., Yasukawa, T., Colmenares, C. and Ishii, S. (2001) The Ski protein family is required for MeCP2-mediated transcriptional repression. *J. Biol. Chem.*, **276**, 34115–34121.

51. Tate, P., Skarnes, W. and Bird, A. (1996) The methyl-CpG binding protein MeCP2 is essential for embryonic development in the mouse. *Nat. Genet.*, **12**, 205–208.
52. Guy, J., Hendrich, B., Holmes, M., Martin, J.E. and Bird, A. (2001) A mouse Mecp2-null mutation causes neurological symptoms that mimic Rett syndrome. *Nat. Genet.*, **27**, 322–326.
53. Chen, R.Z., Akbarian, S., Tudor, M. and Jaenisch, R. (2001) Deficiency of methyl-CpG binding protein-2 in CNS neurons results in a Rett-like phenotype in mice. *Nat. Genet.*, **27**, 327–331.
54. Zimmerman, L., Parr, B., Lendahl, U., Cunningham, M., McKay, R., Gavin, B., Mann, J., Vassileva, G. and McMahon, A. (1994) Independent regulatory elements in the nestin gene direct transgene expression to neural stem cells or muscle precursors. *Neuron*, **12**, 11–24.
55. Tsien, J.Z., Chen, D.F., Gerber, D., Tom, C., Mercer, E.H., Anderson, D.J., Mayford, M., Kandel, E.R. and Tonegawa, S. (1996) Subregion- and cell type-restricted gene knockout in mouse brain. *Cell*, **87**, 1317–1326.
56. Colvin, L., Fyfe, S., Leonard, S., Schiavello, T., Ellaway, C., De Klerk, N., Christodoulou, J., Msall, M. and Leonard, H. (2003) Describing the phenotype in Rett syndrome using a population database. *Arch. Dis. Child*, **88**, 38–43.
57. Nielsen, J.B., Henriksen, K.F., Hansen, C., Silahtaroglu, A., Schwartz, M. and Tommerup, N. (2001) MECP2 mutations in Danish patients with Rett syndrome: high frequency of mutations but no consistent correlations with clinical severity or with the X chromosome inactivation pattern. *Eur. J. Hum. Genet.*, **9**, 178–184.
58. Amir, R.E. and Zoghbi, H.Y. (2000) Rett syndrome: methyl-CpG-binding protein 2 mutations and phenotype-genotype correlations. *Am. J. Med. Genet.*, **97**, 147–152.
59. Cheadle, J.P., Gill, H., Fleming, N., Maynard, J., Kerr, A., Leonard, H., Krawczak, M., Cooper, D.N., Lynch, S., Thomas, N. *et al.* (2000) Long-read sequence analysis of the MECP2 gene in Rett syndrome patients: correlation of disease severity with mutation type and location. *Hum. Mol. Genet.*, **9**, 1119–1129.
60. Hoffbuhr, K.C., Moses, L.M., Jerdonek, M.A., Naidu, S. and Hoffman, E.P. (2002) Associations between MeCP2 mutations, X-chromosome inactivation, and phenotype. *Ment. Retard. Dev. Disabil. Res. Rev.*, **8**, 99–105.
61. Shahbazian, M., Young, J., Yuva-Paylor, L., Spencer, C., Antalffy, B., Noebels, J., Armstrong, D., Paylor, R. and Zoghbi, H. (2002) Mice with truncated MeCP2 recapitulate many Rett syndrome features and display hyperacetylation of histone H3. *Neuron*, **35**, 243–254.
62. Balmer, D., Goldstine, J., Rao, Y.M. and LaSalle, J.M. (2003) Elevated methyl-CpG-binding protein 2 expression is acquired during postnatal human brain development and is correlated with alternative polyadenylation. *J. Mol. Med.*, **81**, 61–68.
63. Shahbazian, M.D., Antalffy, B., Armstrong, D.L. and Zoghbi, H.Y. (2002) Insight into Rett syndrome: MeCP2 levels display tissue- and cell-specific differences and correlate with neuronal maturation. *Hum. Mol. Genet.*, **11**, 115–124.
64. Jung, B.P., Jugloff, D.G., Zhang, G., Logan, R., Brown, S. and Eubanks, J.H. (2003) The expression of methyl CpG binding factor MeCP2 correlates with cellular differentiation in the developing rat brain and in cultured cells. *J. Neurobiol.*, **55**, 86–96.
65. Akbarian, S., Chen, R.Z., Gribnau, J., Rasmussen, T.P., Fong, H., Jaenisch, R. and Jones, E.G. (2001) Expression pattern of the Rett syndrome gene MeCP2 in primate prefrontal cortex. *Neurobiol. Dis.*, **8**, 784–791.
66. Cohen, D.R., Matarazzo, V., Palmer, A.M., Tu, Y., Jeon, O.H., Pevsner, J. and Ronnett, G.V. (2003) Expression of MeCP2 in olfactory receptor neurons is developmentally regulated and occurs before synaptogenesis. *Mol. Cell Neurosci.*, **22**, 417–429.
67. Payen, E., Verkerk, T., Michalovich, D., Dreyer, S.D., Winterpacht, A., Lee, B., De Zeeuw, C.I., Grosveld, F. and Galjart, N. (1998) The centromeric/nucleolar chromatin protein ZFP-37 may function to specify neuronal nuclear domains. *J. Biol. Chem.*, **273**, 9099–9109.
68. Akhmanova, A., Verkerk, T., Langeveld, A., Grosveld, F. and Galjart, N. (2000) Characterisation of transcriptionally active and inactive chromatin domains in neurons. *J. Cell Sci.*, **113** (Pt 24), 4463–4474.
69. Tudor, M., Akbarian, S., Chen, R.Z. and Jaenisch, R. (2002) Transcriptional profiling of a mouse model for Rett syndrome reveals subtle transcriptional changes in the brain. *Proc. Natl Acad. Sci. USA*, **99**, 15536–15541.
70. Nisenbaum, L.K. (2002) The ultimate chip shot: can microarray technology deliver for neuroscience? *Genes Brain Behav.*, **1**, 27–34.
71. Stancheva, I., Collins, A.L., Van den Veyver, I.B., Zoghbi, H. and Meehan, R. (2003) A mutant form of MeCP2 protein associated with human Rett syndrome cannot be displaced from methylated DNA by Notch in Xenopus embryos. *Mol. Cell*, **12**, 425–435.
72. Hendrich, B., Guy, J., Ramsahoye, B., Wilson, V.A. and Bird, A. (2001) Closely related proteins MBD2 and MBD3 play distinctive but interacting roles in mouse development. *Genes Dev.*, **15**, 710–723.
73. Zhao, X., Ueba, T., Christie, B.R., Barkho, B., McConnell, M.J., Nakashima, K., Lein, E.S., Eadie, B.D., Willhoite, A.R., Muotri, A.R. *et al.* (2003) Mice lacking methyl-CpG binding protein 1 have deficits in adult neurogenesis and hippocampal function. *Proc. Natl Acad. Sci. USA*, **100**, 6777–6782.
74. Li, E., Bestor, T.H. and Jaenisch, R. (1992) Targeted mutation of the DNA methyltransferase gene results in embryonic lethality. *Cell*, **69**, 915–926.
75. Fan, G., Beard, C., Chen, R.Z., Csankovszki, G., Sun, Y., Siniaia, M., Biniszkiewicz, D., Bates, B., Lee, P.P., Kuhn, R. *et al.* (2001) DNA hypomethylation perturbs the function and survival of CNS neurons in postnatal animals. *J. Neurosci.*, **21**, 788–797.
76. Hutchins, A.S., Mullen, A.C., Lee, H.W., Sykes, K.J., High, F.A., Hendrich, B.D., Bird, A.P. and Reiner, S.L. (2002) Gene silencing quantitatively controls the function of a developmental trans-activator. *Mol. Cell*, **10**, 81–91.
77. Guan, Z., Giustetto, M., Lomvardas, S., Kim, J.H., Miniaci, M.C., Schwartz, J.H., Thanos, D. and Kandel, E.R. (2002) Integration of long-term-memory-related synaptic plasticity involves bidirectional regulation of gene expression and chromatin structure. *Cell*, **111**, 483–493.
78. Ahmad, K. and Henikoff, S. (2002) Epigenetic consequences of nucleosome dynamics. *Cell*, **111**, 281–284.

Published online March 19, 2004

1818–1823 *Nucleic Acids Research, 2004, Vol. 32, No. 5*
DOI: 10.1093/nar/gkh349

The major form of MeCP2 has a novel N-terminus generated by alternative splicing

Skirmantas Kriaucionis and Adrian Bird*

Wellcome Trust Centre for Cell Biology, University of Edinburgh, The King's Buildings, Edinburgh EH9 3JR, Scotland, UK

Received February 16, 2004; Revised and Accepted March 2, 2004

ABSTRACT

MeCP2 is a methyl-CpG binding protein that can repress transcription of nearby genes. In humans, mutations in the *MECP2* gene are the major cause of Rett syndrome. By searching expressed sequence tag (EST) databases we have found a novel MeCP2 splice isoform (MeCP2α) which encodes a distinct N-terminus. We demonstrate that the MeCP2α mRNA splice variant is more abundant than the previously annotated MeCP2 mRNA (MeCP2β) in mouse tissues and human brain. Furthermore, MeCP2β mRNA has an upstream open reading frame that inhibits its translation. As a result of these differences, >90% of MeCP2 in mouse brain is MeCP2α. Both protein isoforms are nuclear and colocalize with densely methylated heterochromatic foci in mouse cells. The presence of a previously unknown MeCP2 isoform has implications for the genetic screening of Rett syndrome patients and for studies of the functional significance of MeCP2.

INTRODUCTION

In vertebrate genomes, 5-methylcytosine (m^5C) accounts for ~1% of all DNA bases. The minor base arises by post-synthetic modification of cytosine, usually in the context of a CpG dinucleotide that is symmetrically methylated on both strands of DNA. A family of proteins that specifically bind to a methylated CpG pair share a conserved methyl-CpG binding domain (MBD) (1). MeCP2 is the founder member of the MBD protein family and is present in all tested vertebrates. Currently two conserved functional domains have been mapped in MeCP2: the MBD (2), which specifically targets MeCP2 to methylated DNA sequences *in vivo* (3–5), and the transcription repression domain (TRD), which is the minimal domain required to repress transcription *in vitro* and *in vivo* (5–10). MeCP2 repression is sensitive to histone deacetylase (HDAC) inhibitor TSA, indicating that deacetylation may contribute to repression (11,12). GST pulldowns and partial multiprotein complex purification from *Xenopus laevis* oocytes suggest that the TRD interacts with the mSin3A/HDAC co-repressor complex (11,12). As TSA partially alleviates repression, HDAC-independent mechanisms of repression are likely to exist. For example, MeCP2 has been shown to associate with histone methyltransferase activity (13). Other HDAC-independent transcriptional repression mechanisms, involving interactions of the TRD with basal transcriptional repression machinery, have also been proposed (14).

Mutations in the *MECP2* gene are the primary cause of Rett syndrome (15), a neurological disorder that occurs in one in 10 000–22 000 female births. After an initial window of normal development, girls acquire a variety of symptoms including microcephaly, autism, ataxia, stereotypic hand movements, seizures and hyperventilation (16). A wide spectrum of mutations have been mapped throughout the *MECP2* gene, including sites outside the MBD and TRD regions (17). MeCP2 is also essential in mice, as *Mecp2*-null animals have a period of normal postnatal development followed by hindlimb clasping, irregular breathing, reduced mobility and death at around 8 weeks of age (18,19). Mice with *Mecp2* mutations phenotypically mimic several features of Rett syndrome (18–20).

Initially, MeCP2 protein was purified from rat brain as a single 84 kDa protein based on its binding to methylated CpG (21). The results of Edman degradation allowed the design of a degenerate probe which was then used to screen a cDNA library and isolate full-length MeCP2 cDNA (21). Later, the mouse *Mecp2* gene was mapped to Xq28 and shown to be subject to X-inactivation (22). Further analysis of the *Mecp2* transcript identified alternative polyadenylation sites that give rise to two main mRNA variants with different 3′UTRs (10 kb and 2 kb) (23). At this time *Mecp2* was annotated as a three-exon gene, with all exons contributing to the protein (23). Sequencing of the *Mecp2* genomic locus in mouse and human combined with more detailed bioinformatic analysis revealed an additional upstream non-coding exon (24). *Mecp2* is therefore currently recognized as a four-exon gene. Here we report the additional complication that MeCP2 is subject to alternative splicing generating two different N-termini, one of which is significantly more abundant than the other.

MATERIALS AND METHODS

Bioinformatics

Different isoforms encoding expressed sequence tags (ESTs) were found using the NCBI BLAST program. Alignment of genomic DNA with EST sequences was performed with

*To whom correspondence should be addressed. Tel: +44 131 650 5670; Fax: +44 131 650 5379; Email: A.Bird@ed.ac.uk

GeneQuest (DNAStar). Protein alignments were done using ClustalW and T-coffee programs. Alignments were displayed with GeneDoc software.

RNA purification, analysis and RT–PCR

Total RNA from tissue culture cells was purified using TRI-Reagent (Sigma) according to the manufacturer's recommendations. Prior to cDNA synthesis RNA was treated with RQ1 RNase-Free DNase (Promega). cDNA was synthesized by annealing 5 μg of total RNA and 5 μg random hexanucleotides (Amersham) at 70°C for 5 min. Then RT mix [final 1× reaction buffer, 40 U RNAasin ribonuclease inhibitor (Promega), 1 mM dNTP] was added and the solution was incubated for 5 min at 25°C. After addition of M-MLV reverse transcriptase (RNase H Minus, Promega) the 25 μl reaction mix was incubated for 10 min at 25°C and 1 h at 37°C. The reverse transcriptase was inactivated by incubating for 10 min at 70°C. The reaction mixture was diluted to 500 μl, and 2.5 μl was used for PCRs. Mouse exon-specific PCR was carried out using primers me11d (GGTAAAACCCGTCCGGAAAATG) and me31r (TTCAGTGGCTTGTCTCTGAG) at T_a = 61°C. Human exon-specific PCR was performed using me11d and hme31r (CTTGAGGGGTTTGTCCTTGAG) primers at T_a = 61°C. Human brain cDNA was purchased from Ambion (FirstChoice PCR-Ready). Northern blots were performed using standard procedures as described in the Hybond-N+ (Amersham) membrane users' manual. After extraction, RNA was treated with DNase I to remove transfected plasmid. Northern blots were probed with a 1.5 kbp NcoI and NotI fragment of MeCP2 cDNA.

Embryonic stem cell differentiation

Embryonic stem (ES) cells were differentiated as described elsewhere (25). In brief, mouse ES cells were plated on non-adhesive plates without LIF. In these conditions ES cells form embryoid bodies which contain different cell lineage progenitors. Later, embryoid bodies were cultured in the presence of retinoic acid, which was shown to increase the efficiency of neuronal differentiation. In the final stage embryoid bodies were dissociated and cells were plated on serum-free N2 medium which promotes final differentiation and survival of neuronal cells.

Mutagenesis

Site-directed mutagenesis used the QuikChange XL Site-Directed Mutagenesis Kit (Stratagene) according to the manufacturers' recommendations. Primers used for mutagenesis were mumed (CCCGTCCGGAAAAAGGCCGCCG-CTGCCGCC) and mumer (GGCGGCAGCGGCGGCCTTT-TTCCGGACGGG).

Vector construction and transfections

EST clones (BI078224 and BG922233) were received from the I.M.A.G.E. consortium. Plasmids used for transfection are based on pRL-SV40 (Promega). R*luc* gene was excised using NheI and XbaI sites and replaced with appropriate MeCP2 splice variant cDNA. All transfections were done with Lipofectamine reagent (Invitrogen) according to the manufacturer's recommendations. Cells were collected 48 h after transfection.

Table 1. Physical characteristics of human and mouse MeCP2 isoforms

	MW (kDa)	Length (aa)	pI	Charge at pH 7
mMECP2α	53.6	501	9.89	34.9
hMECP2α	53.3	498	9.88	34.8
mMECP2β	52.3	484	9.96	37.8
hMECP2β	52.4	486	9.95	37.8

Western blotting

Western blotting was according to standard protocols. Transfected cells were harvested by scraping, boiled in SDS loading buffer and resolved on 8% SDS–PAGE gels. Mouse brain nuclear extract was kindly provided by Rob Klose. Brain nuclei were purified from whole mouse brain and nuclear proteins were extracted with 400 mM NaCl. Anti-MeCP2 antibodies were purchased from Upstate Biotechnology (no. 07–013).

Immunohistochemistry

Transfected cells were fixed in 4% paraformaldehyde in PBS for 20 min. After two washes with PBS, cells were permeabilized with 0.2% Triton X-100 for 10 min. Blocking was performed in 3% BSA in PBS for 30 min. MeCP2 antibody (Upstate Biotechnology) was diluted 1:200 in blocking solution and incubated with slides for 1 h. After washing three times in PBS, slides were incubated with fluorescein anti-rabbit IgG (Vector Laboratories) at 1:100 dilution. After incubation for 1 h, slides were washed and mounted in Vectaschield mounting medium with DAPI (Vector Laboratories). Slides were examined using a Zeiss microscope.

RESULTS

Identification of an MeCP2 splice variant in EST databases

We searched mouse EST databases for cDNA sequences encoding MeCP2. Alignments revealed that ESTs can be grouped into two categories depending on the presence (BY107013, BI409371) or absence (CA980031, BY244111) of exon 2. Human MECP2 cDNAs with (BC11612, BM923600) and without (BG706068, BI458175) exon 2 also exist in human EST databases. As exon 2 contains the ATG for the initiation of translation, we considered the possibility that the transcript lacking exon 2 is a non-coding RNA. However exon 1 contains an ATG that in the absence of exon 2 initiates a potential open reading frame (ORF) of 501 amino acids (aa) in mice and 498 aa in humans (Table 1). We designate the new exon 2-minus isoform as MeCP2α and the previously described isoform containing exon 2 as MeCP2β. Alignment of α and β predicted protein sequences demonstrates identity except at the extreme N-terminus (Fig. 1a and b). The MeCP2α N-terminus contains polyalanine and polyglycine repeat tracts encoded by GCC and GGA trinucleotides. Comparison of these isoforms with other vertebrate MeCP2 sequences showed that MeCP2α shares a polyalanine tract, serine-glycine residues and EERL motifs with *Xenopus* and zebrafish MeCP2 sequences, whereas

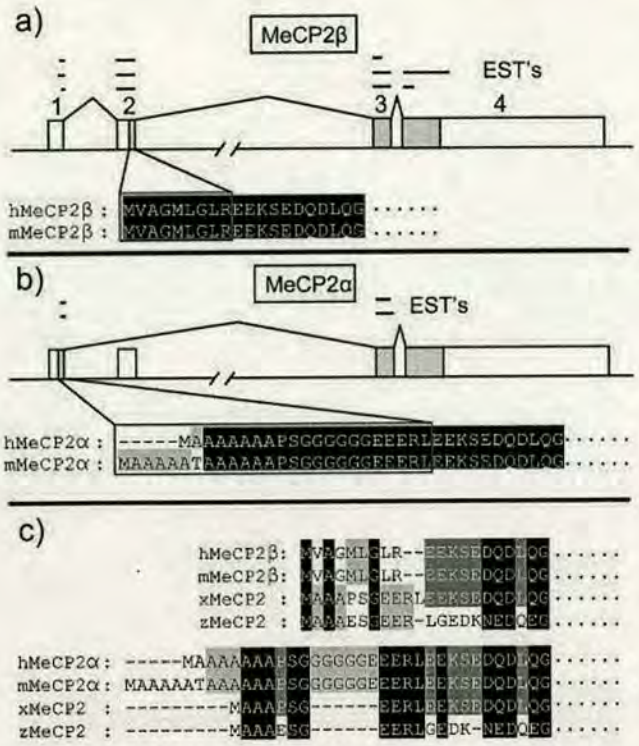

Figure 1. Alternative splicing of MeCP2 mRNA. (**a**) Previously described MeCP2β is encoded when all known exons are sequentially spliced. (**b**) The novel MeCP2α isoform arises when exon 1 is spliced onto exon 3, skipping exon 2. Shaded boxes are protein coding and open boxes are non-coding. ESTs suggesting the occurrence of each isoform *in vivo* are mapped as lines above the genomic DNA. (**c**) Alignment of mouse and human MeCP2β and MeCP2α N-termini with zebrafish and frog MeCP2. MeCP2α is more similar to zebrafish and frog orthologs than is MeCP2β.

MeCP2β lacks these features. The alignment suggested that MeCP2α more closely resembles the ancestral form of MeCP2 than does MeCP2β (Fig. 1c). We have searched the non-mammalian EST databases and failed to find any β-isoform-like EST. Furthermore, examination of zebrafish and *Fugu rubripes* genomic sequences surrounding the MeCP2 gene revealed exon 1 (α), but no potential exon 2 (β). We conclude that the β isoform is either absent or highly diverged compared with the mammalian β sequence.

MeCP2α is the major mRNA splice variant *in vivo*

To confirm *in silico* evidence and assess the relative abundance of the different MeCP2 isoforms *in vivo*, we performed semiquantitative RT–PCR analysis of cDNA derived from different mouse tissues. The two primers were designed to anneal to exon 1 and exon 3, respectively (Fig. 2a). Control amplification of mixed MeCP2α and MeCP2β encoding plasmids showed no significant amplification bias towards the shorter product (Fig. 2a). RT–PCR analysis demonstrated that MeCP2α is more abundant than MeCP2β in most tissues. Relative abundance of MeCP2α was highest in the brain, thymus and lung, whereas an approximately 1:1 isoform ratio was seen in testis and liver. The RT–PCRs (32 cycles) were not saturating and therefore were responsive to template concentration. This was verified for each tissue sample by showing that fewer (30) or more (34) cycles generated less or more product, respectively (data not shown). Similar semiquantitative RT–PCRs provided evidence that both splice variants also exist in human brain; again, the predominant form of mRNA encodes MECP2α (Fig. 2b).

To analyse the abundance of the two isoforms during cellular differentiation, we differentiated mouse ES cells into neurons. Samples from stages of differentiation were assayed for the different isoforms. Semiquantitative RT–PCR showed that MeCP2α mRNA is more abundant than MeCP2β mRNA in ES cells and the proportion of α mRNA appeared to increase during neuronal differentiation (Fig. 2c).

The MeCP2α splice variant is more efficiently translated *in vivo*

Having established that the MeCP2α mRNA splice isoform is abundant in mouse tissues and human brain, we next asked whether MeCP2α mRNA is translated *in vivo*. To address this, we transfected tail fibroblasts from *Mecp2*-null mice (18) with plasmid constructs containing α- or β-isoform cDNA (Fig. 3a). Western blotting with a C-terminal MeCP2 antibody showed that MeCP2α is successfully translated, but we consistently observed only very low amounts of MeCP2β in independent transfections (Fig. 3b). As a potential explanation, we noted a short ORF (39 aa) within the 5′UTR region of MeCP2β that could potentially interfere with its translation. The short ORF starts from the AUG that initiates translation of the MeCP2α isoform, but in MeCP2β mRNA this ORF terminates due to alternative splicing 55 nt (in mouse) upstream of the bona fide MeCP2β translation start site. To test for interference of the upstream ORF, we introduced a point mutation that changed the upstream ATG to AAG (Fig. 3a) and expressed the wild-type and mutant versions of MeCP2β in fibroblasts. Northern blots probed with MeCP2 cDNA showed that similar amounts of mRNA were produced from transfected wild-type MeCP2α, MeCP2β and mutant MeCP2β plasmids (Fig. 3c, lanes 1–3). As before, MeCP2α was efficiently synthesized, but a negligible amount of MeCP2β protein was translated from the wild-type cDNA construct. Mutation of the upstream ATG, however, led to a dramatic increase in the amount of translated MeCP2β (Fig. 3c, lanes 1–3).

Our results indicate that the MeCP2α mRNA is more abundant than MeCP2β mRNA, but also that MeCP2β mRNA is inefficiently translated. Together, these findings suggest that MeCP2α protein will be much more abundant than MeCP2β *in vivo*. To test this prediction, we took advantage of the different sizes of the α and β protein isoforms (Table 1). A high-resolution SDS–PAGE gel of *in vivo* translated α and β forms confirmed that they migrate differently (Fig. 3c). Cotransfection of equal amounts of α- and β-isoform expression constructs showed that MeCP2α is greatly over-represented among the translation products (Fig. 3c, lanes 4 and 5). To investigate whether native MeCP2 also contains predominantly MeCP2α, we loaded different amounts of mouse brain nuclear extract on the same gel (Fig. 3c, lanes 8–10). MeCP2β protein could be detected only with higher amounts of nuclear extract loaded. We estimate conservatively that the MeCP2α protein is at least 10-fold more abundant than MeCP2β in mouse brain extracts. An alternative hypothetical explanation for the difference might be that MeCP2β is poorly extracted from brain nuclei compared with MeCP2α. Given our evidence that MeCP2β mRNA is not only

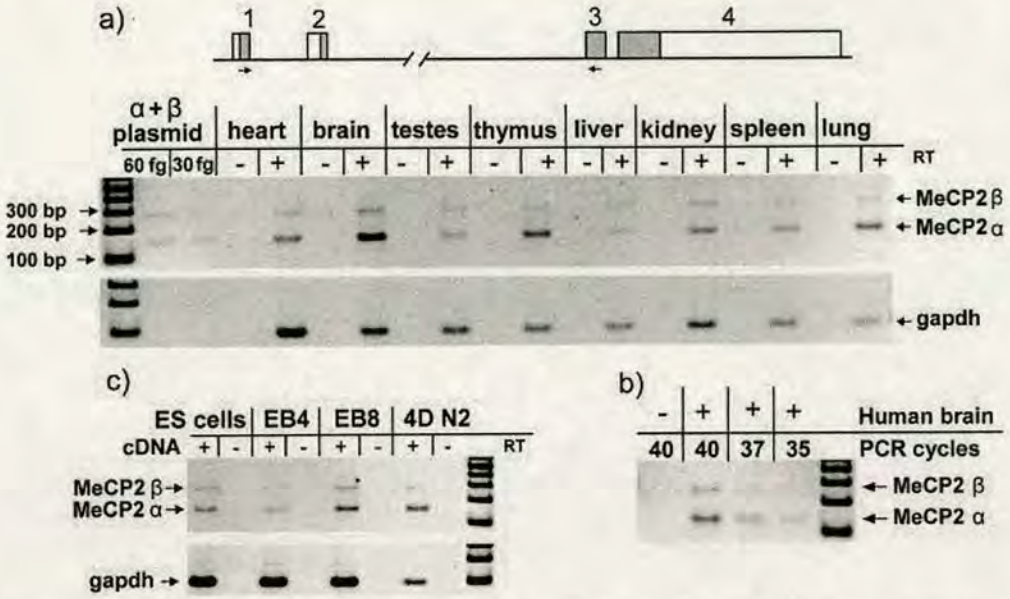

Figure 2. Relative abundance of splice variant mRNAs in mouse tissue, human brain and differentiating ES cells. (**a**) A mouse tissue cDNA panel was analysed by semiquantitative PCR with primers that anneal to exons 1 and 3 (short arrows on map). The α isoform was more abundant in lung, thymus, brain and heart. Amplification of an equimolar mixture of α- and β-encoding plasmids indicated no preference for amplification of either PCR band. (**b**) Human brain cDNA showed dominance of the α isoform mRNA. (**c**) ES cells were differentiated to give embryoid bodies and neuronal cells in culture. EB4 and EB8 refer to embryoid bodies on day 4 and day 8 of differentiation. 4DN2 refers to day 4 after embryoid bodies were split and plated on serum-free neurobasal medium.

less abundant in brain, but also much less well translated than MeCP2α mRNA, we consider it likely that the data accurately reflect the rarity of the β isoform *in vivo*.

Localization of different MeCP2 isoforms in mouse cells

The majority of methylated DNA in mouse cell nuclei is in repeated major satellite sequences, which exhibit punctate staining with DAPI. In mouse cells MeCP2β has previously been shown to colocalize with DAPI bright spots in a DNA methylation-dependent manner (4). To compare localization of the different MeCP2 isoforms in mouse cells, we transfected *Mecp2*-null tail fibroblasts with plasmids expressing the α or β isoforms and stained with an MeCP2 antibody that recognizes the invariant C-terminal domain. Both isoforms were nuclear and colocalized with DAPI bright spots (Fig. 4). The construct encoding the β isoform included the upstream ORF that inhibits translation. Accordingly the number of cells that expressed detectable protein was very low. By comparison, parallel transfections with the α construct gave a much higher percentage of nuclei with easily detectable punctate expression of MeCP2. A few α transfected cells expressed very high protein levels that resulted in saturating fluorescence throughout the nucleus. We suspect that these cells and the few β cells expressing detectable βMeCP2 (Fig. 4, top panel) received by chance a large dose of the transfected expression construct. These experiments reveal no functional difference between α and β MeCP2 isoforms at the level of cellular localization.

DISCUSSION

We report a new splice variant of the MeCP2 gene which we designate MeCP2α. MeCP2α is more similar to frog and zebrafish MeCP2 sequences than the currently known isoform MeCP2β. These findings suggest that MeCP2α is more closely related to the ancestral form of MeCP2 and that the appearance of exon 2 may be a relatively recent event in the evolution of the mammalian gene. The differing size and charge of α and β isoforms permits their separation by gel electrophoresis. This allowed us to demonstrate that both isoforms exist in mouse brain, but that MeCP2α is by far the dominant form. The predominance of MeCP2α can be partly accounted for by the greater abundance of its transcript. In addition, we demonstrate translational interference by an upstream ORF in mRNA of the β isoform. Translational interference by upstream ORFs is well established and has been shown to depend on the distance between the upstream ORF and the AUG of the downstream ORF and also on the structure of 5′UTR RNA (26–29). It is not known whether translational interference of this kind can be modulated in vertebrates as a means of regulating protein synthesis.

The existence of the new isoform has implications for the study of Rett syndrome. Exon 1 was previously thought to be non-coding and has therefore been excluded from many mutational screening programmes. Our finding emphasizes the need for routine inclusion of exon 1 in these screens. Because MeCP2α is the predominant isoform, introduction of a nonsense or frameshift mutation would remove >90% of total MeCP2. This may result in classical Rett syndrome, a milder variant form of Rett syndrome or a related condition such as autism or X-linked mental retardation. We note that the MeCP2α N-terminus contains polyalanine and polyglycine sequences that are encoded by repeated GCC and GGA codons respectively. Expansion of a GCC trinucleotide sequence in the FMR2 gene is reported to cause FRAXE mental retardation (30) and an equivalent expansion may in

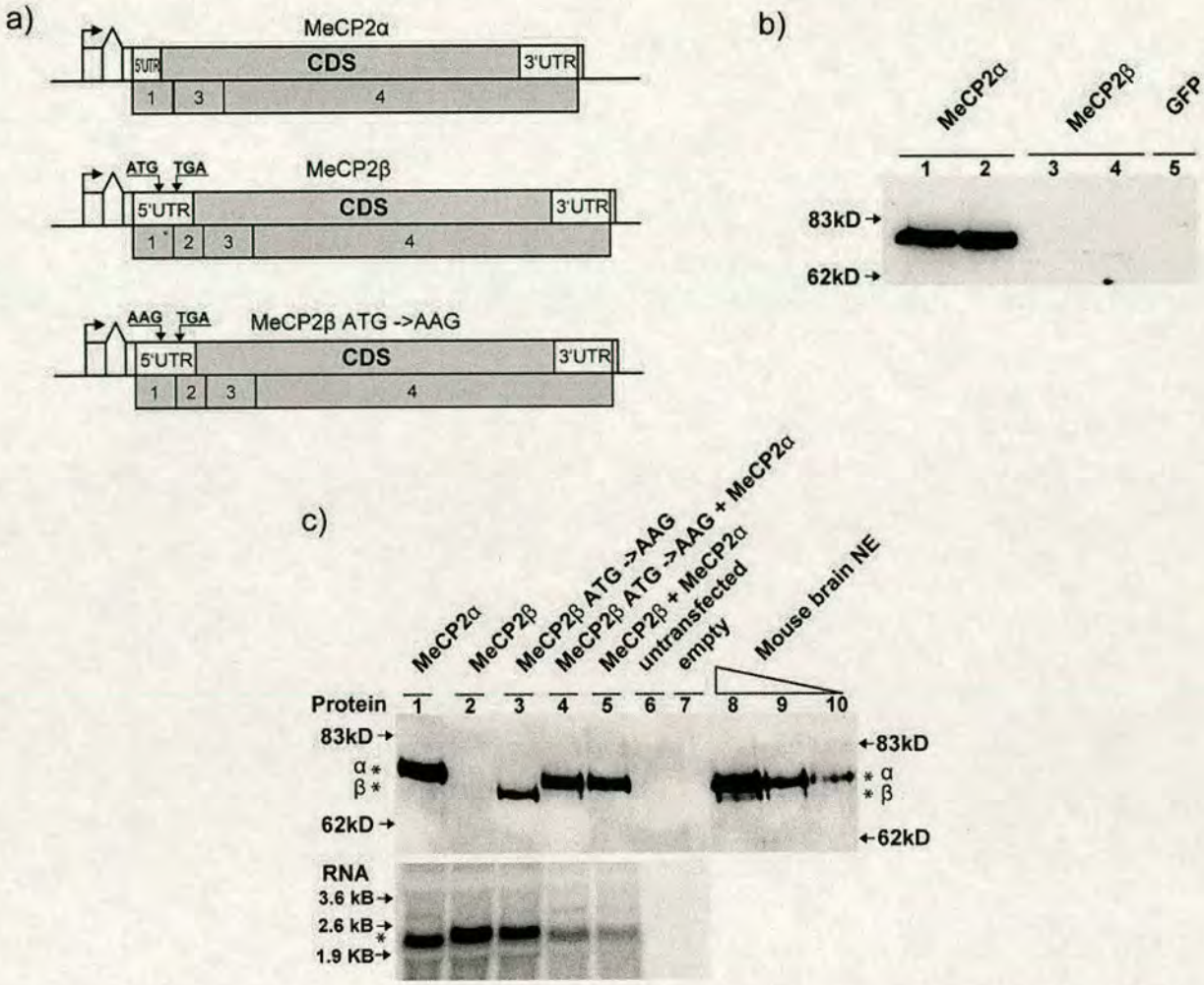

Figure 3. MeCP2β is inefficiently translated to give a protein that can be separated from MeCP2α by PAGE. (**a**) Diagrams of MeCP2α, MeCP2β and mutated MeCP2β constructs used for transfection of *Mecp2*-null tail fibroblasts. An SV-40 promoter and artificial intron is followed by the MeCP2 5′UTR, coding sequence, 3′UTR, MeCP2 polyadenylation signal and SV40 polyadenylation signal. MeCP2 exons are numbered below each map. The start codon of the wild-type upstream ORF in MeCP2β is labeled as ATG (middle diagram) and is mutated to AAG in the MeCP2β ATG-AAG construct (bottom diagram). (**b**) Weak expression of the MeCP2β construct in transfected cells. Two independent plasmid preparations were used for each type of transfection (MeCP2α, lanes 1 and 2; MeCP2β, lanes 3 and 4). The product of the MeCP2β plasmid was barely visible in lane 4 only. (**c**) Western blot analysis (upper panel) of transfected *Mecp2*-null mouse fibroblasts and native MeCP2 from mouse brain nuclear extracts. MeCP2 protein isoforms (asterisks) migrated at different sizes on this 8% PAGE gel (compare lanes 1, 3 and 4). The upstream ORF inhibited the translation of MeCP2β (lanes 2 and 3). MeCP2α is the predominant isoform in mouse brain nuclear extract (lanes 8, 9 and 10). The northern blot (lower panel) showed that different levels of translated MeCP2 protein are not due to differential transcription of the constructs, as similar amounts of MeCP2 mRNA were seen in lanes 1–3. In the absence of transfection, no endogenous MeCP2 RNA is detectable in these *Mecp2*-null cells.

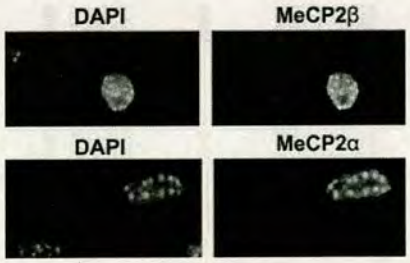

Figure 4. Both MeCP2 isoforms colocalized with methyl-CpG-rich DAPI bright spots when *Mecp2*-null fibroblasts were transfected with wild-type MeCP2α and MeCP2β expression constructs.

theory contribute to Rett syndrome. It is noteworthy that no Rett syndrome mutations in exon 2 have been described. It is possible that exon 2 mutations, which would only affect MeCP2β, are compensated by the more abundant MeCP2α isoform and would therefore have a much less severe phenotypic consequence.

Most previous research on MeCP2 function has utilized the MeCP2β isoform, which we now report to be a minor form *in vivo*. We found that MeCP2 localization in mouse cells is the same for both isoforms, at least in cultured cells. Also, the alternative N-terminus is located outside the previously described functional domains MBD and TRD. It is therefore unlikely that either MBD or TRD function is affected by the N-terminus. Indeed, human MECP2β alone was able to successfully rescue MeCP2 deficiency in frog embryos, whose

endogenous protein more closely resembles MeCP2α (31). Consequently, we expect that the functions of α and β isoforms may overlap significantly. On the other hand, it cannot be ruled out that the two isoforms exert somewhat distinct functions *in vivo*. For example, the MeCP2α N-terminus contains a conserved serine residue that is absent in MeCP2β and which could be a target of phosphorylation. Recently, MeCP2 phosphorylation has been shown to accompany induction of *bdnf* transcription in cultured mouse neurons (32,33). It may be of future interest to determine the functional significance of differing MeCP2 N-termini by the creation of isoform-specific gene disruptions in mice.

ACKNOWLEDGEMENTS

We thank Jim Selfridge for the mouse tissue panel RNA, Rob Klose for mouse brain nuclear extract and comments on the manuscript, Meng Li (ISCR, Edinburgh) for practical advice on ES cell differentiation, Cathy Abbott for helpful discussions and Helle Jorgensen for a critical reading of the manuscript. S.K. is the Darwin Trust scholar. The research was funded by the Wellcome Trust.

REFERENCES

1. Hendrich,B. and Bird,A. (1998) Identification and characterization of a family of mammalian methyl-CpG binding proteins. *Mol. Cell. Biol.*, **18**, 6538–6547.
2. Nan,X., Meehan,R.R. and Bird,A. (1993) Dissection of the methyl-CpG binding domain from the chromosomal protein MeCP2. *Nucleic Acids Res.*, **21**, 4886–4892.
3. El Osta,A. and Wolffe,A.P. (2001) Analysis of chromatin-immunopurified MeCP2-associated fragments. *Biochem. Biophys. Res. Commun.*, **289**, 733–737.
4. Nan,X., Tate,P., Li,E. and Bird,A. (1996) DNA methylation specifies chromosomal localization of MeCP2. *Mol. Cell Biol.*, **16**, 414–421.
5. Lorincz,M.C., Schubeler,D. and Groudine,M. (2001) Methylation-mediated proviral silencing is associated with MeCP2 recruitment and localized histone H3 deacetylation. *Mol. Cell. Biol.*, **21**, 7913–7922.
6. Nan,X., Campoy,F.J. and Bird,A. (1997) MeCP2 is a transcriptional repressor with abundant binding sites in genomic chromatin. *Cell*, **88**, 471–481.
7. Nguyen,C.T., Gonzales,F.A. and Jones,P.A. (2001) Altered chromatin structure associated with methylation-induced gene silencing in cancer cells: correlation of accessibility, methylation, MeCP2 binding and acetylation. *Nucleic Acids Res.*, **29**, 4598–4606.
8. El Osta,A., Baker,E.K. and Wolffe,A.P. (2001) Profiling methyl-CpG specific determinants on transcriptionally silent chromatin. *Mol. Biol. Rep.*, **28**, 209–215.
9. Drewell,R.A., Goddard,C.J., Thomas,J.O. and Surani,M.A. (2002) Methylation-dependent silencing at the H19 imprinting control region by MeCP2. *Nucleic Acids Res.*, **30**, 1139–1144.
10. Rietveld,L.E., Caldenhoven,E. and Stunnenberg,H.G. (2002) *In vivo* repression of an erythroid-specific gene by distinct corepressor complexes. *EMBO J.*, **21**, 1389–1397.
11. Nan,X., Ng,H.H., Johnson,C.A., Laherty,C.D., Turner,B.M., Eisenman,R.N. and Bird,A. (1998) Transcriptional repression by the methyl-CpG-binding protein MeCP2 involves a histone deacetylase complex. *Nature*, **393**, 386–389.
12. Jones,P.L., Veenstra,G.J., Wade,P.A., Vermaak,D., Kass,S.U., Landsberger,N., Strouboulis,J. and Wolffe,A.P. (1998) Methylated DNA and MeCP2 recruit histone deacetylase to repress transcription. *Nature Genet.*, **19**, 187–191.
13. Fuks,F., Hurd,P.J., Wolf,D., Nan,X., Bird,A.P. and Kouzarides,T. (2003) The methyl-CpG-binding protein MeCP2 links DNA methylation to histone methylation. *J. Biol. Chem.*, **278**, 4035–4040.
14. Kaludov,N.K. and Wolffe,A.P. (2000) MeCP2 driven transcriptional repression *in vitro*: selectivity for methylated DNA, action at a distance and contacts with the basal transcription machinery. *Nucleic Acids Res.*, **28**, 1921–1928.
15. Amir,R.E., Van den Veyver, I, Wan,M., Tran,C.Q., Francke,U. and Zoghbi,H.Y. (1999) Rett syndrome is caused by mutations in X-linked MECP2, encoding methyl-CpG-binding protein 2. *Nature Genet.*, **23**, 185–188.
16. Hagberg,B. (2002) Clinical manifestations and stages of Rett syndrome. *Ment. Retard. Dev. Disabil. Res. Rev.*, **8**, 61–65.
17. Kriaucionis,S. and Bird,A. (2003) DNA methylation and Rett syndrome. *Hum. Mol. Genet.*, **12** (Spec. No. 2), R221–R227.
18. Guy,J., Hendrich,B., Holmes,M., Martin,J.E. and Bird,A. (2001) A mouse Mecp2-null mutation causes neurological symptoms that mimic Rett syndrome. *Nature Genet.*, **27**, 322–326.
19. Chen,R.Z., Akbarian,S., Tudor,M. and Jaenisch,R. (2001) Deficiency of methyl-CpG binding protein-2 in CNS neurons results in a Rett-like phenotype in mice. *Nature Genet.*, **27**, 327–331.
20. Shahbazian,M., Young,J., Yuva-Paylor,L., Spencer,C., Antalffy,B., Noebels,J., Armstrong,D., Paylor,R. and Zoghbi,H. (2002) Mice with truncated MeCP2 recapitulate many Rett syndrome features and display hyperacetylation of histone H3. *Neuron*, **35**, 243–254.
21. Lewis,J.D., Meehan,R.R., Henzel,W.J., Maurer-Fogy,I., Jeppesen,P., Klein,F. and Bird,A. (1992) Purification, sequence and cellular localization of a novel chromosomal protein that binds to methylated DNA. *Cell*, **69**, 905–914.
22. Quaderi,N.A., Meehan,R.R., Tate,P.H., Cross,S.H., Bird,A.P., Chatterjee,A., Herman,G.E. and Brown,S.D. (1994) Genetic and physical mapping of a gene encoding a methyl CpG binding protein, Mecp2, to the mouse X chromosome. *Genomics*, **22**, 648–651.
23. Coy,J.F., Sedlacek,Z., Bachner,D., Delius,H. and Poustka,A. (1999) A complex pattern of evolutionary conservation and alternative polyadenylation within the long 3"-untranslated region of the methyl-CpG-binding protein 2 gene (MeCP2) suggests a regulatory role in gene expression. *Hum. Mol. Genet.*, **8**, 1253–1262.
24. Reichwald,K., Thiesen,J., Wiehe,T., Weitzel,J., Poustka,W.A., Rosenthal,A., Platzer,M., Stratling,W.H. and Kioschis,P. (2000) Comparative sequence analysis of the MECP2-locus in human and mouse reveals new transcribed regions. *Mamm. Genome*, **11**, 182–190.
25. Li,M., Pevny,L., Lovell-Badge,R. and Smith,A. (1998) Generation of purified neural precursors from embryonic stem cells by lineage selection. *Curr. Biol.*, **8**, 971–974.
26. Kozak,M. (2001) Constraints on reinitiation of translation in mammals. *Nucleic Acids Res.*, **29**, 5226–5232.
27. Child,S.J., Miller,M.K. and Geballe,A.P. (1999) Translational control by an upstream open reading frame in the HER-2/neu transcript. *J. Biol. Chem.*, **274**, 24335–24341.
28. Xu,G., Rabadan-Diehl,C., Nikodemova,M., Wynn,P., Spiess,J. and Aguilera,G. (2001) Inhibition of corticotropin releasing hormone type-1 receptor translation by an upstream AUG triplet in the 5′ untranslated region. *Mol. Pharmacol.*, **59**, 485–492.
29. Arrick,B.A., Lee,A.L., Grendell,R.L. and Derynck,R. (1991) Inhibition of translation of transforming growth factor-beta 3 mRNA by its 5′ untranslated region. *Mol. Cell. Biol.*, **11**, 4306–4313.
30. Knight,S.J., Flannery,A.V., Hirst,M.C., Campbell,L., Christodoulou,Z., Phelps,S.R., Pointon,J., Middleton-Price,H.R., Barnicoat,A., Pembrey,M.E. *et al.* (1993) Trinucleotide repeat amplification and hypermethylation of a CpG island in FRAXE mental retardation. *Cell*, **74**, 127–134.
31. Stancheva,I., Collins,A.L., Van den Veyver, I, Zoghbi,H. and Meehan,R.R. (2003) A mutant form of MeCP2 protein associated with human Rett syndrome cannot be displaced from methylated DNA by notch in *Xenopus* embryos. *Mol. Cell*, **12**, 425–435.
32. Martinowich,K., Hattori,D., Wu,H., Fouse,S., He,F., Hu,Y., Fan,G. and Sun,Y.E. (2003) DNA methylation-related chromatin remodeling in activity-dependent BDNF gene regulation. *Science*, **302**, 890–893.
33. Chen,W.G., Chang,Q., Lin,Y., Meissner,A., West,A.E., Griffith,E.C., Jaenisch,R. and Greenberg,M.E. (2003) Derepression of BDNF transcription involves calcium-dependent phosphorylation of MeCP2. *Science*, **302**, 885–889.